BIOCOMPATIBLE NANOCARRIER-MEDIATED DRUG DELIVERY FOR THE MANAGEMENT OF DISEASE SEVERITY OF EXPERIMENTAL COLITIS

RAKESH KUMAR MISHRA

A thesis submitted for the partial fulfillment of
the degree of Doctor of Philosophy

Institute of Nano Science and Technology
Sector-81, Knowledge City, Sahibzada Ajit Singh Nagar, Punjab, 140306

Indian Institute of Science Education and Research Mohali
Knowledge city, Sector 81, SAS Nagar, Manauli PO, Mohali 140306, Punjab, India.

July, 2022

Dedicated to

my Family

and Friends

Declaration

The work presented in this thesis has been carried out by me under the guidance of Dr. Rehan Khan at the Institute of Nano Science and Technology Mohali. This work has not been submitted in part or in full for a degree, a diploma, or a fellowship to any other university or institute. Whenever contributions of others are involved, every effort is made to indicate this clearly, with due acknowledgement of collaborative research and discussions. This thesis is a bonafide record of original work done by me and all sources listed within have been detailed in the bibliography.

Rakesh Kumar Mishra

In my capacity as the supervisor of the candidate's thesis work, I certify that the above statements by the candidate are true to the best of my knowledge.

Dr. Rehan Khan

Acknowledgments

ॐ नमः शिवाय
ॐ हनुमते नमः

In the quest for knowledge, search is a means to find the most pertinent information. Similar to that, research is the act of gathering, analysing, and drawing a logical conclusion on a particular topic. All of these things may occur when your karma causes the universe's energy to intensify. I owe a debt of gratitude to each and every person whose well wishes and support helped make my pursuit of Ph.D. possible.

I deem it a proud privileged to express my heartfelt gratitude to my eminent supervisor, **Dr. Rehan Khan** for his guidance, support, motivation and important advice throughout my Ph.D. tenure. I am very grateful to him for allowing me to work in my own way and developing some scientific attitude at the end of my Ph.D. journey. His attitude of always being ready to provide important inputs in terms of scientific as well as personal whenever I required. His continuous reassurance, mental and moral support in the difficult phase and valuable ideas boosted me at every step of my research work. I have enjoyed my work so much and gained vast experience not only for the research prospective but also in life lessons. Not only did I learn to be independent under his guidance, but also developed infinite patience and underwent a significant personality improvement. I want to take this opportunity to thank him from the bottom of my heart for being my Ph.D. supervisor.

I am really grateful to **Dr. Rahul K. Verma** and **Prof. Asish Pal**, members of my doctoral committee, for their insightful remarks, motivation, and time to time evaluations throughout my Ph.D. tenure.

I would like to express my thankful gratitude to **Prof. Amitava Patra**, Director INST for providing research facility and support. I am also thankful to former directors **Prof. H.N. Ghosh** and **Prof. A.K. Ganguli** for basic facility and infrastructure.

I would like to thank Department of Science and Technology, Government of India for providing me fellowship during my Ph.D. tenure.

My sincere gratitude to my collaborators, **Dr. Syed Shadab Raza**, Era Lucknow Medical College and Hospital for providing me animal experimentation facility. I would like to acknowledge Ravi Prakash, Danish and all staffs for supporting me during animal experiments at Era Medical College, Lucknow. I would also like to thank my collaborator **Dr. Jayamurugan Govindasamy** from INST for providing biomaterials for *in-vivo* study. I would also like to acknowledge Dr. Selim and Dr. Arif for their help and support. I acknowledge central instrumentation facility, Panjab University for NMR experimentation. I would also like to thank all the faculty members of INST for their valuable suggestions and support during my Ph.D. coursework. I am thankful to INST administrative and office staffs, security staffs for their cooperation and help. I also thanks to **small laboratory animals** for their sacrifice that made my experiments successful throughout my Ph.D. work.

I take this opportunity to acknowledge my lab mates and alumni for their constant help, support and belief made my Ph.D. journey successful. In this regard I would like to thank **Dr. Anas Ahmad** for his valuable suggestions throughout my research tenure in the lab. I am thankful to my friend and colleague **Ajay** for his help, support and suggestions from M. Pharm to Ph.D. not only professionally but also personally when required. I express my sincere regards to my juniors and friends **Akshay**, **Aneesh**, **Kanika** and **Chandrashekhar** for their help, support and making healthy environment in lab. I also like to express my sincere appreciation to my lab interns Radha, Manisha and Shipra for their affection. I am grateful to **Dr. Vemana** for his support and suggestions. I appreciate **Mrs. Jayashree** for providing a comfortable homely environment outside the lab. I am also thankful to **Dr. Rahul** for his suggestions and support.

I am thankful to my batchmates Chirag, Deepak, Rajat, Priyanka, Mamta, Gagandeep, Sonali, Ridhima, Kritika, Kamaljit, Simerpreet, Navpreet, Arpana, Parvati for their help and support whenever I required.

I would like to express my sincere regards to some of my seniors and friends from INST Dr. Anup Srivastava, Dr. Atul, Dr. Ankur Sood, Dr. Arpit, Dr. Ankur Sharma, Dr. Rashmi, Dr. Naimat, Dr. Neha, Dr. Ruchi, Dr. Renu, Dr. Pulkit, Dr. Rajinder, Dr. Ashmeet, Dr. Jojo, Dr. Sandeep, Dr. Pranjali, Dr. Taru, Dr. Pushpendra, Dr. Ravi, Dr. Krishna, Dr. Aashish, Dr. Navneet, Dr. Ruby, Dr. Sushil, Dr. Soumadri, Dr. Kalpesh, Dr. Rohit, Dr. Deepika, Dr. Babita, Dr. Abhinoy, for their help and support. I also want to sincerely acknowledge my seniors from CSIR-CIMAP, Lucknow Dr. Priyam, Dr. Kuldeep, Dr. Vineet, Dr. Himanshu for their love, affection and motivation. My sincere thanks to my friend **Dr. Arti Joshi** for her constant support, motivation and encouragement.

I take this opportunity to acknowledge some of my friends Jijo, Viani, Avinash, Nadim, Avneet, Eupa, Anjana, Dr. Deepika Rani and juniors Hari Krishna, Varun, Ashish, Shilpa, Raihan, Sourav, Himadri, Dr. Rejaul, Dr. Manisha, Jignesh, Anand, Archana, Silky, Parul, Indranil, Vikas, KK, Prashant, Pradip, Amal, Amit, Raghu, Krishna, Bibek, Debashish for their help and support during my Ph.D. journey.

I would like to acknowledge INST sports coordinators Dr. Debabrata Patra and Dr. Bhanu Prakash for providing sports facility in the campus. I would like to sincerely thanks Dr. Ramesh Jha for his support and valuable suggestions professionally and personally. I would like to sincerely acknowledge my sports team members Dr. Arvinda, Dr. Venu, Dr. Khalid, Dr. Riyaz, Atikur, Ankush, Dr. Nandan, Ajeet, Surjit, Manish, Tanmay, Mujeeb, Dr. Sunil, Dr. Bharat, Himanshu Bhatt, Gaurav, Nausad, Naveen, Dr. Dipankar, Dr. Dipanjan, Dr. Ujjal, Vikas, KK, Liku, Satish, Shumile, Afshan, Prem, Aquib, Ajay Pratap, Shahjad, Hemant, Sudip, Nilkantha, Pradipta, Sonu, Ajay, Ashish, Devender, Himanshu Panda, Vikas Kumar etc.

I would like to thank my friends from INST student body Vibhav, Mayank, Aritra, Mansi and subcommittee members for their support and suggestions for some of the important works beyond the research.

I am thankful to my M. Pharm supervisor Prof. Gaurav Kaithwas, HOD Prof. Shubhini Saraf and school teacher Mr. Umesh Singh for their support and motivation. I sincerely thanks to some of my college and school friends Dr. Rajneesh, Virendra, Swati, Md. Ibrahim, Chetan, Mohit, Ramesh, Vaibhav for their support and motivation.

I want to now convey my sincere gratitude to my family, who I consider to be the most important individuals in my life. It was only because of their support, love, and encouragement that I was able to finish my Ph.D. My sincere gratitude to my grandmother and parents for their unconditional support and belief in me and creating a holistic environment so that I can accomplish my ambitions. My sincere love and affection to my younger brother **Rahul Mishra** (Scientist, IISS Bhopal) for being constant source of motivation and encouragement throughout my academics. I also want to express my gratitude to my elder brothers **Santosh Pandey**, **Rakesh Pandey** and younger sister **Rani** for their unwavering love, motivation and encouragement throughout the way. I also thankful to all my teachers, relatives and the people from my village whose appreciation and motivation made me to cover the journey of my Ph.D.

Above all, I would like to bow my head to the **Almighty** and **Gurus** for their blessings.

Rakesh Kumar Mishra

ABBREVIATIONS

AB-NR	*Alcian blue neutral red*
AFM	*Atomic force microscopy*
BUD	*Budesonide*
CA	*Caffeic acid*
CLX	*Celecoxib*
COX-2	*Cycloxygenase-2*
CRT	*Cortisone*
DAB	*3, 3,-diaminobenzidine*
DLS	*Dynamic light scattering*
DSS	*Dextran sodium sulphate*
DTNB	*5-5'dithio-bis-2-nitrobenzoicacid*
EDTA	*Ethylene diamine tetra-acetic acid*
ELISA	*Enzyme-linked Immunosorbent assay*
EUD	*Eudragit*
FTIR	*Fourier transform infrared*
GPC	*Gel permeation chromatography*
H&E	*Hematoxylin and eosin*
HID	*High iron diamine*
IL-1β	*Interleukin-1 beta*
iNOS	*Inducible nitric oxide synthase*
MTT	*3-(4,5-dimethylthiazol-2-yl)-2,5-diphenyltetrazolium bromide*
MPO	*Myeloperoxidase*
NBT	*Nitrobluetetrazolium*
NSAIDs	*Non-steroidal anti-inflammatory drugs*
PBS	*Phosphate-buffered saline*

PDI	*Poly dispersity index*
SA	*Stearic acid*
SAA	*6-o-Stearoyl-L-ascorbic acid*
SEM	*Scanning electron microscopy*
TEM	*Transmission electron microscopy*
TNF-a	*Tumor necrosis factor-alpha*
UC	*Ulcerative colitis*
UV-Vis	*Ultraviolet-Visible*
XRD	*X-ray diffraction*

TABLE OF CONTENTS

List of Figures

List of Tables

ABSTRACT

Ulcerative colitis (UC) is a chronic mucosal inflammatory condition that adversely affects colon and rectum. Existing conventional approaches in UC and RA treatment include nonsteroidal anti-inflammatory drugs (NSAIDs), mesalazine, corticosteroids, etc. However, these conventional drugs have several inherent limitations like low water solubility, low bioavailability, off-target systemic adverse effects etc., which limit their use in clinics. Nanotechnology based advancements have considerably contributed to the alleviation of inflammation and associated UC disease severity as inflammation greatly contribute in the development of UC. In this thesis, synthesis and characterization of nanoformulation is described for delivery of pharmacological agents such as celecoxib, budesonide etc for targeting inflammation involved in acute experimental colitis. In this thesis, we developed different types of nano-sized delivery systems such as nanostructured lipid carriers (NLCs) and micelles for the delivery of drugs. Importantly, we have used US-FDA approved Generally Recognized as Safe (GRAS) compounds and natural compounds to develop the delivery systems by keeping in mind to develop safe and non-toxic nanoformulation. NLCs were developed by the hot-melt method while nanomicelle were developed by the co-solvent evaporation method. Nanoparticles were characterized for their various physicochemical properties such as particle size, zeta potential, and polydispersity index with dynamic light scattering. Particle shape and surface morphological features were studied with transmission electron microscopy, scanning electron microscopy and atomic force microscopy. Drug loading capacity and drug entrapment efficiency was analyzed with UV-Vis spectroscopy. The developed nanoparticles further used to investigate the cytocompatibility against normal human foreskin fibroblasts (BJ). Furthermore, safety and pharmacological efficacy of these nanoparticles was assessed in-vivo using dextran sodium sulphate (DSS)-induced colitis in Swiss Albino mice models. Results of these studies indicated that nanoparticles possessed favourable physicochemical characteristics in terms of particle size, zeta, polydispersity, shape, surface morphology etc. and delivery of drugs mediated by these, markedly reduced the colitis disease severity in mice model by mitigating the inflammatory biomarkers. Most of the observations in animals, biochemical parameters, and immunohistochemical markers showed a considerably superior degree of restoration by treatment of drug-loaded nanoparticles as compared to free form of drugs alone.

OBJECTIVES

1. Formulation, characterizations and therapeutic efficacy of Eudragit S-100 coated celecoxib loaded lipid based nanocarrier for colitis.

2. Formulation, characterizations and efficacy assessment of cortisone loaded stearoyl ascorbic acid based nanocarrier in colitis model.

3. Assessment of anti-inflammatory activity of copper oxide nanoparticles against animal model of colitis.

4. Formulation, characterizations of caffeic acid based nanomicelle and their therapeutic efficacy study on animal model of ulcerative colitis.

Chapter 1

Introduction

1. Introduction

Inflammation is one of the prominent natural defense mechanisms that protect biological systems against harsh external stimuli like materials that causes irritations to the body, injured/necrotized cells, pathogenic organisms. In response to them biological system undergoes cellular and humoral changes to neutralize the harmful effects. But sometimes inflammatory responses become pathology for different associated diseases such as inflammatory bowel diseases i.e., ulcerative colitis and Crohn`s disease, rheumatoid arthritis, osteoarthritis, various cancers, diabetes mellitus etc.[1]

The physiological role of inflammation is to enhance the tissue repair process after pathological changes and make them to regain the cellular components in their natural originated form via eliminating or terminating the damaged/necrotic/dead cells and local tissues which affected by the external stimuli that initiated inflammatory process.[2] The inflammation is recognized as its hallmark features such as redness (rubor) due to enhanced blood flow in that particular region, rised temperature at inflammatory site called heat (calor), swelling known as tumour, enhanced hypersensitivity as pain (dolor) and functional loss. Inflammation is also regarded as amenable incidence which reflected as response of innate immune system rather than adaptive immunity.

On intensity and incidence inflammation is classified as acute and chronic inflammation. Acute inflammation is short duration and high peak response of body`s against obnoxious stimulus such as tissue injury which arises due to activities like locomotion which initiated because of accumulation and movement of some inflammation responsive cells like granulated leukocytes from blood to inflammatory tissue site.[3] The is inclusive of several biochemical reactions in system that develop quickly and noticed as hallmarks of inflammation viz. heat, swelling, redness, pain and immobilization in terms of functional loss. Whereas, chronic phase inflammation occurs as low peak than acute but for longer duration that may last upto few months or years. Generally, it depends on the cause of inflammation and body`s capability to repair and control of damage.[4] Chronic inflammation mainly occurs in failure response of body if acute phase inflammatory response is not sufficient to overcome from the inflammatory damages and thus gives rise to various diseases.[5,6]

There are three main biochemical and structural implications that have been recognized in all types of inflammation that may include alterations in cellular components, morphological architecture of tissues and vascular changes. It started from vascular responses as increased capillaries permeability and vasodilation. It also causes the movement of blood containing fluids to the tissue site of inflammation from blood vessels and releases various proteins like immunoglobulins and fibrins.[7] Whenever it contacts with pathogens secretion of different inflammatory components take place like vasoactive amines such as serotonin, histamine, prostaglandin E2 etc. that causes alterations at inflammation confined blood capillaries. Then the local endothelial and macrophagic production and release of nitric oxide takes place that enhances blood capillaries` permeability and vasodilation and ensures the distribution of blood from vasculature to inflamed tissue. Thereafter cellular changes take place which may involve infiltration and accumulation of different immune cells.[8,9]

Cellular components of inflammation need cumulated and infiltrated leucocytes from plasma to the inflamed site via extravasation. These infiltrated cells actively engulf pathogens and eliminate injured cells` debris. These cells also secret various mediators like enzymes that actively impair/kill pathogenic factors. Inflammatory mediators are also responsible for initiation and progression of inflammatory events. Normally, acute phase inflammations are the response of granulocytes whereas, chronic inflammations are mediated by lymphocytes and monocytes.[10] Inflammation also proceeds in serial manners that involves neutrophiles localization from blood circulation to tissues vicinity. It undertakes the adherence of leucocyte to endothelium and its depreciation and movement of leucocytes to the inflamed tissue through chemotaxis.[11]

Finally, morphological alterations of inflammation appear in acute as well as chronic inflammatory events that can be visualize in inflamed tissue histological architecture via various staining procedures. These histological changes occur in different manner for various diseases like granulomatous structural components formation in diseases such as syphilis, tuberculosis, leprosy etc., deposition of fibrin in colitis and cancer, accumulation and pus formation, fluid retention or deposition in intestinal ulcers and skin blisters.[12,13] As the involvement of inflammation has been found in various complications and diseases as mentioned above required the target of

inflammation. The vast involvement of inflammation provided motivation for this thesis on an important inflammatory disease ulcerative colitis.

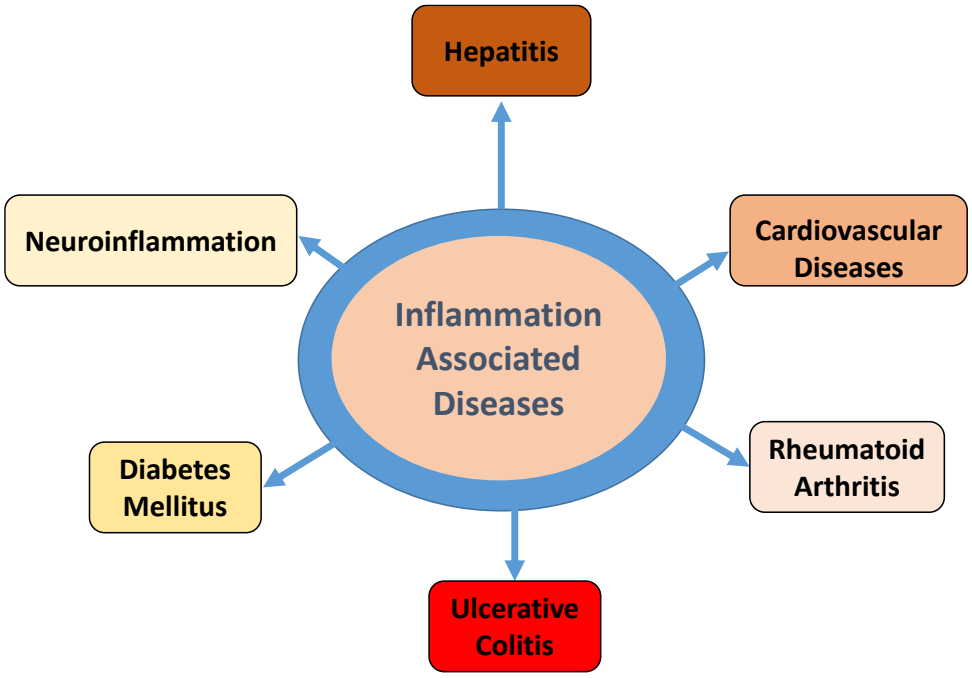

Figure 1.1 Association of inflammation in various metabolic disorders.

1.1 Inflammatory Bowel Diseases

Inflammatory bowel diseases (IBDs) are chronic, relapsing and multifactorial disorders of unknown cause affecting the gastrointestinal tract. On the basis of histological locations IBDs can be recognized as Crohn's disease which affects any portion of g.i.t. whereas the inflammation confined to the colon in ulcerative colitis. The cause of these diseases is not known but resultant of compromised immune response against regulating factors such as microbial and luminal agents in genetic susceptible individuals.[14]

IBD has become a global disease in the 21st century, rapidly expanding throughout industrialized nations, particularly in Eastern Europe, South America, Africa and Asia. It is not now at its peak and is reported to have a low prevalence.[15] According to lancet report over 6.8 million of people are having IBD globally.[16] The approximation of these diseases in North America is 1.5 million whereas more than 2 million Europeans are affected by IBDs. Similarly, its emerging trends have been observed in Asian countries. In South Asian countries mainly in India the prevalence

of these diseases rises 550 thousand cases in 2020 from 212.451 thousand cases in 2017. The futuristic estimation of IBDs cases rise in India in 2035 around 2.2 million. In East Asia regions the prevalence has been increases upto 3 million in 2020 from 2.767 million cases in 2017 and future estimation upto 4.5 million cases in 2035. In Southeast Asian countries its increment of its prevalence has been observed from 103.884 thousand in 2017 to 118 thousand cases in 2020. It is estimated to be rise to 199 thousand upto 2035. These observations indicate that a highly aggressive uprise in IBDs cases in Asia will be faced by 2035.[17]

1.2 Ulcerative Colitis

Ulcerative colitis (UC) is a chronic inflammatory disease that affect lower end of g.i.t. mainly colon and over time it may spread towards rectum. In this disease an ulceration has been occur at colon as well as rectum where it affected. The symptoms of UC are diarrhoea, rectal bleeding, rectal irritation, passage of mucus, tenesmus etc. whereas some extraintestinal symptoms are also observed namely weight loss, anaemia, fever, fatigue, tachycardia etc. Other complications may also appear as dilation of colon, observed inflammations of eyes and joints. If the diseased left untreated or unmanaged for longer duration its progression may lead to colon or rectum cancers.[18,19] The exact etiology of UC is unknown but researchers concluded the involvement of various factors in the development and progressions of UC. The underlying factors includes altered gut microbiota, various environmental factors and association of food habits and life styles, genetic factors, unregulated immune systems etc. UC rates are found higher in developed countries due to sedentary lifestyle and diet. Colon biopsy and colonoscopy have been performed to diagnose UC.[20]

UC starts with diarrhoea along with blood in watery or loose stools which may also include fecal incontinency and frequent enhancement of bowel movements, mucus passage and sometimes nocturnal occurred defecation. The symptoms of disease also depend on the severity. Likewise, abdominal pain and diarrhoea or rectal bleeding have strong association with severity and intensity of pain also differ according to the frequency or intensity of bowel movement and related abdominal cramps. Decreased body mass, enhanced bowel movement, frequent nausea feelings,

fatigue and fever are generally associated with UC. Longer intestinal bleeding and severe inflammation causes the deficiency of iron that culminates into anaemia and ultimately lowers the life span and quality.[21,22] In UC body undergo catabolic state that restrict the absorption of nutrients from the intestine and body weight decreases cause severe fall in body weight.[23]

Utmost severity of colitis is recognized by toxic reactions, excessive abdominal contraction with distensions, colon expansions, profuse bleeding, 10 bowel movements in a day. As the severity of UC enhances the inflammation spread par the colonic mucosa layers and it disturb movements of colon and causes intense colon distensions. Whenever inflammation involves to the serous membrane perforation in colon regions also appears.[24]

1.2.1 Pathophysiology of UC

Normally inflammation in ulcerative colitis originates from rectum and remain there or may extended towards colon completely or partially and affect the mucosa and submucosa layers of colon epithelium. In some severe cases involvement of muscularis layer also observe. In the initial stage of disease mucous membrane become friable and loss of normal pattern of vasculature appear due to the formation of erythematous granules. The extent of disease severity is characterized by the scattered pattern of hemorrhage in some area with large cover area with ulcerated mucosa and some exudates have been observed.[25]

The colon epithelium normally intends for its barrier function and become covered with protective mucin layer that acts as prime mucosal immune defense system that play a physical barrier between luminal microbiota and host immune system. Development and progression of colitis affect the production of specific type of mucin. There are two types of mucins are secreted by colonic cells i.e., sulphomucin and sialomucin. In normal colonic mucosa sulphomucin is predominantly secreted whereas in inflammation or UC sialomucin enhanced. In diseased cases sulfation pattern of either type of mucin is changed. Membrane permeability increases because of the damage of intestinal barrier function and unregulated characteristics of epithelial tight junctions.[26]

Previous literatures suggested that in the pathogenesis of UC various cytokines and enzymes play pivotal role. They are interleukins (ILs), tumor necrosis factors (TNFs), cyclooxygenases (COXs), nitric oxide synthases (NOSs) etc. Role of free radicals and immune responses are also considered in the initiation and development of inflammatory diseases and colitis. Also, the level of TNF-α found overexpressed in blood, faecal and mucosal tissue samples of colitis patients. TNF-α upregulation is also associated with the production of various free radicals that causes DNA damage and elevation of inflammatory effects.[27,28] Furthermore, numerous evidences have found that natural killer T-cells producing interleukins causes cytotoxic effects on colon epithelium together with apoptosis induction and modifying the responsible protein of colonic tight junctions have strong correlation with colitis. These ILs enhances the severity of inflammation and tissue injury via positive feedback action on natural killer cells. In this regard proinflammatory cytokines like IL-13, IL-33, TNF-α plays very crucial role in the progression of disease. In contrast, anti-inflammatory cytokines such as IL-10, IL-33 etc. downregulates the progression of inflammation and disease progression. The imbalance between proinflammatory and anti-inflammatory mediators gives rise to disturbance of colonic homeostasis causes disease initiation and progressions.[29–31] Inflammatory enzyme COX-2 is also reported to be expressed at the sites of inflammation and colitis. COX-2 is inducible enzyme overexpressed at the site of inflammation due to the effects of stimuli. Following the arachidonic acid pathway, it is responsible for the production of various prostanoids viz. prostaglandins, prostacyclins and thromboxanes. These prostanoids have variety of role in the pathogenesis of inflammation, colitis and various malignancies. Moreover, PGE2 have tumor promotor and proinflammatory roles of COX-2 in the pathogenesis of inflammatory diseases.[32,33] Similarly, iNOS leads to the formation of nitric oxide (NO) that have role in inflammatory processes. Normally this enzyme has been found in the mucous membrane of large intestine where it produces nitric oxide (NO) from L-arginine. It is established regulator and mediators of inflammation. It possesses cytotoxic effect against pathogenic vectors but also has destructive effects on host tissue. It also interacts with superoxide anion and molecular oxygen and produces nitrogen free radicals and regulate various cellular functionalities. Thus, iNOS has strong association in the pathogenesis of colitis.[34,35]

The pathogenic pathway of ulcerative colitis is also associated with the recruitment of leucocytes from plasma and their movement to the inflamed/injured mucosa and release of chemoattractants that regulates and enhances the intensity of inflammation. Numerous proinflammatory mediators (cytokines) released at the inflammatory site in colitis upregulates the level of cell adhesion molecules on the surface of mucosal capillary endothelium which further enhances the leucocytes into colonic tissue and further prolonging the inflammatory cycles.

Generally, colonic immune systems regulate and maintain homeostasis between commensal microbes and antigens in ingested diets that provide sufficient response to the intestinal pathogens. Reports from various animal models that exhibit prolonged intestinal inflammation followed by commensal intestinal bacterial colonization but do not develop symptoms when exposed to bacteria suggests that many non-pathogenic intestinal bacteria play a major role in the progression of colitis.[26,36] Similarly evidence from clinical studies supports the role of intestinal microbial flora in the pathophysiology of this disease. In light of this, ulcerative colitis comes from the disruption of the homoeostatic balance between the intestinal microflora and the host's mucosal immune system, which causes aberrant immune responses against commensal and non-pathogenic bacterial organisms.[37,38]

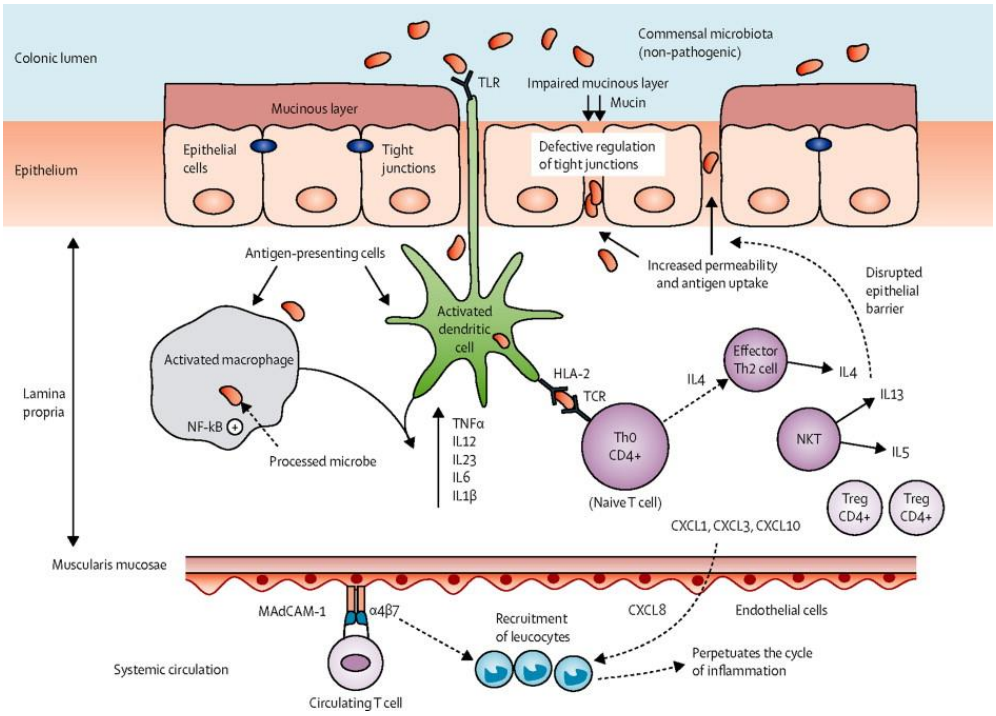

Figure 1.2 Pathophysiological changes in ulcerative colitis (Reprinted from[26]).

1.2.2 Strategies of UC Treatment

Considering the intensity and severity of disease variable therapeutic strategies have been employed aiming to decrease its progression and degree of related pathologies. It starts with the medicinal treatment followed by the maintenance therapy to prevent the disease relapse.[39] The initial effort has been kept to relief the disease symptoms and enhance the mucosal healing damaged in colitis. A sustainable treatment plan is then implemented to prevent further complications. When ulcerative colitis becomes acute and severe, hospitalization may be necessary for infection control and for acute conditions and also a low-fiber diet is advised.[40]

1.2.2.1 Drugs for Treatment of UC

The first line and popular medicine for the treatment of colitis has been used from long back is 5-amino salicylic acid category drugs e.g., sulfasalazine, mesalazine etc.[41] Steroidal drugs like corticosteroid class particularly prednisolone and others are used for healing effects with immunosuppression action, but their long-term use is associated with severe clinical toxicities limits their application. Other biological agents and immunosuppressive agents such as adalimumab, azathioprine and infliximab are used in condition where steroidal drugs and aminosalicylates proves to be ineffective.[42] In moderate to severe disease condition of colitis infliximab and vedolizumab may be administered. Tofacitinib, a medication also used to treat moderate and less severe active instances of ulcerative colitis, is the first oral medication for long-term usage in ulcerative colitis. Budesonide and its formulation have also been used to treat acute ulcerative colitis.[43]

TNF-α inhibitors are biological substances that are frequently used to treat ulcerative colitis and have had notable clinical results in terms of both patient responses and disease remissions. However, when other therapeutics are proven to fail for required potential effects these biological agents are used for treatment. In general, the approaches to treating ulcerative colitis must be highly individualized based on the patients and corresponding drug response.[44]

The use of biological agents in ulcerative colitis is associated with substantial adverse effects and raises the possibility of causing malignancies outside the afflicted areas of the gut. These agents are also linked to heart failure and severe

immune system weakness, both of which can make it difficult for the body to fight off illnesses like tuberculosis. Therefore, individuals on these treatments need to be closely monitored, and it's common to see them being admitted to the hospital for a yearly hepatitis or tuberculosis checkup.[45]

In comparison to Crohn's disease, ulcerative colitis sufferers are less harmed by smoking. Therefore, resuming low dosage nicotine therapy may assist in lowering active ulcerative colitis-related symptoms in a small number of carefully chosen patients with a history of smoking. Transdermal nicotine patches have been shown to improve ulcerative colitis histological and other clinical symptoms. In a double-blind, placebo-controlled clinical research, ulcerative colitis symptoms were significantly improved in almost half of the patients who used nicotine transdermal patches in addition to other usual treatments. However, due to a number of side effects and inconsistent results, nicotine cannot be advised for sustained use.[46,47]

1.2.2.2 Alternative management of UC

Although there is a chance that extra intestinal symptoms will continue to persist, surgically removing the large intestine is another option for treating ulcerative colitis. This procedure must be carried out when the severity of ulcerative colitis is relatively high, intestinal perforations occur, or there is a high propensity for colon cancer. Additionally, patients may think about considering surgery for betterment of their quality of life if they experience severe and incapacitating symptoms or if the disease does not improve with pharmacological therapy.[48,49]

Additionally, numerous randomized clinical trials have shown the potential benefit of probiotics in the management of ulcerative colitis. Some particular probiotics, such as E. Coli Nissle, show the ability to induce ulcerative colitis remission in patients that lasts for up to a year. A probiotic product has been shown to be beneficial in bringing ulcerative colitis into remission, and its effectiveness in preventing the disease relapse is comparable to that of 5-ASA. Additionally, faecal anema injections with human probiotics may be necessary for microbial recolonization.[50] According to a report, microbiota transplantation had a favorable effect on ulcerative colitis response, and around 68 percent of patients have reached the full remission stage.[51]

For the treatment of UC, numerous more alternative therapeutic regimens have been developed, although the outcomes of the majority of these medications have shown quite a few discrepancies. For instance, when used in conjunction with medications like sulfasalazine and mesalazine, curcumin has also demonstrated its pharmacological usefulness in ulcerative colitis. Additionally, it has assisted individuals with latent colitis in keeping their remission. However, it is unknown how curcumin monotherapy would affect ulcerative colitis in its latent stages.[52]

1.2.3 Limitations of Drugs in UC

Numerous problems have been associated with using medications and pharmacological chemicals to treat ulcerative colitis, particularly when using biological medications and immunomodulating medicines. Because ulcerative colitis is a chronic condition, long-term therapy strategies are needed. The therapeutic outcome of any disease is strongly related with patient acceptance.[53] Other aspects of treating colitis include prescription costs, related side effects, and adverse drug reactions. As many as 35–70% of patients have been observed to be noncompliant with anti-inflammatory medication therapy for ulcerative colitis. Patient compliance with these medications is challenged by the prolonged administration of immunomodulating medicines, which strongly require periodic patient monitoring.[54]

Along with adverse effects such gastrointestinal pain, skin rashes, hepatitis, hematological abnormalities, folate insufficiency, lowered sperm count, pancreatitis, etc., standard therapy for ulcerative colitis with mesalamine, mesalazine, etc. also causes intolerance in patients. These medications may also result in hypersensitivity responses, hepatotoxicity with increased aminotransferase activity, hepatomegaly, etc. Thiopurines used to treat ulcerative colitis can also result in hepatotoxicity, flu-like symptoms, severe pancreatitis, and other side effects.[55]

Anti-TNF-drugs are used to treat ulcerative colitis, however doing so significantly increases the risk of developing TB, hypersensitivity responses, infusion reactions, and immune cell malignancies such hepatosplenic T-cell lymphomas. Similarly, using corticosteroids to treat ulcerative colitis has been linked to infections and related side effects. Bowel perforations, peripheral neuropathy, leukopenia, and fever are other side effects and problems associated with medications.[56]

Other ulcerative colitis drugs can affect sexual function and fertility. For example, sulfasalazine can cause male infertility by reducing sperm count, sperm motility, and sperm morphology. Additionally, sulfasalazine has been known to cause congenital malformations, abnormalities, or variations in the fetus. Purine analogues and the usage of corticosteroids during pregnancy both have a connection to congenital issues in newborns.[57]

Pregnant women take Janus kinase inhibitors have been associated to birth malformations and miscarriages. Other adverse effects of medications include headaches, nasopharyngitis, and upper respiratory tract infections. Additionally, gastrointestinal perforations have been brought on by its use in ulcerative colitis.[58]

Inadequate drug accumulation at the desired target site, target non-specificity of pharmacological agents, poor patient compliance or adherence, and a variety of associated off-target effects are just a few of the challenges that have prompted researchers to search for cutting-edge drug delivery systems and treatment paradigms that can fill in the gaps in currently available conventional treatments for ulcerative colitis.

1.2.4 Strategies to overcome drug limitations

Numerous natural and synthetic biomaterials based smart drug delivery systems have entered the picture as a result of the numerous drawbacks of the medications currently used to treat ulcerative colitis. These innovative and advanced deliveries are intended to reduce the side effects of medications, transport pharmacological chemicals to specific sites with precision, and increase the therapeutic efficacy of these compounds as a whole.[59] Natural polymer-based materials offer good biocompatibility with the biological environment, improved adaptability and response to environmental stimuli, and biodegradability with minimal or negligible toxicity issues. To treat ulcerative colitis, several hydrogels, microparticles, and nanoparticles have been developed.[60,61]

For the treatment of ulcerative colitis, hydrogels based on natural polymers such as pectin, chondroitin sulphate, gelatin, hyaluronic acid, heparin, alginates, etc. have been developed. Natural polymers provide various benefits over the synthetic ones and are generally selected for their usefulness in drug delivery. But because of their weaker mechanical and tensile qualities, their employment is

constrained.[61,62] Polypeptides, polyphosphazenes, or polyesters are used in synthetic polymer-based drug delivery systems, which can help with controlled degradability and therefore provide controllable drug release rates in ulcerative colitis. However, since neither a natural polymer nor a synthetic polymer can serve all of the goals in almost all situations, a combinatorial method that combines both natural and synthetic polymers is frequently used.[61,63]

Additionally, a number of microparticulate and nanoparticulate systems for the treatment of ulcerative colitis have been created. These systems, which are based on smart biomaterials, were also developed for use in oral and parenteral drug delivery systems for the targeted and controlled delivery of pharmacological agents. Costas et al. developed pectin-based microspheres loaded with sulfasalazine for its controlled release, which depended on the level of methylation of pectin. They hypothesized that microspheres might be a candidate for solon-specific drug delivery of sulfasalazine.[64] For ulcerative colitis, chitosan-based microspheres have also been developed to release medication at the desired colon-specific locus. Additionally, it was claimed that microspheres could lessen colonic mucosa damage and suppress inflammatory gene expression.[65]

1.2.5 Nanoformulations used in UC

Nanoparticles have been widely used in the treatment of ulcerative colitis to provide the regulated and targeted administration of medications and pharmacological agents. In this regard, a variety of nanoparticulate delivery systems made of both polymeric and metallic materials have been developed. For pH-responsive drug administration, polymeric nanoparticles of both natural and synthetic origin are used, whilst magnetic nanoparticles can be used because of their thermoresponsive capabilities.[61]

Drugs can be delivered to colonic epithelial cells and macrophages specifically by targeting transmembrane protein complexes like CD98 utilizing active targeted nanoparticles in ulcerative colitis. Certain targeting ligands, such as hyaluronic acid, can be employed to create these nanoparticles. Both *in-vitro* and *in-vivo*, these particles have superior effects compared to free or naive drug forms.[66]

They are frequently tailored to prevent the loaded drug from being harshly degraded by gastric acid or enzymatic activity and to deliver the intended drug only to the inflamed mucosa of the colon for localized administration. Nanoparticles can help reduce drug waste caused by enzymatic or acidic hydrolysis and increase the therapeutic efficacy of anti-inflammatory medications in this way. The improved drug loading capacity, *in-vitro* cytocompatibility, *in-vivo* biocompatibility, sheathing characteristics, and well-controlled and sustained release of the loaded drug cargo are just a few additional benefits that these nanoparticles possess.[67,68]

In general, many kinds of nanoformulations have been fabricated for ulcerative colitis in order to achieve a variety of objectives, including the administration of greater and localized medication concentrations at the inflamed mucosa, pharmacological efficacy of medications is increased and prolonged, and drug degradation is decreased, minimizing efficacy loss, lowering the dose and frequency of the drug's dosage, reducing adverse drug reactions and drug toxicity, enhancing drug biodistribution, taking advantage of various stimuli and disease-related responses, and increasing the overall cost-effectiveness of the disease therapy are all ways to treat the disease.[59]

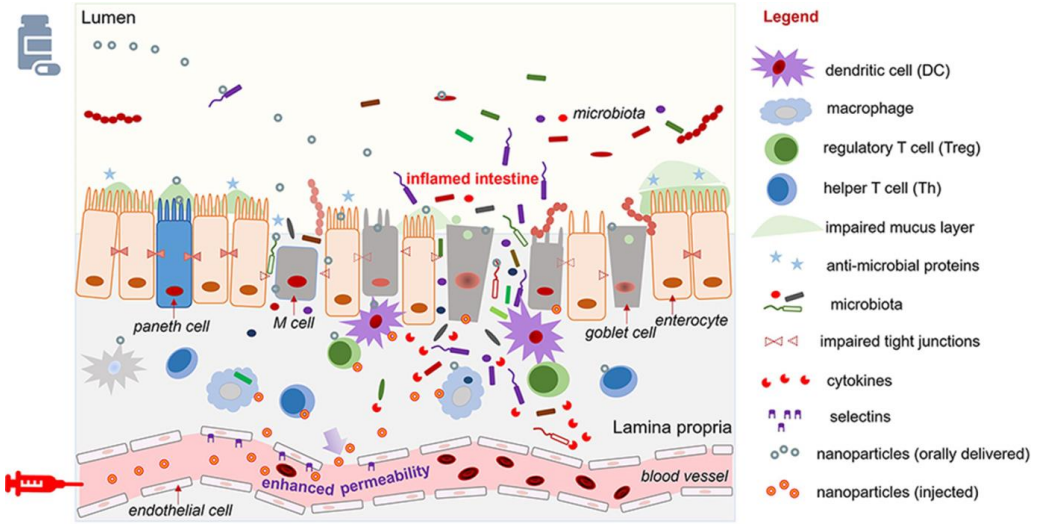

Figure 1.3 Oral and parenteral nanotechnology-based drug delivery systems in ulcerative colitis. (Reprinted from[69]).

1.2.6 Nanotechnology based drug delivery systems for UC management

In the cure and management of ulcerative colitis researchers have developed various drug delivery systems. The USFDA has also approved many of these multi-responsive nanoformulations for the treatment of intestinal inflammation. These nanoformulations were fabricated for disease-related imaging concerns, modulation and management of the immune system response, and targeted medication delivery to achieve the optimum efficacy and potential of active agents. As the efficacy of therapeutics also dependent on the route of administration so these nanoformulations intended for oral as well as intravenous and intrarectal administration of active agents.

By employing lactulose, Katsuma et al. developed a colon-targeting drug delivery system that consists of three parts: a lactulose core containing the medication, an inner layer that is acid soluble, and an outer layer of material that is soluble in the intestine. Here, lactulose triggered the release of the drug in the colon environment. This approach made use of the bacterial activity in the intestine to break down the polymeric nanoparticles and release the 5-ASA-loaded drug cargo.[70] In a different study, non-toxic tailored liposomal nanoformulations containing hyaluronan-liposomal phospholipid conjugates and antibodies that specifically target integrin beta-7 on their surface were created for their unique targeting capabilities. Due to their ability to precisely target intestinal mononuclear leukocytes, these liposomes enabled the anti-inflammatory delivery of siRNA against cyclin D.[71]

The inflammation in the mice model of experimental colitis was also reduced by surface decorated nanoparticles with antibodies against CD98 and loaded with short interfering RNA against CD98. The hydrogel that can be taken orally contains the nanoparticles and can release them to lower the amount of CD98 in the mouse colon. Under fluorescence microscopy, nanoparticles also demonstrated effective cellular absorption in colon cells and had a strong affinity for cells that overexpress CD-98. According to the authors' findings, a variety of physical, biochemical, and histological factors resulted in a reduction in the severity of colitis-related inflammation.[72] Since colonic epithelial cells overexpress peptide transporters, which are oligopeptides, nanoparticles have also been developed to target these peptides, which can increase the absorption capacity of loaded drug cargo. As a

result, in ulcerative colitis, increased membrane proteins and peptides serve as effective targets for nanoparticle-mediated drug delivery systems.[73]

Recently, gastro resistant polymer coated nanoparticles for oral drug administration in the treatment of ulcerative colitis have also been developed. In experimental colitis models, these nanoparticles can deliver the target to certain inflamed colon regions while avoiding the harsh effects of the stomach's acidic environment. By using the solvent evaporation approach, coating is applied to nanoparticles after they have been created, and these nanoparticles have improved drug loading and encapsulating capabilities. The sustained drug release behaviour of these enteric coated nanoformulations, which can lower the dose frequency in colitis patients, is another benefit. In comparison to free or naive forms of drugs, these types of nanoparticles also demonstrate superior therapeutic efficacy due to their increased anti-inflammatory activity.[74,75]

1.3 Bibliography

(1) Bennett, J. M.; Reeves, G.; Billman, G.; Sturmberg, J. P. Inflammation, the Body's Only Efficient Way to Respond to Injuries: Implications for Clinical Care of Chronic Diseases. *Front Med* **2018**, *5*, 316.

(2) Medzhitov, R. Origin and Physiological Roles of Inflammation. *Nature* **2008**, *454* (7203), 428–435. https://doi.org/10.1038/nature07201.

(3) *Indwelling Neural Implants: Strategies for Contending with the In Vivo Environment*; CRC Press, 2007. https://doi.org/10.1201/9781420009309.

(4) Ansar, W.; Ghosh, S. C-Reactive Protein: A Clinical Marker in Cardiovascular Disease. In *Biology of C Reactive Protein in Health and Disease*; Ansar, W., Ghosh, S., Eds.; Springer India: New Delhi, 2016; pp 143–165. https://doi.org/10.1007/978-81-322-2680-2_7.

(5) Hannoodee, S.; Nasuruddin, D. N. Acute Inflammatory Response. In *Stat Pearls*; Stat Pearls Publishing: Treasure Island (FL), 2022.

(6) Suzuki, K. Chronic Inflammation as an Immunological Abnormality and Effectiveness of Exercise. *Biomolecules* **2019**, *9* (6), 223. https://doi.org/10.3390/biom9060223.

(7) Chen, L.; Deng, H.; Cui, H.; Fang, J.; Zuo, Z.; Deng, J.; Li, Y.; Wang, X.; Zhao, L. Inflammatory Responses and Inflammation-Associated Diseases in Organs. *Oncotarget* **2017**, *9* (6), 7204–7218. https://doi.org/10.18632/oncotarget.23208.

(8) Pober, J. S.; Sessa, W. C. Inflammation and the Blood Microvascular System. *Cold Spring Harb Perspect Biol* **2015**, *7* (1), a016345. https://doi.org/10.1101/cshperspect.a016345.

(9) Hart, P. H. Regulation of the Inflammatory Response in Asthma by Mast Cell Products. *Immunology & Cell Biology* **2001**, *79* (2), 149–153. https://doi.org/10.1046/j.1440-1711.2001.00983.x.

(10) Rock, K. L.; Kono, H. The Inflammatory Response to Cell Death. *Annu Rev Pathol* **2008**, *3*, 99–126. https://doi.org/10.1146/annurev.pathmechdis.3.121806.151456.

(11) Muller, W. A. Getting Leukocytes to the Site of Inflammation. *Vet Pathol* **2013**, *50* (1), 7–22. https://doi.org/10.1177/0300985812469883.

(12) Shah, K. K.; Pritt, B. S.; Alexander, M. P. Histopathologic Review of Granulomatous Inflammation. *Journal of Clinical Tuberculosis and Other Mycobacterial Diseases* **2017**, *7*, 1–12. https://doi.org/10.1016/j.jctube.2017.02.001.

(13) Bowler, P. G.; Duerden, B. I.; Armstrong, D. G. Wound Microbiology and Associated Approaches to Wound Management. *Clinical Microbiology Reviews* **2001**, *14* (2), 244–269. https://doi.org/10.1128/CMR.14.2.244-269.2001.

(14) McDowell, C.; Farooq, U.; Haseeb, M. Inflammatory Bowel Disease. In *Stat Pearls*; Stat Pearls Publishing: Treasure Island (FL), 2022.

(15) Ng, S. C.; Shi, H. Y.; Hamidi, N.; Underwood, F. E.; Tang, W.; Benchimol, E. I.; Panaccione, R.; Ghosh, S.; Wu, J. C. Y.; Chan, F. K. L.; Sung, J. J. Y.; Kaplan, G. G. Worldwide Incidence and Prevalence of Inflammatory Bowel Disease in the 21st Century: A Systematic Review of Population-Based Studies. *Lancet* **2017**, *390* (10114), 2769–2778. https://doi.org/10.1016/S0140-6736(17)32448-0.

(16) Jairath, V.; Feagan, B. G. Global Burden of Inflammatory Bowel Disease. *The Lancet Gastroenterology & Hepatology* **2020**, *5* (1), 2–3. https://doi.org/10.1016/S2468-1253(19)30358-9.

(17) Olfatifar, M.; Zali, M. R.; Pourhoseingholi, M. A.; Balaii, H.; Ghavami, S. B.; Ivanchuk, M.; Ivanchuk, P.; Nazari, S. hashemi; shahrokh, S.; Sabour, S.; Khodakarim, S.; Aghdaei, H. A.; Rohani, P.; Mehralian, G. The Emerging Epidemic of Inflammatory Bowel Disease in Asia and Iran by 2035: A Modeling Study. *BMC Gastroenterology* **2021**, *21* (1), 204. https://doi.org/10.1186/s12876-021-01745-1.

(18) do Nascimento, R. de P.; da Fonseca Machado, A. P.; Galvez, J.; Cazarin, C. B. B.; Junior, M. R. M. Ulcerative Colitis: Gut Microbiota, Immunopathogenesis and Application of Natural Products in Animal Models. *Life Sciences* **2020**, *258*, 118129.

(19) Tegtmeyer, D.; Seidl, M.; Gerner, P.; Baumann, U.; Klemann, C. Inflammatory Bowel Disease Caused by Primary Immunodeficiencies—Clinical Presentations, Review of Literature, and Proposal of a Rational Diagnostic Algorithm. *Pediatric Allergy and Immunology* **2017**, *28* (5), 412–429. https://doi.org/10.1111/pai.12734.

(20) Hendrickson, B. A.; Gokhale, R.; Cho, J. H. Clinical Aspects and Pathophysiology of Inflammatory Bowel Disease. *Clinical Microbiology Reviews* **2002**, *15* (1), 79–94. https://doi.org/10.1128/CMR.15.1.79-94.2002.

(21) Kaitha, S.; Bashir, M.; Ali, T. Iron Deficiency Anemia in Inflammatory Bowel Disease. World J Gastrointest Pathophysiol 6: 62–72, 2015.

(22) Zonderman, J.; Vender, R. S. *Understanding Crohn Disease and Ulcerative Colitis*; Univ. Press of Mississippi, 2009.

(23) Abdelmegid, A. M.; Abdo, F. K.; Ahmed, F. E.; Kattaia, A. A. A. Therapeutic Effect of Gold Nanoparticles on DSS-Induced Ulcerative Colitis in Mice with Reference to Interleukin-17 Expression. *Sci Rep* **2019**, *9* (1), 10176. https://doi.org/10.1038/s41598-019-46671-1.

(24) Rubin, D. T.; Ananthakrishnan, A. N.; Siegel, C. A.; Sauer, B. G.; Long, M. D. ACG Clinical Guideline: Ulcerative Colitis in Adults. *Official journal of the American College of Gastroenterology | ACG* **2019**, *114* (3), 384–413. https://doi.org/10.14309/ajg.0000000000000152.

(25) Collins, P.; Rhodes, J. Ulcerative Colitis: Diagnosis and Management. *BMJ* **2006**, *333* (7563), 340–343. https://doi.org/10.1136/bmj.333.7563.340.

(26) Ordás, I.; Eckmann, L.; Talamini, M.; Baumgart, D. C.; Sandborn, W. J. Ulcerative Colitis. *The Lancet* **2012**, *380* (9853), 1606–1619. https://doi.org/10.1016/S0140-6736(12)60150-0.

(27) Luo, C.; Zhang, H. The Role of Proinflammatory Pathways in the Pathogenesis of Colitis-Associated Colorectal Cancer. *Mediators of Inflammation* **2017**, *2017*, e5126048. https://doi.org/10.1155/2017/5126048.

(28) Heller, F.; Fuss, I. J.; Nieuwenhuis, E. E.; Blumberg, R. S.; Strober, W. Oxazolone Colitis, a Th2 Colitis Model Resembling Ulcerative Colitis, Is Mediated by IL-13-Producing NK-T Cells. *Immunity* **2002**, *17* (5), 629–638. https://doi.org/10.1016/S1074-7613(02)00453-3.

(29) Tatiya-aphiradee, N.; Chatuphonprasert, W.; Jarukamjorn, K. Immune Response and Inflammatory Pathway of Ulcerative Colitis. *Journal of Basic and Clinical Physiology and Pharmacology* **2019**, *30* (1), 1–10. https://doi.org/10.1515/jbcpp-2018-0036.

(30) Qiu, X.; Zhang, M.; Yang, X.; Hong, N.; Yu, C. Faecalibacterium Prausnitzii Upregulates Regulatory T Cells and Anti-Inflammatory Cytokines in Treating TNBS-Induced Colitis. *Journal of Crohn's and Colitis* **2013**, *7* (11), e558–e568. https://doi.org/10.1016/j.crohns.2013.04.002.

(31) Mishra, R. K.; Selim, A.; Gowri, V.; Ahmad, A.; Nadeem, A.; Siddiqui, N.; Raza, S. S.; Jayamurugan, G.; Khan, R. Thiol-Functionalized Cellulose-Grafted Copper Oxide Nanoparticles for the Therapy of Experimental Colitis in Swiss Albino Mice. *ACS Biomater. Sci. Eng.* **2022**, *8* (5), 2088–2095. https://doi.org/10.1021/acsbiomaterials.2c00124.

(32) Wang, D.; DuBois, R. N. The Role of COX-2 in Intestinal Inflammation and Colorectal Cancer. *Oncogene* **2010**, *29* (6), 781–788. https://doi.org/10.1038/onc.2009.421.

(33) Yang, Y.-P.; Tong, Q.-Y.; Zheng, S.-H.; Zhou, M.-D.; Zeng, Y.-M.; Zhou, T.-T. Anti-Inflammatory Effect of Fucoxanthin on Dextran Sulfate Sodium-Induced Colitis in Mice. *Natural Product Research* **2020**, *34* (12), 1791–1795. https://doi.org/10.1080/14786419.2018.1528593.

(34) Schreiber, O.; Petersson, J.; Waldén, T.; Ahl, D.; Sandler, S.; Phillipson, M.; Holm, L. INOS-Dependent Increase in Colonic Mucus Thickness in DSS-Colitic Rats. *Plos One* **2013**, *8* (8), e71843. https://doi.org/10.1371/journal.pone.0071843.

(35) Korhonen, R.; Lahti, A.; Kankaanranta, H.; Moilanen, E. Nitric Oxide Production and Signaling in Inflammation. *Curr Drug Targets Inflamm Allergy* **2005**, *4* (4), 471–479. https://doi.org/10.2174/1568010054526359.

(36) Zhao, Y.; Lukiw, W. J. Microbiome-Mediated Upregulation of MicroRNA-146a in Sporadic Alzheimer's Disease. *Frontiers in Neurology* **2018**, *9*.

(37) Frank, D. N.; Robertson, C. E.; Hamm, C. M.; Kpadeh, Z.; Zhang, T.; Chen, H.; Zhu, W.; Sartor, R. B.; Boedeker, E. C.; Harpaz, N.; Pace, N. R.; Li, E. Disease Phenotype and Genotype Are Associated with Shifts in Intestinal-Associated Microbiota in Inflammatory Bowel Diseases. *Inflammatory Bowel Diseases* **2011**, *17* (1), 179–184. https://doi.org/10.1002/ibd.21339.

(38) Belkaid, Y.; Hand, T. W. Role of the Microbiota in Immunity and Inflammation. *Cell* **2014**, *157* (1), 121–141. https://doi.org/10.1016/j.cell.2014.03.011.

(39) Meier, J.; Sturm, A. Current Treatment of Ulcerative Colitis. *World J Gastroenterol* **2011**, *17* (27), 3204–3212. https://doi.org/10.3748/wjg.v17.i27.3204.

(40) Chen, J.-H.; Andrews, J. M.; Kariyawasam, V.; Moran, N.; Gounder, P.; Collins, G.; Walsh, A. J.; Connor, S.; Lee, T. W. T.; Koh, C. E.; Chang, J.; Paramsothy, S.; Tattersall, S.; Lemberg, D. A.; Radford-Smith, G.; Lawrance, I. C.; McLachlan, A.; Moore, G. T.; Corte, C.; Katelaris, P.; Leong, R. W.; IBD Sydney Organisation and the Australian Inflammatory Bowel Diseases Consensus Working Group. Review Article: Acute Severe Ulcerative Colitis – Evidence-Based Consensus Statements. *Alimentary Pharmacology & Therapeutics* **2016**, *44* (2), 127–144. https://doi.org/10.1111/apt.13670.

(41) Ye, B.; van Langenberg, D. R. Mesalazine Preparations for the Treatment of Ulcerative Colitis: Are All Created Equal? *World J Gastrointest Pharmacol Ther* **2015**, *6* (4), 137–144. https://doi.org/10.4292/wjgpt.v6.i4.137.

(42) Xu, C.-T.; Meng, S.-Y.; Pan, B.-R. Drug Therapy for Ulcerative Colitis. *World J Gastroenterol* **2004**, *10* (16), 2311–2317. https://doi.org/10.3748/wjg.v10.i16.2311.

(43) Lichtenstein, G. R.; Hanauer, S. B.; Sandborn, W. J. Emerging Treatment Options in Mild to Moderate Ulcerative Colitis. *Gastroenterol Hepatol (N Y)* **2015**, *11* (3 Suppl 1), 1–16.

(44) Carolina, S. F. F. B., PharmD South University School of Pharmacy Columbia, South Carolina Kelly J. Clark, PharmD Department of Pharmacy Practice South University School of Pharmacy Columbia, South. *Overview of TNF Inhibitors for Treating Inflammatory Bowel Disease*. https://www.uspharmacist.com/article/overview-of-tnf-inhibitors-for-treating-inflammatory-bowel-disease (accessed 2022-07-06).

(45) D'Haens, G. Risks and Benefits of Biologic Therapy for Inflammatory Bowel Diseases. *Gut* **2007**, *56* (5), 725–732. https://doi.org/10.1136/gut.2006.103564.

(46) Guslandi, M. Nicotine Treatment for Ulcerative Colitis. *Br J Clin Pharmacol* **1999**, *48* (4), 481–484. https://doi.org/10.1046/j.1365-2125.1999.00039.x.

(47) Sandborn, W. J.; Tremaine, W. J.; Offord, K. P.; Lawson, G. M.; Petersen, B. T.; Batts, K. P.; Croghan, I. T.; Dale, L. C.; Schroeder, D. R.; Hurt, R. D. Transdermal Nicotine for Mildly to Moderately Active Ulcerative Colitis. *Ann Intern Med* **1997**, *126* (5), 364–371. https://doi.org/10.7326/0003-4819-126-5-199703010-00004.

(48) Frizelle, F. A.; Burt, M. J. *Surgical Management of Ulcerative Colitis*; Zuckschwerdt, 2001.

(49) Parray, F. Q.; Wani, M. L.; Malik, A. A.; Wani, S. N.; Bijli, A. H.; Irshad, I.; Nayeem-Ul-Hassan. Ulcerative Colitis: A Challenge to Surgeons. *Int J Prev Med* **2012**, *3* (11), 749–763.

(50) Fedorak, R. N. Probiotics in the Management of Ulcerative Colitis. *Gastroenterol Hepatol (N Y)* **2010**, *6* (11), 688–690.

(51) Borody, T. J.; Brandt, L. J.; Paramsothy, S. Therapeutic Faecal Microbiota Transplantation: Current Status and Future Developments. *Curr Opin Gastroenterol* **2014**, *30* (1), 97–105. https://doi.org/10.1097/MOG.0000000000000027.

(52) Hanai, H.; Iida, T.; Takeuchi, K.; Watanabe, F.; Maruyama, Y.; Andoh, A.; Tsujikawa, T.; Fujiyama, Y.; Mitsuyama, K.; Sata, M.; Yamada, M.; Iwaoka, Y.; Kanke, K.; Hiraishi, H.; Hirayama, K.; Arai, H.; Yoshii, S.; Uchijima, M.; Nagata, T.; Koide, Y. Curcumin Maintenance Therapy for Ulcerative Colitis: Randomized, Multicenter, Double-Blind, Placebo-Controlled Trial. *Clinical Gastroenterology and Hepatology* **2006**, *4* (12), 1502–1506. https://doi.org/10.1016/j.cgh.2006.08.008.

(53) Pham, A. Q.; Doan, A.; Andersen, M. Pyrazinamide-Induced Hyperuricemia. *P T* **2014**, *39* (10), 695–715.

(54) Curkovic, I.; Egbring, M.; Kullak-Ublick, G. A. Risks of Inflammatory Bowel Disease Treatment with Glucocorticosteroids and Aminosalicylates. *DDI* **2013**, *31* (3–4), 368–373. https://doi.org/10.1159/000354699.

(55) Singh, A.; Mahajan, R.; Kedia, S.; Dutta, A. K.; Anand, A.; Bernstein, C. N.; Desai, D.; Pai, C. G.; Makharia, G.; Tevethia, H. V.; Mak, J. W.; Kaur, K.; Peddi, K.; Ranjan, M. K.; Arkkila, P.; Kochhar, R.; Banerjee, R.; Sinha, S. K.; Ng, S. C.; Hanauer, S.; Verma, S.; Dutta, U.; Midha, V.; Mehta, V.; Ahuja, V.; Sood, A. Use of Thiopurines in Inflammatory Bowel Disease: An Update. *Intest Res* **2022**, *20* (1), 11–30. https://doi.org/10.5217/ir.2020.00155.

(56) Shivaji, U. N.; Sharratt, C. L.; Thomas, T.; Smith, S. C. L.; Iacucci, M.; Moran, G. W.; Ghosh, S.; Bhala, N. Review Article: Managing the Adverse Events Caused by Anti-TNF Therapy in Inflammatory Bowel Disease. *Aliment Pharmacol Ther* **2019**, *49* (6), 664–680. https://doi.org/10.1111/apt.15097.

(57) Shin, T.; Okada, H. Infertility in Men with Inflammatory Bowel Disease. *World J Gastrointest Pharmacol Ther* **2016**, *7* (3), 361–369. https://doi.org/10.4292/wjgpt.v7.i3.361.

(58) Schwartz, D. M.; Kanno, Y.; Villarino, A.; Ward, M.; Gadina, M.; O'Shea, J. J. JAK Inhibition as a Therapeutic Strategy for Immune and Inflammatory Diseases. *Nat Rev Drug Discov* **2017**, *16* (12), 843–862. https://doi.org/10.1038/nrd.2017.201.

(59) Zhang, M.; Merlin, D. Nanoparticle-Based Oral Drug Delivery Systems Targeting the Colon for Treatment of Ulcerative Colitis. *Inflammatory Bowel Diseases* **2018**, *24* (7), 1401–1415. https://doi.org/10.1093/ibd/izy123.

(60) Song, R.; Murphy, M.; Li, C.; Ting, K.; Soo, C.; Zheng, Z. Current Development of Biodegradable Polymeric Materials for Biomedical Applications. *Drug Des Devel Ther* **2018**, *12*, 3117–3145. https://doi.org/10.2147/DDDT.S165440.

(61) Sohail, M.; Mudassir; Minhas, M. U.; Khan, S.; Hussain, Z.; de Matas, M.; Shah, S. A.; Khan, S.; Kousar, M.; Ullah, K. Natural and Synthetic Polymer-Based Smart Biomaterials for Management of Ulcerative Colitis: A Review of Recent Developments and Future Prospects. *Drug Deliv. and Transl. Res.* **2019**, *9* (2), 595–614. https://doi.org/10.1007/s13346-018-0512-x.

(62) Onaciu, A.; Munteanu, R. A.; Moldovan, A. I.; Moldovan, C. S.; Berindan-Neagoe, I. Hydrogels Based Drug Delivery Synthesis, Characterization and Administration. *Pharmaceutics* **2019**, *11* (9), 432. https://doi.org/10.3390/pharmaceutics11090432.

(63) Liechty, W. B.; Kryscio, D. R.; Slaughter, B. V.; Peppas, N. A. Polymers for Drug Delivery Systems. *Annu Rev Chem Biomol Eng* **2010**, *1*, 149–173. https://doi.org/10.1146/annurev-chembioeng-073009-100847.

(64) Costas, L.; Pera, L. M.; López, A. G.; Mechetti, M.; Castro, G. R. Controlled Release of Sulfasalazine Release from "Smart" Pectin Gel Microspheres under Physiological Simulated Fluids. *Appl Biochem Biotechnol* **2012**, *167* (5), 1396–1407. https://doi.org/10.1007/s12010-012-9615-x.

(65) Wang, Q.-S.; Wang, G.-F.; Zhou, J.; Gao, L.-N.; Cui, Y.-L. Colon Targeted Oral Drug Delivery System Based on Alginate-Chitosan Microspheres Loaded with Icariin in the Treatment of Ulcerative Colitis. *International Journal of Pharmaceutics* **2016**, *515* (1), 176–185. https://doi.org/10.1016/j.ijpharm.2016.10.002.

(66) Xiao, B.; Laroui, H.; Ayyadurai, S.; Viennois, E.; Charania, M. A.; Zhang, Y.; Merlin, D. Mannosylated Bioreducible Nanoparticle-Mediated Macrophage-Specific TNF-α RNA Interference for IBD Therapy. *Biomaterials* **2013**, *34* (30), 7471–7482. https://doi.org/10.1016/j.biomaterials.2013.06.008.

(67) Poh, S.; Lin, J. B.; Panitch, A. Release of Anti-Inflammatory Peptides from Thermosensitive Nanoparticles with Degradable Cross-Links Suppresses Pro-Inflammatory Cytokine Production. *Biomacromolecules* **2015**, *16* (4), 1191–1200. https://doi.org/10.1021/bm501849p.

(68) Ahmad, A.; Ansari, Md. M.; Mishra, R. K.; Kumar, A.; Vyawahare, A.; Verma, R. K.; Raza, S. S.; Khan, R. Enteric-Coated Gelatin Nanoparticles Mediated Oral Delivery of 5-Aminosalicylic Acid Alleviates Severity of DSS-Induced Ulcerative Colitis. *Materials Science and Engineering: C* **2021**, *119*, 111582. https://doi.org/10.1016/j.msec.2020.111582.

(69) Yang, C.; Merlin, D. Nanoparticle-Mediated Drug Delivery Systems For The Treatment Of IBD: Current Perspectives. *Int J Nanomedicine* **2019**, *14*, 8875–8889. https://doi.org/10.2147/IJN.S210315.

(70) Katsuma, M.; Watanabe, S.; Kawai, H.; Takemura, S.; Masuda, Y.; Fukui, M. Studies on Lactulose Formulations for Colon-Specific Drug Delivery. *International Journal of Pharmaceutics* **2002**, *249* (1), 33–43. https://doi.org/10.1016/S0378-5173(02)00429-5.

(71) Peer, D.; Park, E. J.; Morishita, Y.; Carman, C. V.; Shimaoka, M. Systemic Leukocyte-Directed SiRNA Delivery Revealing Cyclin D1 as an Anti-Inflammatory Target. *Science* **2008**, *319* (5863), 627–630. https://doi.org/10.1126/science.1149859.

(72) Si, X.-Y.; Merlin, D.; Xiao, B. Recent Advances in Orally Administered Cell-Specific Nanotherapeutics for Inflammatory Bowel Disease. *World J Gastroenterol* **2016**, *22* (34), 7718–7726. https://doi.org/10.3748/wjg.v22.i34.7718.

(73) Wu, Y.; Sun, M.; Wang, D.; Li, G.; Huang, J.; Tan, S.; Bao, L.; Li, Q.; Li, G.; Si, L. A PepT1 Mediated Medicinal Nano-System for Targeted Delivery of Cyclosporine A to Alleviate Acute Severe Ulcerative Colitis. *Biomater. Sci.* **2019**, *7* (10), 4299–4309. https://doi.org/10.1039/C9BM00925F.

(74) Mishra, R. K.; Ahmad, A.; Kumar, A.; Vyawahare, A.; Raza, S. S.; Khan, R. Lipid-Based Nanocarrier-Mediated Targeted Delivery of Celecoxib Attenuate Severity of Ulcerative Colitis. *Materials Science and Engineering: C* **2020**, *116*, 111103. https://doi.org/10.1016/j.msec.2020.111103.

(75) Zeeshan, M.; Ali, H.; Khan, S.; Mukhtar, M.; Khan, M. I.; Arshad, M. Glycyrrhizic Acid-Loaded PH-Sensitive Poly-(Lactic-Co-Glycolic Acid) Nanoparticles for the Amelioration of Inflammatory Bowel Disease. *Nanomedicine* **2019**, *14* (15), 1945–1969. https://doi.org/10.2217/nnm-2018-0415.

Chapter 2

Materials & Methods

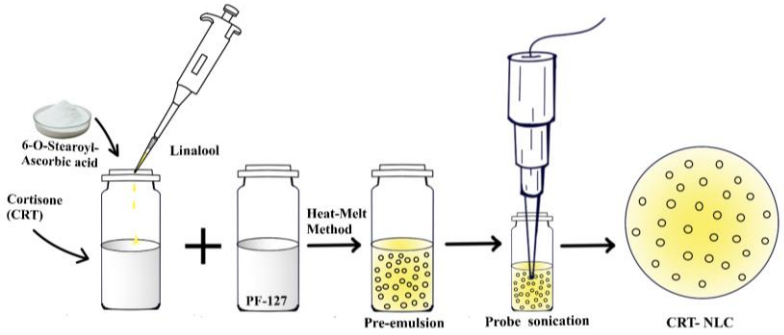
6-O-Stearoyl-
Ascorbic acid
Linalool
Cortisone
(CRT)
PF-127
Heat-Melt
Method
Pre-emulsion
Probe sonication
CRT- NLC

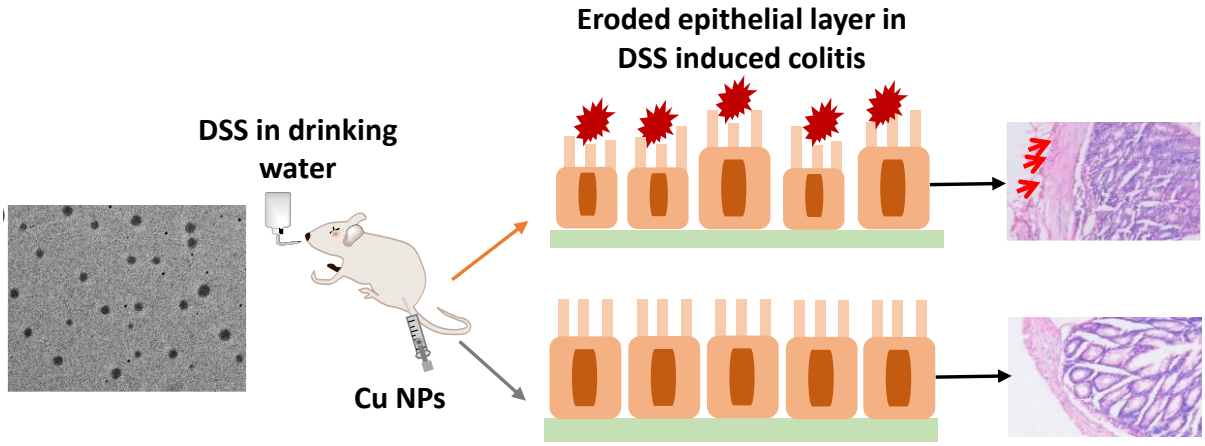
Eroded epithelial layer in
DSS induced colitis
DSS in drinking
water
Cu NPs
Recovered colon
epithelium after
treatment

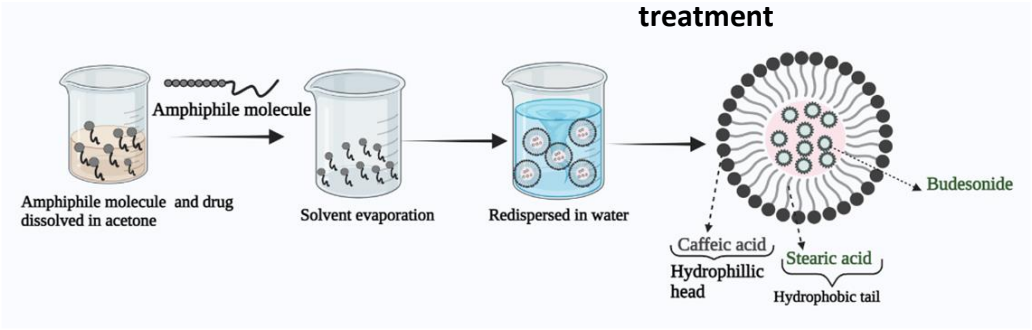
Amphiphile molecule
Amphiphile molecule and drug
dissolved in acetone
Solvent evaporation
Redispersed in water
Budesonide
Caffeic acid
Hydrophillic
head
Stearic acid
Hydrophobic tail

2. Materials and Methods

All of the chemical reagents and techniques utilised in this thesis are described in details in this section. All the studies implicate a combination of formulation methodologies, physical, chemical, spectroscopic and biological characterization approaches. Following sections give meticulous detail of materials and methods employed herein. Further, description has been provided wherever required essential in next chapters.

2.1 Materials

Table 2.1 Used chemicals, Softwares and instruments.

Reagents	Source	Identifier
Chemicals, reagents and solvents		
Alcian blue	Alfa Aesar Chemicals	Cat # 33864-99-2
Anti- iNOS antibody (Rabbit polyclonal)	Invitrogen	Cat # PA5-16524
Anti- COX-2 antibody (Rabbit polyclonal)	Invitrogen	
Bovine serum albumin (BSA)	Himedia laboratories	Cat # 9048-46-8
Budesonide	TCI	Cat # B-3909
Caffeic acid	TCI	Cat # C-0002
Celecoxib	TCI	Cat # C-2816
Cortisone	TCI	Cat # C-1317
Dichloromethane (DCM)	Merck Millipore	Cat # 75092
Dimethyl sulfoxide (DMSO)	Merck Millipore	Cat # 102952
DPX mounting media	Himedia laboratories	Cat # GRM655-500G
Eosin	Himedia laboratories	Cat # 17372-87-1
Ethanol	Merck Millipore	Cat # 64-17-5
Ethylenediamine	TCI	Cat # E-0077
EDC (1-ethyl-3-(3-	Himedia	Cat # 18-17-5

dimethylaminopropy) carbodiimide		
Ethylene diamine tetra-acetic acid (EDTA)	Himedia laboratories	Cat # 60-00-4
Fecal occult blood test kit	Coral chemical system	1108020050
Formic acid	Himedia laboratories	Cat # 64-18-6
Glacial acetic acid	Himedia laboratories	Cat # 64-19-7
Geraniol	TCI	Cat # G-0027
Griess Reagent	Himedia laboratories	Cat # 215-981-2
Glyceryl monostearate	TCI	Cat # G-0085
Hematoxylin	Himedia laboratories	Cat # 517-28-2
HRP-conjugated secondary antibody	Invitrogen	Cat # G-21040
Hydrogen peroxide (H_2O_2)	Himedia laboratories	Cat # 7722-84-1
Linalool	TCI	Cat # L-0048
MTT (3-[4, 5-dimethylthiazol-2-yl]-2, 5 diphenyl tetrazolium bromide)	Himedia laboratories	Cat # 298-93-1
N-Hydroxysuccinimide (NHS)	TCI	Cat # B-0249
Nitrobluetetrazolium (NBT)	Himedia laboratories	Cat # 298-83-9
N-methoxysuccinyl-Ala-Ala-Pro-Val p-nitroanilide	Himedia laboratories	Cat # 70967-90-7
Neutral red	Himedia laboratories	Cat # 553-24-2
6-O-Stearoyl-L-ascorbic Acid	TCI	Cat # A-0617
Paraformaldehyde	Himedia laboratories	Cat # 30525-89-4
Pluronic F-127	Sigma Aldrich	Cat # 9003-11-6

Potassium Chloride (KCl)	Himedia laboratories	Cat # 7447-40-7
Potassium phosphate buffer pH 7.0	Himedia laboratories	Cat # 7778-77-0
Stearic acid	TCI	Cat # S-0163
Sodium Chloride (NaCl)	Himedia laboratories	Cat # 7647-14-5
Thiobarbituric acid (TBA)	Sigma Aldrich	Cat # 504-17-6
Trichloroacetic acid (TCA)	Sigma Aldrich	Cat # 76-03-9
Tris–HCl buffer, (pH 8.0)	Himedia laboratories	Cat # ML013-100ML
3, 3'-diaminobenzidine (DAB)	Himedia laboratories	Cat # 91-95-2
5-5'dithio-bis-2-nitrobenzoicacid (DTNB)	Himedia laboratories	Cat # 69-78-3
Others		
Carbon coated 300 mesh copper grids	Beta Tech Equipment Pvt. Ltd., India	
Culture plates (96-well)	Thermo Fisher Scientific	Cat # 95029330
Disposable folded capillary cell zeta potential cuvettes	Malvern Instruments (Malvern Panalytical)	Cat # DTS1070
Dialysis Membrane-70 (12–14 kDa molecular weight cut off)	HiMedia Laboratories Pvt. Ltd., India	Cat # 68035
EZcount™ MTT Cell Assay Kit	(Himedia)	Cat # CCK003
Swiss albino mice (20-25 gm), 4-6 weeks old	Indian Institute of toxicological research Indian Institute of toxicological research	---
hTERT-immortalized normal	Dr. Robert Weinberg	---

human foreskin fibroblasts (BJ) cells	(MIT Ludwig Center for Molecular Oncology, MIT, Cambridge)	
Silicon wafer	(Ekta Marketing Corporation, India)	Cat # 7440-21-3
Square disposable polystyrene cuvettes (12 mm)	Malvern Instruments (Malvern Panalytical)	Cat # DTS0012

Softwares		
Adobe Illustrator CS6	Adobe System, Inc. USA	https://www.adobe.com/products/illustrator/free-trial-download.html
GraphPad Prism 5.0	GraphPad Software Inc.	https://www.graphpad.com
Nanoscope	Nanoscale world, Bruker, USA	http://nanoscaleworld.bruker-axs.com/nanoscaleworld/forums/t/812.aspx
Origin 8.6	Origin Lab, USA	https://www.originlab.com

Instruments		
Atomic Force Microscopy	Bruker Multimode 8 scanning probe	Bruker, USA
Confocal Laser Scanning Microscope	LSM 880 Confocal microscope	Carl Zeiss AG, Germany

Dynamic light scattering	Nano-ZSP	Malvern, UK
Fourier Transform Infrared Spectroscopy	Cary Agilent 660 IR	Agilent technology
High speed centrifuge	Eppendorf	Hamburg, Germany
Incubator	Eppendorf	Hamburg, Germany
Microtiter Multimode plate reader	Biotek-EonTM	Vermont, USA
Scanning Electron Microscopy	JSM-IT300	JEOL, Japan
Table top centrifuge	Avanti JXN-26,	Beckman Coulter
Transmission Electron Microscopy	JEM 2100	JEOL, Japan
UV-Vis spectrometer	Cary 60 UV	Double Beam Agilent technology
X-ray Diffraction	Bruker ECO D8	Bruker, US
Gel permeation chromatography	CBM-20Alite	Shimadzu, Japan

2.2 Methods

2.2.1 Development of various nanoformulations

2.2.1.1 Formulation of celecoxib loaded nanostructured lipid carriers

The nanostructured lipid carrier (NLC) was prepared according to the protocol of Muller et al.[1] Briefly, glyceryl monostearate (GMS) and geraniol were mixed in 1% w/v and melted above 10°C of their melting points in 70:30 ratio. The aqueous surfactant PF-127 1% w/v was dissolved in distilled water at same temperature. The aqueous phase was incorporated slowly into oil phase over constant stirring of 1500 rpm and kept for 2 hours. After milky emulsion was appeared, it was

sonicated using probe sonicator for 10 minutes (5 seconds on and 5 seconds off cycle at 40 Hz frequency). Same procedure was followed for EUD S100-coated CLX-loaded NLC preparation by taking 1:10 drug and lipid ratio. Prepared NLC was lyophilized and kept for further characterization.

2.2.1.2 Formulation of Eudragit S100-coated NLCs

The enteric coating solution was prepared by dissolving 12% w/v Eudragit S100 (EUD S 100) into acetone. Freshly prepared blank as well as CLX-loaded NLC were separately poured drop by drop into the enteric coating solution (EUD S 100) over constant stirring for 6 hr. Lipid and EUD S100 was taken in 1:1 ratio. Blank EUD S100-coated NLC as well as EUD S100-coated CLX-loaded NLC were finally prepared after coating solvent was evaporated under vacuum evaporator. Prepared NLC was lyophilized and kept for further characterization and biological studies.[2]

2.2.1.3 Formulation of cortisone loaded stearoyl ascorbic acid (SAA NLCs)

Blank and cortisone loaded nanostructured lipid carriers (NLCs) were prepared by following the protocol of Muller et al.[3] Solid lipid, 6-0-stearoyl ascorbic acid (SAA) and liquid lipid, linalool was mixed together and melted to a clear texture. The aqueous emulsifier PF-127 was dissolved in distilled water at same temperature. Both the phases were mixed together till the appearance of milky emulsion. The pre-emulsion was probe sonicated for 10 minutes (at 40 Hz frequency using 5 seconds on and 5 seconds off cycle).

2.2.1.4 Synthesis of thiol-functionalized cellulose grafted copper oxide nanoparticles (C-$Cu^{I/II}O$ NPs)

Copper oxide nanoparticles ($Cu^{I/II}O$ NPs) supported by thiol functionalized cellulose was synthesized in two steps starting from microcrystalline cellulose (MCC). Following the reported procedures, cellulose (MCC) was treated with thioglycolic acid (S) catalyzed by *p*-toluene sulphonic acid (*p*-TsOH) to provide thiol functionalized cellulose (C-SH).[4] The second step was the treatment of ethanolic solution of $CuCl_2$ with the aqueous solution of thiol-functionalized cellulose as

described in the previously published paper[5] to produce $Cu^{I/II}O$ NPs which is discussed in the 2.2. as shown in Scheme 1.

The freshly prepared thiol-functionalized cellulose C-SH (330 mg) was dissolved in deionized (DI) water (20 mL) with the help of ultrasonication for 5 min at 20 °C to make a homogenous solution. With the help of filtration using low-cost cotton rag pulp paper a portion (30–40%) of insoluble cellulose part was discarded, only the homogenously dispersed solution of C-SH filtrate was added slowly an ethanolic solution of $CuCl_2$ (30 mg, 3 mL). Then the resulting mixture was stirred for 10 min at room temperature (25 °C). The colour of the reaction mixture's deep black/brown was changed to colourless followed by the addition of the ethanolic solution of $CuCl_2$ to the aqueous solution of C-SH. After that, the transparent homogeneous solution was solidified by using freeze-dried technique.

2.2.1.5 Formulation of caffeic acid conjugated nanomicelle

2.2.1.5.1 Activation of stearic acid and caffeic acid

Activation of Stearic acid (SA) was performed following the protocol of Chen et al.[6] with slight modification. Briefly, 500 mg SA was dissolved in dimethylformamide at ice cooled water bath. To this solution specified amount of EDC and NHS were added and kept the reaction for 1 h at 0°C under nitrogen atmosphere. Then reaction was continued for 24 h at room temperature. Product was collected by solvent evaporation.

Similarly, Caffeic acid (CA) activation was performed by dissolving 250 MG CA in 10 ml ethanolic aqueous solution (1:1 v/v) and then added specified amount of EDC and NHS. The resulting mixture was stirred for 1 h under ice water bath, then reaction was continued for 24 h at room temperature. Activated CA was collected by evaporating the solvent.[7]

2.2.1.5.2 Synthesis of SA and CA conjugated amphiphile

Specified amount of activated SA and ethylenediamine conjugated CA was added in ethanol and stirred at 80°C for 24 h under reflux. Conjugated product

was collected after solvent evaporation and lyophilized to make powder. Dialysis was performed over 48 hours to minimized the impurities form SA and CA conjugated amphiphile.

2.2.1.5.3 Formulation of caffeic acid conjugated budesonide loaded nanomicelle

Blank and budesonide-loaded micelle was developed by solvent evaporation method using the methodology of Ameli et al.[8] Previously synthesized amphiphile and budesonide was dissolved in acetone. Then distilled water was added slowly for self-assembly of amphiphile and micelle formation. Presuspension was stirred at 1500 rpm for 6 hours followed by solvent evaporation. Hence, prepared micelle was kept for characterizations and further experimentations.

2.2.2 Characterization of nanoformulations

2.2.2.1 Hydrodynamic diameter (particle size) by dynamic light scattering

In 12 mm square disposable polystyrene cuvettes, the mean hydrodynamic diameter (particles size) and polydispersity index (PDI) measurement of nanoformulations were measured using the dual angle dynamic light scattering (DLS) technique (Photon Correlation Spectroscopy; Malvern Instrument Ltd. Worcestershire, UK) (DTS0012; Malvern). A sample of 1 ml of nanoformulations is obtained, placed in disposable cuvettes with an optical path length of 10 mm, and measured. In a particle size distribution diagram, the y-axis represents the percentage and the 'x' axis displays hydrodynamic diameter. At room temperature, measurements were carried out in triplicate, and the average of three separate observations was reported as the average particle size.[9]

2.2.2.2 Zeta potential measurements

By employing the Phase Analysis Light Scattering (PALS) technique with palladium electrodes at 25°C, the Zetasizer Nano ZSP; Model-ZEN5600; Malvern Instruments Ltd, Malvern, UK, measured the zeta-potential of nanoformulations in disposable folding capillary cells (Model-DTS1070; Malvern). The average of three

independent observations was used to calculate the average zeta-potential for experiments that were carried out in triplicate.[10]

2.2.2.3 Scanning electron microscopy

The particle size and surface morphology of nanoformulations were examined by scanning electron microscopy (SEM). For SEM imaging, freshly prepared nanoformulations were diluted sufficiently in double filtered ultrapure type-1 (Milli-Q) water. Samples were drop casted onto a previously cleaned silicon wafer and then dried under vacuum desiccator to prevent any type of contaminations. Drop casted samples were gold coated inside an auto fine coater (JEOL JEC-3000FC; Tokyo, Japan) for 150 sec each at 30 Pascal's. Gold coating was performed to deposit a thin conductive metallic layer on the NLC. Morphology of nanoparticles was then explored using a with JEOL JSM-7600F field emission scanning electron microscope Tokyo, Japan. The accelerating voltage was kept at 20 kV.[11,12]

2.2.2.4 Transmission electron microscopy

To confirm the size and morphology of nanoformulations, we have also performed transmission electron microscopy (TEM), one drop of the diluted nanoformulations were drop casted onto a carbon-coated 300 mesh copper grid (Ted Pella Inc.) and incubated for 30 min for proper adsorption followed by negative staining with uranyl acetate (1%) for 30 sec and then washed it with Milli-Q water. The remaining solution was removed by absorbing filter paper. Sample-loaded grids were then placed inside the vacuum desiccator for overnight drying and were viewed under a tungsten filament at 120 kV using a JEOL JEM-2100 transmission electron microscope (Tokyo, Japan). Transmission electron micrographs were digitally recorded and processed using the camera software Gatan.[13]

2.2.2.5 Atomic force microscopy

For the acquisition of atomic force microscopic (AFM) images, freshly prepared NLC was diluted in double filtered ultrapure type-1 Milli-Q water. It was

drop casted onto a previously cleaned silicon wafer. Sample drop casted silicon wafers were air dried. Imaging of the sample at room temperature and ambient atmosphere were carried out in tapping mode using an AFM (NanoScope 9.1, Bruker Multimode 8).[14,15]

2.2.2.6 Attenuated total reflectance - Fourier transform infrared spectroscopy

The fourier transform infrared (FTIR) spectra of drugs/chemical conjugates/nanoformulations was captured. Spectra of individual components and formulations were recorded in the range of 4000-400 cm^{-1} on 64 scans at 4^{-cm} using Cary Agilent 660 IR spectrophotometer. Software Origin Pro 32-bit Version 8.6 was used to analyse the FTIR spectrum.[16]

2.2.2.7 X-ray diffraction

The D-8 advanced ECO D8 diffractometer (Bruker, Germany), nickel-filtered with Cu K radiation (λ = 1.54060 Å), with a scanning range between 2θ = 5° and 90° at room temperature, at a voltage of 40 kV and a current of 25 mA, was used to analyze dried powdered samples of drugs or nanoformulations for X-ray diffraction (XRD). Powder was placed on a glass sample holder with zero background in order to conduct the analysis, and the wide-angle X-ray diffraction pattern was measured.[17]

2.2.2.8 Ultraviolet-visible spectrophotometry

In UV-Vis, a quartz cell with a 1 cm path length and a 1 nm bandwidth was employed. To determine the concentration of loaded drugs in nanoformulations and unloaded drugs still present in the supernatant, a standard curve of corresponding drugs was plotted. By using a UV-VIS spectrophotometer (Shimadzu UV-2600) at the appropriate wavelengths (celecoxib at 252 nm, budesonide at 246 nm, and cortisone at 242 nm), or in a specific UV range, UV-Visible analysis was carried out.[18]

2.2.2.9 Differential scanning calorimetry (DSC)

Calorimetric study of NLC has been done using DSC Perkin Elmer (STA8000) system. DSC of blank NLC, cortisone and drug loaded NLC were performed at temperature range from 50°C to 300°C with scan rate of 10°C/min.[19]

2.2.2.10 Nuclear magnetic resonance (NMR)

On the Bruker Advance-II spectrometer, ^{1}H NMR of several samples was performed at 400 MHz in certain solvents. Tetramethylsilane (TMS) was retained as an internal reference while the chemical changes were measured in parts per million. All chemical conjugates/samples were dissolved in specific deuterated solvents and NMR spectra were carried out.[20]

2.2.2.11 Gel permeation chromatography (GPC)

GPC of amphiphile was done (OMNISEC Malvern Panalytical Spectris) by dispersing the synthesized amphiphile in tetrahydrofuran (THF) with a concentration of 4mg/ml. The flow rate of solvent was maintained 1ml/min.[21]

2.2.2.12 Determination of drug loading capacity and encapsulation efficiency

For encapsulation efficiency (EE) and drug loading (DL), calibration curve of loaded drug was plotted by preparing 1 mg/ml stock solution of corresponding drug in PBS (pH 7.4) or specific solvents. Serial dilutions of stock solution were prepared and absorbance was read under UV-Vis spectrophotometer (Shimadzu UV-2600) between the wavelength range 200-600 nm. Following successful formulation, these were centrifuged at 15000 rpm for 30 min, and the supernatant was examined spectrophotometrically by UV-Visible spectroscopy to determine the amount of loaded and unloaded drugs in the nanoformulations. Drug loading and entrapment efficiency was calculated using following formula:[2]

$$\text{Amount of drug loaded in formulation} = \text{Total amount of drug added} - \text{drug present in supernatant}$$

$$EE\ (\%) = \frac{Amount\ of\ drug\ in\ formulation}{Total\ amount\ of\ formulation\ taken} X100$$

$$DL\ (\%) = \frac{Amount\ of\ drug\ in\ formulation}{Total\ amount\ of\ formulation\ used} X100$$

2.2.2.13 *In-Vitro* drug release

By using the dialysis bag method, the release behaviour of drugs from nanoformulations was investigated at 37ºC in various physiological solutions, including 0.1 M HCL (pH 2.0), KH2PO4 buffer (pH 4.5), and phosphate buffer saline (PBS) (pH 7.4). These buffers were used to analyse the increasing drug release from nanoformulations. Drug loaded and lyophilized nanoformulations were taken in 2 ml of PBS and kept in previously activated 5 cm long dialysis bag suspended in 100 ml of PBS and for continuous stirring at a speed of 80 to 100 rpm at 37 °C. To maintain sink conditions, 1 ml of release media was taken at specified time periods of 0.25, 0.5, 1, 2, 4, 8, 12, 24 and 48 h and the same volume of fresh PBS was added each time. The UV-Vis spectrophotometer was used to measure the amount of drug released from the drug-loaded nanoformulations at the corresponding wavelengths.[22–24]

2.2.3 *In-Vitro* studies

2.2.3.1 Cytocompatibility of nanoformulations

To determine the cytocompatibility of blank formulations, MTT (3-[4, 5-dimethylthiazol-2-yl]-2, 5 diphenyl tetrazolium bromide) assay was performed against hTERT-immortalized normal human foreskin fibroblasts (BJ) cells. Cells were seeded in 96-well culture plate at a density of 4000 cells/wells. After 24 hours of seeding, the cells were treated with blank formulations at different concentrations for 24 h. The concentration gradient of nanocarrier was selected and set according to previously established studies. After completion of the treatment time, MTT solution was added in each well and incubated for 3-4 h. Formazan crystals were solubilized

using 100 µL solubilization buffer. Then, using the EZcount™ MTT Cell Assay Kit (Himedia) in accordance with the manufacturer's instructions, the viability of the cells was assessed. Plates were then re-incubated for 4-6 hours after incorporation of the MTT solution. Formazan crystals were solubilized using 100 µL solubilization buffer. Absorbance was taken at 590 and 630 nm with ELISA plate reader to estimate % cell viability was calculated against control cells (without treatment) taken as 100% viable.[24,25]

2.2.3.2 *In-Vitro* nitrite (NO) estimation

Anti-inflammatory potential of various drug loaded formulations in the terms of inhibition of nitrite production against LPS (1µg/ml) treated RAW 264.7 cells were estimated using Griess reagent (1% sulphanilamide and 0.1 napthylethelenediamine dihydrochloride) method.[26,27]

2.2.4 *In-Vivo* efficacy studies against DSS induced colitis models

2.2.4.1 Experimental animal ethical statement

Male/Female albino mice (20-25 g), 4-6 weeks old were purchased from Central Animal House Facility of Indian Institute of Toxicology Research (CSIR-IITR), Lucknow. Mice were kept in animal house of Era`s Medical College under an ambient condition of 25 ± 1 °C with 12-hour light /dark cycles for acclimatization of about 1 week. They had free access of standard rodent chew diet and water ad libitum. All procedures for using experimental animals were permitted by "Institutional Animal Ethics Committee (IAEC)" of Era's Lucknow Medical College and Hospital (ELMCH) that is fully accredited by the Committee for Purpose of Control and Supervision on Experimental Animals (CPCSEA) Chennai, India.

2.2.4.2 Induction of colitis in Swiss albino mice

To induce colitis in Swiss albino mice, 4% w/v DSS (Dextran sodium sulfate) was added in drinking water and given ad libitum to mice.[28] Colonic inflammation was evaluated 5 days after DSS administration. Colitis was confirmed by observing the mice for physical activity, stool consistency and rectal bleeding.

2.2.4.3 Treatment of colitis induced mice with EUD S100-coated celecoxib-loaded NLCs

2.2.4.3.1 Study groups and treatment regimen

To study the effectiveness of CLX loaded NLC against DSS induced colitis model 30 male albino mice were randomly divided into 5 groups of 6 animals each.[2]

Group I (Normal control): Mice received basal diet.

Group II (DSS): served as DSS induced colitis group and mice received 4% DSS in drinking water ad libitum for 5 days.

Group III (DSS + CLX): DSS induced colitis mice, treated with CLX suspended in 0.5 % CMC at dose of 10 mg/kg body weight p.o. after induction of colitis for 7 days.

Group IV (DSS + EUD S100-coated CLX-loaded NLC): DSS induced colitis mice, treated with equivalent dose of EUD S100-coated CLX-loaded NLC in 0.5 % CMC p.o. after induction of colitis for 7 days.

Group V (Blank EUD S100-coated NLC): Normal mice treated with equivalent dose of blank Eud S100-coated NLC in 0.5 % CMC p.o. for 7 days.

2.2.4.4 Treatment of colitis induced mice with cortisone-loaded SAA NLCs

2.2.4.4.1 Study groups and treatment regimen

Therapeutic efficacy of CRT (Cortisone) loaded SAA NLC was evaluated on colitis induced male albino mice whereas 36 animals were divided in 6 groups which contain 6 animals in each group. Study and dosing were performed following previously optimized schedule.[29]

Group I (Normal control): Healthy mice fed with free access of basal diet.

Group II (DSS): Diseased group in which mice received 4% DSS in drinking water for 5 days.

Group III (DSS + CRT): Diseased mice treated with 25 mg/kg body weight dose of cortisone in 0.5% CMC intrarectally for 7 days.

Group IV (DSS + CRT loaded NLC): Diseased mice treated with 25 mg/kg body weight equivalent dose of CRT loaded NLC in 0.5% CMC intrarectally for 7 days.

Group V (DSS + Blank): Diseased mice treated with 25 mg/kg body weight equivalent dose of blank NLC in 0.5% CMC intrarectally for 7 days.

Group VI (Safety): Healthy mice treated with 25 mg/kg body weight equivalent dose of blank NLC in 0.5% CMC intrarectally for 7 days.

2.2.4.5 Treatment of colitis induced mice with copper oxide nanoparticles (C-$Cu^{I/II}O$ NPs)

2.2.4.5.1 Study groups and treatment regimen

To evaluate the efficacy of C-$Cu^{I/II}O$ NPs against dextran sulphate sodium (DSS) induced colitis, 36 male albino mice were randomly divided into 6 animals each in 6 groups and followed our previously optimized dosing schedule.[29]

Group 1 (Normal control): Mice of this group fed with basal diet and vehicle control.

Group 2 (DSS): DSS group where mice received 4% DSS in drinking water for 5 days and have free access to water all the time.

Group 3 (DSS + C-$Cu^{I/II}O$ NPs 1): Colitis induced mice treated with C-$Cu^{I/II}O$ NPs (in 0.5 % carboxymethyl cellulose suspension) at dose of 10 mg/kg b. wt. intrarectally after induction of disease for 7 days.

Group 4 (DSS + C-$Cu^{I/II}O$ NPs 2): Colitis induced mice treated with C-$Cu^{I/II}O$ NPs (in 0.5 % carboxymethyl cellulose suspension) at dose of 40 mg/kg b. wt. intrarectally after induction of disease for 7 days.

Group 5 (DSS + 5-aminosalicyclic acid): In this group, 5-aminosalicylic acid was used as a positive control and colitis induced mice treated with 5-aminosalicylic acid (in 0.5 % carboxymethyl cellulose suspension) at dose of 40 mg/kg b. wt. intrarectally after induction of disease for 7 days.

Group 6 (C-$Cu^{I/II}O$ NPs 2): Normal mice, treated with C-$Cu^{I/II}O$ NPs (in 0.5 % carboxymethyl cellulose suspension) at dose of 40 mg/kg b. wt. intrarectally for 7 days.

2.2.4.6 Treatment of colitis induced mice with caffeic acid conjugated budesonide loaded nanomicelle

2.2.4.6.1 Study groups and treatment regimen

To evaluate the efficacy of budesonide loaded micelle against dextran sulphate sodium (DSS) induced colitis, 36 male albino mice were randomly divided into 6 animals each in 6 groups and followed our previously optimized dosing schedule.[29]

Group 1 (Healthy mice): Freely accessed basal diet has been fed to the mice of this group.

Group 2 (DSS): Colitis group where mice fed 4% DSS in drinking water upto 5 days.

Group 3 (DSS + BUD): Colitis induced mice administered with 300µg/kg body weight dose of budesonide in 0.25% CMC intrarectally for 7 days.

Group 4 (DSS + CRT loaded micelle): Colitis induced mice administered with 300µg/kg body weight equivalent dose of BUD loaded micelle in 0.25% CMC intrarectally for 7 days.

Group 5 (DSS + Blank micelle): Colitis induced mice administered with 300µg/kg body weight equivalent dose of blank micelle in 0.25% CMC intrarectally for 7 days.

Group 6 (Safety): Normal mice administered with 300µg/kg body weight equivalent dose of blank micelle in 0.25% CMC intrarectally for 7 days.

After 24 hours of administration of 7th dose of the treatment regimens mice were anaesthetized with mild anaesthesia and sacrificed by cervical dislocation on day 13.

2.2.5 Assessment of disease activity index and weight variation

It includes three different physical parameters which may be associated with colitis. They are physical activity, stool consistency and rectal bleeding. Physical activity has been scored on the basis of observation of experimental animals (0-normal or highly active, 1-mild active, 2-low active and 3-sedentary). Stool

consistency has been observed and scored (0-normal pellet, 1-soft, 2-loose watery stool, 3-stickiness, 4-diarrhoea).[2] Similarly, after the induction of colitis rectal bleeding of each group has been observed and scored (0-no bleeding and 1-bleeding). Weight variation in the mice among different groups has been determined using following formula:[30]

$$Weight\ variation\ (\%) = \frac{Final\ weight - Initial\ weight}{Final\ weight} X100$$

2.2.6. Colon length and fecal occult blood test

After completion of study animals were sacrificed by light ether anaesthesia followed by cervical dislocation. Colons of all the study groups were removed and physically observed for any changes after DSS treatment. Similarly, fecal occult blood test (FOBT) was performed to check any traces of hidden blood in feces of experimental animals. Briefly, on the FOBT paper strip faeces of animals was kept and then developer solution was applied. A blue color spot on the paper shows the presence of hidden blood in faeces.[29]

2.2.7 Histological observations

2.2.7.1 Hematoxylin and Eosin staining

The colons were excised, flushed with saline, cut open longitudinally along the main axis, and then again washed with saline. These colonic sections were fixed in 10% buffered formalin for at least 24 h and after fixation, the specimens were dehydrated in ascending grades of ethanol, cleared in benzene, and embedded in paraffin wax. Blocks were made and 5 µm thick sections were cut from the distal colon. The paraffin embedded colonic tissue sections were deparaffinized using xylene and ethanol. The slides were washed with phosphate buffered saline (PBS) and permeabilized with permeabilization solution (0.1 M citrate, 0.1% Triton X-100). These sections stained with hematoxylin and eosin and were observed under light microscope at 10X, 20X and 40X magnifications to investigate the histoarchitecture of colonic mucosa.[31]

2.2.7.2 Goblet cells staining

Paraffin embedded 5 µm thick colon sections were deparaffinized in xylene followed by rehydration with graded series of alcohol to water. Sections were stained with 1% Alcian blue (pH-2.5) in 3% acetic acid solution for 10 min and then rinsed for 1 min in 3% acetic acid solution to prevent non-specific staining. After washing with distilled water sections were then counter stained with 0.5 % aqueous solution of neutral red for 20 seconds. Again, washed the sections, dehydrated with alcohol and mounted with mounting media.[32]

2.2.7.3 Mucins staining

Paraffin embedded 5 µm thick colon sections were deparaffinized in xylene followed by rehydration with graded series of alcohol to water. Sections were then stained with high iron diamine solution for 20 hours and kept it at room temperature in dark. Then washed in running water for 20 minutes and rinsed three times in distilled water. Stained the sections in 1 % Alcian blue solution (prepared in 3 % acetic acid) for 30 minutes. Washed with distilled water, dehydrated in alcohol, cleared in xylene and mounted with the help of mounting media.[32]

2.2.7.4 Mast cells staining

Paraffin embedded 5 µm thick colon sections were deparaffinized in xylene followed by rehydration with graded series of alcohol to water. Stained in 0.1 % toluidine blue solution prepared in 1 % sodium chloride for 5 minutes. Slides were then washed three times in distilled water and dehydrated quickly in alcohol. Cleared in xylene and mounted with mounting media.[32]

2.2.7.5 Immunohistochemical staining

Immunohistochemistry for iNOS and COX-2 was performed using paraffin embed sections of colon tissue of 5µm thickness. Sections were deparaffinized three times in xylene dehydrated in graded ethanol followed by rehydration in running tap water. Antigen retrieval was performed by boiling of sections in 10 mM citrate buffer (pH 6.0) for 10-15 min. Non-specific staining was minimized by incubating the sections in hydrogen peroxide for 15 min and then

rinsed three times (5 minutes each) with 1X PBST (0.05% Tween-20). Blocking solution was applied for 10 minutes and then sections were incubated with rabbit polyclonal anti-iNOS antibody (dilution 1:300; PA5-16524, Invitrogen) and rabbit polyclonal anti- COX-2 antibody (dilution 1:400; PA5-17614) for overnight at 4°C in a humid chamber then sections were incubated with HRP-conjugated secondary antibody (dilution 1: 3000; FNSA – 0004, Invitrogen) for 1 hr at room temperature. Finally incubate sections with 3, 3,-diaminobenzidine (DAB), counterstained with hematoxylin, air dried, mounted with DPX and covered with cover slips. Imaging and analysis were performed at 40X magnification. On the basis of appearance of DAB staining, sections were graded as 0 (no staining), 1 (staining, 25%), 2 (staining between 25% and 50%), 3 (staining between 50% and 75%), or 4 (staining >75%). Similarly, staining intensity was the basis for the sections graded as follows: 0 (no staining), 1 (weak but detectable staining), 2 (distinct staining) or 3 (intense staining). Immunohistochemical staining scores were obtained by adding the diffuseness and intensity scores. All the analysis were performed using a Leica microsystems bright field microscope at 20X/40X magnification.[31]

2.2.7.5.1 Semiquantitative analysis of iNOS and COX-2 expression

Immunohistochemically processed colon sections for iNOS and COX-2 were also observed semi-quantitatively and corresponding histogram has been plotted on the basis of their staining scores.

2.2.8 *In-Vivo* cytokines estimations

2.2.8.1 Serum TNF-α measurement

In the pathogenesis of DSS-induced colitis tumor necrosis factor-alpha (TNF-α) play very crucial role. In mice serum TNF-α level was quantified using ELISA kit (eBioscience, Inc., San Diego, USA) as per the manufacturer instructions.[29]

2.2.8.2 Tissue nitrite level measurement

Tissue nitrite level was measured in 10% tissue homogenate of different treatment groups in KCl buffer as described elsewhere. Briefly, supernatants from

homogenates of all the groups and Griess reagent were taken in 1:2 ratio respectively and incubated at room temperature in dark for 10 minutes. The absorbance was recorded at 540 nm in microplate reader. Calculations were performed according to manufacturer`s protocol.[33]

2.2.8.3 Tissue myeloperoxidase (MPO) level

MPO assay was performed to estimate neutrophils infiltration in the colonic tissue of different treatment groups. Assay was performed as reported and myeloperoxidase activity represented as U/gram of protein.[34]

2.2.9 Statistical analysis

All data in this study were expressed as mean ± standard error of mean/standard deviation and analyzed by one-way ANOVA and followed by Bonferroni's post tests for the significant differentiation between the various groups. *p ≤ 0.05, **p ≤ 0.01, ***p ≤ 0.001, ###p ≤ 0.001, ##p ≤ 0.01, #p ≤ 0.05, were considered as statistically significant. Graph Pad Prism 5 was used for statistical analysis.

Note: Reprinted with permission from:-

(1) Mishra, R. K.; Ahmad, A.; Kumar, A.; Vyawahare, A.; Raza, S. S.; Khan, R. Lipid-Based Nanocarrier-Mediated Targeted Delivery of Celecoxib Attenuate Severity of Ulcerative Colitis. *Materials Science and Engineering: C* **2020**, *116*, 111103. https://doi.org/10.1016/j.msec.2020.111103.

(2) Mishra, R. K.; Selim, A.; Gowri, V.; Ahmad, A.; Nadeem, A.; Siddiqui, N.; Raza, S. S.; Jayamurugan, G.; Khan, R. Thiol-Functionalized Cellulose-Grafted Copper Oxide Nanoparticles for the Therapy of Experimental Colitis in Swiss Albino Mice. *ACS Biomater. Sci. Eng.* **2022**, *8* (5), 2088–2095. https://doi.org/10.1021/acsbiomaterials.2c00124.

2.3 Bibliography

(1) Muller, W. A. Getting Leukocytes to the Site of Inflammation. *Vet Pathol* **2013**, *50* (1), 7–22. https://doi.org/10.1177/0300985812469883.

(2) Mishra, R. K.; Ahmad, A.; Kumar, A.; Vyawahare, A.; Raza, S. S.; Khan, R. Lipid-Based Nanocarrier-Mediated Targeted Delivery of Celecoxib Attenuate Severity of Ulcerative Colitis. *Materials Science and Engineering: C* **2020**, *116*, 111103. https://doi.org/10.1016/j.msec.2020.111103.

(3) Müller, R. H.; Mäder, K.; Gohla, S. Solid Lipid Nanoparticles (SLN) for Controlled Drug Delivery – a Review of the State of the Art. *European Journal of Pharmaceutics and Biopharmaceutics* **2000**, *50* (1), 161–177. https://doi.org/10.1016/S0939-6411(00)00087-4.

(4) Kaur, S.; Mukhopadhyaya, A.; Selim, A.; Gowri, V.; Neethu, K. M.; Dar, A. H.; Sartaliya, S.; Ali, M. E.; Jayamurugan, G. Tuning of Cross-Glaser Products Mediated by Substrate–Catalyst Polymeric Backbone Interactions. *Chem. Commun.* **2020**, *56* (17), 2582–2585. https://doi.org/10.1039/C9CC08565C.

(5) Selim, A.; Neethu, K. M.; Gowri, V.; Sartaliya, S.; Kaur, S.; Jayamurugan, G. Thiol-Functionalized Cellulose Wrapped Copperoxide as a Green Nano Catalyst for Regiospecific Azide-Alkyne Cycloaddition Reaction: Application in Rufinamide Synthesis. *Asian Journal of Organic Chemistry* **2021**, *10* (12), 3428–3433. https://doi.org/10.1002/ajoc.202100658.

(6) Chen, Q.; Sun, Y.; Wang, J.; Yan, G.; Cui, Z.; Yin, H.; Wei, H. Preparation and Characterization of Glycyrrhetinic Acid-Modified Stearic Acid-Grafted Chitosan Micelles. *Artificial Cells, Nanomedicine, and Biotechnology* **2015**, *43* (4), 217–223. https://doi.org/10.3109/21691401.2013.845570.

(7) Chuysinuan, P.; Pavasant, P.; Supaphol, P. Preparation and Characterization of Caffeic Acid-Grafted Electrospun Poly (l-Lactic Acid) Fiber Mats for Biomedical Applications. *ACS Appl. Mater. Interfaces* **2012**, *4* (6), 3031–3040. https://doi.org/10.1021/am300404v.

(8) Ameli, H.; Alizadeh, N. Targeted Delivery of Capecitabine to Colon Cancer Cells Using Nano Polymeric Micelles Based on Beta Cyclodextrin. *RSC Advances* **2022**, *12* (8), 4681–4691. https://doi.org/10.1039/D1RA07791K.

(9) Ahmad, A.; Fauzia, E.; Kumar, M.; Mishra, R. K.; Kumar, A.; Khan, M. A.; Raza, S. S.; Khan, R. Gelatin-Coated Polycaprolactone Nanoparticle-Mediated Naringenin Delivery Rescue Human Mesenchymal Stem Cells from Oxygen Glucose Deprivation-Induced Inflammatory Stress. *ACS Biomater. Sci. Eng.* **2019**, *5* (2), 683–695. https://doi.org/10.1021/acsbiomaterials.8b01081.

(10) Ahmad, A.; Gupta, A.; Ansari, Md. M.; Vyawahare, A.; Jayamurugan, G.; Khan, R. Hyperbranched Polymer-Functionalized Magnetic Nanoparticle-Mediated Hyperthermia and Niclosamide Bimodal Therapy of Colorectal Cancer Cells. *ACS Biomater. Sci. Eng.* **2020**, *6* (2), 1102–1111. https://doi.org/10.1021/acsbiomaterials.9b01947.

(11) García-Betancourt, M. L.; Magaña-Zavala, C.; Crespo-Sosa, A. Structural and Optical Properties Correlated with the Morphology of Gold Nanoparticles Embedded in Synthetic Sapphire: A Microscopy Study. *J Microsc Ultrastruct* **2018**, *6* (2), 72–82. https://doi.org/10.4103/JMAU.JMAU_19_18.

(12) Bari, N. K.; Kumar, G.; Hazra, J. P.; Kaur, S.; Sinha, S. Functional Protein Shells Fabricated from the Self-Assembling Protein Sheets of Prokaryotic Organelles. *J. Mater. Chem. B* **2020**, *8* (3), 523–533. https://doi.org/10.1039/C9TB02224D.

(13) Naydenova, K.; McMullan, G.; Peet, M. J.; Lee, Y.; Edwards, P. C.; Chen, S.; Leahy, E.; Scotcher, S.; Henderson, R.; Russo, C. J. CryoEM at 100 KeV: A Demonstration and Prospects. *IUCrJ* **2019**, *6* (6), 1086–1098. https://doi.org/10.1107/S2052252519012612.

(14) Zhu, C.; Soldatov, A.; P. Mathew, A. Advanced Microscopy and Spectroscopy Reveal the Adsorption and Clustering of Cu (Ii) onto TEMPO-Oxidized Cellulose Nanofibers. *Nanoscale* **2017**, *9* (22), 7419–7428. https://doi.org/10.1039/C7NR01566F.

(15) Tang, C.; Fan, Y.; Lü, J. Atomic Force Microscopy-Based Single Molecule Force Spectroscopy for Biological Application. In *Atomic Force Microscopy in Molecular and Cell Biology*; Cai, J., Ed.; Springer: Singapore, 2018; pp 29–40. https://doi.org/10.1007/978-981-13-1510-7_2.

(16) Lawson, G.; Ogwu, J.; Tanna, S. Quantitative Screening of the Pharmaceutical Ingredient for the Rapid Identification of Substandard and Falsified Medicines Using

Reflectance Infrared Spectroscopy. *PLOS ONE* **2018**, *13* (8), e0202059. https://doi.org/10.1371/journal.pone.0202059.

(17) Kozachuk, O.; Yusenko, K.; Noei, H.; Wang, Y.; Walleck, S.; Glaser, T.; Fischer, R. A. Solvothermal Growth of a Ruthenium Metal–Organic Framework Featuring HKUST-1 Structure Type as Thin Films on Oxide Surfaces. *Chem. Commun.* **2011**, *47* (30), 8509–8511. https://doi.org/10.1039/C1CC11107H.

(18) Sahu, D. K.; Rai, J.; Rai, M. K.; Banjare, M. K.; Nirmal, M.; Wani, K.; Sahu, R.; Pandey, S. G.; Mundeja, P. Detection of Flonicamid Insecticide in Vegetable Samples by UV–Visible Spectrophotometer and FTIR. *Results in Chemistry* **2020**, *2*, 100059. https://doi.org/10.1016/j.rechem.2020.100059.

(19) Nahak, P.; Karmakar, G.; Chettri, P.; Roy, B.; Guha, P.; Besra, S. E.; Soren, A.; Bykov, A. G.; Akentiev, A. V.; Noskov, B. A.; Panda, A. K. Influence of Lipid Core Material on Physicochemical Characteristics of an Ursolic Acid-Loaded Nanostructured Lipid Carrier: An Attempt To Enhance Anticancer Activity. *Langmuir* **2016**, *32* (38), 9816–9825. https://doi.org/10.1021/acs.langmuir.6b02402.

(20) Wang, X.-Z.; Meng, Q.-Y.; Zhong, J.-J.; Gao, X.-W.; Lei, T.; Zhao, L.-M.; Li, Z.-J.; Chen, B.; Tung, C.-H.; Wu, L.-Z. The Singlet Excited State of BODIPY Promoted Aerobic Cross-Dehydrogenative-Coupling Reactions under Visible Light. *Chem. Commun.* **2015**, *51* (56), 11256–11259. https://doi.org/10.1039/C5CC03421C.

(21) Wu, Y.; Li, Q.; Cao, J.; Liu, Y.; Wang, Z.; Shangguan, L.; Zhu, H. Pillararene-Peptide Nanogels and Their Biomimetic Mineralization Hybrids for Heterogeneous Catalysis. *ACS Appl. Nano Mater.* **2021**, *4* (10), 11126–11133. https://doi.org/10.1021/acsanm.1c02585.

(22) Alopaeus, J. F.; Hagesæther, E.; Tho, I. Micellisation Mechanism and Behaviour of Soluplus®–Furosemide Micelles: Preformulation Studies of an Oral Nanocarrier-Based System. *Pharmaceuticals* **2019**, *12* (1), 15. https://doi.org/10.3390/ph12010015.

(23) Cheng, K.; Sun, S.; Gong, X. Preparation, Characterization, and Antiproliferative Activities of Biotin-Decorated Docetaxel-Loaded Bovine Serum Albumin Nanoparticles. *Braz. J. Pharm. Sci.* **2018**, *54*. https://doi.org/10.1590/s2175-97902018000217295.

(24) Ahmad, A.; Fauzia, E.; Kumar, M.; Mishra, R. K.; Kumar, A.; Khan, M. A.; Raza, S. S.; Khan, R. Gelatin-Coated Polycaprolactone Nanoparticle-Mediated Naringenin Delivery Rescue Human Mesenchymal Stem Cells from Oxygen Glucose Deprivation-Induced Inflammatory Stress. *ACS Biomater. Sci. Eng.* **2019**, *5* (2), 683–695. https://doi.org/10.1021/acsbiomaterials.8b01081.

(25) Gupta, A.; Ahmad, A.; Singh, H.; Kaur, S.; K M, N.; Ansari, Md. M.; Jayamurugan, G.; Khan, R. Nanocarrier Composed of Magnetite Core Coated with Three Polymeric Shells Mediates LCS-1 Delivery for Synthetic Lethal Therapy of BLM-Defective Colorectal Cancer Cells. *Biomacromolecules* **2018**, *19* (3), 803–815. https://doi.org/10.1021/acs.biomac.7b01607.

(26) Soni, J. M.; Sardoiwala, M. N.; Choudhury, S. R.; Sharma, S. S.; Karmakar, S. Melatonin-Loaded Chitosan Nanoparticles Endows Nitric Oxide Synthase 2 Mediated Anti-Inflammatory Activity in Inflammatory Bowel Disease Model. *Materials Science and Engineering: C* **2021**, *124*, 112038. https://doi.org/10.1016/j.msec.2021.112038.

(27) Yang, S.-T.; Chang, H.-H. Nitric Oxide of Neuronal Origin Mediates NMDA-Induced Cerebral Hyperemia in Rats. *NeuroReport* **1998**, *9* (3), 415–418.

(28) Laroui, H.; Ingersoll, S. A.; Liu, H. C.; Baker, M. T.; Ayyadurai, S.; Charania, M. A.; Laroui, F.; Yan, Y.; Sitaraman, S. V.; Merlin, D. Dextran Sodium Sulfate (DSS) Induces Colitis in Mice by Forming Nano-Lipocomplexes with Medium-Chain-Length Fatty Acids in the Colon. *PLOS ONE* **2012**, *7* (3), e32084. https://doi.org/10.1371/journal.pone.0032084.

(29) Mishra, R. K.; Selim, A.; Gowri, V.; Ahmad, A.; Nadeem, A.; Siddiqui, N.; Raza, S. S.; Jayamurugan, G.; Khan, R. Thiol-Functionalized Cellulose-Grafted Copper Oxide Nanoparticles for the Therapy of Experimental Colitis in Swiss Albino Mice. *ACS Biomater. Sci. Eng.* **2022**, *8* (5), 2088–2095. https://doi.org/10.1021/acsbiomaterials.2c00124.

(30) Mishra, R. K.; Sammi, S. R.; Rawat, J. K.; Roy, S.; Singh, M.; Gautam, S.; Yadav, R. K.; Devi, U.; Ansari, M. N.; Saeedan, A. S.; Saraf, S. A.; Pandey, R.; Kaithwas, G. Palonosetron Attenuates 1,2-Dimethyl Hydrazine Induced Preneoplastic Colon Damage through Downregulating Acetylcholinesterase Expression and up-Regulating

Synaptic Acetylcholine Concentration. *RSC Adv.* **2016**, *6* (46), 40527–40538. https://doi.org/10.1039/C6RA04614B.

(31) Ansari, Md. M.; Ahmad, A.; Mishra, R. K.; Raza, S. S.; Khan, R. Zinc Gluconate-Loaded Chitosan Nanoparticles Reduce Severity of Collagen-Induced Arthritis in Wistar Rats. *ACS Biomater. Sci. Eng.* **2019**, *5* (7), 3380–3397. https://doi.org/10.1021/acsbiomaterials.9b00427.

(32) Khan, R.; Khan, A. Q.; Lateef, A.; Rehman, M. U.; Tahir, M.; Ali, F.; Hamiza, O. O.; Sultana, S. Glycyrrhizic Acid Suppresses the Development of Precancerous Lesions via Regulating the Hyperproliferation, Inflammation, Angiogenesis and Apoptosis in the Colon of Wistar Rats. *PLOS ONE* **2013**, *8* (2), e56020. https://doi.org/10.1371/journal.pone.0056020.

(33) Guevara, I.; Iwanejko, J.; Dembińska-Kieć, A.; Pankiewicz, J.; Wanat, A.; Anna, P.; Gołąbek, I.; Bartuś, S.; Malczewska-Malec, M.; Szczudlik, A. Determination of Nitrite/Nitrate in Human Biological Material by the Simple Griess Reaction. *Clinica Chimica Acta* **1998**, *274* (2), 177–188. https://doi.org/10.1016/S0009-8981(98)00060-6.

(34) Lefkowitz, D. L.; Gelderman, M. P.; Fuhrmann, S. R.; Graham, S.; Starnes, J. D.; Lefkowitz, S. S.; Bollen, A.; Moguilevsky, N. Neutrophilic Myeloperoxidase–Macrophage Interactions Perpetuate Chronic Inflammation Associated with Experimental Arthritis. *Clinical Immunology* **1999**, *91* (2), 145–155. https://doi.org/10.1006/clim.1999.4696.

Chapter 3

Celecoxib-loaded nanostructured lipid carrier for ulcerative colitis

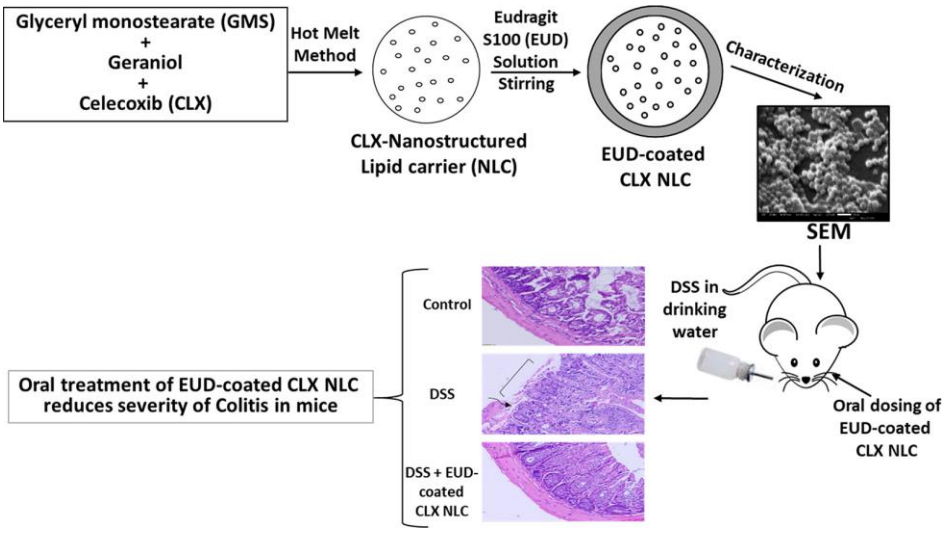

Graphical abstract

3.1 Introduction

Ulcerative colitis (UC) is a chronic inflammatory disease which primarily affects the rectum and spreads toward the lower end of the colon.[1] Damage to the intestinal epithelium enables the lumen microbiota to evoke inflammatory responses because of the activation of immune system and cytokine production. UC can lead to several complications like abdominal pain, diarrhea, rectal bleeding etc.[2] and if the disease is left untreated it may further lead to the development of colorectal cancer.[3–5]

The conventional and currently prevailing therapeutic regimens for ulcerative colitis include antibiotics, immunosuppressive agents, aminosalicylates, corticosteroids and biologics, but they provide symptomatic treatment and are associated with long term adverse drug reactions. Furthermore, these drugs have limited efficacy because of other factors like drug inactivation in harsh gastric acid surroundings, high first pass metabolism, low solubility and as a result low bioavailability.[6–8] Non-steroidal anti-inflammatory drugs (NSAIDs) have been mostly used to manage the disease-associated pain and inflammation.[9] Celecoxib (CLX) is a NSAID, which selectively inhibits cyclooxygenase-2 (COX-2) enzyme. It is commonly prescribed in the management of rheumatoid arthritis and osteoarthritis for the pain management but higher dose consumptions have been associated with increased risk of adverse cardiovascular, renal and gastrointestinal events.[10,11] COX-2 is an inducible enzyme which is reported to get overexpressed in inflamed colonic mucosa by producing different inflammatory cytokines and is well reported in UC.[12,13] CLX treatment minimizes the gastric side effects of conventional NSAIDs and may produce significant therapeutic effects in UC. As CLX is able to selectively inhibit COX-2 enzyme without affecting another isoform i.e. COX-1, it helps to alleviate inflammation, fever and pain together with minimized side effects like gastric ulcers and gastric mucosal erosions which are strongly associated with COX-1 inhibition.[14–16] Despite the diverse advantages of CLX, it has some limitations such as poor water solubility, large volume of distribution and low oral bioavailability.[17]

To overcome the aforementioned drug limitations, several nanotechnology based drug delivery systems have been developed to address drugs

and pharmaceuticals concerns, that were able to significantly aid in drug solubilization, reduce side effects, increase bioavailability, and finally enhance their pharmacological activity.[18,19] Advancement in the field of drug delivery brought lipid-based carrier systems which can potentially enhance the bioavailability of highly hydrophobic, poorly water soluble and/or lipophilic drugs.[20,21] In lipid nanoformulations, solid lipid nanoparticles (SLN) are lipidic colloidal carrier which contain solid lipid, dispersed in water or in an aqueous surfactant solution. Generally, these are submicron sized particles, with range between 100-1000 nm. The advantages of SLNs are to protect the drug form chemical decomposition and regulate drug release.[22,23] In conventional SLNs only solid lipid is there which have some limitations like restricted drug loading capacity, regulation of release rate and drug exclusion during storage.[24,25] To surpass these problems advancement in SLNs lead to nanostructured lipid carriers (NLCs) which contain liquid lipid in solid lipid matrix stabilized with biocompatible emulsifier. The NLCs have potential to encapsulate large amount of drug and even after formulation process, possesses very less ordered lipid matrix imperfections.[5,26–28] NLCs are easily produced and are entirely devoid of any organic solvent. They have good stability on long term storage and can be sterilized with ease by steam sterilization as well as lyophilization.[29–31] Moreover, NLCs have been established as potential carriers for oral administration of poorly water soluble and low bioavailable drugs and are well reported for the treatment of UC.[32–34]

The present study aimed to prepare CLX-loaded Eudragit S100 coated NLCs for the treatment of dextran sodium sulfate (DSS)-induced colitis in Swiss albino mice. For the fabrication of the NLC, glyceryl monostearate (GMS) was employed as solid lipid, geraniol as liquid lipid and PF-127 as water soluble emulsifier. This composition makes the formulation quite novel and unique. Both, GMS and geraniol are generally recognized as safe (GRAS), approved by US-FDA, which are non-toxic, safe for enteral human use, low-cost materials and have been used in various industries like pharmaceuticals, foods, cosmetics with no signs of toxicity. GMS is a fatty acid present in various plant derived oils and geraniol is also plant origin component of the proposed formulation such that it renders the

formulation as biocompatible and non-toxic delivery system.[35,36] Therefore, we have chosen GMS and geraniol to develop NLC. Furthermore, the primary requirement for any colon targeted formulation is to resist the drug degradation at gastric pH and successfully deliver it to colon. After formulation of CLX NLCs, coating performed with gastric resistant colon specific polymer Eudragit S100 (EUD S100) to ensure the protection of CLX in harsh gastric environment and site-specific delivery of CLX-loaded NLC in the colon.

3.2 Results and discussion

3.2.1 Formulation and characterization of NLCs

Celecoxib loaded Eudragit S-100 coated nanostructured lipid carriers (EUD-S-100 coated CLX NLCs) were prepared by hot melt technique (**Figure 3.1)** followed by probe sonication.

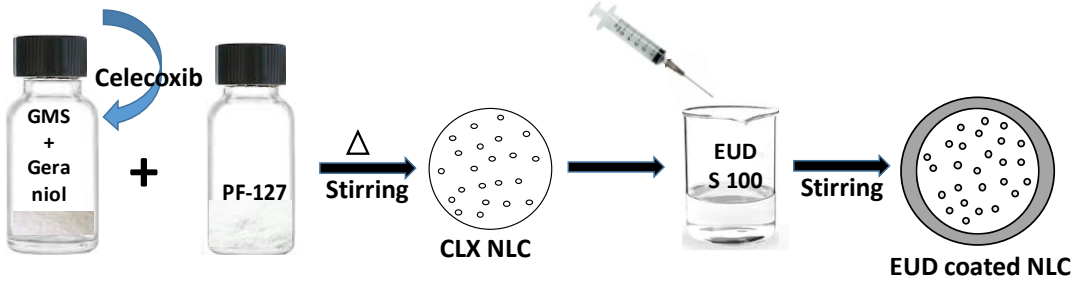

Figure 3.1 Schematic representation of formulation of EUD S 100 coated CLX loaded NLCs.

The optimization was carried out using various combinations of different ingredients **(Table 3.1)**.

Table 3.1 Composition of different batches of NLC. Blank formulation (B1-B7), CLX-loaded NLC (B7D), (q.s. – quantity sufficient).

S. No.	Ingredients (mg)	Batches							
		B1	B2	B3	B4	B5	B6	B7	B7D
1.	SAA	90	90	60	45	105	140	70	70
2.	Linalool	60	60	40	30	45	60	30	30
3.	PF-127	100	150	100	100	100	200	100	100
4.	Drug	-	-	-	-	-	-	-	15
6.	D. Water (ml)	q.s.	q.s.	q.s.	q.s.	q.s.	q.s.	q.s.	q.s.

Initially NLC formulation was dependent upon two variables viz. lipid concentration and surfactant concentration. On the basis of preliminary studies, optimized lipid concentration 0.75 – 2% and surfactant concentration 1 – 2% were selected.[37] Batches were prepared by varying concentrations of independent variables and were observed for their corresponding particle size as well as physical deformation. At higher concentration of lipid and lower concentration of surfactant a bigger particle size and separation of lipid and aqueous phases was observed. Moreover, at lower concentration of lipid and higher concentration of surfactant sedimentation rate of NLC suspension was high. Therefore, the concentration range of lipid and surfactant were precisely selected to cover the particle size (200 – 300 nm) in nanometer range to aid the delivery of CLX to the site of action with good physical stability attributes. After optimization of blank NLCs the drug and lipid ratio (0.5:10, 1:10 and 1.5:10) was screened for particle size and encapsulation efficacy. At lower lipid: surfactant ratio (≤0.5:10) a low encapsulation efficacy was observed while at higher ratio (≥1.5:10) an increase in particle size with signs of sedimentation were seen. Stable NLC suspensions with the most optimum particle size were obtained at 1:10**:** drug: lipid ratio. CLX-loaded nanostructured lipid carriers (uncoated) and EUD S100-coated CLX-loaded NLCs possess the mean

hydrodynamic diameter 161.20 nm **(Figure 3.2A)** and 250.90 nm **(Figure 3.2B)** respectively. It is important to consider particle size and polydispersity index (PDI) of the carriers as they directly affect various physicochemical properties of the system. For lipid based nanocarriers, PDI value 0.3 or below is acceptable and represent homogeneous and monodispersed particles. The uncoated blank NLC and EUD S100-coated blank NLC were also prepared during optimization which were slightly smaller in size in comparison to EUD S100-coated CLX-loaded NLC **(Figure 3.3).**

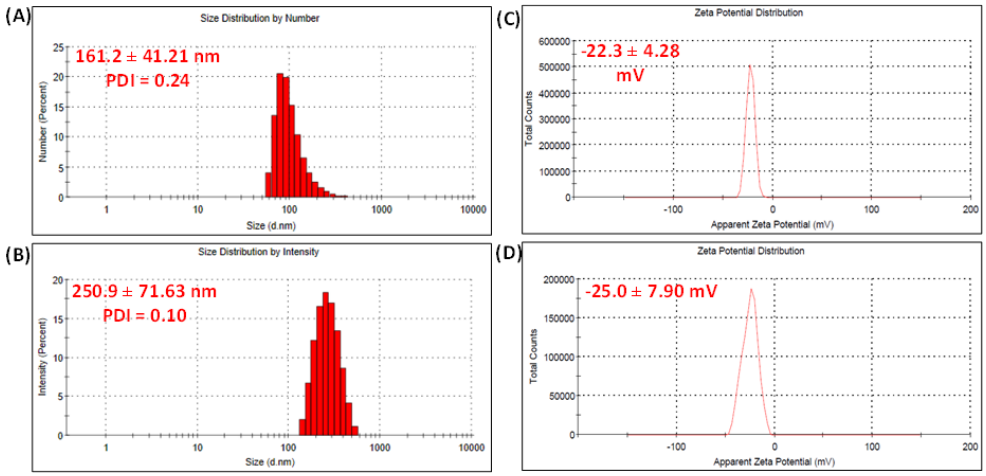

Fig 3.2 Particle size distribution histogram and poly dispersity index (PDI) analysis of CLX-loaded NLC (uncoated) and EUD S100-coated CLX-loaded NLC (A & B) and mean zeta potential of CLX-loaded NLC (uncoated) and EUD S100-coated CLX-loaded NLC (C & D). The data are reported as Mean ± SD of three independent sets of observations (n=3).

In both the cases, particles showed good PDI as 0.24 and 0.10 which may be suitable to consider NLCs as monodisperse.[38] These NLCs have zeta potential values between – 22 to – 25 mV **(Figure 3.2 C&D)** which showed good stability as the particles repel each other and remain dispersed throughout the medium.

Long term stability studies of nanocarriers in terms of their hydrodynamic diameter and zeta potential were performed by storing nanocarriers at room temperature for an extended period of 30 days and then measuring particle size

and zeta potential values. After the specified time period, no significant alteration in either particle size (hydrodynamic diameter) or zeta potential was observed which established that nanocarriers could retain their size and charge and prevented particle aggregation and settling down **(Figure 3.3E-F)**.

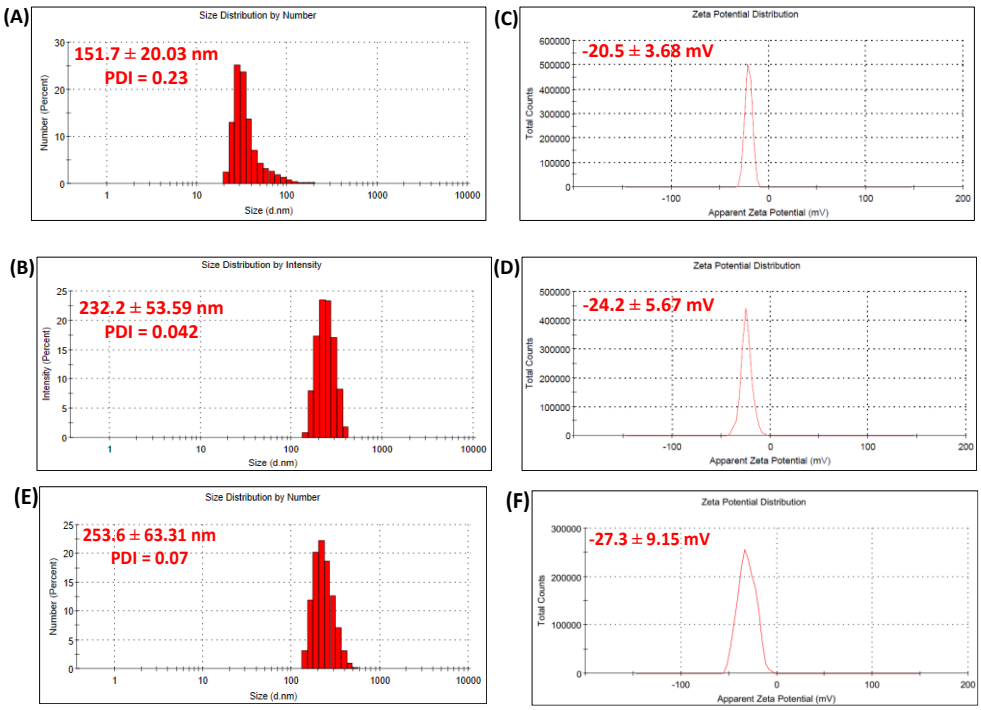

Figure 3.3 Mean hydrodynamic particle size distribution histogram and poly dispersity index (PDI) analysis of blank NLC (uncoated) and EUD S100-coated NLC (A & B); and mean zeta potential values of blank NLC (uncoated) and EUD S100-coated NLC (C & D) by photon correlation spectroscopy. The data is reported as Mean ± SD (n=3). (E) Mean hydrodynamic particle size distribution histogram and poly dispersity index (PDI) and (F) zeta potential values after the stability testing of nanoformulation.

The size, shape and surface morphology of CLX-loaded NLCs (uncoated) and EUD S100-coated CLX-loaded NLCs was also substantiated by different microscopic methods as TEM, SEM and AFM. The particles showed spherical morphology in shape and were observed without any aggregation **(Figure 3.4 and Figure 3.5).**

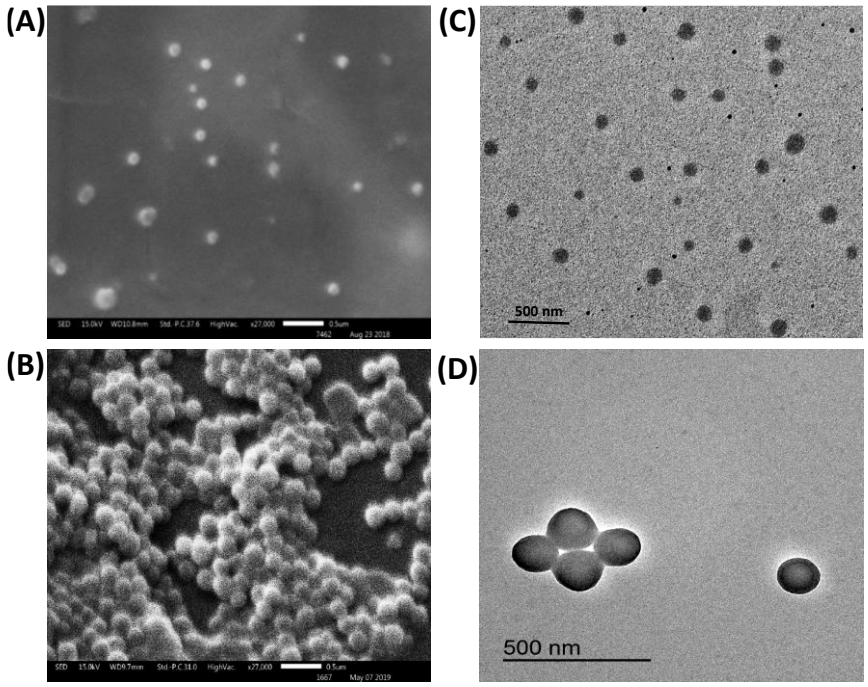

Figure 3.4 Microscopic images of CLX-loaded NLC (uncoated) and EUD S100-coated CLX-loaded NLC. SEM of CLX-loaded NLC (uncoated) (A) and EUD S100-coated CLX-loaded NLC (B). TEM of CLX-loaded NLC (uncoated) (C) and EUD S100-coated CLX-loaded NLC (D). Scale bar = 500 nm.

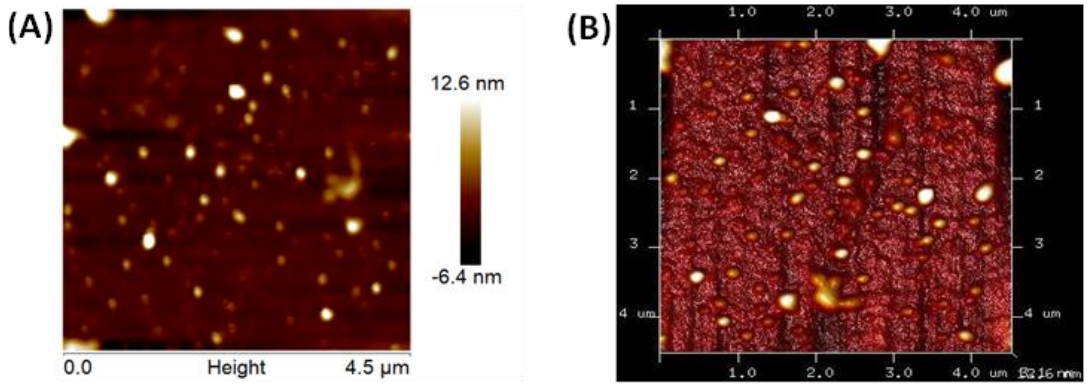

Figure 3.5 Atomic Force Microscopic image of CLX-loaded NLC (uncoated) (A) 2D-AFM image (B) 3D-AFM image. (Scale bar = 4.5 µm).

3.2.2 Drug loading and release

The loading of CLX in EUD S100-coated NLC is confirmed by XRD and ATR-FTIR techniques. In XRD spectrum, CLX shows characteristic peaks at 2θ =

16.3ºand 21.5º. The similar peaks were found in EUD S100-coated CLX-loaded NLCs **(Figure 3.6)**.

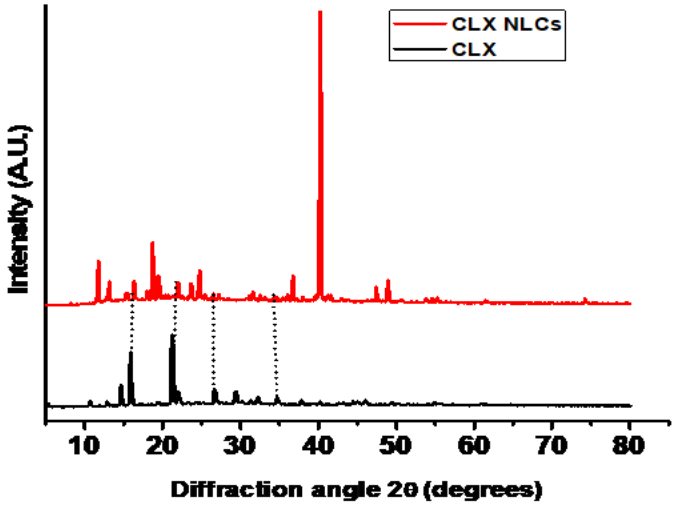

Figure 3.6 Comparative X-Ray diffraction (XRD) spectra of CLX and EUD S-100 coated CLX-loaded NLC.

The loading capacity and encapsulation efficiency were determined by UV-VIS spectroscopy at 252 nm (λmax of CLX) absorbance wavelength **(Figure 3.7)** and found to be 8.55±0.05% and 59.89±0.41% respectively.

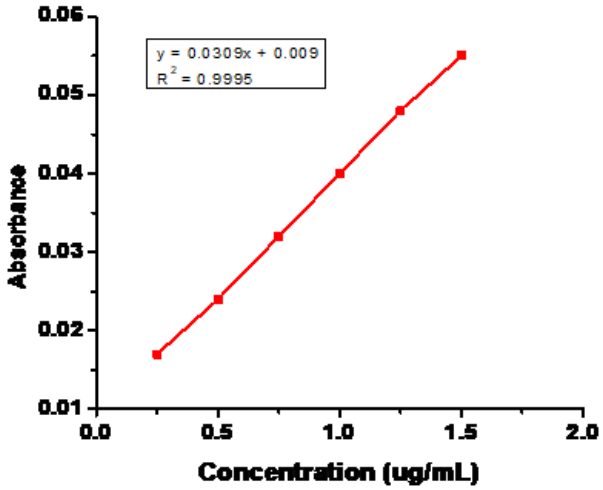

Figure 3.7 Standard plot of CLX with UV-Vis spectra of serially diluted specific concentrations of CLX in aqueous solvent at its λ_{max}.

Again, ATR spectra of CLX and individual components of the formulation

have some common peaks that were observed in EUD S100-coated CLX-loaded NLCs **(Figure 3.8)**.

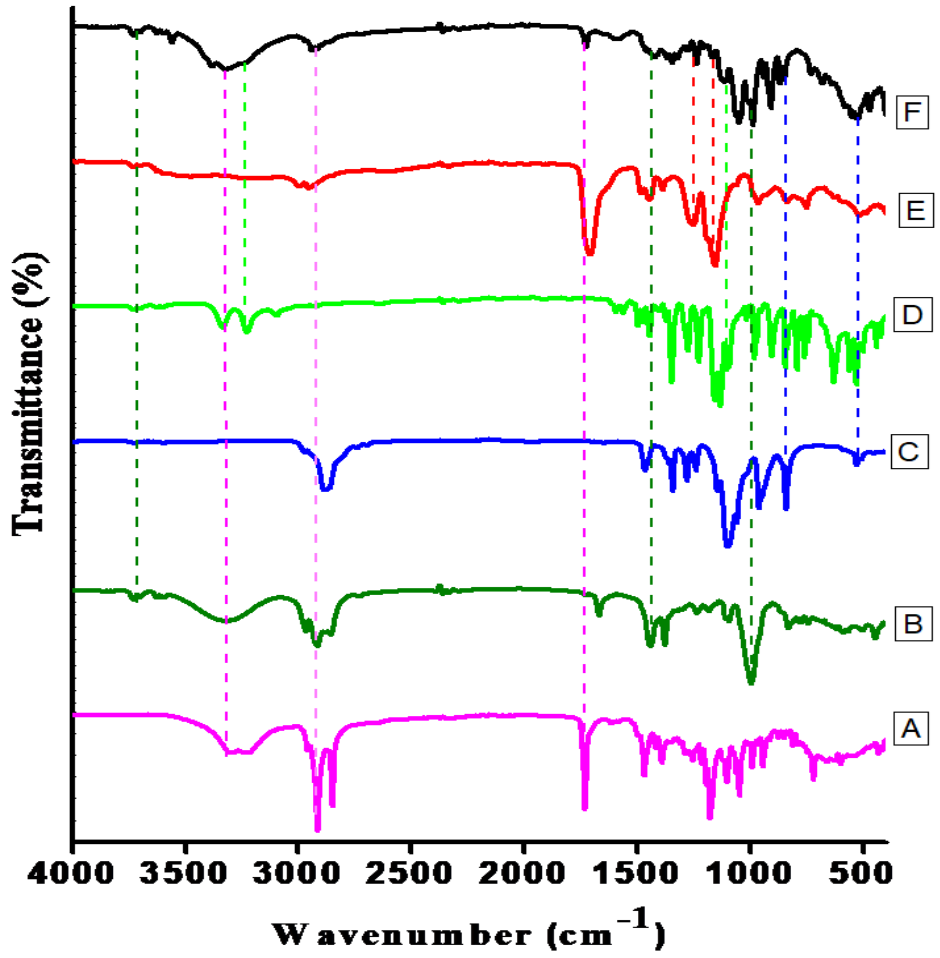

Figure 3.8 Comparative ATR-FTIR spectral analysis of (A) GMS, (B) Geraniol, (C) PF-127, (D) EUD S100, (E) CLX and (F) EUD S100-coated CLX loaded NLC. Dotted lines show common peaks of the ATR-FTIR spectra of GMS, geraniol, PF-127, EUD S-100, CLX and EUD S100-coated CLX loaded NLCs.

The release study of CLX from EUD S100-coated NLCs was performed in simulated gastrointestinal fluids at different pH values as 0.1 M Hcl (pH – 2.0), KH_2PO_4 buffer (pH – 4.5) and phosphate buffer saline (PBS) (pH – 7.4) at room temperature as described previously, with slight modification **(Figure 3.9 and Figure 3.10).**[39,40] Initially for 2 hours release of CLX was very low (>1 %) in acidic condition as the drug was protected by EUD S-100 layer in gastric environment. After 2 hours upto 4-6 hours slight increase in CLX release was observed from EUD

S-100 coated CLX NLC in KH_2PO_4 buffer. After 6 hours significantly marked increase in CLX amount in release media PBS (pH – 7.4) was observed as the coating of EUD S-100 getting dissolved. Release pattern revealed the sustain release of CLX from EUD S100-coated CLX-loaded NLC as evidenced by 90% of drug was released in 24 hours. Sustained release profile of CLX from EUD S100-coated CLX-loaded NLCs may be beneficial to avoid the multiple dosing.

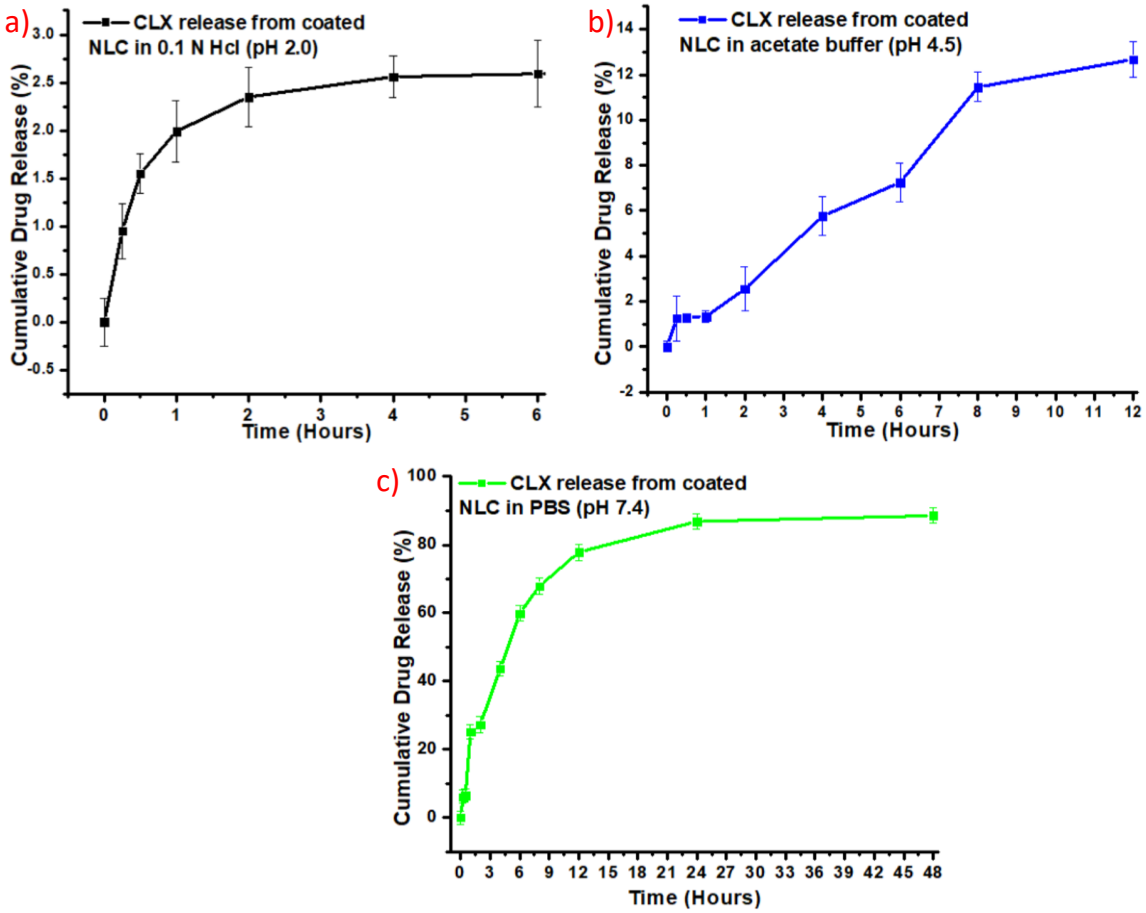

Figure 3.9 Release profile of CLX from EUD S100 coated NLC in simulated gastrointestinal fluids. (a) Release in 0.1 M Hcl (pH – 2.0), (b) KH_2PO_4 buffer (pH – 4.5) and (c) PBS (pH – 7.4). The experiments were performed in triplicate (n=3) and data are presented as mean ± standard deviation of three independent sets of observations.

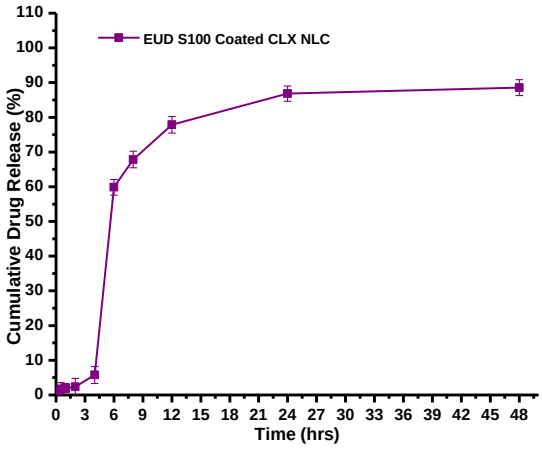

Figure 3.10 Release profile of CLX from EUD S100 coated NLC in 0.1 M Hcl (pH 2.0 for 0-2 hours), KH_2PO_4 buffer (pH – 4.5 for 2-4 hours) and PBS (pH 7.4 for 6-48 hours). The experiments were performed in triplicate (n=3) and data are presented as mean ± standard deviation of three independent sets of observations.

3.2.3 Cytocompatibility of NLC

Further, the cytocompatibility of blank EUD S100-coated NLCs in previously established concentration gradients[39,41] was assessed against normal human fibroblast cells (hTERT-BJ) for 24 hours **(Figure 3.11)**. At the dose of 200 µg/ml, slight decrease in cell viability was observed but was statistically non-significant. This study suggested that formulation was cytocompatible upto a dose of 200 µg/ml without exerting cytotoxic effects.

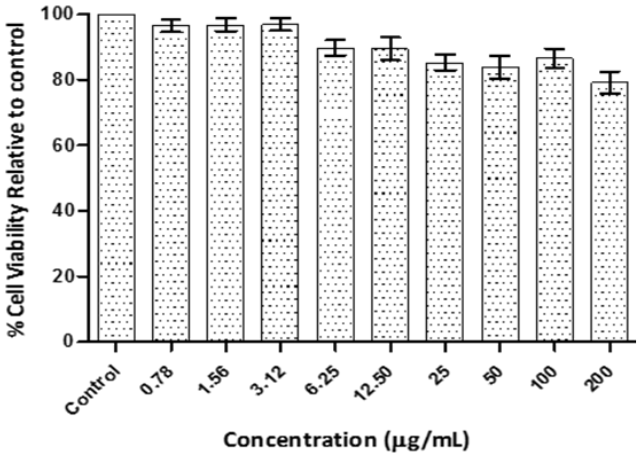

Figure 3.11 Cytocompatibility of blank EUD S100-coated NLCs at different concentrations against normal human foreskin fibroblasts (hTERT-BJ) cells. The experiments were performed in triplicate (n=3) and data are presented as mean ± standard deviation of three independent sets of observations.

3.2.4 *In-Vivo* Therapeutic Efficacy Study

After the synthesis, characterization and *in-vitro* cytocompatibility evaluation of NLC, we performed the *in-vivo* therapeutic efficacy study of EUD S100-coated CLX-loaded NLC against dextran sulfate sodium (DSS)-induced colitis mouse model.

3.2.4.1 Disease activity index and weight variation

During the study period, experimental animals were examined physically for their normal activities. In this line, we observed disease activity index which includes parameters like stool consistency, physical activity and rectal bleeding **(Table 3.2)**. In normal control and blank EUD S100-coated NLC group, above mentioned parameters were normal. After induction of colitis in DSS group diarrhea (watery stool) was observed. In the same group, mice underwent sedentary activity and some had severe rectal bleeding. Treatment with CLX leads to the normalization of conditions i.e., stool became soft from diarrhea, physical activity tends to mild and there was no rectal bleeding observed. In EUD S100-coated CLX-loaded NLC treatment group stool consistency was soft with normal activity of mice and there was no rectal bleeding observed.

Table 3.2 Physical observations of various parameters on experimental animals over the study period. Values are expressed in the table are average observational values.

S.No.	Groups	Observations		
		Stool Consistency	Physical Activity	Rectal Bleeding
1.	Normal Control	0	0	0
2.	DSS	4	3	1
3.	CLX	1	1	0
4.	EUD S100-coated CLX-loaded NLC	1	0	0
5.	Blank EUD S100-coated NLC	0	0	0

Stool Consistency	**Physical Activity**	**Rectal Bleeding**
0-Normal Pellet (Hard)	0-Normal active (Highly)	0-No bleeding
1-Soft Pellet	1-Mild active	1-Bleeding
2-Loose watery stool	2-Low active	
3-Stickiness	3-Sedentary	
4-Diarrhoea		

Further, the weight variation of mice over the study period was also observed. Intestinal inflammation may be marked as weight loss and reflect inflammatory state of IBD that restrict the nutrient absorption and leads to catabolic state of the system.[42] After the induction of colitis in DSS treated group, weight of mice was significantly decreased (***p≤0.001) in comparison to normal control. Treatment with CLX as well as EUD S100-coated CLX-loaded NLC, body weight was significantly increased (###p≤0.001) in comparison to DSS group **(Figure 3.12)**. Percentage weight variations from starting to the end of the study has also been observed **(Figure 3.13)**.

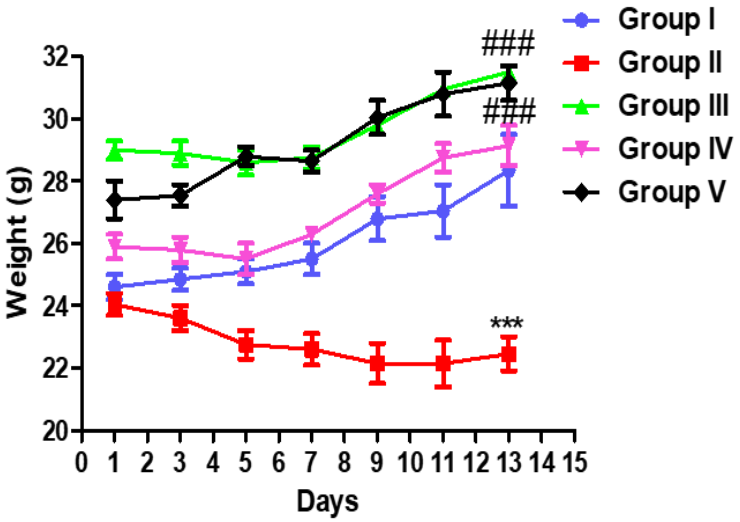

Figure 3.12 Weight variation in mice among different groups during the study period. Group I, Normal Control: mice received basal diet. Group II, DSS: mice received 4% DSS in drinking water upto 5 days. Group III, DSS + CLX: DSS induced colitis mice, treated with CLX suspended in 0.5 % CMC at dose of 10 mg/kg body weight p.o. after induction of colitis. Group IV, DSS + EUD S100-coated CLX-loaded NLC: DSS induced colitis mice, treated with equivalent dose of CLX loaded

NLCs in 0.5 % CMC p.o. after induction of colitis. Group V, Blank EUD S100-coated NLC: Normal mice treated with blank EUD S100-coated NLC in 0.5 % CMC p.o. (values are presented as mean ± SD). Comparisons were made on the basis of the one-way ANOVA followed by Bonferroni post-test. All groups were compared to the DSS-treated group (p≤0.001, ###p≤0.001).***

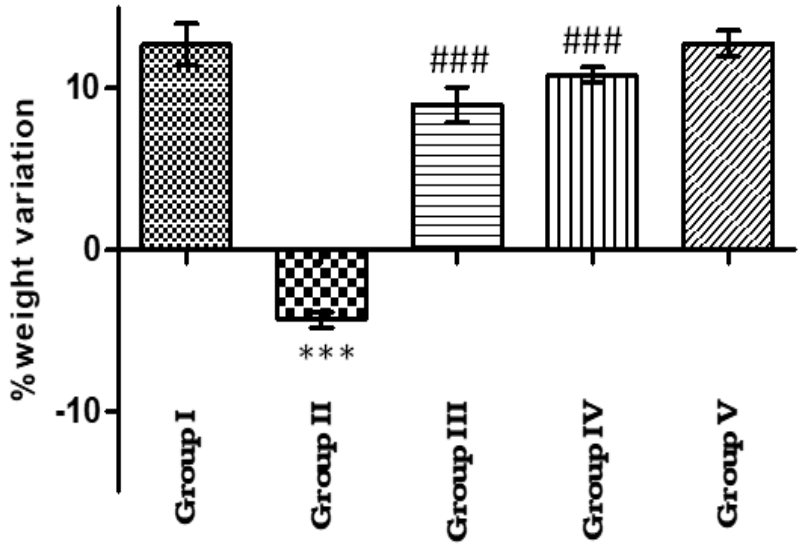

Figure 3.13 Shows % weight variation of in mice over the study period. Group I – Normal Control, Group II – DSS, Group III – DSS + CLX, Group IV – DSS + EUD S100-coated CLX-loaded NLC, Group V – Blank EUD S100-coated NLC. Comparisons were made on the basis of the one-way ANOVA followed by Bonferroni post-test. All groups were compared to the DSS group (*p < 0.001, ###p < 0.001). (Values are presented as mean ± SD).**

Colon length of experimental animals in different treatment groups was observed. DSS treatment led to marked decreased in colon length while EUD S100-coated CLX-loaded NLC regained the colon length. Blank EUD S100-coated NLC group did not show any marked variation **(Figure 3.14I-V)**. Similarly, fecal occult blood test (FOBT) was also carried out in all treatment groups. In DSS treated group as well as CLX treated groups presence of fecal blood was observed while there was no fecal blood was observed in the group treated with EUD S-100 coated CLX-loaded NLC **(Figure 3.14A-E)**.

Figure 3.14 Physical observation of colon length of all mice of different groups after completion of study. I – Normal Control, II – DSS, III – DSS + CLX, IV – DSS + EUD S100-coated CLX-loaded NLC, V – Blank EUD S100-coated NLC and A – E are corresponding fecal occult blood test (FOBT) images.

3.2.4.2 Histological observations

Histological study revealed that complete colon integrity was present in normal control group. It contains mucosa which has intact goblet cells and submucosa was surrounded by intact muscularis layer. Treatment with DSS causes induction of colitis that leads to significant alteration in normal colon architect. In DSS-induced colitis group goblet cells were significantly depleted from the mucosa and abnormal crypts, ulcerated mucosa layer and damaged muscularis have been observed. Significant gap between muscularis and mucosa appeared that was recognized as submucosal widening which was correlated with collagen deposition or inflammatory cell infiltrations in DSS group. In our study, DSS-induced colonic histological changes were in close corroboration with the previous reports.[42–44] Treatment with CLX causes significant recovery in the damaged colon linings. Goblet cells were appeared in mucosa as well as submucosal layer was intact between mucosa and muscularis. In EUD S100-coated CLX-loaded NLC treatment group complete colon morphology was regained. The normal arrangement of colon in this group was

observed where mucosa, submucosa and muscularis layers were present. Numerous goblet cells were intact in mucosa and normal crypts were also observed. There were no signs of morphological alteration observed in blank EUD S100-coated NLC treated group **(Figure 3.15)**.

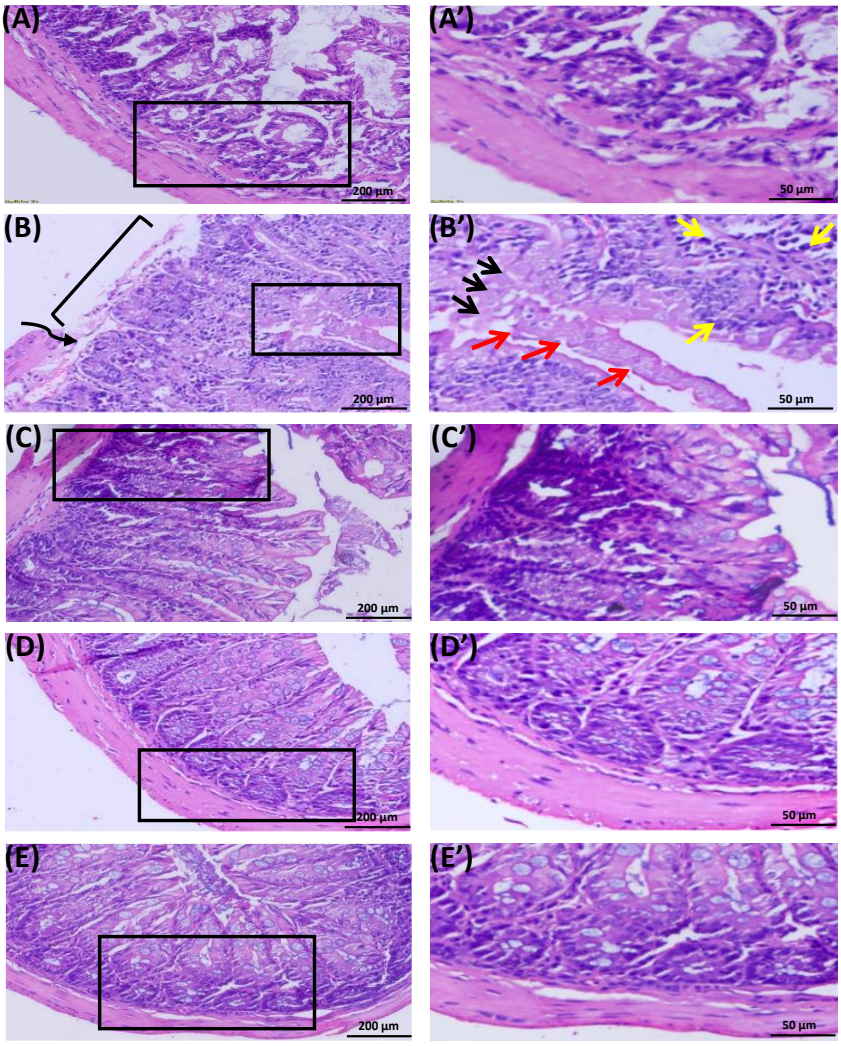

Figure 3.15 Microscopic images of H&E-stained mice colon. (A) Normal Control: showed normal colonic histoarchitecture. (B) DSS: showed depleted goblet cells (black arrows), ulcerated mucosa (red arrows), abnormal crypts (yellow arrows), damaged muscularis layer (single bracket) and submucosal widening (curved arrow). (C) DSS + CLX: showed goblet cells were appeared in mucosa as well as submucosal layer was intact between mucosa and muscularis. (D) DSS + EUD S100-coated CLX-loaded NLC: showed complete colon morphology was regained. (E) Blank EUD S100-coated NLC: similar to normal control group. Images were taken at the magnification of 20X with scale bar = 200 µm (A-E) and 40X with scale bar = 50 µm (A'-E').

To check the integrity of mucin layer, goblet cell staining was performed with Alcian blue and neutral red (AB-NR). Mucins are high molecular weight glycosylated proteins which are secreted from colonic epithelial cells i.e., goblet cells that forms protective viscous mucous layer in the inner wall of intestine. Any disruption of mucous layer may induce inflammation in that particular region because of direct exposure of noxious agent of intestinal tract.[45,46] In normal control group, goblet cells were present as evidenced by stained acidic mucin (blue color). In this study, DSS-induced colitis resulted in disintegration of goblet cells as observed by drastically reduced blue color staining in this group. Treatment with CLX alleviated the diminished goblet cells and thus enhanced acidic mucins were present as evidenced by blue color stain. Treatment with EUD S100-coated CLX-loaded NLC was able to significantly overcome the inflammatory conditions and goblet cells were significantly in this group. Acidic mucins (blue color) in blank EUD S100-coated NLC treated group was presented similar to normal control group **(Figure 3.16)**.

Furthermore, to analyze the predominance of type of mucins, colon sections were stained with high-iron diamine and alcian blue (HID-AB) dyes. There are two types of mucins present in the colon i.e. sulfomucin and sialomucin and it is reported that normal colonic mucosa predominantly secretes sulfomucins, whereas in case of colonic inflammation or colon cancer, predominantly sialomucin get secreted in the colon.[47,48] HID dye stains sulphomucin (which imparts brown color) while AB dye stain sialomucin (which imparts blue color). In our study, sulphomucin (brown color) was predominantly present in normal control group in comparison to sialomucin (blue color). While in DSS-induced colitis, sulfomucin and sialomucin both were reduced due to disintegration of goblet cells and extensive damage to mucosal layer of the colon. Treatment with CLX enhanced the mucin productions as evidenced by the presence of both sialomucin and sulfomucin in similar fashion as shown by stained blue and brown color. In EUD S100-coated CLX-loaded NLC treated group, there was significant predominance of sulfomucin in comparison to sialomucin was observed.

The mucin staining pattern in blank EUD S100-coated NLC group was

similar to normal control group **(Figure 3.17)**. These observations suggested that EUD S100-coated CLX-loaded NLC treatment was able to exert the protective effect on colon by promoting secretion of sulphomucin and suppress the transformation of sulphomucin to sialomucin.

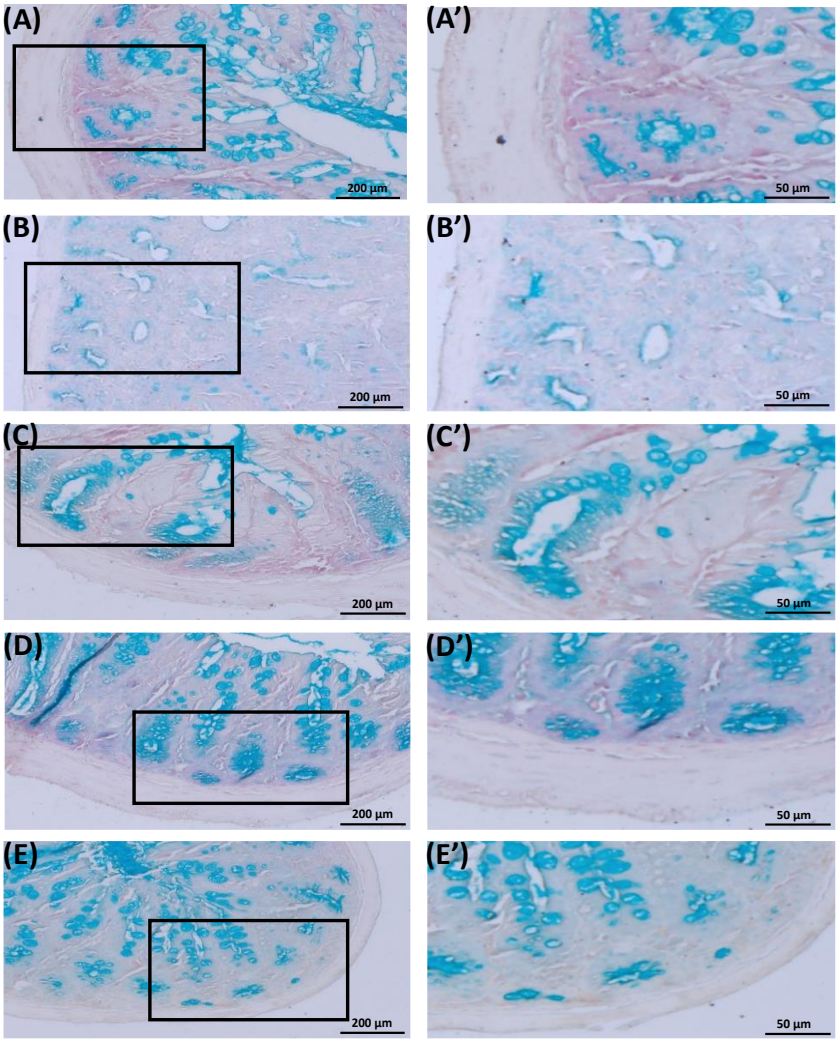

Figure 3.16. Microscopic images of AB-NR-stained mouse colon. (A) Normal Control: showed blue color-stained images of goblet cells. (B) DSS: significantly reduced blue color stain shows disintegration of goblet cells. (C) DSS + CLX: showed recovered goblet cells. (D) DSS + EUD S100-coated CLX-loaded NLC: showed significant increased blue color. (E) Blank EUD S100-coated NLC: showed goblet cells staining similar to normal control. Images were taken at the magnification of 20X (A-E) scale bar = 200 µm and 40X (A'-E') scale bar = 50 µm.

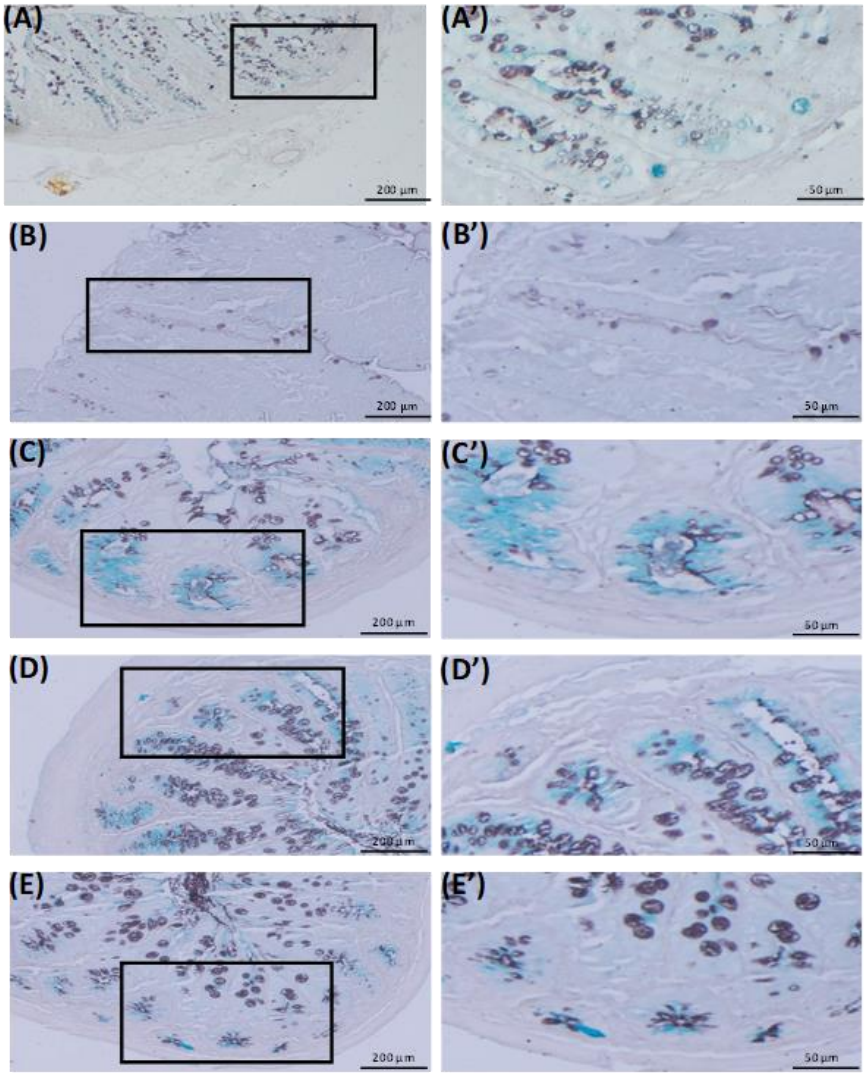

Figure 3.17 Microscopic images of HID-AB-stained colonic sections. (A) Normal Control: showed more sulfomucin (brown color) than sialomucin (blue color). (B) DSS: showed loss of both types of mucins. (C) DSS + CLX: showed enhancement of the mucin productions as evidenced by blue and brown stains. (D) DSS + EUD S100-coated CLX-loaded NLC: exhibited predominance of sulfomucin in comparison to sialomucin. (E) Blank EUD S100-coated NLC: showed mucin staining pattern similar to normal control group. Images were taken at the magnification of 20X (A-E) scale bar = 200 µm and 40X (A'-E') scale bar = 50 µm.

Mast cells are pro-inflammatory cells and play a crucial role in intestinal inflammatory conditions. Histamine is one of the most prevalent inflammatory mediators that gets released from activated mast cells. It causes allergic reactions by imparting tissue and vascular changes. Mast cells infiltration has been noted in colitis and other inflammatory diseases.[49,50] In DSS induced colitis, mast cells infiltration

was observed in sub-mucosa and muscularis layers. Treatment with CLX and EUD S100-coated CLX-loaded NLC attenuated the mast cells infiltration in these groups. In normal control and blank EUD S100-coated NLC group mast cells infiltration was not observed **(Figure 3.18)**. The findings suggest that nanoformulation of CLX reduced the infiltration of mast cells which may lead to reduce the harshness of colitis induced by DSS.

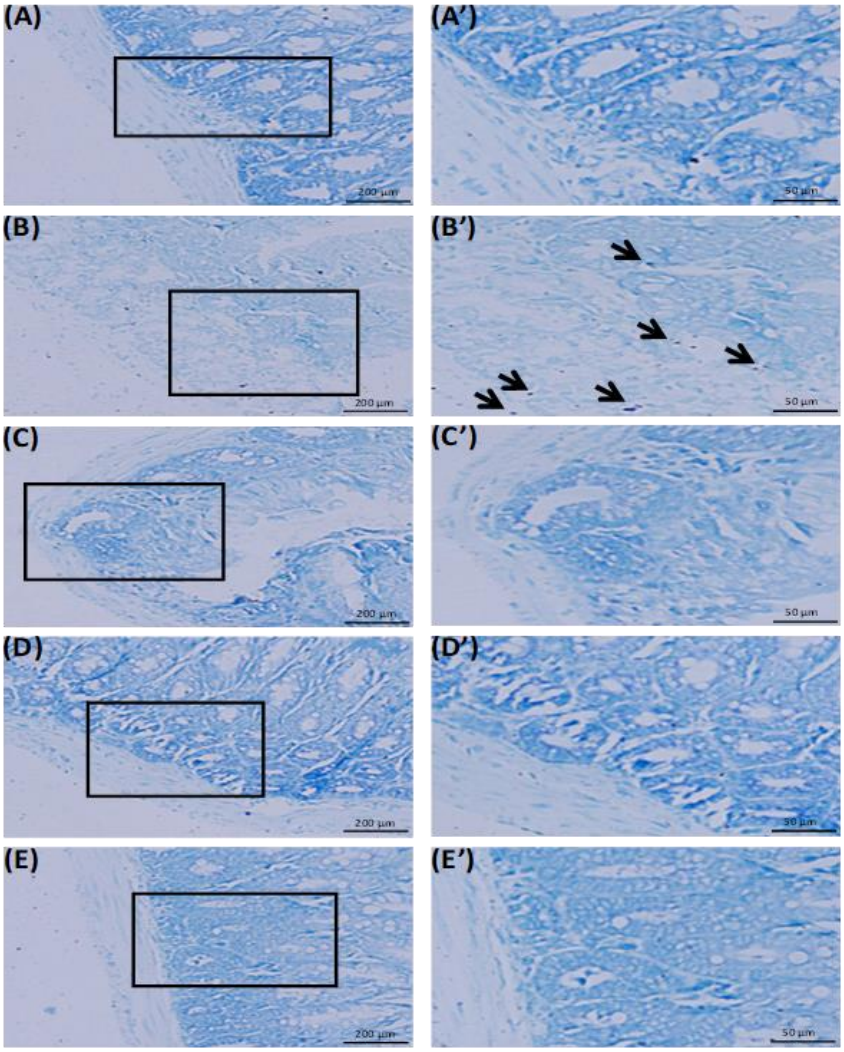

Figure 3.18 Microscopic images of colonic sections stained with toluidine blue. (A) Normal Control: showed no mast cells infiltration in colon section, (B) DSS: showed infiltration of mast cells as purplish-blue color indicated by black arrows, (C) DSS + CLX: (D) DSS + EUD S100-coated CLX-loaded NLC: there were no infiltrated mast cells, (E) Blank EUD S100-coated NLC: did not observed mast cells infiltration. Images were taken at the magnification of 20X (A-E) scale bar = 200 µm and 40X (A'-E') scale bar = 50 µm.

3.2.4.2.1 Immunohistochemical analysis

Cyclooxygenase-2 (COX-2) is an inducible enzyme which in case of inflammatory bowel diseases such as Crohn`s disease and UC, is reported to get overexpressed in colon.[51] While inducible nitric oxide synthase (iNOS) leads to the formation of nitric oxide (NO) that have role in inflammatory processes.[52] Immunohistochemistry for COX-2 and iNOS were also performed to evaluate the potential of EUD S100-coated CLX-loaded NLC in alleviating the expression of inflammatory biomarkers such as COX-2 and iNOS. Additionally, we have also performed semi-quantitative analysis of COX-2 and iNOS expression **(Figure 3.19)**.

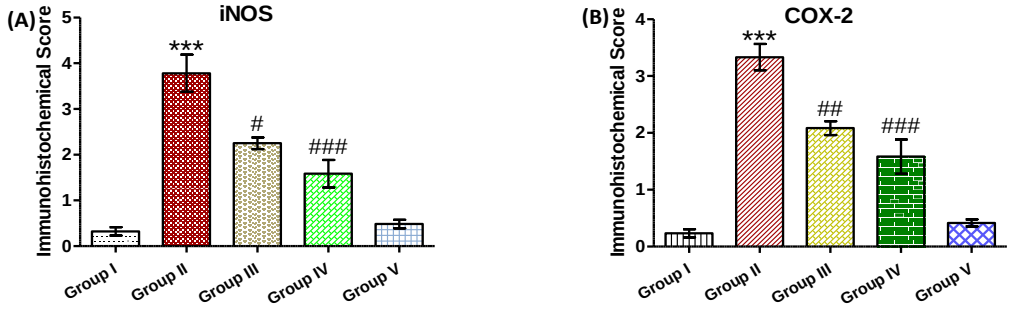

Figure 3.19 Semi-quantitative evaluation of (A) iNOS and (B) COX-2 expression. Group I – Normal Control, Group II – DSS, Group III – DSS + CLX, Group IV – DSS + EUD S100-coated CLX-loaded NLC, Group V – Blank EUD S100-coated NLC. Significant differences were indicated by ***p ≤ 0.001, as compared to control and #p ≤ 0.05, ##p ≤ 0.01 and ###p ≤0.001 as compared to DSS group. The experiments were performed in triplicate (n = 3) and data are presented as mean ± standard deviation of three independent sets of observations.

In normal control and blank EUD S100-coated NLC treated group, remarkably less iNOS- and COX-2-immunopositive cells (brown color) were observed. In DSS-treated group, there was a significant overexpression of iNOS (***p≤0.001) and COX-2 (***p≤0.001) in comparison to normal control. Treatment with CLX (#p≤0.05) and EUD S100-coated CLX-loaded NLC (###p≤0.001) were able to downregulate the overexpression of iNOS in comparison to DSS group **(Figure 3.19A and Figure 3.20)**. Similarly, treatment with CLX (##p≤0.01) and EUD S100-coated CLX-loaded NLC (###p≤0.001) was able to downregulate the

overexpression of COX-2 in comparison to DSS group. **(Figure 3.19B and Figure 3.20)**. The results suggest that EUD S100-coated CLX-loaded NLC have strong potential to attenuate the expression of inflammatory biomarkers.

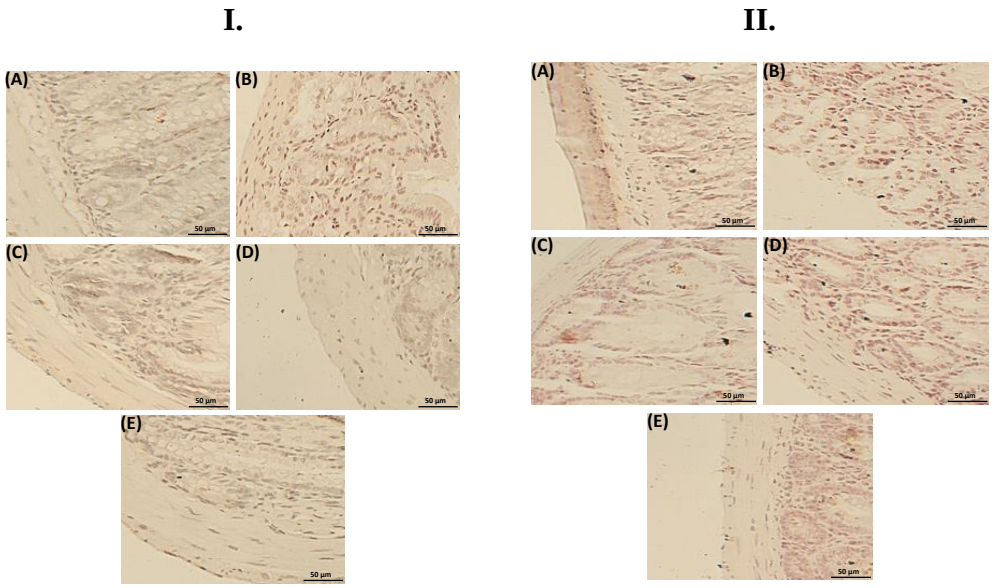

Figure 3.20 Immunohistochemical staining of (I) iNOS, and (II) COX-2. Microscopic images of colonic sections representing immunohistochemical analyses, brown color indicates specific immunostaining of iNOS and COX-2, while light blue color indicates counter staining of hematoxylin. (A) Normal Control: showed very low expression of iNOS and COX-2 in comparison to DSS group. (B) DSS: exhibited enhanced expression of iNOS and COX-2 in comparison to normal control. (C) DSS + CLX: exhibited decreased expression of iNOS and COX-2 as compared to DSS group. (D) DSS + EUD S100-coated CLX-loaded NLC: exhibited reduced iNOS and COX-2 expression in comparison to DSS group (E) Blank EUD S100-coated NLC: showed very low expression of iNOS similar to normal control. Images were taken at the magnification of 40X (A'-E') Scale Bar = 50 µm.

3.3 Conclusion

In the present study, a novel biocompatible nanoformulation for celecoxib drug has been developed with colon specific characteristic. Importantly, nanocarrier was developed using generally recognized as safe (GRAS) compounds, approved by US-FDA, which are non-toxic, safe for enteral human use and cost-effective. This study suggests that EUD S100-coated CLX-loaded NLC is a convenient

nanoformulation that adequately target colon tissue. The NLC possessed favourable characteristics, showed sustained release of CLX in physiological buffer solution and were cytocompatible for the normal cells. EUD S100-coated CLX-loaded NLC effectively overcame the inflammatory changes induced by DSS.

Note: Reprinted with permission from: -

Mishra, R. K.; Ahmad, A.; Kumar, A.; Vyawahare, A.; Raza, S. S.; Khan, R. Lipid-Based Nanocarrier-Mediated Targeted Delivery of Celecoxib Attenuate Severity of Ulcerative Colitis. *Materials Science and Engineering: C* **2020**, *116*, 111103. https://doi.org/10.1016/j.msec.2020.111103.

3.4 Bibliography

(1) Gopi, S.; Amalraj, A.; Jude, S.; Varma, K.; Sreeraj, T. R.; Haponiuk, J. T.; Thomas, S. Preparation, Characterization and Anti-Colitis Activity of Curcumin-Asafoetida Complex Encapsulated in Turmeric Nanofiber. *Materials Science and Engineering: C* **2017**, *81*, 20–31. https://doi.org/10.1016/j.msec.2017.07.037.

(2) Lv, J.; Zhang, Y.; Tian, Z.; Liu, F.; Shi, Y.; Liu, Y.; Xia, P. Astragalus Polysaccharides Protect against Dextran Sulfate Sodium-Induced Colitis by Inhibiting NF-KB Activation. *International Journal of Biological Macromolecules* **2017**, *98*, 723–729. https://doi.org/10.1016/j.ijbiomac.2017.02.024.

(3) Sharara, A. I.; Awadhi, S. A.; Alharbi, O.; Dhahab, H. A.; Mounir, M.; Salese, L.; Singh, E.; Sunna, N.; Tarcha, N.; Mosli, M. Epidemiology, Disease Burden, and Treatment Challenges of Ulcerative Colitis in Africa and the Middle East. *Expert Review of Gastroenterology & Hepatology* **2018**, *12* (9), 883–897. https://doi.org/10.1080/17474124.2018.1503052.

(4) Chen, Q.; Gou, S.; Ma, P.; Song, H.; Zhou, X.; Huang, Y.; Kwon Han, M.; Wan, Y.; Kang, Y.; Xiao, B. Oral Administration of Colitis Tissue-Accumulating Porous

Nanoparticles for Ulcerative Colitis Therapy. *International Journal of Pharmaceutics* **2019**, *557*, 135–144. https://doi.org/10.1016/j.ijpharm.2018.12.046.

(5) Gaba, B.; Fazil, M.; Khan, S.; Ali, A.; Baboota, S.; Ali, J. Nanostructured Lipid Carrier System for Topical Delivery of Terbinafine Hydrochloride. *Bulletin of Faculty of Pharmacy, Cairo University* **2015**, *53* (2), 147–159. https://doi.org/10.1016/j.bfopcu.2015.10.001.

(6) Serrano-Olvera, A.; Cetina, L.; Coronel, J.; Dueñas-González, A. Emerging Drugs for the Treatment of Cervical Cancer. *Expert Opinion on Emerging Drugs* **2015**, *20* (2), 165–182. https://doi.org/10.1517/14728214.2015.1002768.

(7) Ashton, J. J.; Mossotto, E.; Ennis, S.; Beattie, R. M. Personalising Medicine in Inflammatory Bowel Disease—Current and Future Perspectives. *Transl Pediatr* **2019**, *8* (1), 56–69. https://doi.org/10.21037/tp.2018.12.03.

(8) Meier, J.; Sturm, A. Current Treatment of Ulcerative Colitis. *World J Gastroenterol* **2011**, *17* (27), 3204–3212. https://doi.org/10.3748/wjg.v17.i27.3204.

(9) Wallace, J. L. Nonsteroidal Anti-Inflammatory Drugs and Gastroenteropathy: The Second Hundred Years. *Gastroenterology* **1997**, *112* (3), 1000–1016. https://doi.org/10.1053/gast.1997.v112.pm9041264.

(10) van Midwoud, P. M.; Sandker, M.; Hennink, W. E.; de Leede, L. G. J.; Chan, A.; Weinans, H. In Vivo Pharmacokinetics of Celecoxib Loaded Endcapped PCLA-PEG-PCLA Thermogels in Rats after Subcutaneous Administration. *European Journal of Pharmaceutics and Biopharmaceutics* **2018**, *131*, 170–177. https://doi.org/10.1016/j.ejpb.2018.07.026.

(11) Shin, S. Safety of Celecoxib versus Traditional Nonsteroidal Anti-Inflammatory Drugs in Older Patients with Arthritis. *J Pain Res* **2018**, *11*, 3211–3219. https://doi.org/10.2147/JPR.S186000.

(12) Kim, E. R.; Chang, D. K. Colorectal Cancer in Inflammatory Bowel Disease: The Risk, Pathogenesis, Prevention and Diagnosis. *World J Gastroenterol* **2014**, *20* (29), 9872–9881. https://doi.org/10.3748/wjg.v20.i29.9872.

(13) Spisni, E.; Valerii, M. C.; De Fazio, L.; Cavazza, E.; Borsetti, F.; Sgromo, A.; Candela, M.; Centanni, M.; Rizello, F.; Strillacci, A. Cyclooxygenase-2 Silencing for the Treatment of Colitis: A Combined In Vivo Strategy Based on RNA

Interference and Engineered Escherichia Coli. *Molecular Therapy* **2015**, *23* (2), 278–289. https://doi.org/10.1038/mt.2014.222.

(14) Cooper, D. L.; Harirforoosh, S. Effect of Formulation Variables on Preparation of Celecoxib Loaded Polylactide-Co-Glycolide Nanoparticles. *PLoS One* **2014**, *9* (12). https://doi.org/10.1371/journal.pone.0113558.

(15) Goldenberg, M. M. Celecoxib, a Selective Cyclooxygenase-2 Inhibitor for the Treatment of Rheumatoid Arthritis and Osteoarthritis. *Clinical Therapeutics* **1999**, *21* (9), 1497–1513. https://doi.org/10.1016/S0149-2918(00)80005-3.

(16) Pereira, P. A. T.; Trindade, B. C.; Secatto, A.; Nicolete, R.; Peres-Buzalaf, C.; Ramos, S. G.; Sadikot, R.; Bitencourt, C. da S.; Faccioli, L. H. *Celecoxib Improves Host Defense through Prostaglandin Inhibition during Histoplasma capsulatum Infection*. Mediators of Inflammation. https://www.hindawi.com/journals/mi/2013/950981/ (accessed 2020-04-22). https://doi.org/10.1155/2013/950981.

(17) Bazan, L.; Bendas, E. R.; Gazayerly, O. N. E.; Badawy, S. S. Comparative Pharmaceutical Study on Colon Targeted Micro-Particles of Celecoxib: In-Vitro–in-Vivo Evaluation. *Drug Delivery* **2016**, *23* (9), 3339–3349. https://doi.org/10.1080/10717544.2016.1178824.

(18) Patra, J. K.; Das, G.; Fraceto, L. F.; Campos, E. V. R.; Rodriguez-Torres, M. del P.; Acosta-Torres, L. S.; Diaz-Torres, L. A.; Grillo, R.; Swamy, M. K.; Sharma, S.; Habtemariam, S.; Shin, H.-S. Nano Based Drug Delivery Systems: Recent Developments and Future Prospects. *Journal of Nanobiotechnology* **2018**, *16* (1), 71. https://doi.org/10.1186/s12951-018-0392-8.

(19) Lombardo, D.; Kiselev, M. A.; Caccamo, M. T. *Smart Nanoparticles for Drug Delivery Application: Development of Versatile Nanocarrier Platforms in Biotechnology and Nanomedicine*. Journal of Nanomaterials. https://www.hindawi.com/journals/jnm/2019/3702518/ (accessed 2020-04-20). https://doi.org/10.1155/2019/3702518.

(20) Geszke-Moritz, M.; Moritz, M. Solid Lipid Nanoparticles as Attractive Drug Vehicles: Composition, Properties and Therapeutic Strategies. *Mater Sci Eng C Mater Biol Appl* **2016**, *68*, 982–994. https://doi.org/10.1016/j.msec.2016.05.119.

(21) Lu, H.; Wang, J.; Wang, T.; Zhong, J.; Bao, Y.; Hao, H. *Recent Progress on Nanostructures for Drug Delivery Applications*. Journal of Nanomaterials. https://www.hindawi.com/journals/jnm/2016/5762431/ (accessed 2020-04-20). https://doi.org/10.1155/2016/5762431.

(22) Singh, A. P.; Biswas, A.; Shukla, A.; Maiti, P. Targeted Therapy in Chronic Diseases Using Nanomaterial-Based Drug Delivery Vehicles. *Signal Transduction and Targeted Therapy* **2019**, *4* (1), 1–21. https://doi.org/10.1038/s41392-019-0068-3.

(23) Huang, Z.; Hua, S.; Yang, Y.; Fang, J. Development and Evaluation of Lipid Nanoparticles for Camptothecin Delivery: A Comparison of Solid Lipid Nanoparticles, Nanostructured Lipid Carriers, and Lipid Emulsion. *Acta Pharmacologica Sinica* **2008**, *29* (9), 1094–1102. https://doi.org/10.1111/j.1745-7254.2008.00829.x.

(24) Mukherjee, S.; Ray, S.; Thakur, R. S. Solid Lipid Nanoparticles: A Modern Formulation Approach in Drug Delivery System. *Indian J Pharm Sci* **2009**, *71* (4), 349–358. https://doi.org/10.4103/0250-474X.57282.

(25) Shirodkar, R. K.; Kumar, L.; Mutalik, S.; Lewis, S. Solid Lipid Nanoparticles and Nanostructured Lipid Carriers: Emerging Lipid Based Drug Delivery Systems. *Pharmaceutical Chemistry Journal* **2019**, *53* (5), 440–453. https://doi.org/10.1007/s11094-019-02017-9.

(26) Kraisit, P.; Sarisuta, N. Development of Triamcinolone Acetonide-Loaded Nanostructured Lipid Carriers (NLCs) for Buccal Drug Delivery Using the Box-Behnken Design. *Molecules* **2018**, *23* (4), 982. https://doi.org/10.3390/molecules23040982.

(27) Khan, S.; Baboota, S.; Ali, J.; Khan, S.; Narang, R. S.; Narang, J. K. Nanostructured Lipid Carriers: An Emerging Platform for Improving Oral Bioavailability of Lipophilic Drugs. *International Journal of Pharmaceutical Investigation* **2015**, *5* (4), 182. https://doi.org/10.4103/2230-973X.167661.

(28) Cirri, M.; Maestrini, L.; Maestrelli, F.; Mennini, N.; Mura, P.; Ghelardini, C.; Mannelli, L. D. C. Design, Characterization and in Vivo Evaluation of Nanostructured Lipid Carriers (NLC) as a New Drug Delivery System for

Hydrochlorothiazide Oral Administration in Pediatric Therapy. *Drug Delivery* **2018**, *25* (1), 1910–1921. https://doi.org/10.1080/10717544.2018.1529209.

(29) Bondì, M. L.; Emma, M. R.; Botto, C.; Augello, G.; Azzolina, A.; Di Gaudio, F.; Craparo, E. F.; Cavallaro, G.; Bachvarov, D.; Cervello, M. Biocompatible Lipid Nanoparticles as Carriers To Improve Curcumin Efficacy in Ovarian Cancer Treatment. *J. Agric. Food Chem.* **2017**, *65* (7), 1342–1352. https://doi.org/10.1021/acs.jafc.6b04409.

(30) Zhang, X.-G.; Miao, J.; Dai, Y.-Q.; Du, Y.-Z.; Yuan, H.; Hu, F.-Q. Reversal Activity of Nanostructured Lipid Carriers Loading Cytotoxic Drug in Multi-Drug Resistant Cancer Cells. *International Journal of Pharmaceutics* **2008**, *361* (1), 239–244. https://doi.org/10.1016/j.ijpharm.2008.06.002.

(31) Wang, M.; Jin, Y.; Yang, Y.; Zhao, C.; Yang, H.; Xu, X.; Qin, X.; Wang, Z.; Zhang, Z.; Jian, Y.; Huang, Y. In Vivo Biodistribution, Anti-Inflammatory, and Hepatoprotective Effects of Liver Targeting Dexamethasone Acetate Loaded Nanostructured Lipid Carrier System. *Int J Nanomedicine* **2010**, *5*, 487–497.

(32) Zai, K.; Hirota, M.; Yamada, T.; Ishihara, N.; Mori, T.; Kishimura, A.; Suzuki, K.; Hase, K.; Katayama, Y. Therapeutic Effect of Vitamin D3-Containing Nanostructured Lipid Carriers on Inflammatory Bowel Disease. *Journal of Controlled Release* **2018**, *286*, 94–102. https://doi.org/10.1016/j.jconrel.2018.07.019.

(33) Jaiswal, P.; Gidwani, B.; Vyas, A. Nanostructured Lipid Carriers and Their Current Application in Targeted Drug Delivery. *Artificial Cells, Nanomedicine, and Biotechnology* **2016**, *44* (1), 27–40. https://doi.org/10.3109/21691401.2014.909822.

(34) Beloqui, A.; del Pozo-Rodríguez, A.; Isla, A.; Rodríguez-Gascón, A.; Solinís, M. Á. Nanostructured Lipid Carriers as Oral Delivery Systems for Poorly Soluble Drugs. *Journal of Drug Delivery Science and Technology* **2017**, *42*, 144–154. https://doi.org/10.1016/j.jddst.2017.06.013.

(35) Sachs, C.; Brittain, H.; Cohen, E. *Synopsis*; 1989.

(36) Tiwari, M.; Kakkar, P. Plant Derived Antioxidants – Geraniol and Camphene Protect Rat Alveolar Macrophages against t-BHP Induced Oxidative Stress.

Toxicology in Vitro **2009**, *23* (2), 295–301. https://doi.org/10.1016/j.tiv.2008.12.014.

(37) Gaba, B.; Fazil, M.; Khan, S.; Ali, A.; Baboota, S.; Ali, J. Nanostructured Lipid Carrier System for Topical Delivery of Terbinafine Hydrochloride. *Bulletin of Faculty of Pharmacy, Cairo University* **2015**, *53* (2), 147–159. https://doi.org/10.1016/j.bfopcu.2015.10.001.

(38) Danaei, M.; Dehghankhold, M.; Ataei, S.; Hasanzadeh Davarani, F.; Javanmard, R.; Dokhani, A.; Khorasani, S.; Mozafari, M. R. Impact of Particle Size and Polydispersity Index on the Clinical Applications of Lipidic Nanocarrier Systems. *Pharmaceutics* **2018**, *10* (2), 57. https://doi.org/10.3390/pharmaceutics10020057.

(39) Ahmad, A.; Fauzia, E.; Kumar, M.; Mishra, R. K.; Kumar, A.; Khan, M. A.; Raza, S. S.; Khan, R. Gelatin-Coated Polycaprolactone Nanoparticle-Mediated Naringenin Delivery Rescue Human Mesenchymal Stem Cells from Oxygen Glucose Deprivation-Induced Inflammatory Stress. *ACS Biomater. Sci. Eng.* **2019**, *5* (2), 683–695. https://doi.org/10.1021/acsbiomaterials.8b01081.

(40) Tsai, S.-W.; Yu, D.-S.; Tsao, S.-W.; Hsu, F.-Y. Hyaluronan–Cisplatin Conjugate Nanoparticles Embedded in Eudragit S100-Coated Pectin/Alginate Microbeads for Colon Drug Delivery. *Int J Nanomedicine* **2013**, *8*, 2399–2407. https://doi.org/10.2147/IJN.S46613.

(41) Gupta, A.; Ahmad, A.; Singh, H.; Kaur, S.; K M, N.; Ansari, Md. M.; Jayamurugan, G.; Khan, R. Nanocarrier Composed of Magnetite Core Coated with Three Polymeric Shells Mediates LCS-1 Delivery for Synthetic Lethal Therapy of BLM-Defective Colorectal Cancer Cells. *Biomacromolecules* **2018**, *19* (3), 803–815. https://doi.org/10.1021/acs.biomac.7b01607.

(42) Abdelmegid, A. M.; Abdo, F. K.; Ahmed, F. E.; Kattaia, A. A. A. Therapeutic Effect of Gold Nanoparticles on DSS-Induced Ulcerative Colitis in Mice with Reference to Interleukin-17 Expression. *Sci Rep* **2019**, *9* (1), 1–16. https://doi.org/10.1038/s41598-019-46671-1.

(43) Balaha, M.; Kandeel, S.; Elwan, W. Garlic Oil Inhibits Dextran Sodium Sulfate-Induced Ulcerative Colitis in Rats. *Life Sciences* **2016**, *146*, 40–51. https://doi.org/10.1016/j.lfs.2016.01.012.

(44) Islam, J.; Sato, S.; Watanabe, K.; Watanabe, T.; Ardiansyah; Hirahara, K.; Aoyama, Y.; Tomita, S.; Aso, H.; Komai, M.; Shirakawa, H. Dietary Tryptophan Alleviates Dextran Sodium Sulfate-Induced Colitis through Aryl Hydrocarbon Receptor in Mice. *The Journal of Nutritional Biochemistry* **2017**, *42*, 43–50. https://doi.org/10.1016/j.jnutbio.2016.12.019.

(45) Khan, R.; Khan, A. Q.; Lateef, A.; Rehman, M. U.; Tahir, M.; Ali, F.; Hamiza, O. O.; Sultana, S. Glycyrrhizic Acid Suppresses the Development of Precancerous Lesions via Regulating the Hyperproliferation, Inflammation, Angiogenesis and Apoptosis in the Colon of Wistar Rats. *PLOS ONE* **2013**, *8* (2), e56020. https://doi.org/10.1371/journal.pone.0056020.

(46) Larsson, J. M. H.; Karlsson, H.; Crespo, J. G.; Johansson, M. E. V.; Eklund, L.; Sjövall, H.; Hansson, G. C. Altered O-Glycosylation Profile of MUC2 Mucin Occurs in Active Ulcerative Colitis and Is Associated with Increased Inflammation. *Inflamm Bowel Dis* **2011**, *17* (11), 2299–2307. https://doi.org/10.1002/ibd.21625.

(47) Croix, J. A.; Carbonero, F.; Nava, G. M.; Russell, M.; Greenberg, E.; Gaskins, H. R. On the Relationship between Sialomucin and Sulfomucin Expression and Hydrogenotrophic Microbes in the Human Colonic Mucosa. *PLOS ONE* **2011**, *6* (9), e24447. https://doi.org/10.1371/journal.pone.0024447.

(48) Deplancke, B.; Gaskins, H. R. Microbial Modulation of Innate Defense: Goblet Cells and the Intestinal Mucus Layer. *Am J Clin Nutr* **2001**, *73* (6), 1131S-1141S. https://doi.org/10.1093/ajcn/73.6.1131S.

(49) Luchini, A. C.; Costa de Oliveira, D. M.; Pellizzon, C. H.; Di Stasi, L. C.; Gomes, J. C. *Relationship between Mast Cells and the Colitis with Relapse Induced by Trinitrobenzesulphonic Acid in Wistar Rats*. Mediators of Inflammation. https://www.hindawi.com/journals/mi/2009/432493/abs/ (accessed 2019-11-16). https://doi.org/10.1155/2009/432493.

(50) Branco, A. C. C. C.; Yoshikawa, F. S. Y.; Pietrobon, A. J.; Sato, M. N. *Role of Histamine in Modulating the Immune Response and Inflammation*. Mediators of Inflammation. https://www.hindawi.com/journals/mi/2018/9524075/abs/ (accessed 2019-11-16). https://doi.org/10.1155/2018/9524075.

(51) Spisni, E.; Valerii, M. C.; De Fazio, L.; Cavazza, E.; Borsetti, F.; Sgromo, A.; Candela, M.; Centanni, M.; Rizello, F.; Strillacci, A. Cyclooxygenase-2 Silencing for the Treatment of Colitis: A Combined In Vivo Strategy Based on RNA Interference and Engineered Escherichia Coli. *Molecular Therapy* **2015**, *23* (2), 278–289. https://doi.org/10.1038/mt.2014.222.

(52) Schreiber, O.; Petersson, J.; Waldén, T.; Ahl, D.; Sandler, S.; Phillipson, M.; Holm, L. INOS-Dependent Increase in Colonic Mucus Thickness in DSS-Colitic Rats. *PLOS ONE* **2013**, *8* (8), e71843. https://doi.org/10.1371/journal.pone.0071843.

Lipid-based nanocarrier-mediated targeted delivery of celecoxib attenuate severity of ulcerative colitis

Author:
Rakesh Kumar Mishra,Anas Ahmad,Ajay Kumar,Akshay Vyawahare,Syed Shadab Raza,Rehan Khan

Publication: Materials Science and Engineering: C

Publisher: Elsevier

Date: November 2020

Journal Author Rights

BACK CLOSE WINDOW

Materials Science & Engineering C 116 (2020) 111103

Contents lists available at ScienceDirect

Materials Science & Engineering C

journal homepage: www.elsevier.com/locate/msec

Lipid-based nanocarrier-mediated targeted delivery of celecoxib attenuate severity of ulcerative colitis

Rakesh Kumar Mishra[a], Anas Ahmad[a], Ajay Kumar[a], Akshay Vyawahare[a], Syed Shadab Raza[b], Rehan Khan[a,*]

[a] Institute of Nano Science and Technology, Habitat Centre, Phase - 10, Sector 64, Mohali, Punjab 160062, India
[b] Laboratory for Stem Cell and Restorative Neurology, Department of Biotechnology, Era's Lucknow Medical College Hospital, Sarfarazganj, Lucknow 226003, India

ARTICLE INFO

Keywords:
Ulcerative colitis
Celecoxib
Lipid nanocarrier
Drug delivery
Inflammation

ABSTRACT

Ulcerative colitis is a chronic mucosal inflammatory condition that adversely affects colon and rectum. Celecoxib is a selective inhibitor of inducible cyclooxygenase-2 (COX-2) and is prescribed for the management of pain and other inflammatory disorders. The physicochemical properties of celecoxib limit its clinical potency. Here we developed nanostructured lipid carriers (NLCs) using Generally Recognized as Safe and US-FDA approved compounds for encapsulating celecoxib. Present study was aimed to evaluate efficacy of eudragit-S100-coated celecoxib-loaded NLCs against DSS-induced colitis in mice. NLCs were formulated by hot-melt method and possessed the average particle size of 250.90 nm and entrapment efficiency (%) was 59.89%. Furthermore, size, shape and morphology of NLCs were confirmed using TEM, SEM and AFM. The blank NLCs were cytocompatible against hTERT-BJ cells up to a dose of 200 μg/ml. Treatment with celecoxib-loaded NLCs alleviated severity of colitis as demonstrated by disease activity index, colon length, fecal occult blood test, and histopathological analysis. Moreover, treatment with celecoxib-loaded NLCs reduced disintegration of goblets cells and restores sulfomucin in colon. Celecoxib-nanoformulation markedly reduced colonic inflammation as evidenced by decreased immunohistochemical expression of COX-2 and iNOS. The observations of study suggest that lipid-based colon specific delivery of celecoxib may be used for management of colitis.

1. Introduction

Ulcerative colitis (UC) is a chronic inflammatory disease which primarily affects the rectum and spreads toward the lower end of the colon [1]. Damage to the intestinal epithelium enables the lumen microbiota to evoke inflammatory responses because of the activation of immune system and cytokine production. UC can lead to several complications like abdominal pain, diarrhea, rectal bleeding etc. [2] and if the disease is left untreated it may further lead to the development of colorectal cancer [3,4].

The conventional and currently prevailing therapeutic regimens for ulcerative colitis include antibiotics, immunosuppressive agents, aminosalicylates, corticosteroids and biologics, but they provide symptomatic treatment and are associated with long term adverse drug reactions. Furthermore, these drugs have limited efficacy because of other factors like drug inactivation in harsh gastric acid surroundings, high first pass metabolism, low solubility and as a result low bioavailability [6–8]. Non-steroidal anti-inflammatory drugs (NSAIDs) have been mostly used to manage the disease-associated pain and inflammation [9]. Celecoxib (CLX) is a NSAID, which selectively inhibits cyclooxygenase-2 (COX-2) enzyme. It is commonly prescribed in the management of rheumatoid arthritis and osteoarthritis for the pain management but higher dose consumptions have been associated with increased risk of adverse cardiovascular, renal and gastrointestinal events [10,11]. COX-2 is an inducible enzyme which is reported to get overexpressed in inflamed colonic mucosa by producing different inflammatory cytokines and is well reported in UC [12,13]. CLX treatment minimizes the gastric side effects of conventional NSAIDs and may produce significant therapeutic effects in UC. As CLX is able to selectively inhibit COX-2 enzyme without affecting another isoform i.e. COX-1, it helps to alleviate inflammation, fever and pain together with minimized side effects like gastric ulcers and gastric mucosal erosions which are strongly associated with COX-1 inhibition [14–16]. Despite the diverse advantages of CLX, it has some limitations such as poor water solubility, large volume of distribution and low oral bioavailability [17].

To overcome the aforementioned drug limitations, several nanotechnology based drug delivery systems have been developed to address

* Corresponding author.
E-mail address: rehankhan@inst.ac.in (R. Khan).

https://doi.org/10.1016/j.msec.2020.111103
Received 30 January 2020; Received in revised form 2 May 2020; Accepted 18 May 2020
Available online 20 May 2020
0928-4931/

Chapter 4

Cortisone loaded stearoyl ascorbic acid nanostructured lipid carrier for ulcerative colitis

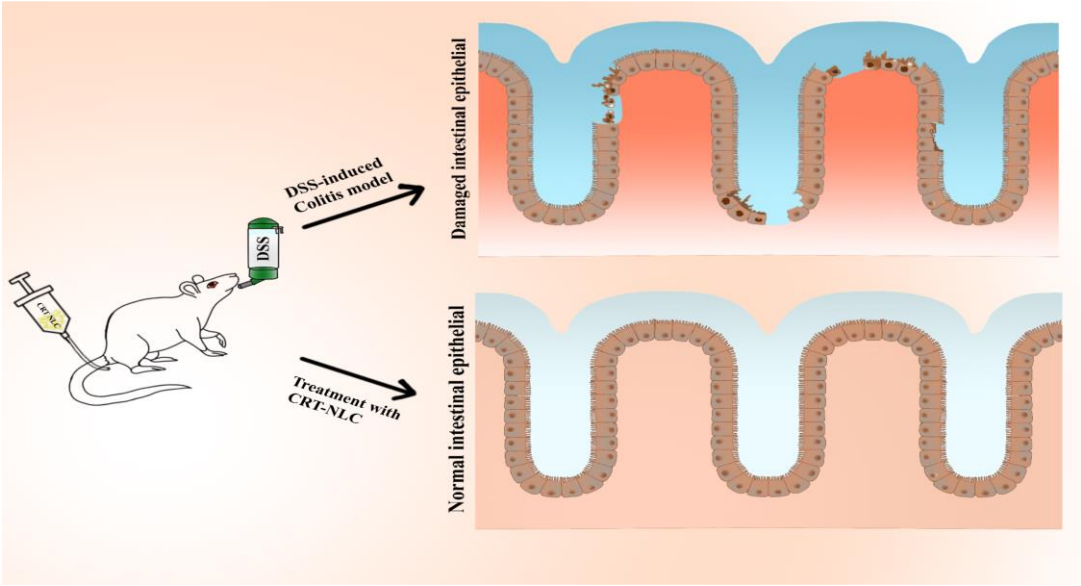

Graphical abstract

4.1 Introduction

Ulcerative colitis (UC) is one of chronic inflammatory bowel disease that primarily affect the rectum and spread over the distal end of colon. UC is recognized by irregular inflammatory reactions and severe disturbance of epithelial barrier lining of colon.[1,2] Any harm to the intestinal epithelium causes immune system activation and cytokines production. Overproduction of various reactive oxygen species or imbalance between generation of free radicals and antioxidant defense machinery are the key promotors of inflammatory disease like UC.[3] These may also recruit various proinflammatory enzymes and cytokines that further enhances the inflammatory reactions and play as a modulator for the pathological conditions of UC.[4] This may affect the important functionalities of colon and if left unmanaged it may develop life threatening colon cancer disease. Rectal bleeding, weight loss, intestinal mucosal damage etc. are some of the prominent features of UC.[5,6]

The existing and conventional therapy for the treatment of UC includes aminosalicylates, antibiotics, immunosuppressants etc. where these provides symptomatic relief but associated with various side effects. They also possess different physicochemical limitations like enhanced first pass metabolism, drug degradation in gastric environment etc.[7,8]

From very long back corticosteroids are also used for the management of UC. In this cortisone is very efficacious to relief the inflammatory conditions in UC patients. There are reports that concluded, if this drug is used for limited times and with low doses its efficacy is very high for inflammatory disease like colitis and other inflammatory bowel diseases. But cortisone also have some limitations like low water solubility as well as very short half-life that compromises its therapeutic efficacy and potency.[9,10]

To conquer above drug related problems, different nanoscience based novel drug delivery systems have been evolved to rationalize the therapeutic outcomes of drug and delivery systems. These delivery systems markedly enhance bare drug related problems like solubility, bioavailability, unwanted effects and combinedly regulate pharmacological outcome of treatment.[11,12] Lipid based delivery systems are the advancement of drug delivery technology that may significantly

upgrade the solubility of poorly water-soluble/hydrophobic drugs and enhances its bioavailability.[13,14] Advanced solid lipid nanoparticles that are also known as nanostructured lipid carriers (NLCs) are 100-1000 nm carriers which proved to enhance drug encapsulation and loading capacity, ensure regulated drug release profile and limits drug leakage etc. from formulations.[15,16] The production as well as sterilization process of NLCs are quite easy and they are more stable on long term storage. In this way, NLCs are potential carrier reported for administration of very low water soluble, less bioavailable and highly lipophilic drugs for colitis treatment.

In this study we have prepared cortisone (CRT) encapsulated stearoyl ascorbic acid NLCs and tested against dextran sodium sulfate (DSS)-induced colitic mice. For the formulation of NLC, 6-o-stearoyl ascorbic acid (SAA) was incorporated as solid lipid, linalool as liquid lipid and PF-127 as hydrophilic emulsifier. SAA is a stearyl ester of ascorbic acid which is an antioxidant molecule and form amphiphile with stearic acid. It is USFDA approved material for drug and pharmaceuticals use and categorized generally recognized as safe (GRAS) and linalool is also plant originated compound in the formulation which is known for its antioxidant, anti-inflammatory, antimicrobial activities. Together with CRT the proposed composition of formulation enhances the anti-inflammatory activity and also provide defence from oxidative stress towards the colonic inflammation. As this formulation fabricated with USFDA GRAS materials it makes the formulation as non-toxic as well as biocompatible delivery system.

4.2 Results and discussion

4.2.1 Formulation and characterization of NLCs

In the present study CRT encapsulated SAA NLCs were formulated by hot melt technique (**Figure 4.1**) following the previously optimized parameters in our lab.

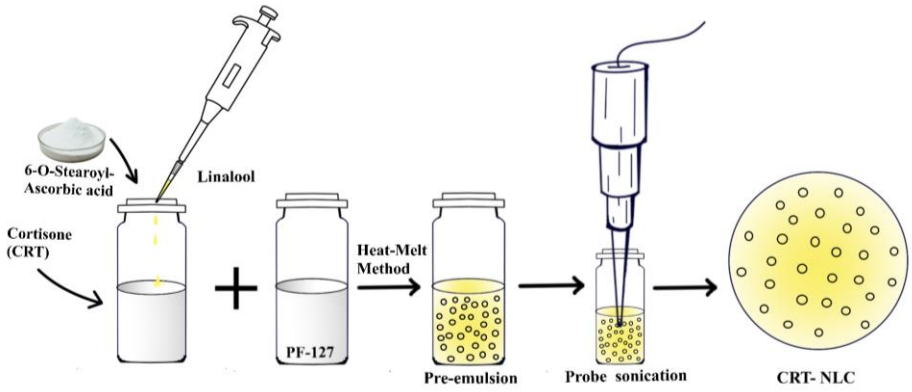

Figure 4.1 Scheme of NLC development.

By varying the concentration of all the ingredients different batches has been prepared (**Table 4.1**). Initial optimization and characterizations were also performed accordingly.[17]

Table 4.1: Shows different batches (F1-F7) along with ingredients and their amounts. SAA - 6-O-Stearoyl-L-Ascorbic Acid, PF-127- Pluronic F-127, D. Water- Distilled water.

S. No.	Ingredients (mg)	Batches							
		B1	B2	B3	B4	B5	B6	B7	B7D
1.	SAA	90	90	60	45	105	140	70	70
2.	Linalool	60	60	40	30	45	60	30	30
3.	PF-127	100	150	100	100	100	200	100	100
4.	Drug	-	-	-	-	-	-	-	15
6.	D. Water (ml)	q.s.	q.s.	q.s.	q.s.	q.s.	q.s.	q.s.	q.s.

By varying the concentration of all the employed ingredients of NLCs optimization were done. Initial characterizations were performed for hydrodynamic diameter and zeta potential with the help of Zetasizer. The hydrodynamic diameter of blank NLC was 151.7 nm which slightly enhanced after drug loading as 182 nm. The

polydispersity index of blank as well as CRT loaded NLC was found to be 0.06 and 0.11 respectively which shows nanocarriers were monodispersed. Similarly, zeta potential of blank NLC as well as CRT loaded NLC was -30.9 mV and -29.5 mV makes the formulation stable as they repel to each other in the dispersion medium (**Figure 4.2**).

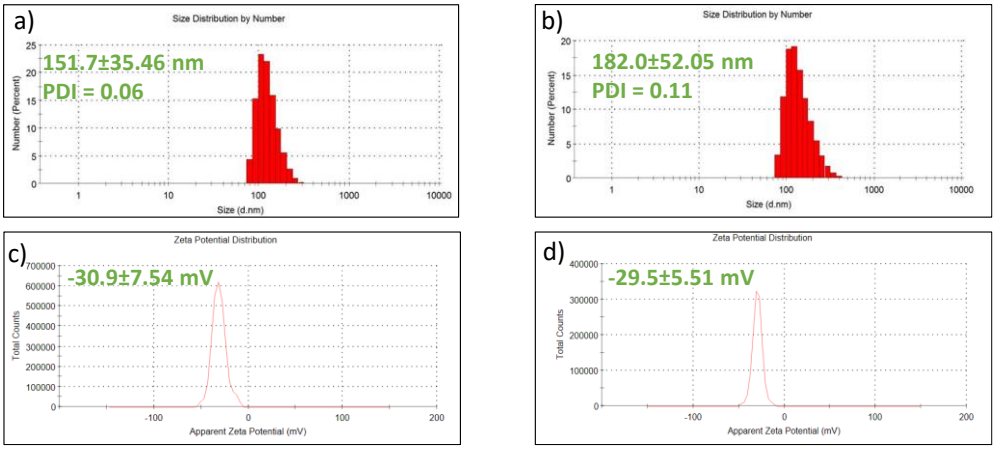

Figure 4.2 Size, PDI and Zeta of blank and CRT loaded NLCs by DLS. Hydrodynamic size a) blank nanostructured lipid carriers, b) CRT loaded nanostructured lipid carriers. Zeta potential c) blank nanostructured lipid carriers and d) CRT loaded nanostructured lipid carriers.

The shape, morphology and size of blank NLC and after CRT loading was also validated by various microscopic techniques such as transmission electron microscopy (TEM), atomic force microscopy (AFM) and transmission electron microscopy (TEM). Observation of these techniques showed spherical particle that were evenly distributed (**Figure 4.3**).

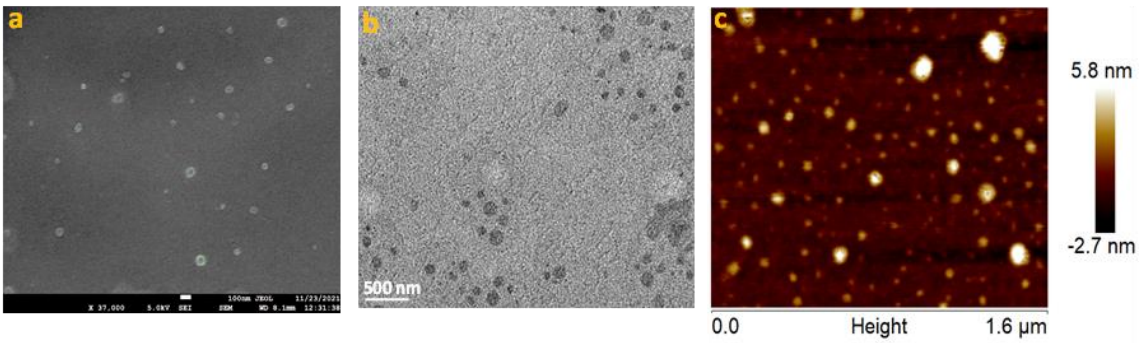

Figure 4.3 Microscopic images of CRT loaded NLCs. a) SEM, b) TEM and c) AFM.

4.2.2 Drug loading and release

ATR spectral analysis shows presence of all the components of formulated nanocarrier with characteristics peaks presented in CRT loaded NLC (**Figure 4.4**). The drug loading (11.23±0.39%) and encapsulation efficacy (81.14±2.79%) of CRT loaded NLC were calculated by employing UV-VIS spectroscopy.

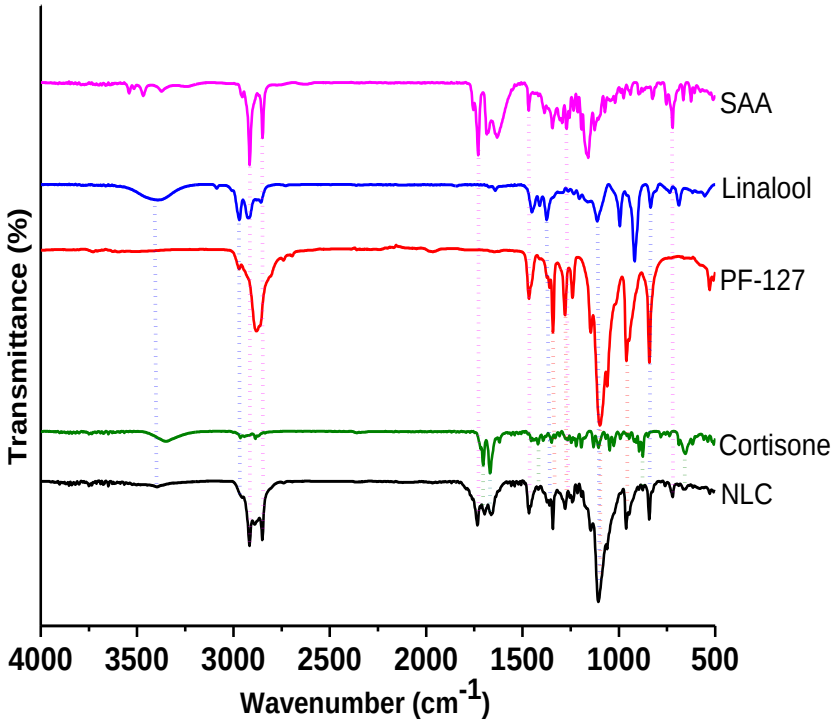

Figure 4.4 ATR-FTIR spectrum analysis of SAA, Linalool, PF-127, cortisone and cortisone loaded NLCs. Common peaks of the ATR-FTIR spectra of SAA, linalool, PF-127, cortisone and cortisone loaded NLCs represented by dotted lines.

To confirm the incorporation of CRT in SAA NLC differential scanning colorimetry has been performed (**Figure 4.5**). Graph shows the melting peak of blank NLC approximately at 129°C due to melting of stearoyl ascorbic acid. CRT melting peak appeared near 230°C. CRT loaded NLC shows melting peak near the melting point of SAA. The disappearance of CRT peak in the formulation confirms the amorphous transformation of drug after incorporation in SAA NLC [18].

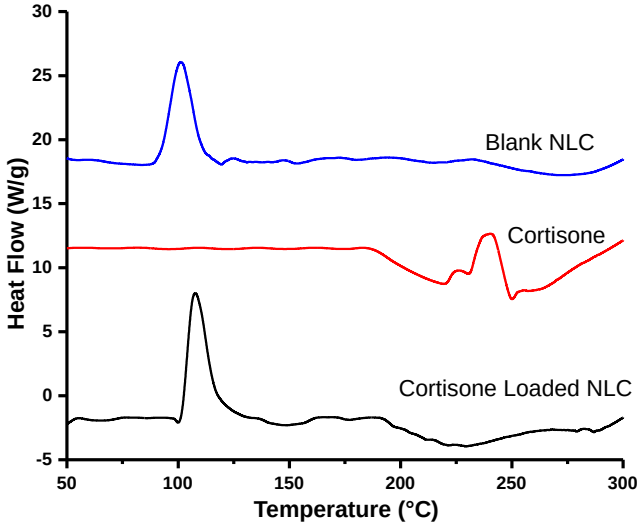

Figure 4.5 Differential scanning colorimetry heating curves of NLCs.

The *in-vitro* release of CRT from SAA NLC was performed by using phosphate buffer saline (PBS pH 7.4) as release medium at room temperature according to our previously optimized parameters. The obtained graph shown that more than 80% of CRT has been released in 48 hours. This observation revealed the sustained release behaviour of formulated NLC. This SAA NLCs might be valuable to minimize the multiple dose administration (**Figure 4.6**).

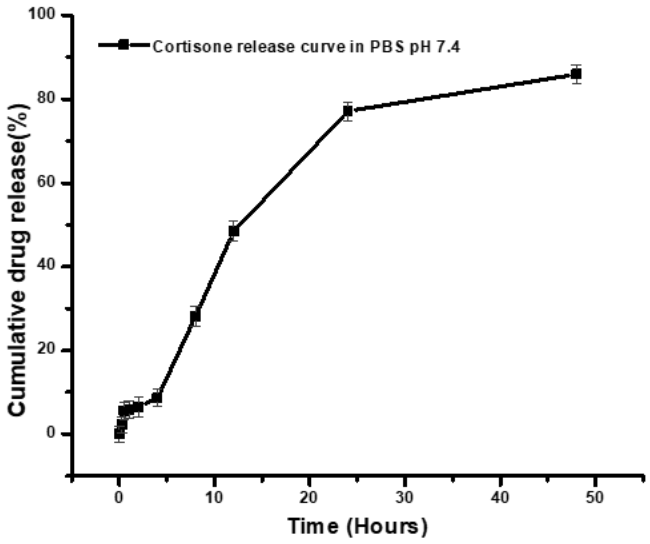

Figure 4.6 CRT Release profile from NLCs. Presented data as mean ± SD of three sets of experiments.

4.2.3 Cytocompatibility of NLC

Further, to check the safety of NLC composition, cytocompatibility of blank NLC was evaluated for 24 hours on normal human fibroblast cells (hTERT-BJ). The dose more than 250 µg/ml shows insignificant reduction of cell viability. Upto the dose of 500 µg/ml more than 85% of the cells were alive which showed cytocompatible characteristics of SAA NLC (**Figure 4.7**).

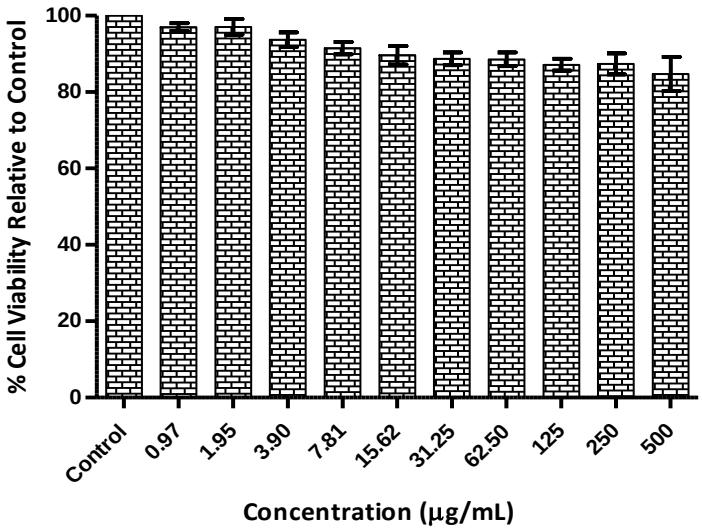

Figure 4.7 Cytocompatibility of blank nanostructured lipid carriers at shown concentrations on normal human foreskin fibroblasts (hTERT-BJ) cells. Presented data as mean ± SD of three sets of experiments.

4.2.4. *In-Vitro* inflammatory marker

To check the in-vitro anti-inflammatory activity of CRT loaded SAA NLC nitrite estimation was performed in LPS (1µg/ml) treated RAW 264.7 cells. As nitrite level is directly affect the intensity of inflammation and membrane damage and is well reported in UC.[5] In our study the significant increased level of nitrite has been observed in LPS treated group when compared to normal. After treatment with CRT as well as CRT NLC, it was significantly reduced (***$p \leq 0.001$) after comparing with LPS treated group at each concentration. In comparison to CRT treated group with CRT NLC group (*$p \leq 0.05$) significant difference in the nitrite level was found (**Figure 4.8**). In our study dose dependent effect after treatment with

CRT and CRT NLC was found in the reduction of nitrite level. Blank SAA NLC was also able to reduce the nitrite production markedly which aid in the potency of CRT loaded NLC.[19,20]

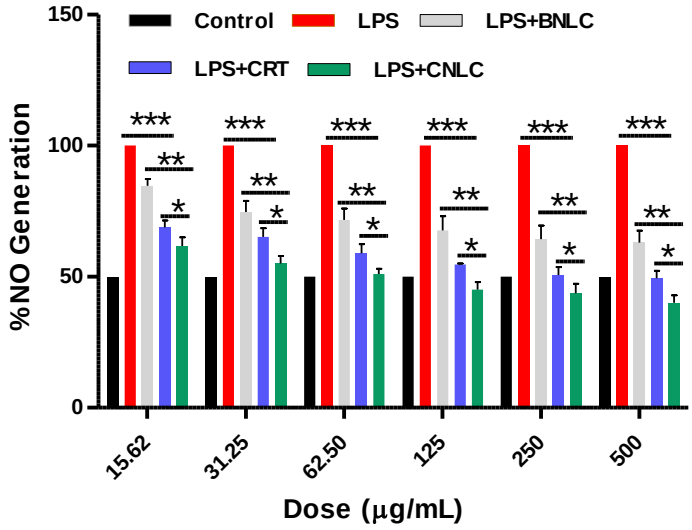

Figure 4.8 Shows in-vitro NO generation against LPS activated RAW 264.7 cell line. Significant differences were indicated by ***p ≤ 0.001, **p ≤ 0.01, *p ≤ 0.05. Presented data as mean ± SD of three sets of experiments.

4.2.5 *In-Vivo* Therapeutic Efficacy Study

After formulation development and *in-vitro* assessments of CRT loaded SAA NLC, *in-vivo* study was done on DSS induced colitis model to evaluate the therapeutic efficacy of prepared NLC.

4.2.5.1 Assessment of activity and weight changes

In time of *in-vivo* study mice were observed for their weight changes following the various treatment regimens. In intestinal inflammation significant reduction in weight has been reported that is correlated with the restriction of nutrient absorption in the inflammatory condition and reflect catabolic state of the biological system.[21] In our study DSS treatment caused marked reduction in body weight in diseased group (***p≤0.001) compared to normal. CRT as well as CRT loaded NLC treatment causes marked increment in body weight (###p≤0.001) compared to colitis group. Treatment with blank NLC after induction of colitis there was slight increase

in body weight was observed (which shows protective role of composition of NLC against inflammation) in comparison to colitis group but it was insignificant (**Figure 4.9**).

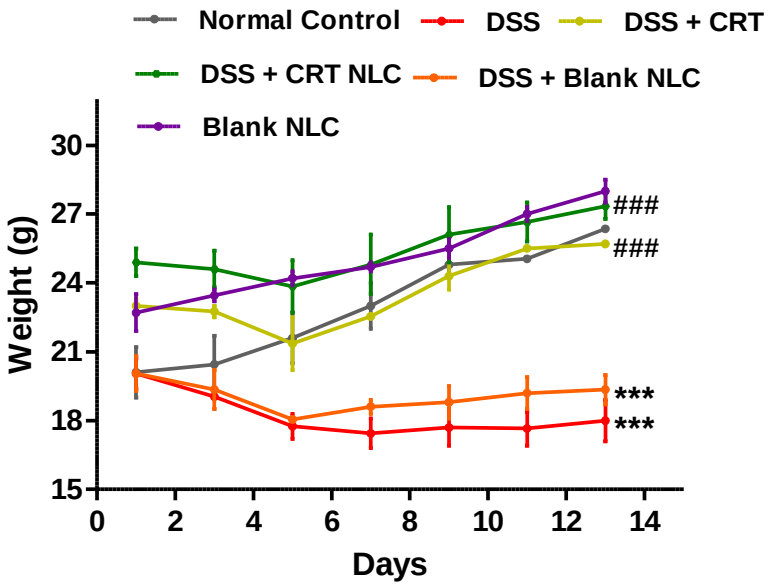

Figure 4.9 Shows weight changes of experimental animals throughout study period. Group I – Normal Control, Group II – DSS, Group III – DSS + CRT, Group IV – DSS + CRT NLC, Group V – DSS + Blank NLC, Group VI – Blank NLC. Statistical differences were signified using one-way ANOVA and Bonferroni test. All study groups were compared to colitis group and normal control. (###p < 0.001, ***p < 0.001). (Represented values as mean ± SD).

Percentage loss or gain in body weight was also calculated after completion of the study (**Figure 4.10**).

Following the treatment schedule animals were also observed for disease activity indices like physical activity, rectal bleeding, stool consistency etc. In normal control and blank treated group all the observation were normal. Colitis group shows abnormalities in these parameters as the stool was observed watery or diarrhoea, physical activity was sedentary with rectal bleeding. Treatment of diseased animal with blank NLC slight improvement was observed. After treatment with CRT stool consistency was soft, animal activity was low and there was no rectal bleeding has been found. In CRT loaded NLC treated group all the observations were normal. Blank NLC group shows physically observed parameters similar to normal control group (**Table 4.2**).

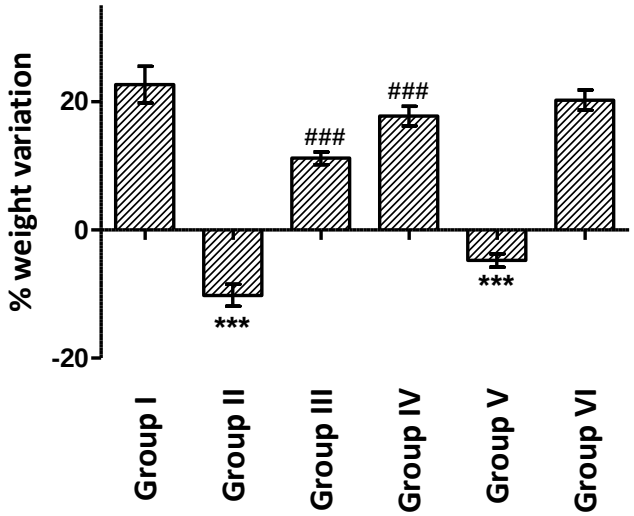

Figure 4.10 Shows % weight variation of mice after completion of study. Group I – Normal Control, Group II – DSS, Group III – DSS + CRT, Group IV – DSS + CRT-loaded NLC, Group V – DSS + Blank NLC, Group VI – Blank NLC. Comparisons were made on the basis of the one-way ANOVA followed by Bonferroni post-test. All groups were compared to the DSS group (p < 0.001, ###p < 0.001). (Values are presented as mean ± SD).***

Table 4.2 Physical observations of various parameters on experimental animals over the study period. Values are expressed in the table are average observational values.

S.No.	Groups	Observations		
		Stool Consistency	Physical Activity	Rectal Bleeding
1.	Normal Control	0	0	0
2.	DSS	4	3	1
3.	CRT	1	2	0
4.	CRT-loaded NLC	0	0	0
5.	Blank	3	2	1
6.	Safety	0	0	0

Stool Consistency
0-Normal Pellet (Hard)
1-Soft Pellet
2-Loose watery stool
3-Stickiness
4-Diarrhoea

Physical Activity
0-Normal active (Highly)
1-Mild active
2-Low active
3-Sedentary

Rectal Bleeding
0-No bleeding
1-Bleeding

Following the treatment schedule after completion of study colon was physically measured and observed for any pathological changes. A notable decrease in the colon length following the DSS treatment has been observed. CRT and CRT loaded NLC treatment caused colon length retainment. Diseased animal treated with blank NLCs had similar effect like DSS induced colitis group but low intensity. Colon length of safety as well as control groups animal observed similar (**Figure 4.11A**). To check any traces of hidden blood in stools, fecal occult blood test (FOBT) was also performed. In colitis group, CRT treated group and colitis animal treated with blank NLC were observed blue color on FOBT strip that confirms presence of fecal blood. After treatment with CRT loaded NLC there was no sign of hidden blood in faeces was observed. Similarly in normal and safety groups also no fecal blood was present (**Figure 4.11B**).

(A) (B)

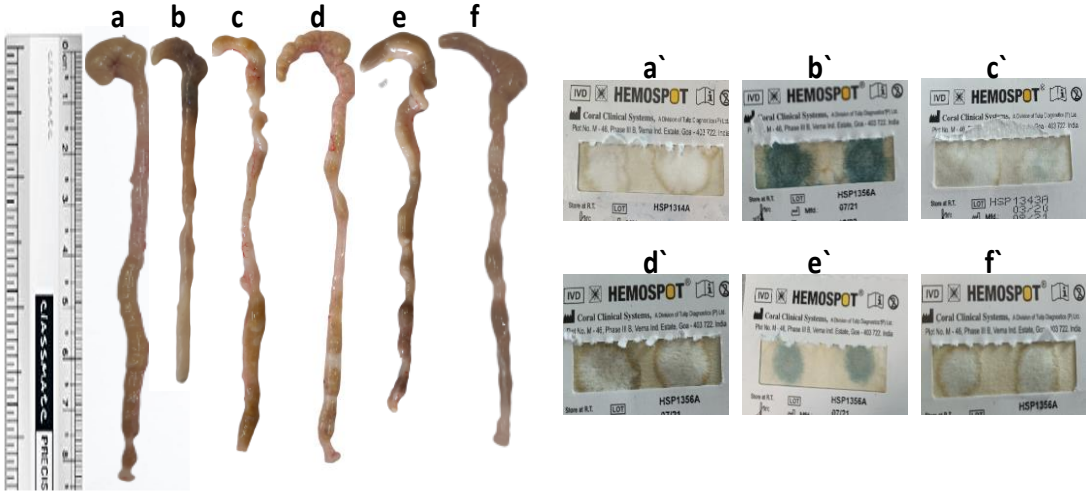

Figure 4.11 Representative images of (A) colon form each experimental group. a – Normal Control, b – DSS, c – DSS + CRT, d – DSS + CRT-loaded NLC, e – DSS + Blank NLC and f – Blank NLC and (B) a` – f` are corresponding FOBT imaging.

4.2.5.2 Histological observations

H&E staining of colon sections confirms the normal histology of colon in control animals. Analysis of healthy animals` colon exhibited complete colon morphology as mucosa, submucosa and muscularis layer in their intact form. DSS treatment causes the induction of colitis where colon histology was markedly disrupts. During colonic inflammation and colitis, it is reported that abnormal colonic cells combined in form of tube and gives rise to aberrant crypt of foci.[22] After induction of colitis following the DSS treatment disruption of colon morphology was appeared. In this group depletion in goblet cells as well destructed muscularis layer appeared. In correlation to the healthy animals, DSS induced colitis group possessed submucosal widening due to collagen deposition and inflammatory cells infiltration as reported previously.[23] Treatment with CRT improved the histological alterations upto some extent which appeared after induction of colitis. In CRT loaded NLC treatment group there was marked recovery in the linings of colon have been observed. In this group healthy appearance of goblet cells in mucosa layer was observed that were surrounded by submucosa and intact muscularis layer. Diseased animal treated with blank NLC shows destructed colon morphology but low intense in comparison to DSS group because of protective role of SAA against oxidative damage. In blank and safety group healthy colon morphology was observed (**Figure 4.12**).

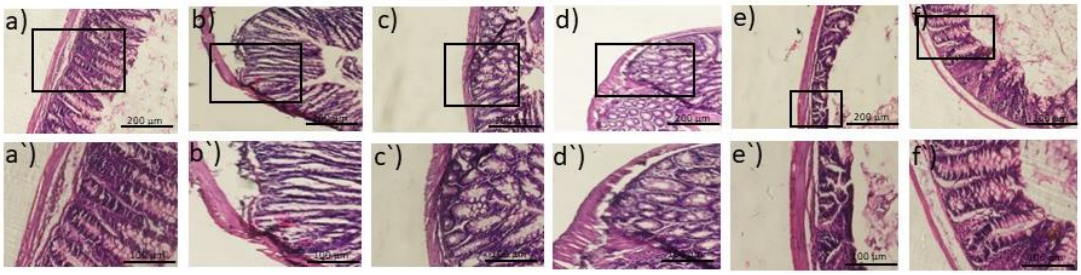

Figure 4.12 H&E-stained mice colonic sections microscopic image. a) Normal Control: Healthy histoarchitect of colon appeared. b) DSS: Damaged mucosa and muscularis layer. c) DSS + CRT: Recovered muscularis and mucosa observed. d) DSS + CRT NLCs: Colon morphology consisted of regained healthy mucosa, submucosa and muscularis layer. e) DSS + Blank NLCs: Damaged colonic epithelial cells observed. f) Blank NLCs: showed healthy colonic morphology as healthy animals. Image magnification of 10X, scale bar = 200 µm (a-f) and 20X, scale bar = 100 µm (a'-f').

Integrity of mucin layer which forms protective layer in colonic lining via the production of mucus was confirmed by goblet cells staining with AB-NR. Abruption of mucus layer in colon is more susceptible to inflammation and colitis where noxious agents' exposure occurs. Notable appearance of goblet cells has been observed in control group as confirmed by acidic mucin stained with blue color. In DSS group there was very low blue color stains confirmed the induction of colitis where diminished goblet cells observed. After treatment with CRT goblet cells increased which shows enhanced blue color-stained mucins. CRT loaded NLC treatment significantly lowers the destructive changes occurs in goblet cells because of colitis induction. In this group notable increment in goblet cells observed. Less goblet cells damage has been appeared in colitis animals treated with blank NLC in comparison to DSS group. Goblet cells observations has been found similar in normal control and safety animals (**Figure 4.13**).

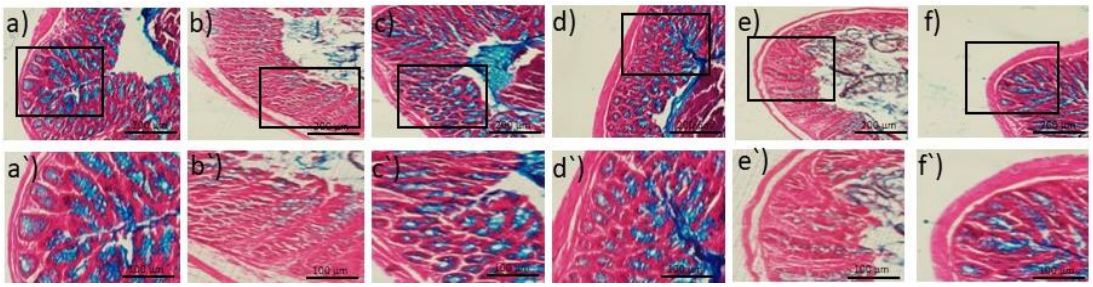

Figure 4.13 AB-NR-stained mice colonic sections microscopic image. a) Normal Control: Sufficiently appeared goblet cells in colonic mucosa stained in blue color. b) DSS: Very low blue color in mucosa appeared damaged goblet cells. c) DSS + CRT: Goblet cells recovery observed. d) DSS + CRT NLCs: Enhancement of blue color shows significantly recovered goblet cells. e) DSS + Blank NLCs: Diminished goblet cells in mucosa. f) Blank NLCs: Appeared blue colored stained goblet cells as healthy mouse. Image magnification of 10X, scale bar = 200 µm (a-f) and 20X, scale bar = 100 µm (a'-f').

Two types of mucins are secreted by goblet cells in the colon which are sialomucin and sulphomucin. Colonic inflammation/cancer recognizes with more secreted sialomucin than normal colonic mucosa secretes more sulphomucin.[24,25] To establish the correlation of type of mucin and UC HID-AB staining was performed. Sialomucin is observed blue color stained with AB as well as sulphomucin appeared

brown in color which is stained by HID dye. This study possessed predominantly brown color stained sulphomucin in comparison to blue color-stained predominant presence of sialomucin in DSS induced colitis group. CRT treatment caused sulphomucin which appeared as more brown color stain. CRT NLC treatment sufficiently enhanced the secretion of sulphomucin by goblet cells as this group observed increased brown color staining. Predominant presence of sulphomucin in normal control group as well as safety group was similar (**Figure 4.14**).

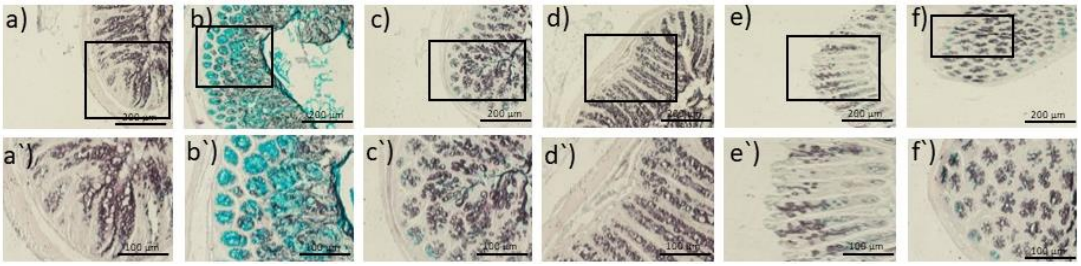

Figure 4.14 HID-AB-stained mice colonic sections microscopic image. a) Normal Control: Predominant (brown color) sulfomucin compared to sialomucin (bluish color). b) DSS: Observed enhanced blue colored stained sialomucin. c) DSS + CRT: Sulfomucin appeared more than sialomucin. d) DSS + CRT NLCs: Significant enhancement of sulfomucin than sialomucin. e) DSS + Blank NLCs: Washed mucin layers shows decreased both type of mucins. f) Blank NLCs: Mucin staining comparable to healthy animals. Images magnification 10X, scale bar = 200 µm (a-f) and 20X, scale bar = 1000 µm (a'-f').

Presence of infiltrated proinflammatory mast cells is directly correlated with intestinal inflammations and UC. Upon activation these cells release histamine which acts as inflammatory mediator which further enhances inflammation by imparting tissue and vascular changes at inflammatory sites.[26,27] TB staining shows the enhancement in infiltrated mast cells in DSS induced colitis group in comparison to normal control where only physiological presence was appeared. Treatment with CRT as well CRT loaded NLC markedly reduced the infiltration of mast cells in these groups. Colitis animals treated with blank NLC also observed lower mast cells because of defensive role of SAA against oxidative damage and inflammation but it was not prominent. In normal control and safety group no mast cells observed. Treatment with CRT loaded NLC markedly lowers the intensity of colitic

inflammation and suppressed mast cells infiltration at the inflammatory site (**Figure 4.15**).

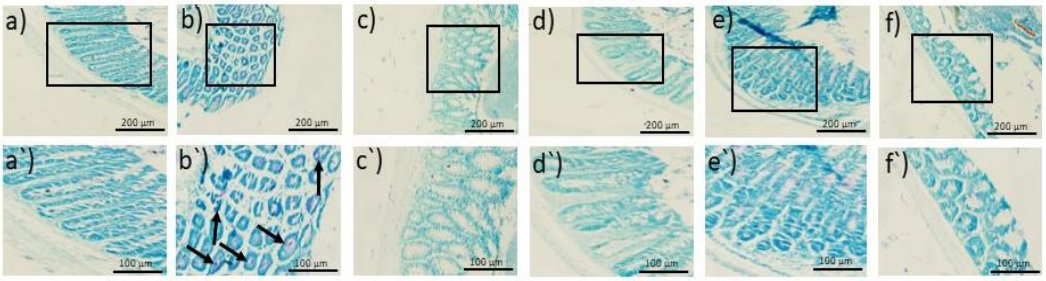

Figure 4.15 Toluidine blue-stained mice colonic sections microscopic image. a) Normal Control: No mast cells infiltration in colonic section. b) DSS: Black arrow indicated infiltrated mast cells in diseased animals' colonic section. c) DSS + CRT: No observed mast cells. d) DSS + CRT NLCs: Infiltrated mast cells not appeared. e) DSS + Blank NLCs: Infiltrated mast cells appeared in mucosa. f) Blank NLCs: No mast cells as normal control group. Images magnification 10X, scale bar = 200 µm (a-f) and 20X, scale bar = 1000 µm (a'-f').

4.2.5.2.1 Immunohistochemical analysis

In IBDs like UC and Chron`s disease it is reported that cyclooxygenase-2 is overexpressed whereas iNOS is responsible for production of NO at diseased site that directly worsen the inflammation and enhances severity of disease like UC.[28,29] IHC for the estimation of iNOS and COX-2 has been performed to assess the potency of CRT loaded NLC in suppression of overexpressed these enzymes (**Figure 4.16**).

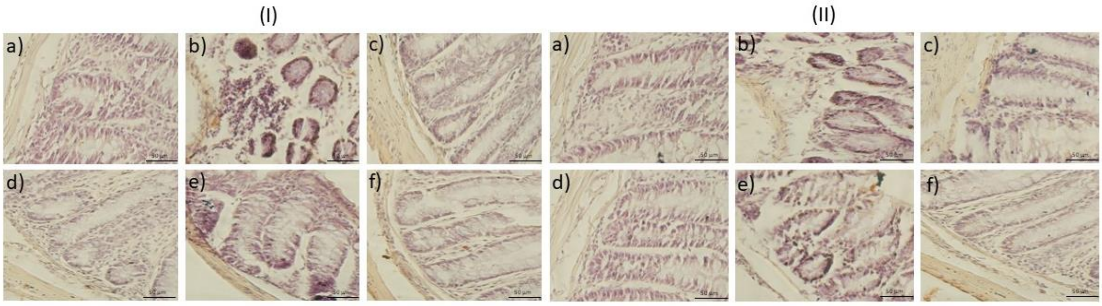

Figure 4.16 IHC staining of (I) iNOS and (II) COX-2 expression. a) Normal Control: Less iNOS as well as COX-2 expressed compared to diseased group. b) DSS: Appeared overexpressed iNOS and COX-2 level than healthy group. c) DSS + CRT: iNOS as well as COX-2 expression lower than diseased group. d) DSS + CRT NLCs: Significantly low iNOS and COX-2 in comparison to diseased

animals. e) DSS + Blank NLCs: Observed enhanced iNOS and COX-2 expression. f) Blank NLCs: iNOS and COX-2 expression as healthy mice. Image magnification 40X, scale bar = 50 µm (a-f).

From IHC images semi quantitatively expression of iNOS (**Figure 4.17a**) and COX-2 (**Figure 4.17b**) was estimated. In control and safety group there was very low level of COX-2 and iNOS expression (brown-colored immune cells) appeared. After administration of DSS significant upsurge of COX-2 (***p ≤ 0.001) and iNOS (***p ≤ 0.001) (Fig.) compared to control group was observed. CRT (##p ≤ 0.01) and CRT NLC treatment (###p ≤ 0.001) significantly downregulated the overexpression of iNOS and COX-2. Results of these observations suggests that CRT loaded SAA NLCs have enough capability to regulate the overexpression of biomarkers of inflammation.

(a) (b)

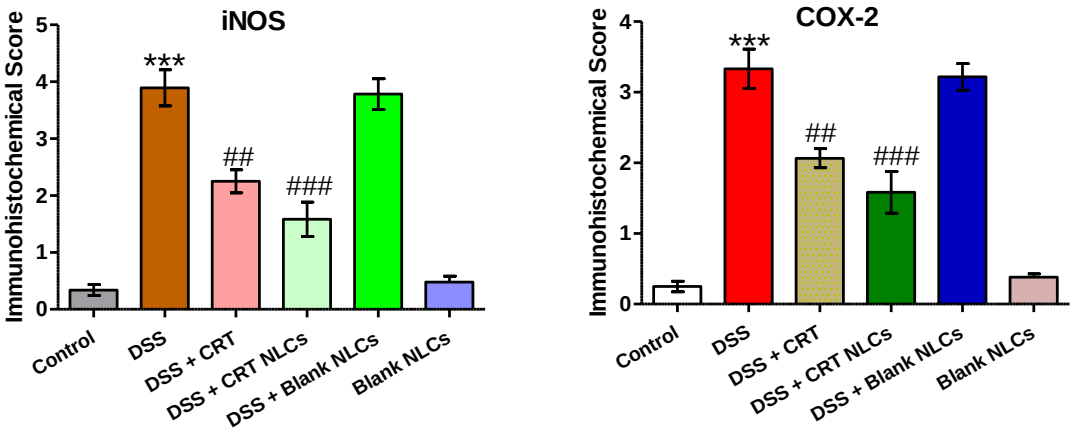

Figure 4.17 Semi-quantitative evaluation of (a) iNOS and (b) COX-2 expression. Group I – Normal Control, Group II – DSS, Group III – DSS + CRT, Group IV – DSS + CRT-loaded NLC, Group V – DSS + Blank NLC. Group VI – Blank NLCs. Significant differences were indicated by ***p ≤ 0.001, as compared to control and #p ≤ 0.05, ##p ≤ 0.01 and ###p ≤0.001 as compared to DSS group. The experiments were performed in triplicate (n = 3) and data are presented as mean ± standard deviation of three independent sets of observations.

4.2.5.3 *In-Vivo* cytokines assay

Infiltrated mast cells are present in the activated form at the inflammatory sites and via innate immunity expresses the level of various cytokines, interleukins (ILs), tumor necrosis factor (TNF-α).[30] These inflammatory mediators are responsible for the initiation and progression of various inflammatory diseases like UC.[26,27] The imbalance between proinflammatory cytokines and anti-inflammatory cytokines leads to negatively affect the homeostasis of colon which gives rise to the initiation and spread of colonic diseases.[31,32] In this study, DSS treatment significantly upregulated the level of TNF-α (***$p \leq 0.001$) if correlated with normal control. CRT (##$p \leq 0.01$) and CRT loaded NLC (###$p \leq 0.001$) treated group found significant downregulation of TNF-α. DSS induced colitis animals treated with blank NLC had lower expressions of TNF-α level but statistically insignificant. This cytokine level in blank NLCs treated animals was similar to healthy animals (**Figure 4.18c**). These results indicated that CRT loaded NLC effectively downregulates the increased TNF-α and limits inflammation and UC progression.

Tissue nitrite estimation have direct correlation with inflammation and disease progression in UC. It is a prominent biomarker reported in colonic inflammation and UC.[33,34] In the present study DSS treatment (***$p \leq 0.001$) significantly enhanced nitrite level compared to control group. CRT (#$p \leq 0.05$) and CRT NLC (##$p \leq 0.01$) treatment significantly decreased the level of tissue nitrite. Diseased animal treated with blank NLC have similar level of nitrite was found (**Figure 4.18b**). Tissue nitrite level in safety group was similarly expressed like normal control. These results are in close collaboration of previous reports.[35,36]

Myeloperoxidase (MPO) is reported as a proinflammatory marker with enhanced expression in the progression of UC.[37–39] In this study treatment with DSS causes the overexpression of MPO (***$p \leq 0.001$) if compared to normal. Administration of CRT (#$p \leq 0.05$) as well as CRT loaded NLC (###$p \leq 0.001$) significantly downregulated the level of MPO and proved the protective role against DSS induced colitis. Blank treatment of colitis induced animals also decreased the MPO level but insignificant with CRT as well as CRT loaded NLCs groups. In safety group there was very low expressed MPO level was estimated as normal control

(**Figure 4.18a**). Various studies reported that in UC and other inflammatory diseases level of MPO is found very high which may prominently enhanced severity of disease.[40,41]

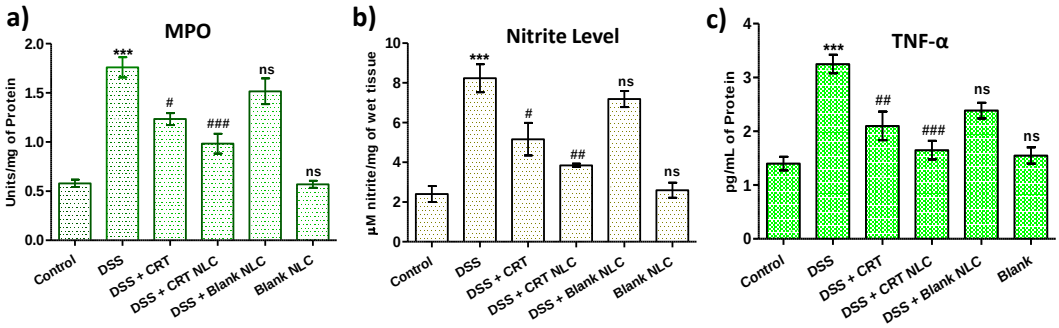

Figure 4.18 Shows a) MPO, b) nitrite level in colon tissue and c) TNF-α quantification in mice serum. Control group was compared with DSS and safety whereas DSS group compared with various treatment groups. (p ≤ 0.001, ###p ≤ 0.001, ##p ≤ 0.01, #p ≤ 0.05, ns = nonsignificant). (Represented values as mean ± SD).***

4.3 Conclusion

In the reported study, a novel lipid nanocarrier has been formulated by utilizing biocompatible composition of USFDA approved GRAS materials. This NLC have good physicochemical properties in terms of its morphological appearance and sustained release profile of encapsulated drug CRT. In vitro cytocompatibility study and efficacy study shows its potential role for the alleviation of inflammatory cytokines. The in vivo study against DSS induced colitis shows biocompatible behaviour of prepared NLC whereas efficacy study proved its significant role in the favour of colitis severity treatment as findings like histological observations and inhibition of inflammatory cytokines.

4.4 Bibliography

(1) Ng, S. C.; Shi, H. Y.; Hamidi, N.; Underwood, F. E.; Tang, W.; Benchimol, E. I.; Panaccione, R.; Ghosh, S.; Wu, J. C. Y.; Chan, F. K. L.; Sung, J. J. Y.; Kaplan, G. G. Worldwide Incidence and Prevalence of Inflammatory Bowel Disease in the 21st Century: A Systematic Review of Population-Based Studies. *The Lancet* **2017**, *390* (10114), 2769–2778. https://doi.org/10.1016/S0140-6736(17)32448-0.

(2) Oshi, M. A.; Lee, J.; Naeem, M.; Hasan, N.; Kim, J.; Kim, H. J.; Lee, E. H.; Jung, Y.; Yoo, J.-W. Curcumin Nanocrystal/PH-Responsive Polyelectrolyte Multilayer Core–Shell Nanoparticles for Inflammation-Targeted Alleviation of Ulcerative Colitis. *Biomacromolecules* **2020**, *21* (9), 3571–3581. https://doi.org/10.1021/acs.biomac.0c00589.

(3) Li, J.; Wang, F.; Zhang, H.-J.; Sheng, J.-Q.; Yan, W.-F.; Ma, M.-X.; Fan, R.-Y.; Gu, F.; Li, C.-F.; Chen, D.-F.; Zheng, P.; Gu, Y.-P.; Cao, Q.; Yang, H.; Qian, J.-M.; Hu, P.-J.; Xia, B. Corticosteroid Therapy in Ulcerative Colitis: Clinical Response and Predictors. *World Journal of Gastroenterology: WJG* **2015**, *21* (10), 3005. https://doi.org/10.3748/wjg.v21.i10.3005.

(4) Ahmad, A.; Ansari, M. M.; Kumar, A.; Bishnoi, M.; Raza, S. S.; Khan, R. Aminocellulose - Grafted Polycaprolactone-Coated Core–Shell Nanoparticles Alleviate the Severity of Ulcerative Colitis: A Novel Adjuvant Therapeutic Approach. *Biomater. Sci.* **2021**, *9* (17), 5868–5883. https://doi.org/10.1039/D1BM00877C.

(5) Guo, T.; Lin, Q.; Li, X.; Nie, Y.; Wang, L.; Shi, L.; Xu, W.; Hu, T.; Guo, T.; Luo, F. Octacosanol Attenuates Inflammation in Both RAW264.7 Macrophages and a Mouse Model of Colitis. *J. Agric. Food Chem.* **2017**, *65* (18), 3647–3658. https://doi.org/10.1021/acs.jafc.6b05465.

(6) Yang, W.; Ren, D.; Zhao, Y.; Liu, L.; Yang, X. Fuzhuan Brick Tea Polysaccharide Improved Ulcerative Colitis in Association with Gut Microbiota-Derived Tryptophan Metabolism. *J. Agric. Food Chem.* **2021**, *69* (30), 8448–8459. https://doi.org/10.1021/acs.jafc.1c02774.

(7) Xie, F.; Ding, X.; Zhang, Q.-Y. An Update on the Role of Intestinal Cytochrome P450 Enzymes in Drug Disposition. *Acta Pharmaceutica Sinica B* **2016**, *6* (5), 374–383. https://doi.org/10.1016/j.apsb.2016.07.012.

(8) Gavhane, Y. N.; Yadav, A. V. Loss of Orally Administered Drugs in GI Tract. Saudi Pharm. J. 20 (4), 331–344, 2012.

(9) Blonski, W.; Buchner, A. M.; Lichtenstein, G. R. Treatment of Ulcerative Colitis. *Current Opinion in Gastroenterology* **2014**, *30* (1), 84–96. https://doi.org/10.1097/MOG.0000000000000031.

(10) Yasir, M.; Goyal, A.; Sonthalia, S. Corticosteroid Adverse Effects. In *StatPearls*; Stat Pearls Publishing: Treasure Island (FL), 2022.

(11) Patra, J. K.; Das, G.; Fraceto, L. F.; Campos, E. V. R.; Rodriguez-Torres, M. del P.; Acosta-Torres, L. S.; Diaz-Torres, L. A.; Grillo, R.; Swamy, M. K.; Sharma, S.; Habtemariam, S.; Shin, H.-S. Nano Based Drug Delivery Systems: Recent Developments and Future Prospects. *Journal of Nanobiotechnology* **2018**, *16* (1), 71. https://doi.org/10.1186/s12951-018-0392-8.

(12) Lombardo, D.; Kiselev, M. A.; Caccamo, M. T. Smart Nanoparticles for Drug Delivery Application: Development of Versatile Nanocarrier Platforms in Biotechnology and Nanomedicine. *Journal of Nanomaterials* **2019**, *2019*, e3702518. https://doi.org/10.1155/2019/3702518.

(13) Chen, Q.; Si, X.; Ma, L.; Ma, P.; Hou, M.; Bai, S.; Wu, X.; Wan, Y.; Xiao, B.; Merlin, D. Oral Delivery of Curcumin via Porous Polymeric Nanoparticles for Effective Ulcerative Colitis Therapy. *J. Mater. Chem. B* **2017**, *5* (29), 5881–5891. https://doi.org/10.1039/C7TB00328E.

(14) Lu, H.; Wang, J.; Wang, T.; Zhong, J.; Bao, Y.; Hao, H. Recent Progress on Nanostructures for Drug Delivery Applications. *Journal of Nanomaterials* **2016**, *2016*, e5762431. https://doi.org/10.1155/2016/5762431.

(15) Shirodkar, R. K.; Kumar, L.; Mutalik, S.; Lewis, S. Solid Lipid Nanoparticles and Nanostructured Lipid Carriers: Emerging Lipid Based Drug Delivery Systems. *Pharm Chem J* **2019**, *53* (5), 440–453. https://doi.org/10.1007/s11094-019-02017-9.

(16) Mukherjee, S.; Ray, S.; Thakur, R. S. Solid Lipid Nanoparticles: A Modern Formulation Approach in Drug Delivery System. *Indian J Pharm Sci* **2009**, *71* (4), 349–358. https://doi.org/10.4103/0250-474X.57282.

(17) Mishra, R. K.; Ahmad, A.; Kumar, A.; Vyawahare, A.; Raza, S. S.; Khan, R. Lipid-Based Nanocarrier-Mediated Targeted Delivery of Celecoxib Attenuate Severity of Ulcerative Colitis. *Materials Science and Engineering: C* **2020**, *116*, 111103. https://doi.org/10.1016/j.msec.2020.111103.

(18) Nahak, P.; Karmakar, G.; Chettri, P.; Roy, B.; Guha, P.; Besra, S. E.; Soren, A.; Bykov, A. G.; Akentiev, A. V.; Noskov, B. A.; Panda, A. K. Influence of Lipid Core Material on Physicochemical Characteristics of an Ursolic Acid-Loaded Nanostructured Lipid Carrier: An Attempt To Enhance Anticancer Activity. *Langmuir* **2016**, *32* (38), 9816–9825. https://doi.org/10.1021/acs.langmuir.6b02402.

(19) Pravda, J. Hydrogen Peroxide and Disease: Towards a Unified System of Pathogenesis and Therapeutics. *Molecular Medicine* **2020**, *26* (1), 41. https://doi.org/10.1186/s10020-020-00165-3.

(20) Piechota-Polanczyk, A.; Fichna, J. Review Article: The Role of Oxidative Stress in Pathogenesis and Treatment of Inflammatory Bowel Diseases. *Naunyn-Schmiedeberg's Arch Pharmacol* **2014**, *387* (7), 605–620. https://doi.org/10.1007/s00210-014-0985-1.

(21) Abdelmegid, A. M.; Abdo, F. K.; Ahmed, F. E.; Kattaia, A. A. A. Therapeutic Effect of Gold Nanoparticles on DSS-Induced Ulcerative Colitis in Mice with Reference to Interleukin-17 Expression. *Sci Rep* **2019**, *9* (1), 10176. https://doi.org/10.1038/s41598-019-46671-1.

(22) Mishra, R. K.; Selim, A.; Gowri, V.; Ahmad, A.; Nadeem, A.; Siddiqui, N.; Raza, S. S.; Jayamurugan, G.; Khan, R. Thiol-Functionalized Cellulose-Grafted Copper Oxide Nanoparticles for the Therapy of Experimental Colitis in Swiss Albino Mice. *ACS Biomater. Sci. Eng.* **2022**, *8* (5), 2088–2095. https://doi.org/10.1021/acsbiomaterials.2c00124.

(23) Balaha, M.; Kandeel, S.; Elwan, W. Garlic Oil Inhibits Dextran Sodium Sulfate-Induced Ulcerative Colitis in Rats. *Life Sciences* **2016**, *146*, 40–51. https://doi.org/10.1016/j.lfs.2016.01.012.

(24) Croix, J. A.; Carbonero, F.; Nava, G. M.; Russell, M.; Greenberg, E.; Gaskins, H. R. On the Relationship between Sialomucin and Sulfomucin Expression and Hydrogenotrophic Microbes in the Human Colonic Mucosa. *PLOS ONE* **2011**, *6* (9), e24447. https://doi.org/10.1371/journal.pone.0024447.

(25) Deplancke, B.; Gaskins, H. R. Microbial Modulation of Innate Defense: Goblet Cells and the Intestinal Mucus Layer. *The American Journal of Clinical Nutrition* **2001**, *73* (6), 1131S-1141S. https://doi.org/10.1093/ajcn/73.6.1131S.

(26) Luchini, A. C.; Costa de Oliveira, D. M.; Pellizzon, C. H.; Di Stasi, L. C.; Gomes, J. C. Relationship between Mast Cells and the Colitis with Relapse Induced by Trinitrobenzesulphonic Acid in Wistar Rats. *Mediators of Inflammation* **2009**, *2009*, e432493. https://doi.org/10.1155/2009/432493.

(27) Branco, A. C. C. C.; Yoshikawa, F. S. Y.; Pietrobon, A. J.; Sato, M. N. Role of Histamine in Modulating the Immune Response and Inflammation. *Mediators of Inflammation* **2018**, *2018*, e9524075. https://doi.org/10.1155/2018/9524075.

(28) Yang, Y.-P.; Tong, Q.-Y.; Zheng, S.-H.; Zhou, M.-D.; Zeng, Y.-M.; Zhou, T.-T. Anti-Inflammatory Effect of Fucoxanthin on Dextran Sulfate Sodium-Induced Colitis in Mice. *Natural Product Research* **2020**, *34* (12), 1791–1795. https://doi.org/10.1080/14786419.2018.1528593.

(29) Schreiber, O.; Petersson, J.; Waldén, T.; Ahl, D.; Sandler, S.; Phillipson, M.; Holm, L. INOS-Dependent Increase in Colonic Mucus Thickness in DSS-Colitic Rats. *PLOS ONE* **2013**, *8* (8), e71843. https://doi.org/10.1371/journal.pone.0071843.

(30) Medicherla, K.; Sahu, B. D.; Kuncha, M.; Kumar, J. M.; Sudhakar, G.; Sistla, R. Oral Administration of Geraniol Ameliorates Acute Experimental Murine Colitis by Inhibiting Pro-Inflammatory Cytokines and NF-KB Signaling. *Food Funct.* **2015**, *6* (9), 2984–2995. https://doi.org/10.1039/C5FO00405E.

(31) Kaur, H.; Ali, S. A. Probiotics and Gut Microbiota: Mechanistic Insights into Gut Immune Homeostasis through TLR Pathway Regulation. *Food Funct.* **2022**. https://doi.org/10.1039/D2FO00911K.

(32) Ramadan, Q.; Gijs, M. A. M. In Vitro Micro-Physiological Models for Translational Immunology. *Lab Chip* **2015**, *15* (3), 614–636. https://doi.org/10.1039/C4LC01271B.

(33) Gawrońska, B.; Matowicka-Karna, J.; Kralisz, M.; Kemona, H. Markers of Inflammation and Influence of Nitric Oxide on Platelet Activation in the Course of Ulcerative Colitis. *Oncotarget* **2017**, *8* (40), 68108–68114. https://doi.org/10.18632/oncotarget.19202.

(34) Nagata, J.; Yokodera, H.; Maeda, G. In Vitro and in Vivo Studies on Anti-Inflammatory Effects of Traditional Okinawan Vegetable Methanol Extracts. *ACS Omega* **2019**, *4* (13), 15660–15664. https://doi.org/10.1021/acsomega.9b02178.

(35) Soufli, I.; Toumi, R.; Rafa, H.; Touil-Boukoffa, C. Overview of Cytokines and Nitric Oxide Involvement in Immuno-Pathogenesis of Inflammatory Bowel Diseases. *World J Gastrointest Pharmacol Ther* **2016**, *7* (3), 353–360. https://doi.org/10.4292/wjgpt.v7.i3.353.

(36) Avdagić, N.; Zaćiragić, A.; Babić, N.; Hukić, M.; Šeremet, M.; Lepara, O.; Nakaš-Ićindić, E. Nitric Oxide as a Potential Biomarker in Inflammatory Bowel Disease. *Bosn J Basic Med Sci* **2013**, *13* (1), 5–9.

(37) Chami, B.; Martin, N. J. J.; Dennis, J. M.; Witting, P. K. Myeloperoxidase in the Inflamed Colon: A Novel Target for Treating Inflammatory Bowel Disease. *Archives of Biochemistry and Biophysics* **2018**, *645*, 61–71. https://doi.org/10.1016/j.abb.2018.03.012.

(38) Garrity-Park, M.; Loftus, E. V., Jr; Sandborn, W. J.; Smyrk, T. C. Myeloperoxidase Immunohistochemistry as a Measure of Disease Activity in Ulcerative Colitis: Association with Ulcerative Colitis-Colorectal Cancer, Tumor Necrosis Factor Polymorphism and RUNX3 Methylation. *Inflammatory Bowel Diseases* **2012**, *18* (2), 275–283. https://doi.org/10.1002/ibd.21681.

(39) Bastaki, S. M. A.; Al Ahmed, M. M.; Al Zaabi, A.; Amir, N.; Adeghate, E. Effect of Turmeric on Colon Histology, Body Weight, Ulcer, IL-23, MPO and Glutathione in Acetic-Acid-Induced Inflammatory Bowel Disease in Rats. *BMC Complementary and Alternative Medicine* **2016**, *16* (1), 72. https://doi.org/10.1186/s12906-016-1057-5.

(40) Hansberry, D. R.; Shah, K.; Agarwal, P.; Agarwal, N. Fecal Myeloperoxidase as a Biomarker for Inflammatory Bowel Disease. *Cureus* **2017**, *9* (1). https://doi.org/10.7759/cureus.1004.

(41) Iwao, Y.; Tomiguchi, I.; Domura, A.; Mantaira, Y.; Minami, A.; Suzuki, T.; Ikawa, T.; Kimura, S.; Itai, S. Inflamed Site-Specific Drug Delivery System Based on the Interaction of Human Serum Albumin Nanoparticles with Myeloperoxidase in a Murine Model of Experimental Colitis. *European Journal of Pharmaceutics and Biopharmaceutics* **2018**, *125*, 141–147. https://doi.org/10.1016/j.ejpb.2018.01.016.

Chapter 5

Copper oxide nanoparticles for ulcerative colitis

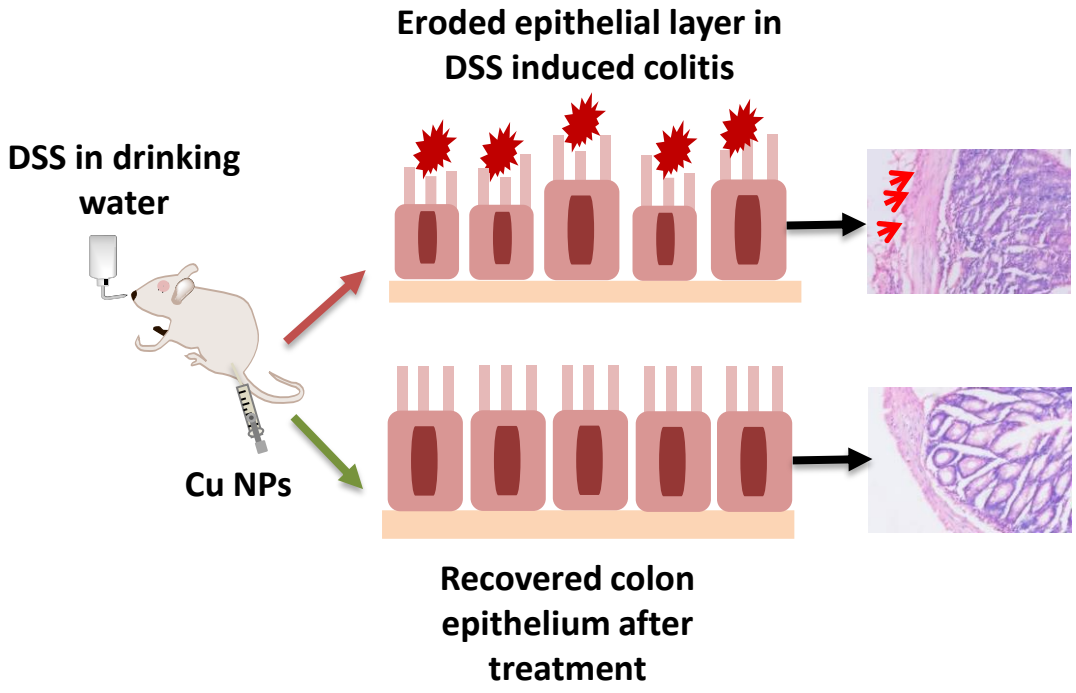

Graphical abstract

5.1 Introduction

Ulcerative colitis (UC) is a chronic idiopathic disease that affects lower end of gastrointestinal tract (g.i.t.) i.e., rectum and colon.[1] Complication like rectal bleeding, diarrhea, abdominal pain etc.[2] led are caused by UC, and it may develop colon cancer if left untreated.[3,4] It affects the colonic inflammatory homeostasis and causes disturbance in intestinal barrier functions. Intestinal tissue damage leads to the activation of the immune system and induces inflammatory processes and cytokine production. It compromises the crucial part of various cytokines and chemokines, including interleukins and TNF-α, which have significant role in the initiation as well as development of UC via the regulation of immune and inflammatory responses.[5,6]

The traditional therapy for UC management includes antibiotics, aminosalicylates, corticosteroids, immunosuppressive and biological agents, but their long term use causes adverse effects and provide symptomatic treatment.[7] Moreover, these drugs have restricted efficacy due to essential factors like low solubility and bioavailability and also high first-pass metabolism[8], drug inactivation in an acidic gastric environment, especially for oral delivery.[9–11]

Stress plays a crucial role in the pathogenesis of UC caused due to the injury in g.i.t. as a result of lipid peroxidation. This process is mediated by the interaction of hydroxy radicals with the cell membrane, and other lipid-derived free radicals are produced.[12–14] Oxidative stress is also an essential factor in initiating inflammatory bowel diseases.[15,16] Study also reported that compounds with antioxidant activity and efficacy against inflammatory cytokines are significant candidates for augmenting the condition of UC.[17] In the recent past, researchers tried to synthesize chemical compounds with gastroprotective and anti-inflammatory properties.

Copper-based complexes have been reported for their antiarthritic and antiulcer activity and have a proven potential role towards in-vivo models of inflammatory diseases.[18] Copper is an crucial element that has an essential role in metabolism and cellular physiology. Its ionic form redox activity makes it very cytotoxic so that the intracellular level of copper ion required to be attenuate for its

beneficial effect in human body.[19] Copper aspirinate and copper tryptophanate have been reported for wound healing activity in ulcers. Copper-based complexes have also been investigated for their antiulcer and anti-inflammatory activity better than some nonsteroidal anti-inflammatory drugs like ibuprofen and enefenamic acid.[20] Some copper complexes work as cytotoxic agents by the generation of free radicals, and some are reported as antioxidant based on their superoxide scavenging activity.[21,22]

In our earlier work, microcrystalline cellulose and aminocelluloses functionalized with thiol group provide 20-52 nm stable $Cu^{I/II}O$ NPs with water-soluble colloidal dispersion, which was used for homo and cross Glaser coupling reactions.[23] Our recent work demonstrated that smaller-sized (1-10 nm) homogenous colloidal dispersion of copper oxide (C-$Cu^{I/II}O$) nanoparticles (NPs) capping with thiol-functionalized cellulose act as efficient catalyst copper-mediated azide-alkyne cycloaddition (CuAAC) reaction under environmental-friendly conditions.[24] Though the previous works were performed for catalysis, the biocompatibility and its application in biology has not been tested for C-$Cu^{I/II}O$ NPs. Hence, in this study, we have tested the activity of smaller-sized C-$Cu^{I/II}O$ NPs against the UC. The synthesized nanoparticles were administered intra-rectally to avoid the oral limitations of anticolitic therapeutics. The homogenous water-soluble colloidal dispersion of C-$Cu^{I/II}O$ NPs supported by thiol functionalized cellulose was showed excellent activity against UC due to the inclusion of $Cu^{I/II}O$ NPs with the bio-compatible polymeric cellulose backbone.

5.2 Results and discussion

5.2.1 Synthesis and characterization of nanoparticles

Thiol-functionalized cellulose grafted copper oxide NPs (C-$Cu^{I/II}O$ NPs) was synthesized (**Figure 5.1**) and characterized in our previously published study by PXRD, FT-IR, TEM, and XPS in Figure 5.2 and Figure 5.3 respectively. The details are discussed in the published articles.[24]

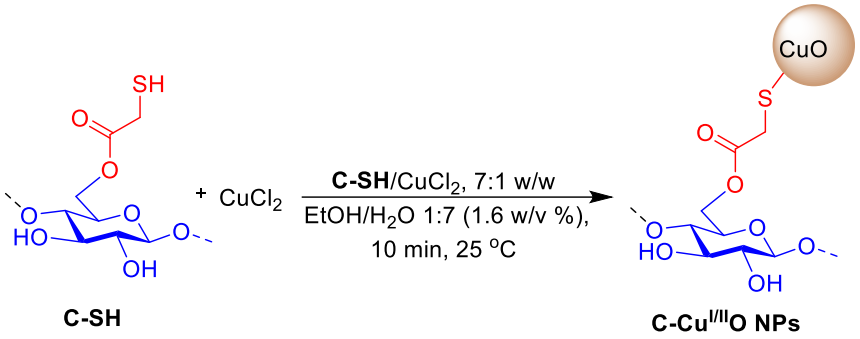

Figure 5.1 Synthesis of thiol-functionalized cellulose grafted copper oxide nanoparticles (C-Cu$^{I/II}$O NPs). Adapted from ref.[24] Copyright 2011 Wiley-VCH.

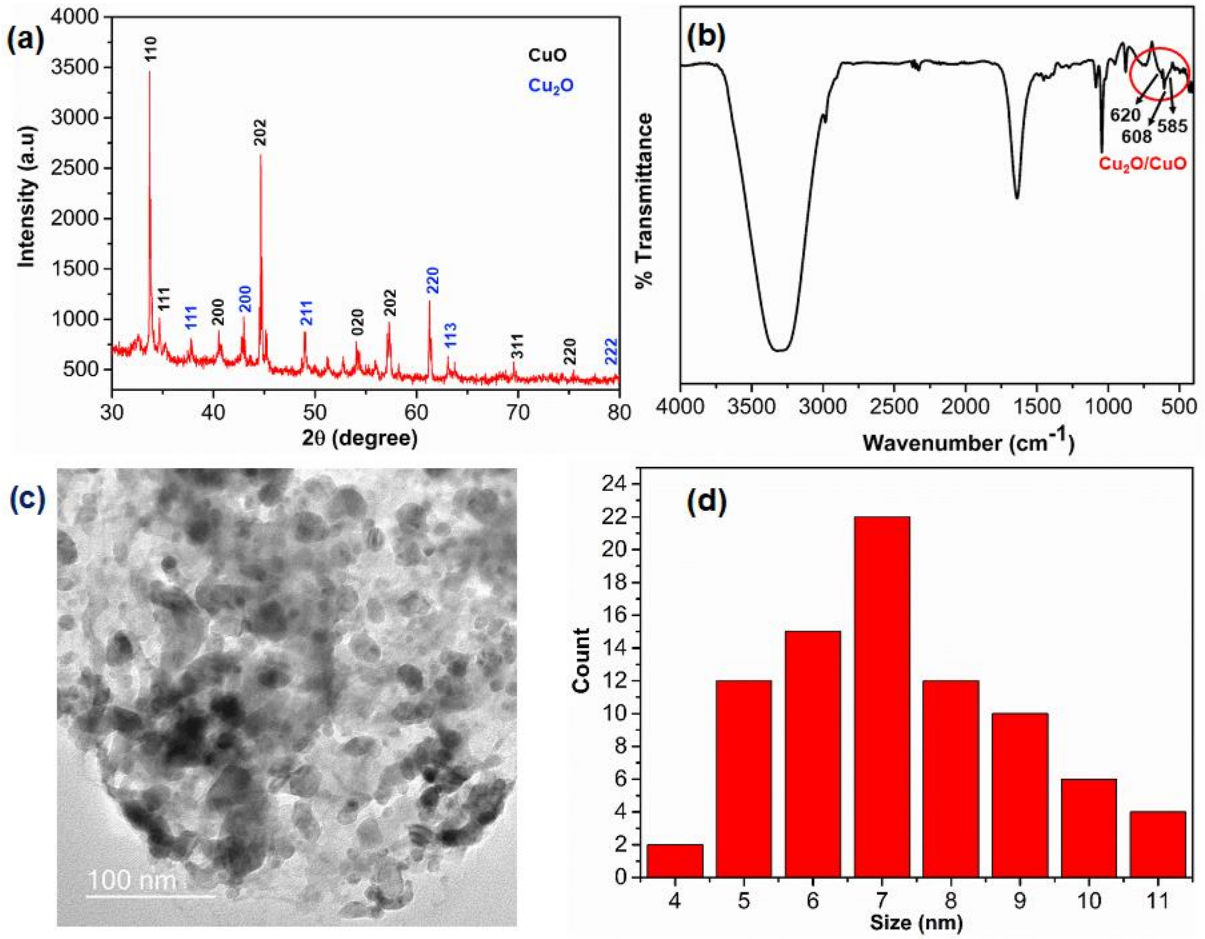

Figure 5.2 (a) XRD, (b) FT-IR, (c) TEM, and (d) particles size distributions of the C-Cu$^{I/II}$O NPs. Adapted from ref.[24] Copyright 2011 Wiley-VCH.

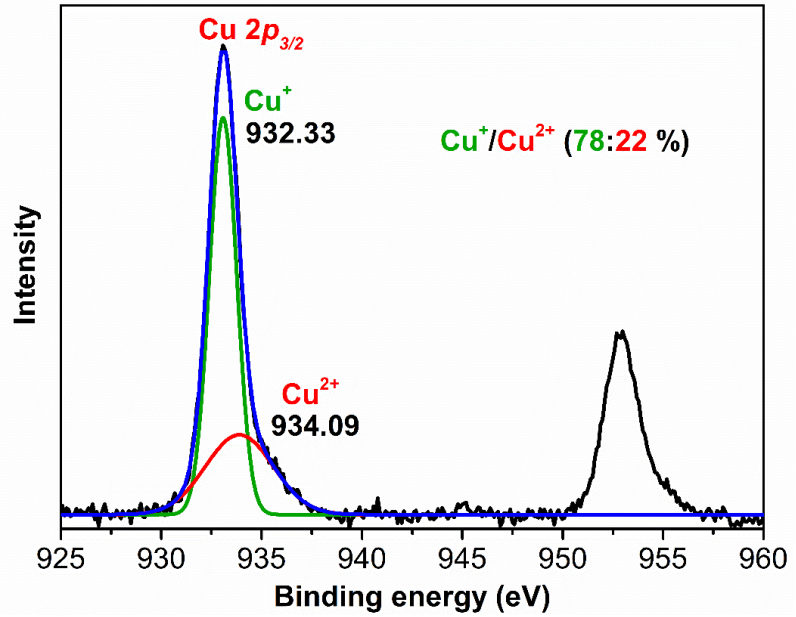

Figure 5.3 XPS of the C-Cu$^{I/II}$O NPs . Adapted from ref.*[24] *Copyright 2011 Wiley-VCH.

5.2.2 *In-vivo* Therapeutic Efficacy Study

After synthesis and characterizations of C-Cu$^{I/II}$O NPs, *in-vivo* therapeutic efficacy study performed against colitis mouse induced with dextran sulfate sodium.

5.2.2.1 Weight variation and disease activity index

Throughout experimentation period, mice were physically observed for parameters such as rectal bleeding, physical activity and stool consistency (**Table 5.1**). In normal control and safety groups, all the observed parameters were normal. In DSS group after induction of colitis diarrhoea (watery stool) was observed. In this group, some mice had severe rectal bleeding and almost all underwent sedentary activity. After treatment with C-Cu$^{I/II}$O NPs **1** stool consistency became soft, physical activity was mild and no rectal bleeding was observed. In C-Cu$^{I/II}$O NPs 2 treatment and standard groups, all physical activities tend to normal. Stool texture found soft without rectal bleeding and mice activity found normal.

Table 5.1 Physical observations of various parameters on experimental animals over the study period. Values are expressed in the table are average observational values.

S.No.	Groups	Observations		
		Stool Consistency	**Physical Activity**	**Rectal Bleeding**
1.	Normal Control	0	0	0
2.	DSS	4	3	1
3.	CNP1	1	1	0
4.	CNP2	0	0	0
5.	5-ASA	0	0	0
6.	Safety	0	0	0

Stool Consistency
0-Normal Pellet (Hard)
1-Soft Pellet
2-Loose watery stool
3-Stickiness
4-Diarrhoea

Physical Activity
0-Normal active (Highly)
1-Mild active
2-Low active
3-Sedentary

Rectal Bleeding
0-No bleeding
1-Bleeding

The variation in body weight of experimental animals through the study was also noticed. In intestinal inflammatory conditions weight loss has been observed which shows inflammatory state of Inflammatory bowel diseases (IBD) that leads to the restriction of nutrient absorption and ultimately represents the catabolism of the biological system.[25] At the end of study it was noticed that in DSS induced colitis group mice weight was severely affected and found drastically reduced (***$p \leq 0.001$) when compare to normal control group. Treatment with CNP and 5-ASA, percentage weight was positively affected and significant weight gain (###$p \leq 0.001$) was observed in comparison to colitis group. The % weight variation of normal control and safety groups were found similar (**Figure 5.4**).

After sacrificing animals' colons, all the study groups were observed physically for any changes. The previous studies reported that the mice colon is reduced in acute UC.[7,26]

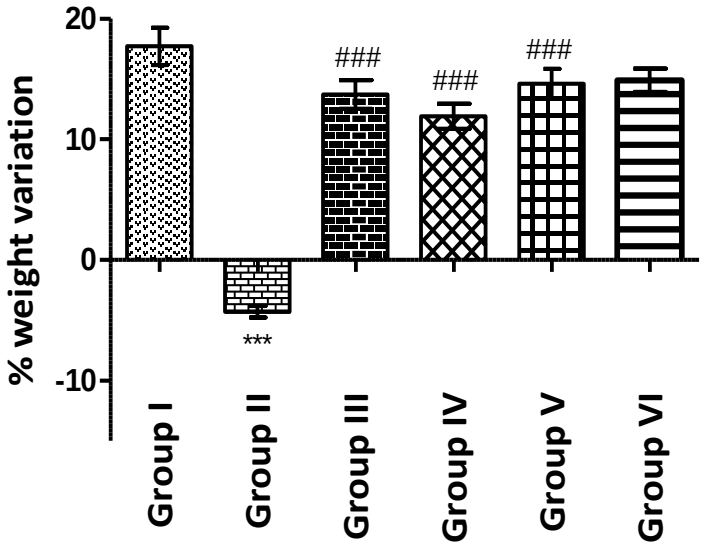

Figure 5.4 Weight variation in mice among different groups during the study period. Group I, Normal Control: mice received basal diet. Group II, DSS: mice received 4% DSS in drinking water upto 5 days. Group III, DSS + CNP1: DSS induced colitis mice, treated with Copperoxide nanoparticles suspended in 0.5 % CMC at dose of 10 mg/kg body weight intrarectally after induction of colitis. Group IV, DSS + CNP2: DSS induced colitis mice, treated with Copperoxide nanoparticles in 0.5 % CMC at dose of 40mg/kg body weight intrarectally after induction of colitis. Group V, DSS + 5-ASA: DSS induced colitis mice, treated with 5-ASA in 0.5 % CMC at dose of 30mg/kg body weight intrarectally after induction of colitis. (Values are presented as mean ± SD). Comparisons were made on the basis of the one-way ANOVA followed by Bonferroni post-test. All groups were compared to the DSS-treated group (p≤0.001, ###p≤0.001).***

DSS treatment causes shrinkage in colon led to marked decreased in colon length (*p≤0.05). After treatment with C-$Cu^{I/II}$O NPs as well as 5-ASA colon length regained (##p≤0.01) to its normal condition and significant difference was found in compared to colitis induced mice. Normal control as well as safety groups did not show marked changes **(Figure 5.5a).** Further, fecal occult blood test (FOBT) was also performed to check any hidden blood in faeces associated with diseases. In DSS treated group fecal blood was observed and also in C-$Cu^{I/II}$O NPs 1 group very slight traces of fecal blood was observed as evidenced by blue colour spot. After treatment with C-$Cu^{I/II}$O NPs 2 and 5-ASA, no fecal blood was observed together with normal control and safety groups **(Figure 5.5b).**

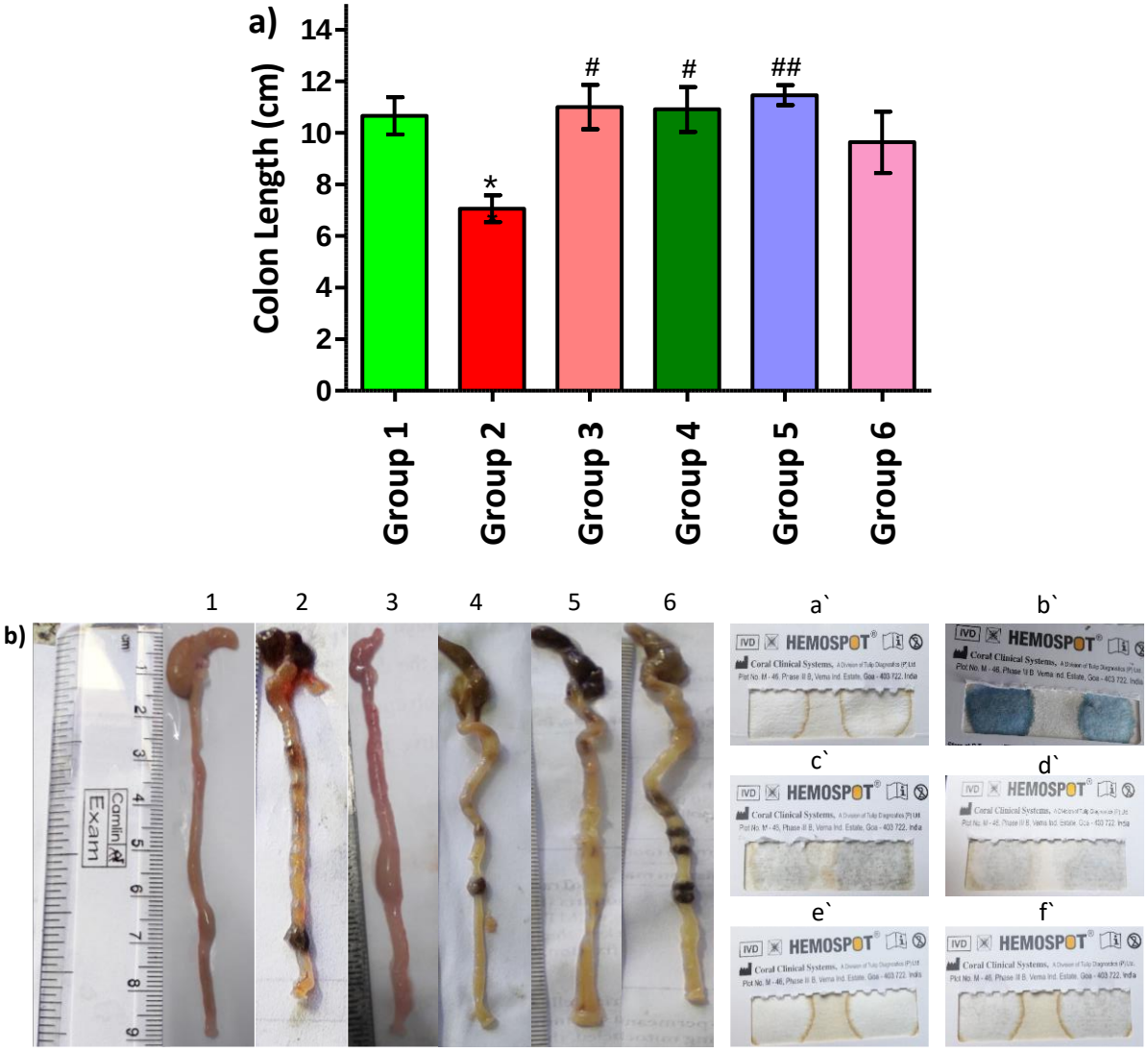

Figure 5.5a Colon length and Figure 5.5b. Representative images of colon and corresponding FOBT (a` - f`) in mice among different experimental groups. Group 1, Normal Control, Group 2, DSS, Group 3, DSS + C-Cu$^{I/II}$O NPs 1, Group 4, DSS + C-Cu$^{I/II}$O NPs 2, Group 5, DSS + 5-ASA, Group 6, C-Cu$^{I/II}$O NPs 2. (Presented values are mean ± SD). Data were compared based on the one-way ANOVA with Bonferroni post-test. Comparison was performed with normal control and colitis groups with all experimental groups (*p≤0.05, ##p≤0.01).

5.2.2.2 Histological findings

Analysis of colon histology of experimental animals suggested that complete colon histoarchitecture was found in healthy animals. In this group intact

muscularis layer surrounded submucosa and in mucosa layer normal goblet cells were appeared. After treatment with DSS, colitis induction took place which leads to significant alteration of colon histology. Sometimes the clusters of abnormal cells combined and forms tube like structures particularly known as aberrant crypt of foci. These are developed as precancerous lesion in colonic inflammation as well colitis.[27,28] In DSS group damaged muscularis layer appeared and depleted goblet cells were found. Comparing to normal control marked space linking the mucosa and muscularis appeared leads to submucosal widening which caused due to inflammatory cell infiltrations and collagen deposition in colitis group. In this study, changes in colonic histological patterns were found similar to previous reports.[25,29,30] After treatment with C-$Cu^{I/II}O$ NPs 1 colon lining recovered as recognized by appearance of goblet cells in mucosa and intacted layer of submucosa between muscularis as well as mucosa. In C-$Cu^{I/II}O$ NPs 2 treatment group regained colon morphology was found. 5-ASA treatment also revealed that complete colon morphology was found which consisted of mucosa, submucosa and muscularis. After treatment with C-$Cu^{I/II}O$ NPs 2 in normal animal to check the safety of the formulated nanoparticle there was no morphological alteration found in this group (**Figure 5.6**).

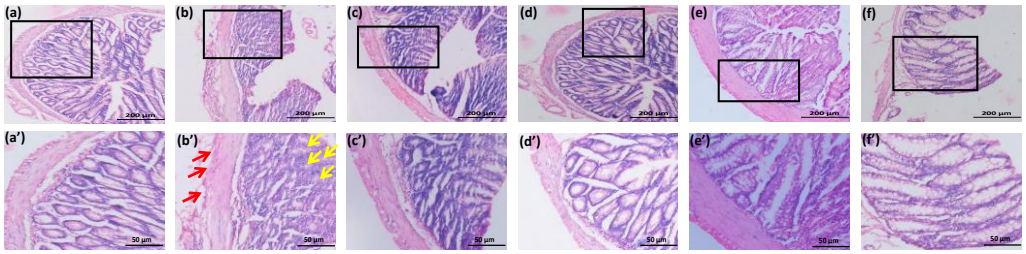

Figure 5.6 H&E-stained microscopic images of mice colon sections. (a) Normal Control: exhibited healthy histology of colon. (b) DSS: showed destructed goblet cells (yellow arrows) and damaged muscularis layer (red arrows). (c) DSS + C-$Cu^{I/II}O$ NPs 1: observed goblet cells appearance in mucosa as well as submucosa was intact between muscularis and mucosa. (d) DSS + C-$Cu^{I/II}O$ NPs 2: shows proper colon morphology was recovered. (e) DSS + 5-ASA: detailed colon morphology was regained. (f) C-$Cu^{I/II}O$ NPs 2: colon morphology found similar to healthy animals. Images magnification, 20X = 200 µm scale bar (a-e) and 40X = 50 µm scale bar (a'-e').

To analyse the coherence of mucin layer, alcian blue and neutral red staining of goblet cells was performed. Goblet cells secrete mucin which is glycosylated proteins of high molecular weight that constructs protective layer of intestinal lining. The depleted mucosa is more prone to inflammation in a particular region of the intestinal tract where direct exposure of noxious agents occurs.[31,32] In normal control group, blue color stained acidic mucin shown the presence of goblet cells. After induction of colitis on the administration of DSS led to the disrupted goblet cells which evidenced by extremely diminished blue colored stain. After administration of C-$Cu^{I/II}O$ NPs **1** recovery of goblet cells appeared, which regulated the increment of acidic mucin as evidenced by increased blue-colored stains. C-$Cu^{I/II}O$ NPs **2** treatment significantly reduced the inflammation and goblet cells were markedly increased. Upon treatment with 5-ASA similar result like C-$Cu^{I/II}O$ NPs **2** treatment group was found. In this group significant upsurge in blue color stain was found. The safety group where only C-$Cu^{I/II}O$ NPs **2** treatment was given goblet cells were similar to the normal control group (**Figure 5.7**).

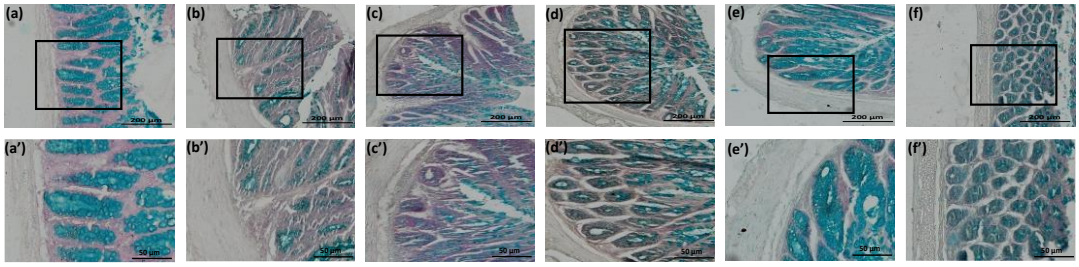

Figure 5.7 AB-NR-stained microscopic images of mice colon. (a) Normal Control: In this group goblet cells observed in blue color stains. (b) DSS: Noticeable reduction in blue color stain represents goblet cells disintegration. (c) DSS + C-$Cu^{I/II}O$ NPs 1: Goblet cells recovery following the treatment. (d) DSS + C-$Cu^{I/II}O$ NPs 2: showed significantly increased goblet cells. (e) DSS + 5-ASA: showed increased goblet cells. (f) C-$Cu^{I/II}O$ NPs 2: showed goblet cells appearance comparable to normal control. Images magnification, 20X = 200 µm scale bar (a-e) and 40X = 50 µm scale bar (a'-e').

Goblet cells in the colon secreted two types of mucins: sulfomucin and sialomucin. In colonic inflammation or colon cancer, colonic mucosa mainly secretes

sialomucin whereas normal colonic mucosa predominantly secretes sulfomucin.[33,34] To know the type of mucin and its correlation with UC high iron diamine and alcian blue (HID-AB) dyes were used to stain the colon sections. Sulfomucins stained by HID that imparts brown color whereas AB stains sialomucin of blue colour. In the present study, the normal control group represented brown color stained sulfomucin predominantly compared to blue colored sialomucin. In DSS induced colitis group significant enhancement of sialomucin mucins found in comparison to sulfomucin. Treatment with C-$Cu^{I/II}$O NPs **1** slightly enhances the sulfomucin, evidenced by increased brown color. In C-$Cu^{I/II}$O NPs **2** treatment group marked increment of sulfomucin in comparison to sialomucin observed as evidenced by enhanced brown color than blue color. In 5-ASA treatment group sulfomucin was predominantly observed than sialomucin. Safety group where C-$Cu^{I/II}$O NPs **2** treatment administered in healthy animals shows mucin pattern similar to normal control (**Figure 5.8**). The promoted secretion of sulfomucin and marked decreased transformation of sulfomucin to sialomucin suggested that C-$Cu^{I/II}$O NPs treatment was accomplished to employ protective effect in colonic inflammation.

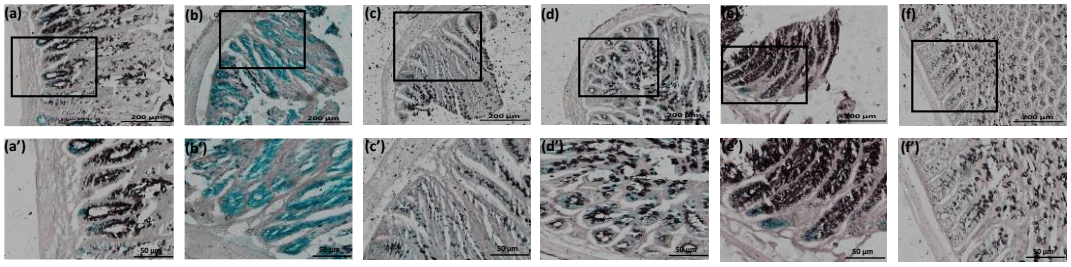

Figure 5.8 HID-AB-stained microscopic images of mice colon. (a) Normal Control: exhibited increased sulfomucin (in brown color) comparing to sialomucin (in blue color). (b) DSS: represented significant increment in sialomucin. (c) DSS + C-$Cu^{I/II}$O NPs 1: blue and brown stains showed enhancement in the production of mucin. (d) DSS + C-$Cu^{I/II}$O NPs 2: marked enhancement of sulfomucin than sialomucin in colon. (e) DSS + 5-ASA: showed more sulfomucin than sialomucin. (f) C-$Cu^{I/II}$O NPs 2: showed mucin staining pattern like normal control. Images magnification, 20X = 200 µm scale bar (a-e) and 40X = 50 µm scale bar (a'-e').

Intestinal inflammations are directly associated with the infiltration of proinflammatory mast cells. Activation of mast cells in inflammatory conditions are

responsible for the release of mediators like histamine. It leads to the allergic reactions by vascular and tissue changes at the site of inflammation. Like other inflammatory diseases infiltration of mast cells has been also noticed in UC.[35,36] In colitis group infiltration of mast cells was spotted in muscularis as well as submucosa. After administration of C-$Cu^{I/II}O$ NPs 1, C-$Cu^{I/II}O$ NPs **2** and 5-ASA mast cells infiltration was marked diminished. Also, in normal control and C-$Cu^{I/II}O$ NPs **2** treatment groups there was no mast cells were observed (**Figure 5.9**). The toluidine blue staining suggested that treatment with C-$Cu^{I/II}O$ NPs nanoparticles supressed the mast cells infiltration which may significantly decrease the intensity of DSS induced colitis.

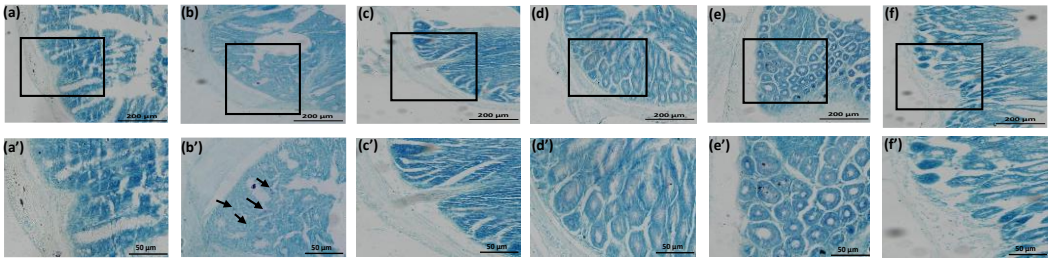

Figure 5.9 Microscopic images of toluidine blue stained colon sections. (a) Normal Control: colon section observed without infiltrated mast cells. (b) DSS: black arrows indicated purplish-blue color infiltrated mast cells. (c) DSS + C-$Cu^{I/II}O$ NPs 1: no mast cells infiltration. (d) DSS + C-$Cu^{I/II}O$ NPs 2: no infiltrated mast cells infiltration exhibited. (e) DSS + 5-ASA: no mast cells infiltration. (f) C-$Cu^{I/II}O$ NPs 2: no observed mast cells infiltration. Images magnification, 20X = 200 µm scale bar (a-e) and 40X = 50 µm scale bar (a'-e').

5.2.2.3 *In-Vivo* cytokines estimation

Granulated pro-inflammatory mast cells contain histamine and regulate innate immunity. These are also accumulated at the site of inflammation and responsible for the release of histamine and various inflammatory cytokines like IL-1β and TNF-α. These mediators are directly correlated with various inflammatory diseases including UC where these potentially marks for initiation and progression of disease.[37–39] Moreover, proinflammatory cytokines like TNF-α, IL-13, IL-33 etc. play crucial role in progress of disease whereas anti-inflammatory cytokines like IL-

10, IL-33 etc. causes the downregulation of disease progression. The imbalance between these two types of cytokines also causes the disturbance of colonic homeostasis and initiation and progression of disease may take place.[40,41] In our study DSS induced colitis group possessed enhanced level of TNF-α (***p≤0.001) in corelation of normal control group. Administration of C-Cu$^{I/II}$O NPs **1** (#p≤0.05) as well as C-Cu$^{I/II}$O NPs **2** (###p≤0.001) significantly reduced TNF-α. 5-ASA treatment also downregulate the level of TNF-α significantly (###p≤0.001). In safety group its level was found similar to normal control (**Figure 5.10**). These finding suggested that the synthesized C-Cu$^{I/II}$O NPs are able to suppress the overexpression of TNF-α, an inflammatory cytokine and inhibit the further progression of UC.

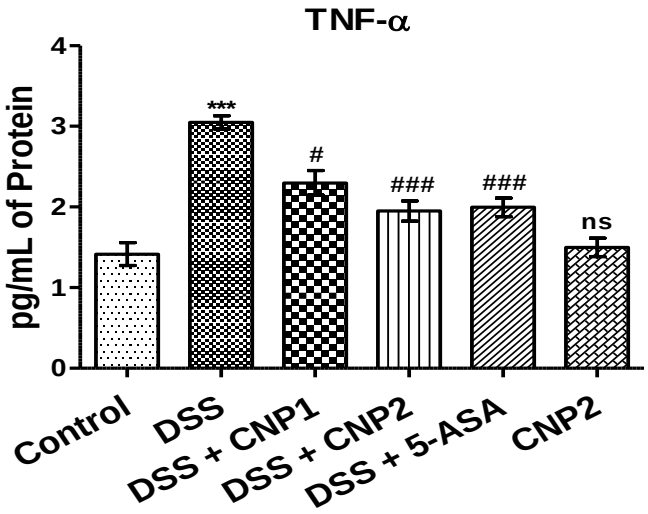

Figure 5.10 TNF-α level in serum. Indicated significant differences ***p ≤ 0.001, in comparison to control and #p ≤ 0.05 and ###p ≤0.001 in comparison to DSS induced colitis group, control group is also compared with C-Cu$^{I/II}$O NPs 2 (ns = non-significant). Represented data as mean ± standard deviation for experiments in triplicate (n = 3).

Tissue nitrite level is associated with inflammation as it is biomarker of inflamed tissue damage which is directly correlated with UC pathophysiology.[42,43] In our study DSS induced colitis group significant enhancement of tissue nitrite level (***p ≤ 0.001) found in collation to normal group. After administration of C-Cu$^{I/II}$O NPs **1** (##p ≤0.01) and C-Cu$^{I/II}$O NPs **2** (###p ≤0.001) nitrite level was markedly

downregulated. Tissue nitrite level in safety group (C-Cu$^{I/II}$O NPs 2) was similar to normal group (**Figure 5.11**). These finds were closely corroborated with previous reports. Significant enhancement in the nitrite level is reported in the tissue of UC patients where it governs the disease severity and progression.[44,45]

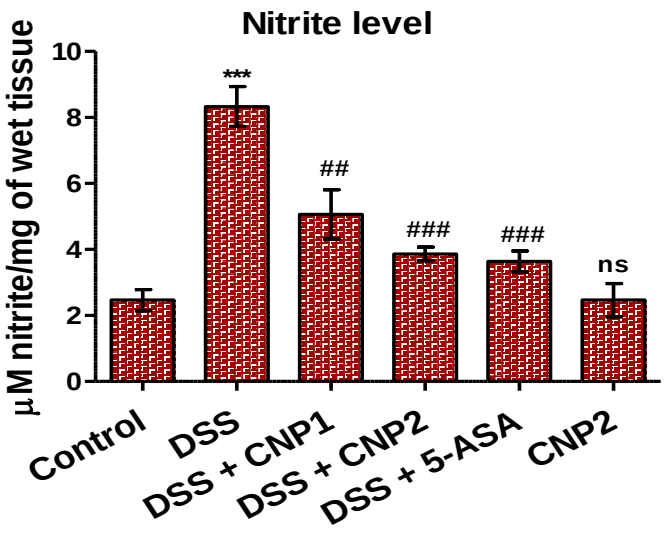

Figure 5.11 The level of nitrite in mice colon tissue. ***p ≤ 0.001, in comparison to control and ##p ≤ 0.01 and ###p ≤0.001 in comparison to DSS group, control group is also compared with C-Cu$^{I/II}$O NPs 2 (ns = non-significant) indicated the significant differences. Represented data as mean ± standard deviation for experiments in triplicate (n = 3).

Myeloperoxidase (MPO) is also an inflammatory marker largely overexpressed by inflammatory cells and is associated with UC.[46–48] In our study DSS induced colitis group significant enhanced MPO level (***p ≤ 0.001) was measured in collation to normal group. Administration of C-Cu$^{I/II}$O NPs 1 (#p ≤ 0.05) and CNP2 (###p ≤ 0.001) shown protective role as evidenced by marked reduction in MPO level. 5-ASA treatment also significantly reduced the MPO level (###p ≤ 0.001). In safety group MPO was similar to normal group (**Figure 5.12**). MPO level in our study is found similar to previous reports. Patient with colonic inflammatory disease found high level of MPO which is also a leading cause to enhance the disease severity.[49,50]

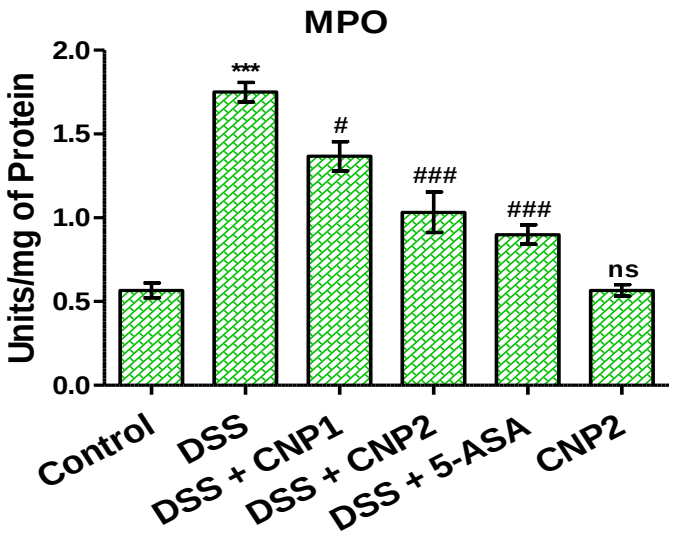

Figure 5.12 The level of MPO in mice colon tissue. Indicated significant differences ***p ≤ 0.001, in comparison to control and #p ≤ 0.05 and ###p ≤0.001 in comparison to DSS induced colitis group, control group is also compared with C-Cu$^{I/II}$O NPs 2 (ns = non-significant). Represented data as mean ± standard deviation for experiments in triplicate (n = 3).

5.3 Conclusion

In this study, a thiol-functionalized cellulose grafted biocompatible copper oxide nanoparticles (C-Cu$^{I/II}$O NPs) has been developed following the environmental-friendly approach for the therapy of DSS induced colitis. This formulated nanoparticle was assessed in acute experimental colitis in mice for various biochemical, physical and histological parameters. The nanoparticle was effective enough in alleviating mostly observed inflammatory indexes associated with the acute experimental colitis. This nanoparticle shows convenience for rectal administration *via* water dispersion. Furthermore, therapeutic efficacy of C-Cu$^{I/II}$O NPs was also evidenced in terms of the restoration of colon histo-architecture after the treatment. The anti-inflammatory activities of this nanoparticle was established in a dose-dependent manner. This study suggested that cellulose-based C-Cu$^{I/II}$O NPs effectively conquered the inflammatory changes associated with DSS induced colitis.

Note: Reprinted with permission from:-

Ahmad, A.; Ansari, Md. M.; Mishra, R. K.; Kumar, A.; Vyawahare, A.; Verma, R. K.; Raza, S. S.; Khan, R. Enteric-Coated Gelatin Nanoparticles Mediated Oral Delivery of 5-Aminosalicylic Acid Alleviates Severity of DSS-Induced Ulcerative Colitis. *Materials Science and Engineering: C* **2021**, *119*, 111582. https://doi.org/10.1016/j.msec.2020.111582.

5.4 Bibliography

(1) Gopi, S.; Amalraj, A.; Jude, S.; Varma, K.; Sreeraj, T. R.; Haponiuk, J. T.; Thomas, S. Preparation, Characterization and Anti-Colitis Activity of Curcumin-Asafoetida Complex Encapsulated in Turmeric Nanofiber. *Materials Science and Engineering: C* **2017**, *81*, 20–31. https://doi.org/10.1016/j.msec.2017.07.037.

(2) Lv, J.; Zhang, Y.; Tian, Z.; Liu, F.; Shi, Y.; Liu, Y.; Xia, P. Astragalus Polysaccharides Protect against Dextran Sulfate Sodium-Induced Colitis by Inhibiting NF-KB Activation. *International Journal of Biological Macromolecules* **2017**, *98*, 723–729. https://doi.org/10.1016/j.ijbiomac.2017.02.024.

(3) Ahmad, A.; Ansari, M. M.; Kumar, A.; Bishnoi, M.; Raza, S. S.; Khan, R. Aminocellulose - Grafted Polycaprolactone-Coated Core–Shell Nanoparticles Alleviate the Severity of Ulcerative Colitis: A Novel Adjuvant Therapeutic Approach. *Biomater. Sci.* **2021**, *9* (17), 5868–5883. https://doi.org/10.1039/D1BM00877C.

(4) Sharara, A. I.; Al Awadhi, S.; Alharbi, O.; Al Dhahab, H.; Mounir, M.; Salese, L.; Singh, E.; Sunna, N.; Tarcha, N.; Mosli, M. Epidemiology, Disease Burden, and Treatment Challenges of Ulcerative Colitis in Africa and the Middle East. *Expert Review of Gastroenterology & Hepatology* **2018**, *12* (9), 883–897. https://doi.org/10.1080/17474124.2018.1503052.

(5) Chen, Q.; Gou, S.; Ma, P.; Song, H.; Zhou, X.; Huang, Y.; Kwon Han, M.; Wan, Y.; Kang, Y.; Xiao, B. Oral Administration of Colitis Tissue-Accumulating Porous Nanoparticles for Ulcerative Colitis Therapy. *International Journal of Pharmaceutics* **2019**, *557*, 135–144. https://doi.org/10.1016/j.ijpharm.2018.12.046.

(6) Gaba, B.; Fazil, M.; Khan, S.; Ali, A.; Baboota, S.; Ali, J. Nanostructured Lipid Carrier System for Topical Delivery of Terbinafine Hydrochloride. *Bulletin of Faculty of Pharmacy, Cairo University* **2015**, *53* (2), 147–159. https://doi.org/10.1016/j.bfopcu.2015.10.001.

(7) Lee, Y.; Sugihara, K.; Gillilland, M. G.; Jon, S.; Kamada, N.; Moon, J. J. Hyaluronic Acid–Bilirubin Nanomedicine for Targeted Modulation of Dysregulated Intestinal Barrier, Microbiome and Immune Responses in Colitis. *Nat. Mater.* **2020**, *19* (1), 118–126. https://doi.org/10.1038/s41563-019-0462-9.

(8) Gavhane, Y. N.; Yadav, A. V. Loss of Orally Administered Drugs in GI Tract. *Saudi Pharmaceutical Journal* **2012**, *20* (4), 331–344. https://doi.org/10.1016/j.jsps.2012.03.005.

(9) Serrano-Olvera, A.; Cetina, L.; Coronel, J.; Dueñas-González, A. Emerging Drugs for the Treatment of Cervical Cancer. *Expert Opinion on Emerging Drugs* **2015**, *20* (2), 165–182. https://doi.org/10.1517/14728214.2015.1002768.

(10) Ashton, J. J.; Mossotto, E.; Ennis, S.; Beattie, R. M. Personalising Medicine in Inflammatory Bowel Disease—Current and Future Perspectives. *Transl Pediatr* **2019**, *8* (1), 56–69. https://doi.org/10.21037/tp.2018.12.03.

(11) Meier, J.; Sturm, A. Current Treatment of Ulcerative Colitis. *World J Gastroenterol* **2011**, *17* (27), 3204–3212. https://doi.org/10.3748/wjg.v17.i27.3204.

(12) Rana, S. V.; Sharma, S.; Prasad, K. K.; Sinha, S. K.; Singh, K. Role of Oxidative Stress & Antioxidant Defence in Ulcerative Colitis Patients from North India. *Indian J Med Res* **2014**, *139* (4), 568–571.

(13) Bourgonje, A. R.; Feelisch, M.; Faber, K. N.; Pasch, A.; Dijkstra, G.; van Goor, H. Oxidative Stress and Redox-Modulating Therapeutics in Inflammatory Bowel Disease. *Trends in Molecular Medicine* **2020**, *26* (11), 1034–1046. https://doi.org/10.1016/j.molmed.2020.06.006.

(14) Gallelli, C. A.; Calcagnini, S.; Romano, A.; Koczwara, J. B.; De Ceglia, M.; Dante, D.; Villani, R.; Giudetti, A. M.; Cassano, T.; Gaetani, S. Modulation of the Oxidative Stress and Lipid Peroxidation by Endocannabinoids and Their Lipid Analogues. *Antioxidants* **2018**, *7* (7), 93. https://doi.org/10.3390/antiox7070093.

(15) Dong, Y.; Hou, Q.; Lei, J.; Wolf, P. G.; Ayansola, H.; Zhang, B. Quercetin Alleviates Intestinal Oxidative Damage Induced by H2O2 via Modulation of GSH: In Vitro Screening and In Vivo Evaluation in a Colitis Model of Mice. *ACS Omega* **2020**, *5* (14), 8334–8346. https://doi.org/10.1021/acsomega.0c00804.

(16) Wang, X.; Gao, Y.; Wang, L.; Yang, D.; Bu, W.; Gou, L.; Huang, J.; Duan, X.; Pan, Y.; Cao, S.; Gao, Z.; Cheng, C.; Feng, Z.; Xie, J.; Yao, R. Troxerutin Improves Dextran Sulfate Sodium-Induced Ulcerative Colitis in Mice. *J. Agric. Food Chem.* **2021**, *69* (9), 2729–2744. https://doi.org/10.1021/acs.jafc.0c06755.

(17) Chen, Y.; Yang, B.; Ross, R. P.; Jin, Y.; Stanton, C.; Zhao, J.; Zhang, H.; Chen, W. Orally Administered CLA Ameliorates DSS-Induced Colitis in Mice via Intestinal Barrier Improvement, Oxidative Stress Reduction, and Inflammatory Cytokine and Gut Microbiota Modulation. *J. Agric. Food Chem.* **2019**, *67* (48), 13282–13298. https://doi.org/10.1021/acs.jafc.9b05744.

(18) Conner, E. M.; Reglinski, J.; Smith, W. E.; Zeitlin, I. J. Schiff Base Complexes of Copper and Zinc as Potential Anti-Colitic Compounds. *Biometals* **2017**, *30* (3), 423–439. https://doi.org/10.1007/s10534-017-0016-z.

(19) Hussain, A.; AlAjmi, M. F.; Rehman, M. T.; Amir, S.; Husain, F. M.; Alsalme, A.; Siddiqui, M. A.; AlKhedhairy, A. A.; Khan, R. A. Copper(II) Complexes as Potential Anticancer and Nonsteroidal Anti-Inflammatory Agents: In Vitro and in Vivo Studies. *Sci Rep* **2019**, *9* (1), 5237. https://doi.org/10.1038/s41598-019-41063-x.

(20) Hajrezaie, M.; Golbabapour, S.; Hassandarvish, P.; Gwaram, N. S.; Hadi, A. H. A.; Ali, H. M.; Majid, N.; Abdulla, M. A. Acute Toxicity and Gastroprotection Studies of a New Schiff Base Derived Copper (II) Complex against Ethanol-Induced Acute Gastric Lesions in Rats. *PLOS ONE* **2012**, *7* (12), e51537. https://doi.org/10.1371/journal.pone.0051537.

(21) Psomas, G. Copper(II) and Zinc(II) Coordination Compounds of Non-Steroidal Anti-Inflammatory Drugs: Structural Features and Antioxidant Activity. *Coordination Chemistry Reviews* **2020**, *412*, 213259. https://doi.org/10.1016/j.ccr.2020.213259.

(22) Boulsourani, Z.; Katsamakas, S.; Geromichalos, G. D.; Psycharis, V.; Raptopoulou, C. P.; Hadjipavlou-Litina, D.; Yiannaki, E.; Dendrinou-Samara, C. Synthesis, Structure Elucidation and Biological Evaluation of Triple Bridged Dinuclear Copper(II) Complexes as Anticancer and Antioxidant/Anti-Inflammatory Agents. *Mater Sci Eng C Mater Biol Appl* **2017**, *76*, 1026–1040. https://doi.org/10.1016/j.msec.2017.03.157.

(23) Kaur, S.; Mukhopadhyaya, A.; Selim, A.; Gowri, V.; Neethu, K. M.; Dar, A. H.; Sartaliya, S.; Ali, M. E.; Jayamurugan, G. Tuning of Cross-Glaser Products Mediated by Substrate–Catalyst Polymeric Backbone Interactions. *Chem. Commun.* **2020**, *56* (17), 2582–2585. https://doi.org/10.1039/C9CC08565C.

(24) Selim, A.; Neethu, K. M.; Gowri, V.; Sartaliya, S.; Kaur, S.; Jayamurugan, G. Thiol-Functionalized Cellulose Wrapped Copperoxide as a Green Nano Catalyst for Regiospecific Azide-Alkyne Cycloaddition Reaction: Application in Rufinamide Synthesis. *Asian Journal of Organic Chemistry* **2021**, *10* (12), 3428–3433. https://doi.org/10.1002/ajoc.202100658.

(25) Abdelmegid, A. M.; Abdo, F. K.; Ahmed, F. E.; Kattaia, A. A. A. Therapeutic Effect of Gold Nanoparticles on DSS-Induced Ulcerative Colitis in Mice with Reference to Interleukin-17 Expression. *Sci Rep* **2019**, *9* (1), 10176. https://doi.org/10.1038/s41598-019-46671-1.

(26) Hu, B.; Yu, S.; Shi, C.; Gu, J.; Shao, Y.; Chen, Q.; Li, Y.; Mezzenga, R. Amyloid–Polyphenol Hybrid Nanofilaments Mitigate Colitis and Regulate Gut Microbial Dysbiosis. *ACS Nano* **2020**, *14* (3), 2760–2776. https://doi.org/10.1021/acsnano.9b09125.

(27) Jin, B.-R.; Chung, K.-S.; Cheon, S.-Y.; Lee, M.; Hwang, S.; Noh Hwang, S.; Rhee, K.-J.; An, H.-J. Rosmarinic Acid Suppresses Colonic Inflammation in Dextran

Sulphate Sodium (DSS)-Induced Mice via Dual Inhibition of NF-KB and STAT3 Activation. *Sci Rep* **2017**, *7*, 46252. https://doi.org/10.1038/srep46252.

(28) Periasamy, S.; Liu, C.-T.; Wu, W.-H.; Chien, S.-P.; Liu, M.-Y. Dietary Ziziphus Jujuba Fruit Influence on Aberrant Crypt Formation and Blood Cells in Colitis-Associated Colorectal Cancer Mice. *Asian Pacific Journal of Cancer Prevention* **2015**, *16* (17), 7561–7566. https://doi.org/10.7314/APJCP.2015.16.17.7561.

(29) Balaha, M.; Kandeel, S.; Elwan, W. Garlic Oil Inhibits Dextran Sodium Sulfate-Induced Ulcerative Colitis in Rats. *Life Sciences* **2016**, *146*, 40–51. https://doi.org/10.1016/j.lfs.2016.01.012.

(30) Islam, J.; Sato, S.; Watanabe, K.; Watanabe, T.; Ardiansyah; Hirahara, K.; Aoyama, Y.; Tomita, S.; Aso, H.; Komai, M.; Shirakawa, H. Dietary Tryptophan Alleviates Dextran Sodium Sulfate-Induced Colitis through Aryl Hydrocarbon Receptor in Mice. *The Journal of Nutritional Biochemistry* **2017**, *42*, 43–50. https://doi.org/10.1016/j.jnutbio.2016.12.019.

(31) Khan, R.; Khan, A. Q.; Lateef, A.; Rehman, M. U.; Tahir, M.; Ali, F.; Hamiza, O. O.; Sultana, S. Glycyrrhizic Acid Suppresses the Development of Precancerous Lesions via Regulating the Hyperproliferation, Inflammation, Angiogenesis and Apoptosis in the Colon of Wistar Rats. *PLOS ONE* **2013**, *8* (2), e56020. https://doi.org/10.1371/journal.pone.0056020.

(32) Larsson, J. M. H.; Karlsson, H.; Crespo, J. G.; Johansson, M. E. V.; Eklund, L.; Sjövall, H.; Hansson, G. C. Altered O-Glycosylation Profile of MUC2 Mucin Occurs in Active Ulcerative Colitis and Is Associated with Increased Inflammation. *Inflammatory Bowel Diseases* **2011**, *17* (11), 2299–2307. https://doi.org/10.1002/ibd.21625.

(33) Croix, J. A.; Carbonero, F.; Nava, G. M.; Russell, M.; Greenberg, E.; Gaskins, H. R. On the Relationship between Sialomucin and Sulfomucin Expression and Hydrogenotrophic Microbes in the Human Colonic Mucosa. *PLOS ONE* **2011**, *6* (9), e24447. https://doi.org/10.1371/journal.pone.0024447.

(34) Deplancke, B.; Gaskins, H. R. Microbial Modulation of Innate Defense: Goblet Cells and the Intestinal Mucus Layer. *The American Journal of Clinical Nutrition* **2001**, *73* (6), 1131S-1141S. https://doi.org/10.1093/ajcn/73.6.1131S.

(35) Luchini, A. C.; Costa de Oliveira, D. M.; Pellizzon, C. H.; Di Stasi, L. C.; Gomes, J. C. Relationship between Mast Cells and the Colitis with Relapse Induced by Trinitrobenzesulphonic Acid in Wistar Rats. *Mediators of Inflammation* **2009**, *2009*, e432493. https://doi.org/10.1155/2009/432493.

(36) Branco, A. C. C. C.; Yoshikawa, F. S. Y.; Pietrobon, A. J.; Sato, M. N. Role of Histamine in Modulating the Immune Response and Inflammation. *Mediators of Inflammation* **2018**, *2018*, e9524075. https://doi.org/10.1155/2018/9524075.

(37) Serhan, N.; Basso, L.; Sibilano, R.; Petitfils, C.; Meixiong, J.; Bonnart, C.; Reber, L. L.; Marichal, T.; Starkl, P.; Cenac, N.; Dong, X.; Tsai, M.; Galli, S. J.; Gaudenzio, N. House Dust Mites Activate Nociceptor-Mast Cell Clusters to Drive Type 2 Skin Inflammation. *Nat Immunol* **2019**, *20* (11), 1435–1443. https://doi.org/10.1038/s41590-019-0493-z.

(38) Wernersson, S.; Pejler, G. Mast Cell Secretory Granules: Armed for Battle. *Nat Rev Immunol* **2014**, *14* (7), 478–494. https://doi.org/10.1038/nri3690.

(39) Liu, D.; Viennois, E.; Fang, J.; Merlin, D.; Iyer, S. S. Toward Point-of-Care Diagnostics to Monitor MMP-9 and TNF-α Levels in Inflammatory Bowel Disease. *ACS Omega* **2021**, *6* (10), 6582–6587. https://doi.org/10.1021/acsomega.0c05115.

(40) Tatiya-aphiradee, N.; Chatuphonprasert, W.; Jarukamjorn, K. Immune Response and Inflammatory Pathway of Ulcerative Colitis. *Journal of Basic and Clinical Physiology and Pharmacology* **2019**, *30* (1), 1–10. https://doi.org/10.1515/jbcpp-2018-0036.

(41) Qiu, X.; Zhang, M.; Yang, X.; Hong, N.; Yu, C. Faecalibacterium Prausnitzii Upregulates Regulatory T Cells and Anti-Inflammatory Cytokines in Treating TNBS-Induced Colitis. *Journal of Crohn's and Colitis* **2013**, *7* (11), e558–e568. https://doi.org/10.1016/j.crohns.2013.04.002.

(42) Gawrońska, B.; Matowicka-Karna, J.; Kralisz, M.; Kemona, H. Markers of Inflammation and Influence of Nitric Oxide on Platelet Activation in the Course of

Ulcerative Colitis. *Oncotarget* **2017**, *8* (40), 68108–68114. https://doi.org/10.18632/oncotarget.19202.

(43) Nagata, J.; Yokodera, H.; Maeda, G. In Vitro and in Vivo Studies on Anti-Inflammatory Effects of Traditional Okinawan Vegetable Methanol Extracts. *ACS Omega* **2019**, *4* (13), 15660–15664. https://doi.org/10.1021/acsomega.9b02178.

(44) Soufli, I.; Toumi, R.; Rafa, H.; Touil-Boukoffa, C. Overview of Cytokines and Nitric Oxide Involvement in Immuno-Pathogenesis of Inflammatory Bowel Diseases. *World J Gastrointest Pharmacol Ther* **2016**, *7* (3), 353–360. https://doi.org/10.4292/wjgpt.v7.i3.353.

(45) Avdagić, N.; Zaćiragić, A.; Babić, N.; Hukić, M.; Šeremet, M.; Lepara, O.; Nakaš-Ićindić, E. Nitric Oxide as a Potential Biomarker in Inflammatory Bowel Disease. *Bosn J Basic Med Sci* **2013**, *13* (1), 5–9.

(46) Chami, B.; Martin, N. J. J.; Dennis, J. M.; Witting, P. K. Myeloperoxidase in the Inflamed Colon: A Novel Target for Treating Inflammatory Bowel Disease. *Archives of Biochemistry and Biophysics* **2018**, *645*, 61–71. https://doi.org/10.1016/j.abb.2018.03.012.

(47) Garrity-Park, M.; Loftus, E. V., Jr; Sandborn, W. J.; Smyrk, T. C. Myeloperoxidase Immunohistochemistry as a Measure of Disease Activity in Ulcerative Colitis: Association With Ulcerative Colitis-Colorectal Cancer, Tumor Necrosis Factor Polymorphism and RUNX3 Methylation. *Inflammatory Bowel Diseases* **2012**, *18* (2), 275–283. https://doi.org/10.1002/ibd.21681.

(48) Bastaki, S. M. A.; Al Ahmed, M. M.; Al Zaabi, A.; Amir, N.; Adeghate, E. Effect of Turmeric on Colon Histology, Body Weight, Ulcer, IL-23, MPO and Glutathione in Acetic-Acid-Induced Inflammatory Bowel Disease in Rats. *BMC Complementary and Alternative Medicine* **2016**, *16* (1), 72. https://doi.org/10.1186/s12906-016-1057-5.

(49) Hansberry, D. R.; Shah, K.; Agarwal, P.; Agarwal, N. Fecal Myeloperoxidase as a Biomarker for Inflammatory Bowel Disease. *Cureus 9* (1), e1004. https://doi.org/10.7759/cureus.1004.

(50) Iwao, Y.; Tomiguchi, I.; Domura, A.; Mantaira, Y.; Minami, A.; Suzuki, T.; Ikawa, T. Kimura, S. Ichiro, Itai, S., 2018. Inflamed Site-Specific Drug Delivery System Based on the Interaction of Human Serum Albumin Nanoparticles with Myeloperoxidase in a Murine Model of Experimental Colitis. *Eur. J. Pharm. Biopharm 125*, 141–147.

Thiol-Functionalized Cellulose-Grafted Copper Oxide Nanoparticles for the Therapy of Experimental Colitis in Swiss Albino Mice

Author: Rakesh Kumar Mishra, Abdul Selim, Vijayendran Gowri, et al
Publication: ACS Biomaterials Science & Engineering
Publisher: American Chemical Society
Date: May 1, 2022

PERMISSION/LICENSE IS GRANTED FOR YOUR ORDER AT NO CHARGE

This type of permission/license, instead of the standard Terms and Conditions, is sent to you because no fee is being charged for your order. Please note the following:

- Permission is granted for your request in both print and electronic formats, and translations.
- If figures and/or tables were requested, they may be adapted or used in part.
- Please print this page for your records and send a copy of it to your publisher/graduate school.
- Appropriate credit for the requested material should be given as follows: "Reprinted (adapted) with permission from {COMPLETE REFERENCE CITATION}. Copyright {YEAR} American Chemical Society." Insert appropriate information in place of the capitalized words.
- One-time permission is granted only for the use specified in your RightsLink request. No additional uses are granted (such as derivative works or other editions). For any uses, please submit a new request.

If credit is given to another source for the material you requested from RightsLink, permission must be obtained from that source.

BACK CLOSE WINDOW

ACS Biomaterials SCIENCE & ENGINEERING

pubs.acs.org/journal/abseba

Article

Thiol-Functionalized Cellulose-Grafted Copper Oxide Nanoparticles for the Therapy of Experimental Colitis in Swiss Albino Mice

Rakesh Kumar Mishra,[▽] Abdul Selim,[▽] Vijayendran Gowri, Anas Ahmad, Ahmed Nadeem, Nahid Siddiqui, Syed Shadab Raza, Govindasamy Jayamurugan,* and Rehan Khan*

Cite This: *ACS Biomater. Sci. Eng.* 2022, 8, 2088−2095

Read Online

ACCESS | Metrics & More | Article Recommendations | Supporting Information

ABSTRACT: Ulcerative colitis (UC) is a chronic inflammatory disease, which deleteriously affects the lower end of the gastrointestinal tract, i.e., the colon and the rectum. UC affects colonic inflammatory homeostasis and disrupts intestinal barrier functions. Intestinal tissue damage activates the immune system and collectively worsens the disease condition via the production of various cytokines. Ongoing therapeutics of UC have marked limitations like rapid clearance, extensive first-pass metabolism, poor drug absorption, very low solubility, bioavailability, etc. Because of these restrictions, the management of UC demands a rational approach that selectively delivers the drug at the site of action to overcome the therapeutic limiting factors. Metallic nanoparticles (NPs) have good therapeutic efficacy against colitis, but their uses are limited due to adverse effects on the biological system. In this study, we have used biocompatible thiol-functionalized cellulose-grafted copper oxide nanoparticles (C-$Cu^{I/II}O$ NPs) to treat UC. The metal NPs alleviated the colitis condition as evidenced by the colon length and observed physical parameters. Analysis of histopathology demonstrated the recovery of the colon architecture damaged by dextran sulfate sodium-induced colitis. Treatment with C-$Cu^{I/II}O$ NPs reduced the disintegration of goblet cells and the retainment of sulfomucin. Significant downregulation of inflammatory markers like MPO activity, as well as levels of nitrite and TNF-α, was found following C-$Cu^{I/II}O$ NP treatment. The observations from the study suggested that intrarectal treatment of colitis with cellulose-based C-$Cu^{I/II}O$ NPs successfully combated the intestinal inflammatory condition.

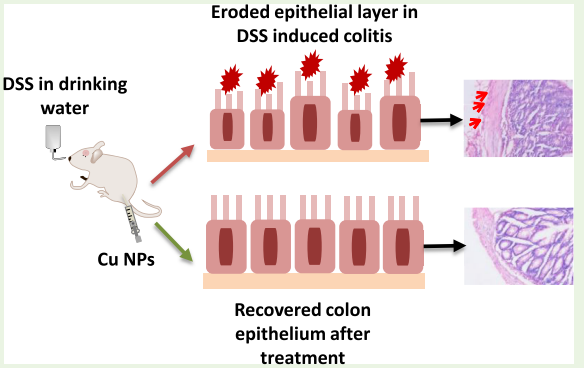

KEYWORDS: *copper oxide nanoparticles, cellulose, ulcerative colitis, inflammatory disease*

1. INTRODUCTION

Ulcerative colitis (UC) is a chronic disease that adversely impacts the lower end of the gastrointestinal tract (g.i.t.), i.e., the rectum and the colon.[1] Complications like rectal bleeding, diarrhea, abdominal pain, etc.[2] are caused by UC, and it may develop colon cancer if left untreated.[3,4] It affects the colonic inflammatory homeostasis and causes disturbance in intestinal barrier functions. Intestinal tissue damage leads to the activation of the immune system and induces inflammatory processes and cytokine production. It compromises the crucial part of various cytokines and chemokines, including interleukins and TNF-α, which have a significant role in the initiation as well as the development of UC via the regulation of immune and inflammatory responses.[5,6]

The traditional therapy for UC management includes 5-aminosalicylic acid, corticosteroids, immunosuppressants, and biologics, but their prolonged use causes adverse effects and provides symptomatic treatment.[7] Moreover, these drugs have restricted efficacy due to essential factors like low solubility and bioavailability, first-pass metabolism,[8] and drug inactivation in an acidic gastric environment, especially for oral delivery.[9−11]

Stress plays a crucial role in the pathogenesis of UC caused by an injury in the g.i.t. as a result of lipid peroxidation. This process is initiated by the interaction of hydroxy radicals with the cell membrane, and other lipid-derived free radicals are produced.[12−14] Oxidative stress is also an essential factor in initiating inflammatory bowel diseases.[15,16] A study also reported that compounds with antioxidant activity and efficacy against inflammatory cytokines are significant candidates for augmenting the condition of UC.[17] In the recent past, researchers tried to synthesize chemical compounds with gastroprotective and anti-inflammatory properties.

Copper-based complexes have been reported for their antiarthritic and antiulcer activity and have a proven potential role toward in vivo models of inflammatory diseases.[18] Copper

Received: January 30, 2022
Accepted: April 11, 2022
Published: April 22, 2022

Chapter 6

Caffeic acid conjugated budesonide-loaded nanomicelle for ulcerative colitis

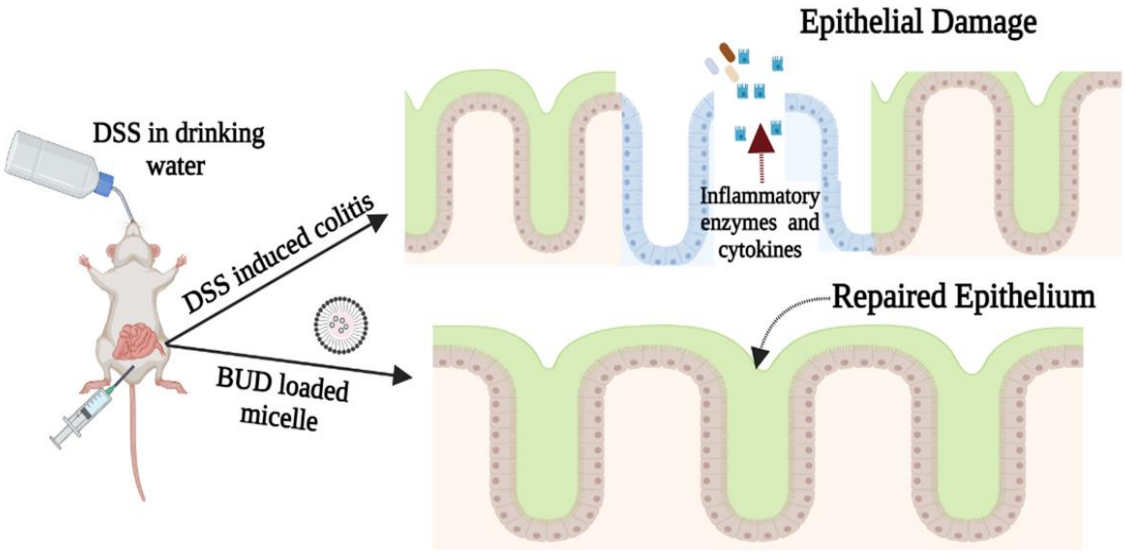

Graphical abstract

6.1 Introduction

Ulcerative colitis (UC) is a multifactorial disease of gastrointestinal tract (g.i.t.) that causes chronic inflammation to the specified portion of large intestine mainly colon and may spread to the rectum. It is a type of inflammatory bowel disease (IBD) that affects more than 6 million population in the world.[1–3] It is associated with food habits and industrialization and is found more frequently in America and European countries. However, its current trend is found rises in Asian countries also.[4]

Most observed symptoms in UC is found to be rectal bleeding, weight loss, diarrhea etc.[5] Disturbance in the intestinal homeostasis is found important factor in the initiation and development of intestinal diseases including UC. During the intestinal inflammatory reactions colonic mucosal layer damaged and is more prone to the obnoxious effects of external materials because of in this condition intestinal barrier function has been compromised.[6,7] The pathology of UC may cause disrupted colon resistance function, dysregulated colonic immunity, uncertainty in gut microbiota that collectively resulted in severe inflammatory processes.[8,9] These unwanted intestinal events give rise to many cytokines and chemokines including interleukins and TNF-α. Their role is reported as considerable factor in the development of inflammatory diseases like UC as regulator of immune and inflammatory response. These inflammatory mediators then start and recruit inflammatory cells and overexpress inflammatory enzymes like iNOS and COX-2 at the site of inflammation and further causes inflammatory changes to the colon epithelium.[10,11] If this intestinal inflammation left unmanaged it may cause the development of colon cancer.[12]

The traditional therapy for the treatment of UC is aminosalicylates, biologicals, hormone therapy, antibiotics, immunosuppressive agents etc. These therapeutic regimens are associated with symptomatic relief and precipitated various side effects[13] on long term administration. Many of these medications have very low water solubility resulting decreased bioavailability, hepatic metabolism is quite high, on oral administration they possess degradation in acidic stomach environment. All

these factors lead to compromised therapeutic efficacy of conventional therapy of UC.[14,15]

Budesonide (BUD) is a synthetically available second generation corticosteroidal drug with potent local anti-inflammatory activity. It is reported to be used for the management of inflammatory diseases including UC. On oral administration it undergoes extensive first pass metabolism and quite limited bioavailability and thus limits its therapeutic efficacy.[16–18]

To conquer above discussed drug related problems novel drug carriers have brought in context that may effectively address the therapeutic requirements. These were markedly able to enhanced drug solubility, manage unwanted effects and enhance availability of drug at the diseased site and thus potentiate therapeutic efficacy of active ingredients.[19,20] In our study we have developed nanosized micelle for the delivery of BUD in the management of UC. Micelles are aggregated structures of amphiphile that forms hydrophilic shell and hydrophobic core after self-assembly in aqueous media. Micelle as a delivery carrier has been reported with several advantages such as enhanced hydrophilic/hydrophobic drug loading, ease for chemical modification as delivery requirement, stability in physiological conditions, enhanced circulation time so that maximally available in the system at the site of disease etc. and is convenient for UC management.[1,21–24]

The aim of present study is to develop BUD loaded caffeic acid conjugated micelle for the management of DSS induced experimental colitis. For the development of micelle an amphiphile containing stearic acid and caffeic acid conjugated with ethylenediamine was synthesized. The components of micelle are USFDA approved generally recognized as safe (GRAS) material for drugs and pharmaceutical use. These are biocompatible, non-toxic and safe for use in clinics as components of therapy. Stearic acid is long chain saturated fatty acid obtained from plant as well as animal originated product which makes hydrophobic portion of amphiphile reported for pharmaceutical preparations.[25,26] Caffeic acid (CA) is a phenolic acid reported for its antioxidant, anti-inflammatory as well as anticarcinogenic activities which makes hydrophilic portion of amphiphile. CA is also

reported to inhibit NF-kB, COX-2 and various proinflammatory cytokines at the site of inflammation and alleviate the inflammatory condition in UC.[27–29] The synthesized amphiphile in aqueous media self-assemble in such a way that stearic acid makes hydrophobic core that sufficiently encapsulated model drug BUD whereas, CA make hydrophilic tails that possess good aqueous dispersibility of micelle for convenient rectal administration in mice model of UC.

6.2 Results and discussion

6.2.1 Formulation and characterization of nanomicelle

For the development of micelle an amphiphile has been synthesized by conjugation of stearic acid and caffeic acid conjugated by ethylenediamine. The synthesis and corresponding characterizations have been given in figures (**Figure 6.1-6.7**).

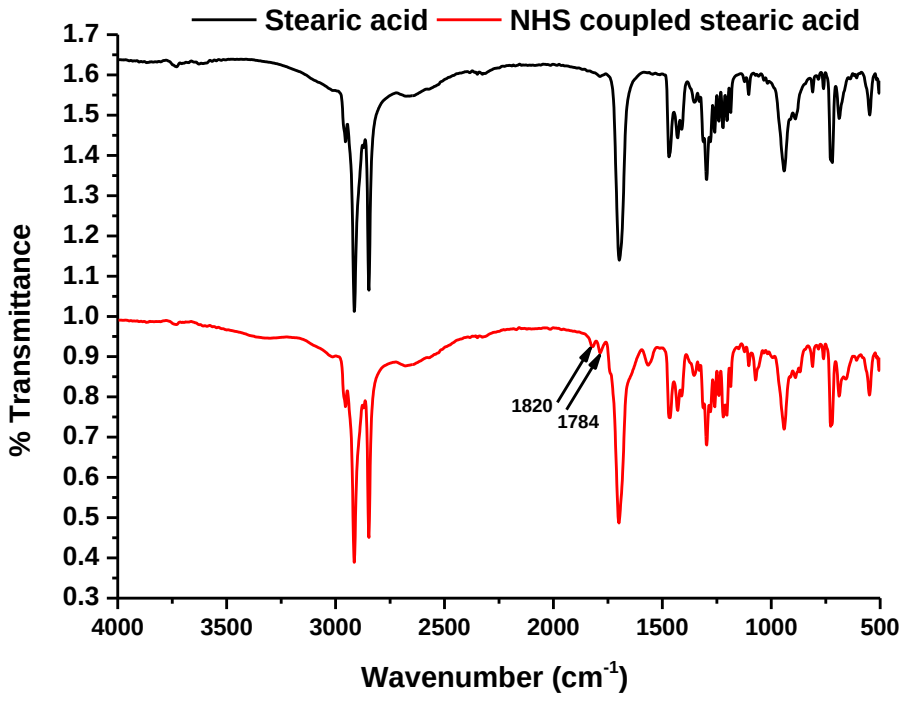

Figure 6.1 ATR-FTIR spectra of NHS coupled stearic acid.

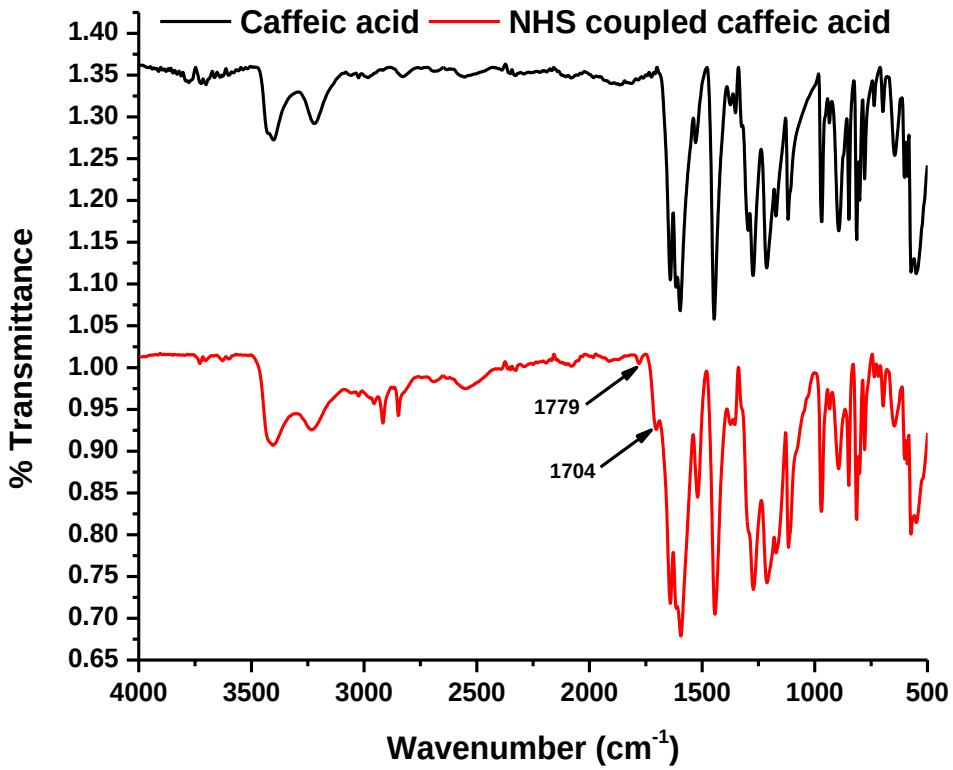

Figure 6.2 ATR-FTIR spectra of NHS coupled caffeic acid.

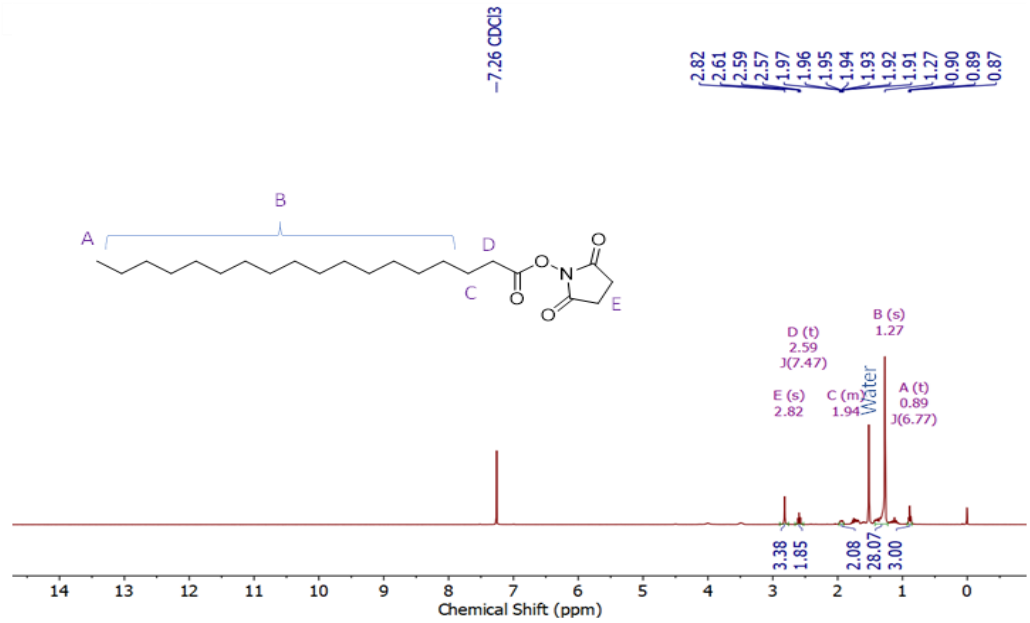

Figure 6.3 ^{1}H NMR spectra of NHS coupled stearic acid.

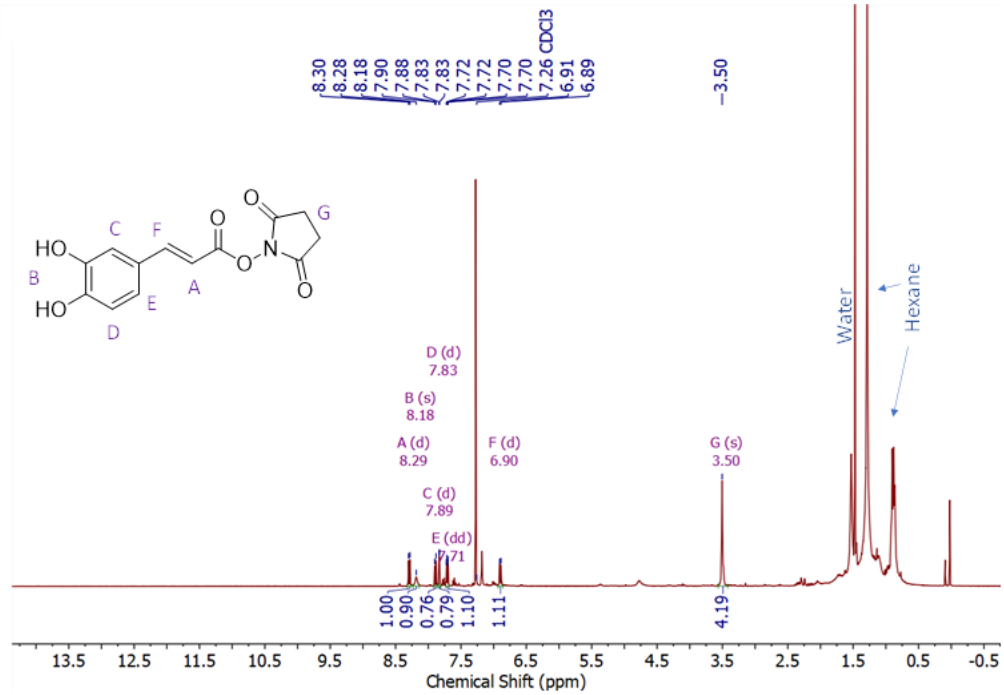

Figure 6.4 ^{1}H NMR spectra of NHS coupled caffeic acid.

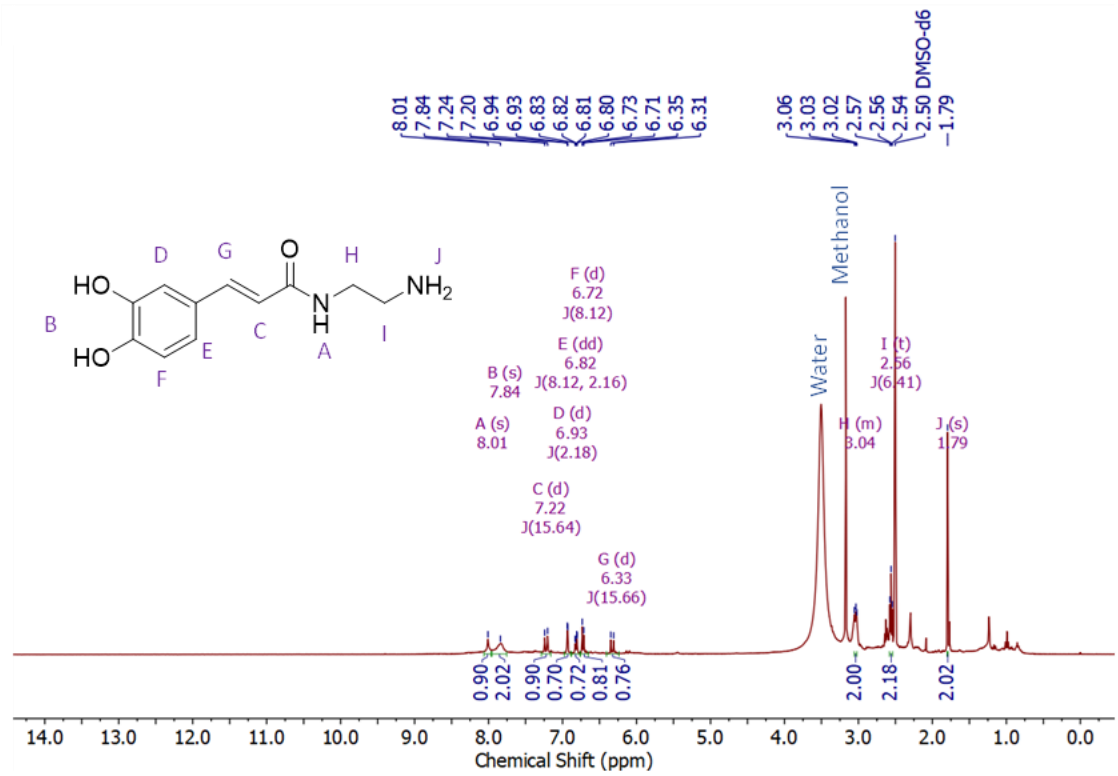

Figure 6.5 ^{1}H NMR spectra of conjugated caffeic acid.

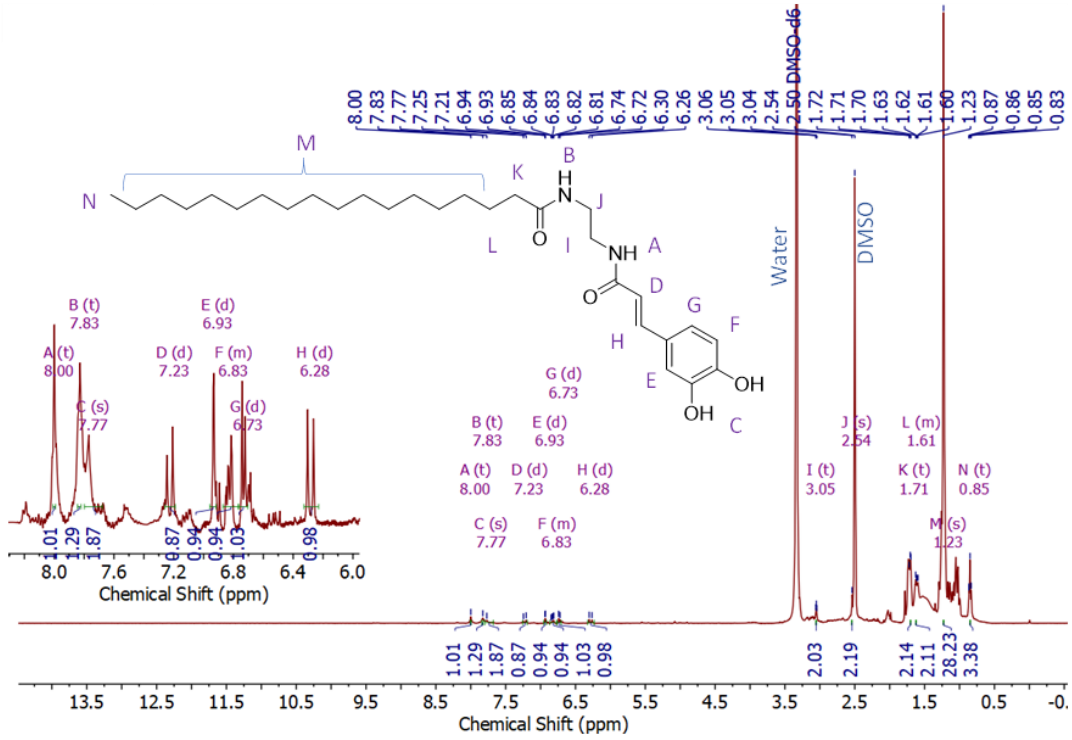

Figure 6.6 ^{1}H NMR spectra of SA and CA conjugated amphiphile.

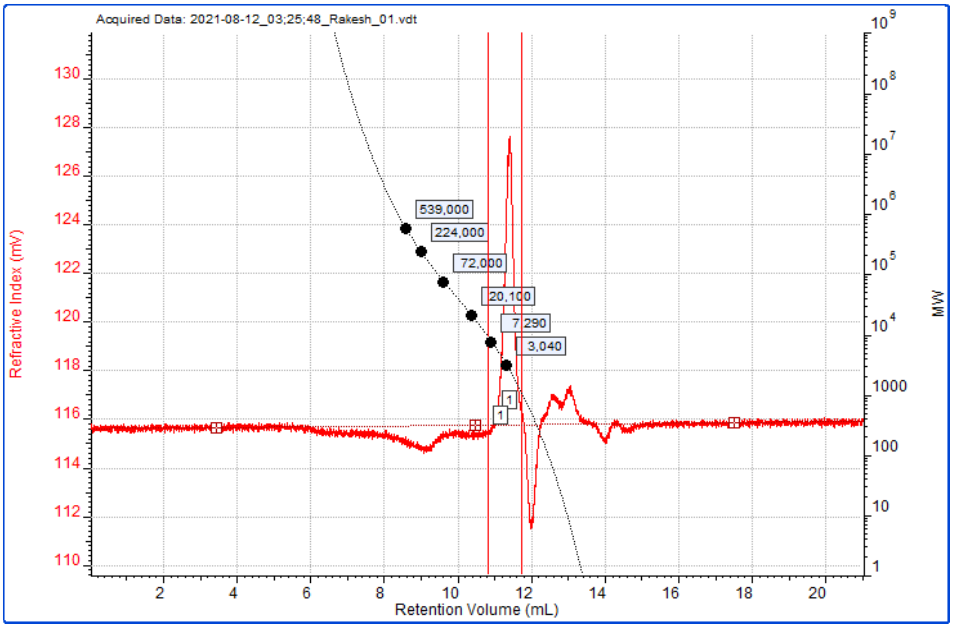

Figure 6.7 Gel permeation chromatograph of amphiphile.

By incorporating the drug and previously synthesized amphiphile micelles has been developed using solvent evaporation method (**Figure 6.8**).

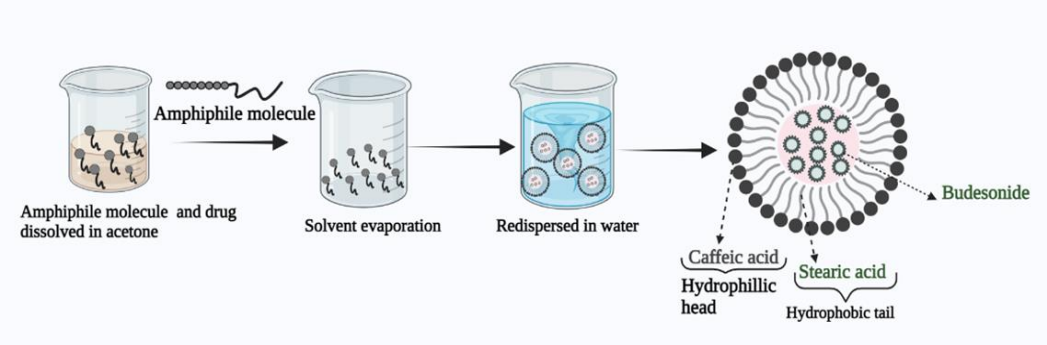

Figure 6.8 Scheme of nanomicelle formulations from synthesized amphiphile.

Prepared micelles were processed for characterizations with different techniques. Hydrodynamic size of blank micelle was 139 nm which found slightly bigger after drug loading as 152.9 nm measured by Zetasizer. The polydispersity index of blank as well as BUD-loaded nanosized micelle was 0.39 and 0.32 respectively which shows micelles were monodispersed. The surface charge of micelles in terms of zeta potential was found -27.4mV of blank micelle and -28.7mV of BUD-loaded micelles. These zeta potential values are found good to maintain stability of micelles as they repel to each other in dispersion medium (**Figure 6.9**).

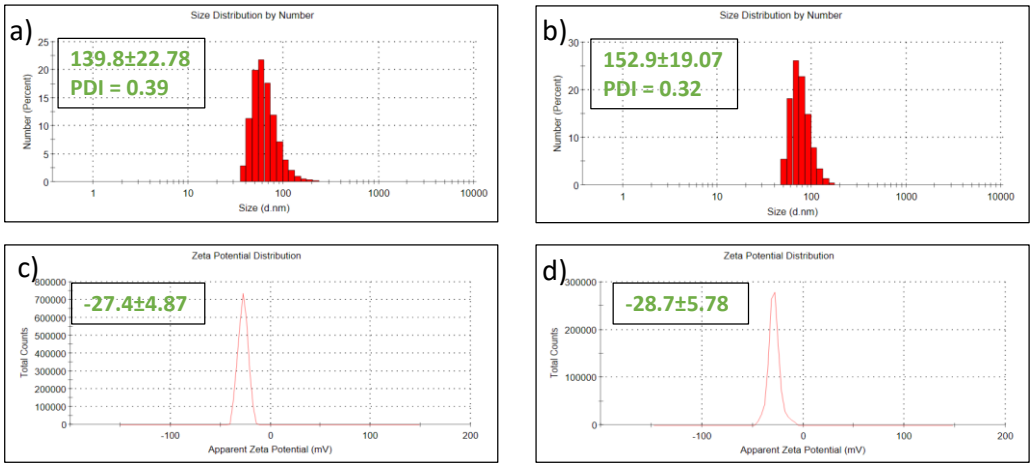

Figure 6.9 Hydrodynamic size and zeta potentials of micelles. a) Size of blank micelles, b) Size of BUD-loaded micelles, c) Zeta potential of blank micelles and d) Zeta potential of BUD-loaded micelles.

The size and morphology of BUD-loaded micelle was also confirmed by different microscopic techniques such as AFM, SEM and TEM. The micrographs

produced by these techniques shows the micelles were spherical in shape and were distributed evenly (**Figure 6.10**).

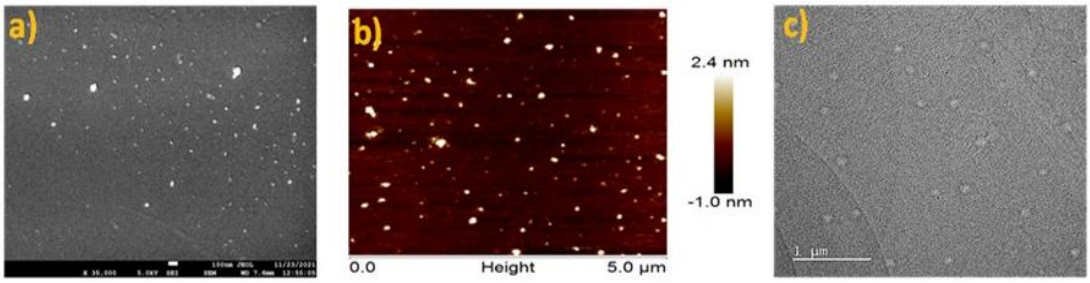

Figure 6.10 Images of BUD-loaded micelles under microscopes. a) SEM, b) AFM and c) TEM. Image magnifications – 500nm and 1µm.

The critical micelle concentration (CMC) is important determinant to confirm the self-assembly of amphiphiles and micelle formation. The CMC of blank micelle was estimated using pyrene assay method and found to be 650ng/ml. The very low CMC value shows that micellization has been started at very low concentration that signifies the stability of micelles (**Figure 6.11**).

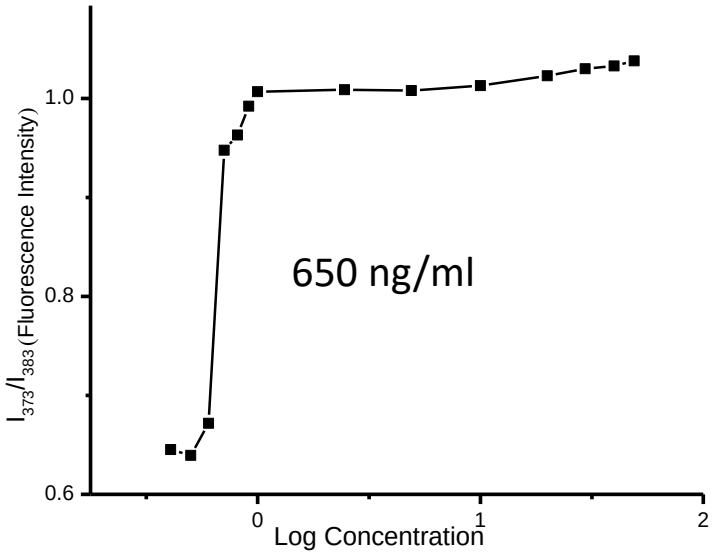

Figure 6.11 Critical micelle concentration graph of amphiphile.

6.2.2 Drug loading and release

The content of budesonide in micelles has been estimated by UV-VIS spectroscopy. It was found that micelles have 13.56±1.39% drug loading as well as encapsulation efficacy was 91.16±3.75%.

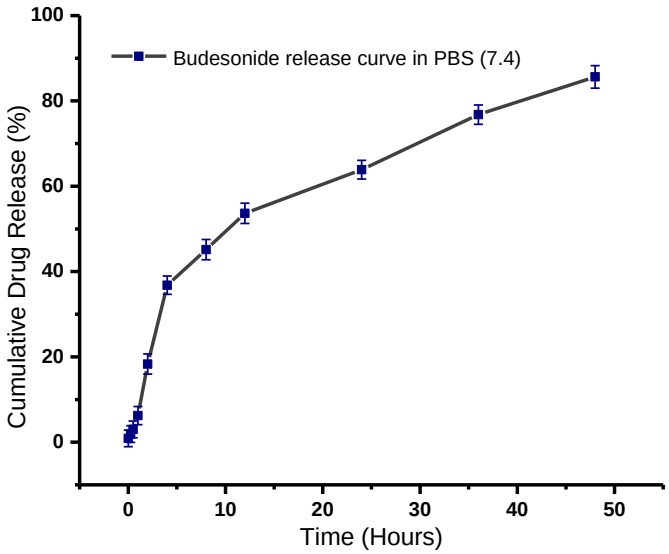

Figure 6.12 Release behaviour of BUD from micelles. Representation of data in average ± standard deviation.

The release profile of BUD from BUD-loaded micelles in-vitro release experiment has been performed in phosphate buffer saline (PBS pH 7.4) following previously optimized methodology. The release graph shows approximately 85% of drug has been released upto 48 hours. This obtained release profile revealed that micelles have sufficiently drug holding capability which provides sustained release of drug. This BUD-loaded micelle has potential to lower the administration of multiple doses (**Figure 6.12**).

6.2.3 Cytocompatibility of nanomicelle

To confirm the safety of micelle, cytocompatibility of blank micelles has been estimated on normal hTERT-BJ fibroblast cells for upto 24 hours. The dose upto 500 µg/ml shows cell viability more than 85% which confirmed cytocompatible properties of the composition of developed micelle (**Figure 6.13**).

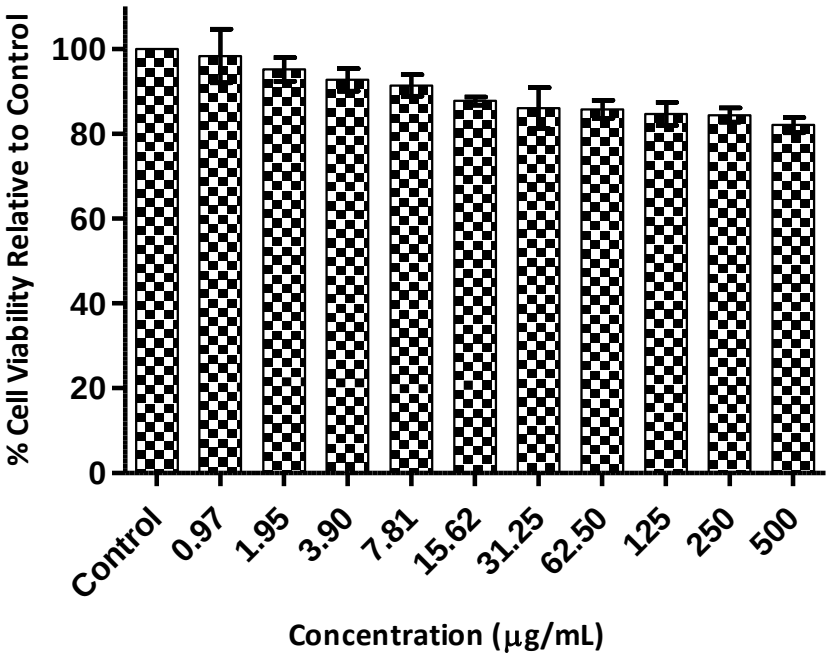

Figure 6.13 Estimation of cytocompatible property of blank micelles at represented concentrations against hTERT-BJ cell line.

6.2.4 *In-Vitro* nitrite estimation

To assess the anti-inflammatory potential of BUD-loaded micelle in-vitro estimation of nitrite has been performed against RAW 264.7 cells treated with LPS (1µg/ml). In inflammation and diseases like UC the correlation of inflammatory damage is directly reported with disease intensity.[30] In this study marked enhancement after LPS treatment has been observed. When treated with BUD and BUD-loaded micelles, nitrite level was markedly reduced (***$p \leq 0.001$) at used concentrations. There was also a significant difference was found in nitrite inhibition compared to BUD and BUD-loaded micelle (*$p \leq 0.05$) treatment groups (**Figure 6.14**). Treatment with BUD and BUD-loaded micelles reflected dose dependant effect in terms of nitrite inhibition. In blank micelle treatment group inhibition of nitrite level is also noticed. This inhibition was due to the caffeic acid presence in micelle that make the micelle formulation more effective.

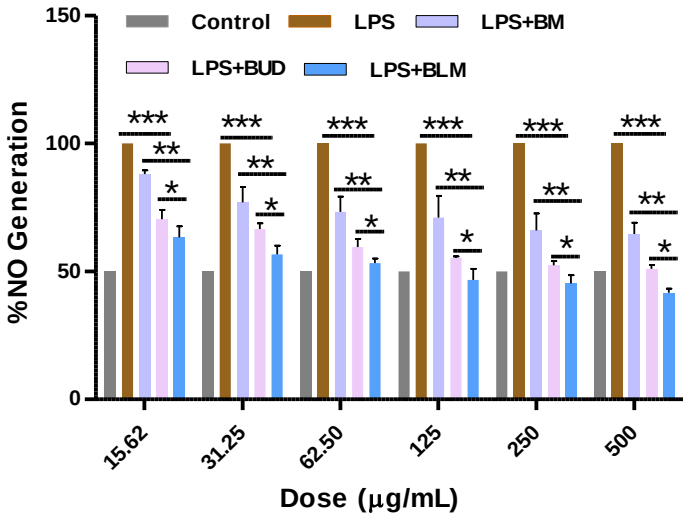

Figure 6.14 Nitric oxide production in LPS treated RAW 264.7 cells. One-way ANOVA has been applied to calculate statistical significance denoted by *p ≤ 0.05, **p ≤ 0.01, ***p ≤ 0.001(Representation of data in average± standard deviation).

6.2.5 *In-Vivo* Therapeutic Efficacy Study

After development and characterizations of BUD-loaded micelle and *in-vitro* cytocompatibility assessment of blank micelle, *in-vivo* efficacy study was performed to assess the therapeutic potential of BUD-loaded micelles.

6.2.5.1 Analysis of disease activity and body weight changes

Following the dosing schedule disease activity of mice was also analyzed in terms of rectal bleeding, physical activity and stool texture. In healthy animals and blank micelle administered animals all the observed parameters were normal. Diseased animals reflected abnormal observations as diarrheal stool, sedentary physical activity and rectal bleeding was also observed. When diseased animals were administered blank micelle slightly improved response (but insignificant) in disease activity indices were observed due to caffeic acid content in micelle. Whenever diseased animals administered with BUD the observation of no rectal bleeding, mild physical activity with soft stool texture were appeared. Treatment of diseased animals with BUD-loaded micelles all the observed parameters tend to normalized. The

observation of these parameters in blank micelle and healthy groups were found similar **(Table 6.1)**.

Table 6.1 Physical observations of various parameters on experimental animals over the study period. Values are expressed in the table are average observational values.

S.No.	Groups	Observations		
		Stool Consistency	**Physical Activity**	**Rectal Bleeding**
1.	Healthy	0	0	0
2.	DSS	4	3	1
3.	BUD	1	1	0
4.	BUD-loaded Micelles	0	0	0
5.	Blank	3	2	1
6.	Safety	0	0	0

Stool Consistency
0-Normal Pellet (Hard)
1-Soft Pellet
2-Loose watery stool
3-Stickiness
4-Diarrhoea

Physical Activity
0-Normal active (Highly)
1-Mild active
2-Low active
3-Sedentary

Rectal Bleeding
0-No bleeding
1-Bleeding

UC or intestinal inflammatory condition are directly associated with weight reduction due to catabolic conditions which happens because of the low absorption of nutrient materials and weaken the strength of body.[31] In this study body weight changes during the study were also observed. In healthy group consistent weight gain of experimental animals has been appeared which was markedly dropped (***$p \leq 0.001$) after colitis induction. Upon administration of BUD and BUD-loaded micelle enhancement of body weight (###$p \leq 0.001$) observed in contrast to diseased group. Diseased animals treated with blank micelle shown less body weight drop due to protective role of caffeic acid in inflammatory condition. In healthy and blank micelle administered animals positive weight gain has been observed (**Figure 6.15**).

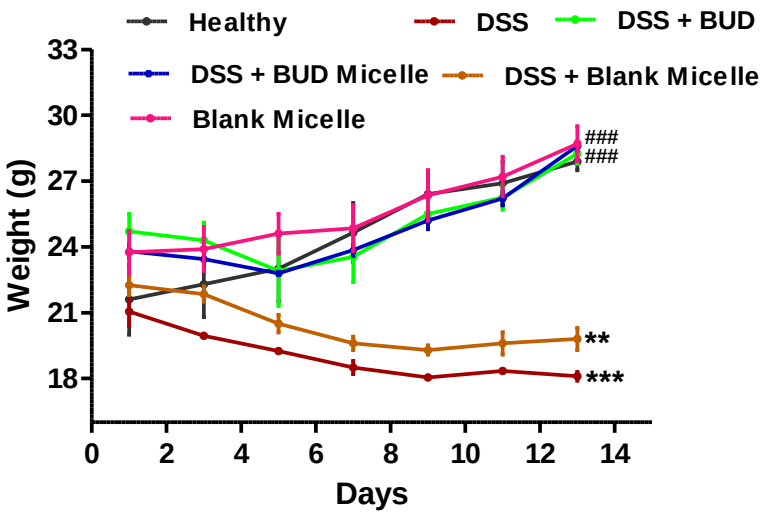

Figure 6.15 Animals weight variations over in-vivo study. Group I – Healthy, Group II – DSS, Group III – DSS + BUD, Group IV – DSS + BUD-loaded Micelles, Group V – DSS + Blank Micelles, Group VI – Blank Micelles. One-way ANOVA has been applied to calculate statistical significance. Treatment groups were compared to colitis group and healthy animals. (###p < 0.001, **p < 0.01 ***p < 0.001). (Representation of data in average± standard deviation).

Percentage weight changes upon completion of experiment has been also estimated (**Figure 6.16**).

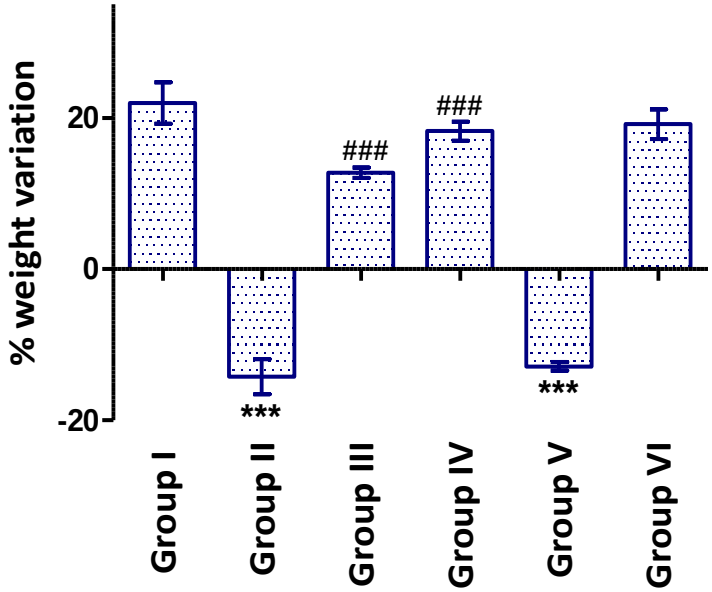

Figure 6.16 Shows % weight variation of mice after completion of study. Group I – Healthy, Group II – DSS, Group III – DSS + BUD, Group IV – DSS + BUD-loaded Micelles, Group V – DSS + Blank Micelles, Group VI – Blank Micelles. Comparisons were made on the basis of the one-way

ANOVA followed by Bonferroni post-test. All groups were compared to the DSS group (p < 0.001, ###p < 0.001). (Values are presented as mean ± SD).***

After subsequent competing the treatments, animals were sacrificed and colons were excised for physical observations and to analyze the changes in diseased conditions. In diseased group marked decrement in colon length was appeared. Treatment with BUD and BUD-loaded micelle reflected regained colon length. Colitis animals when administered blank micelles slight increased colon length than diseased animals were found. Colon length in blank micelle administered and healthy animals were found comparable (**Figure 6.17A**).

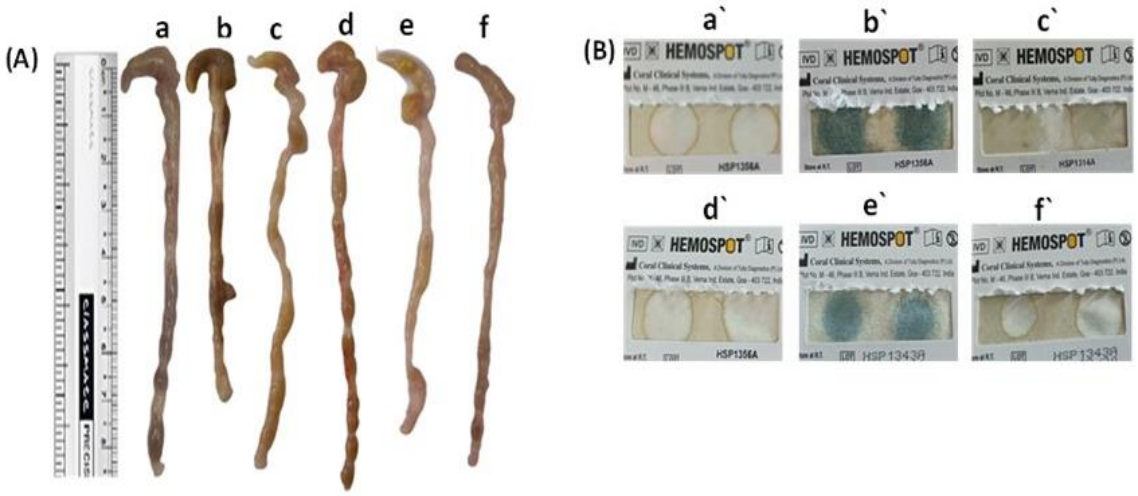

Figure 6.17 Image representation of (A) Physically observed colons. a – Healthy, b – DSS, c – DSS + BUD, d – DSS + BUD-loaded Micelles, e – DSS + Blank Micelles and f – Blank Micelles whereas (B) a` – f` are related FOBT examination.

A qualitative FOBT test to examine any evidence of blood in faeces has been performed. The blue colored spot on FOBT strip shows the presence of blood in faeces of diseased animals. The hidden blood was disappeared after administration of BUD and BUD-loaded micelles. Blue colored spot on FOBT strip of diseased animals treated with blank micelles observed shows presence of hidden blood. FOBT negative test in healthy and blank micelle administered groups observed which concluded the absence of blood in faecal matter (**Figure 6.17B**).

6.2.5.2 Analysis of histopathology

A detailed morphology of healthy animals was confirmed by observation of H&E-stained sections of colon in this group. Analysis of colon sections of healthy mice shows the normal histological presence of muscularis, submucosa as well as mucosa layers. In case of UC and intestinal inflammation, injured cells construct tubular structure and appeared as foci of aberrant crypts.[32] After administration of DSS disturbance in histological appearance of colon was observed due to colitis induction. A marked disruption in goblet cells and damaged muscularis observed in colitis group. An enhanced submucosal widening correlated with collagen aggregation was observed if compared with healthy animals which is also reported earlier.[33] Colitis induction caused marked changes in colon histology which observed ameliorated after BUD administration. When BUD-loaded micelles administered to colitic animals' significant improvement in histological features have been observed in terms of goblet cells and tissue linings of colon. Administration of blank micelles to the colitic animals slightly improved the architecture in contrast to diseased animals. This improvement was due to conjugation of caffeic acid in amphiphile that forms micelles. In blank micelles treated and healthy animals' similar colon architecture was appeared (**Figure 6.18**).

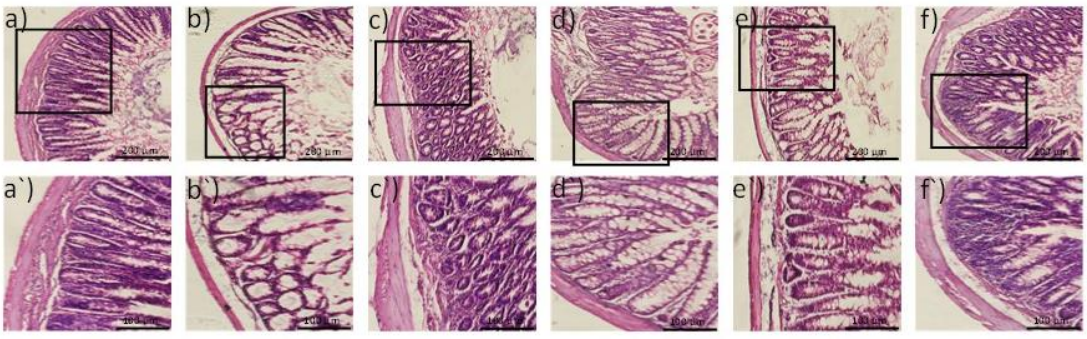

Figure 6.18 Colon images of H&E staining. a) Healthy: Observations of normal colonic histoarchitect. b) DSS: Destructed colonic muscularis and mucosal layers. c) DSS + BUD: Improved colon histology. d) DSS + BUD-loaded Micelles: Regained colon histoarchitect. e) DSS + Blank Micelles: Abrupted colon epithelium. f) Blank Micelles: Normal colon morphology. Magnification of images at 10X, scale bar = 200 µm (a-f), 20X, scale bar = 100 µm (a'-f').

Goblet cells in colon is responsible for the production of protective mucous layer in lining of colon. Coherence of mucin layer in colon was confirmed by AB-NR staining of goblet cells. Mucus layer disruption in colon makes more susceptibility towards obnoxious matters exposure that may leads worsen the disease condition in colitis. Marked presence of goblet cells evidenced by blue colored stained acidic mucins observed in healthy animals. After administration of DSS damage in goblet cells observed as very low blue color staining exhibited. Administering BUD markedly improved the appearance of stained mucins shows the enhancement of goblet cells. In BUD-loaded micelles administered group notable increased goblet cells observed as evidenced by enhanced staining. From this observation it is analyzed that BUD-loaded micelles treatment sufficiently enhances the goblet cells damaged due to the induction of colitis following DSS administration. Colitic animals treated with blank micelle slightly improved appearance of goblet cells observation than diseased animals. Goblet cells staining in blank and healthy animals was similar (**Figure 6.19**).

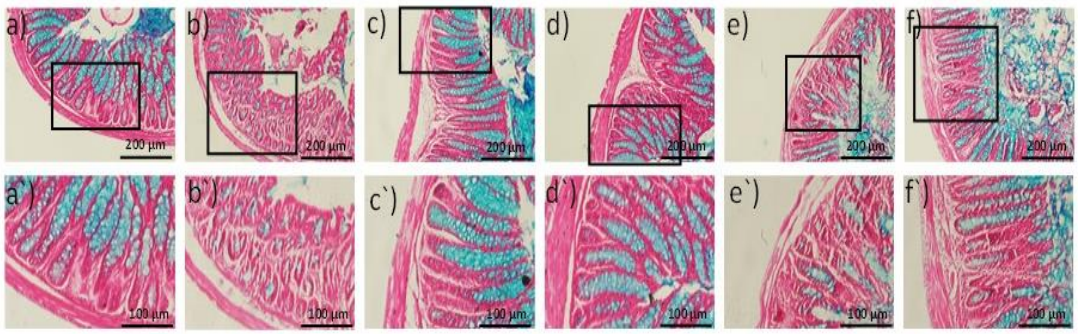

Figure 6.19 Colon images of AB-NR staining. a) Healthy: Observation of blue color-stained goblet cells. b) DSS: Diminished goblet cells shows less blue color. c) DSS + BUD: Observed recovered goblet cells. d) DSS + BUD-loaded Micelles: Enhanced staining shown sufficient recovery of goblet cells. e) DSS + Blank Micelles: Disintegrated goblet cells. f) Blank Micelles: Normal appearance of goblet cells. Magnification of images at 10X, scale bar = 200 µm (a-f), 20X, scale bar = 100 µm (a'-f').

Goblet cells secretes two types of mucins i.e., sulphomucin and sialomucin. It is reported that in intestinal inflammation or cancer more sialomucin has been secreted in comparison to normal mucosa that secretes predominantly

sulfomucin.[34,35] HID-AB staining has been performed to differentiate the mucins in relation to inflammation/UC. In HID-AB-stained sections HID dye stains sulphomucin that observed in brown color whereas blue color appeared sialomucin is stained by AB. In this staining it was observed more sulphomucin in healthy animals' colon than that of diseased animals possess predominantly blue stained sialomucin. BUD administration improved the secretion of sulphomucin whereas BUD-loaded micelles administration markedly enhances the sulphomucin secreted by colonic goblet cells. Observations of mucin staining in healthy and blank group found similar (**Figure 6.20**).

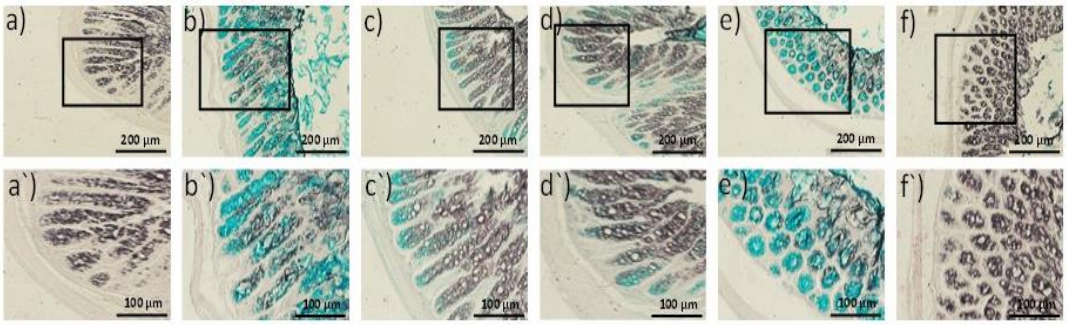

Figure 6.20 Colon images of HID-AB staining. a) Healthy: More sulfomucin than sialomucin observed. b) DSS: More sialomucin in blue color than brown colored sulfomucin. c) DSS + BUD: Comparatively enhanced sulfomucin observed. d) DSS + BUD-loaded Micelles: Marked increment of sulfomucin compared to sialomucin. e) DSS + Blank Micelles: Markedly enhanced sialomucin. f) Blank Micelles: Observed mucin stains similar to normal. Magnification of images at 10X, scale bar = 200 µm (a-f), 20X, scale bar = 100 µm (a'-f').

Infiltrations of proinflammatory mast cells has been observed in inflammation and found related to colitis. At the site of inflammation activation of inflammatory mast cells evidenced by the release of histamine that actively participates and contribute to inflammatory changes via cellular and humoral events.[36,37] TB staining has been performed to observe the presence of purple colored stained infiltrated mast cells. In healthy group physiological appearance of mast cells observed while in diseased group increased level of inflammatory mast cells observed denoted by black arrows. Administration of BUD and BUD-loaded micelles notably decreased the infiltrated mast cells number. Blank micelles administered to the

diseased animals also effectively lowers the infiltration of mast cells due to the conjugated caffeic acid in micelles. Healthy and blank micelles administered groups did not show the observation of mast cells. Observations of TB staining concluded that treatment with BUD-loaded micelles effectively inhibited the infiltration of mast cells and successfully improved the inflammatory changes in colitis (**Figure 6.21**).

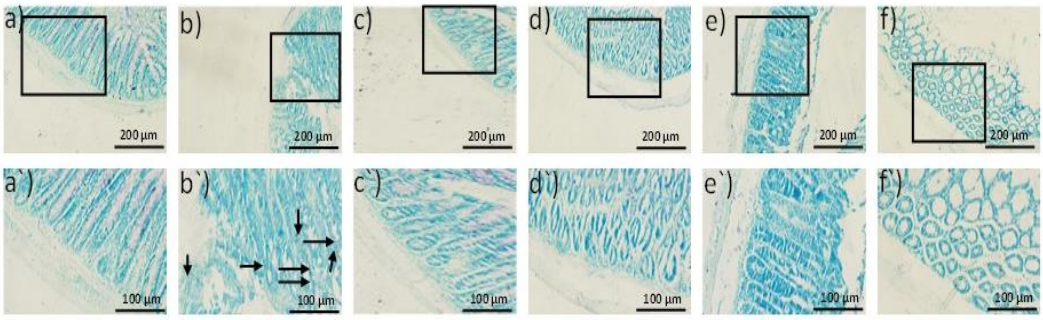

Figure 6.21 Colon images of toluidine blue staining. a) Healthy: Infiltration of mast cells not observed. b) DSS: Dotted appearances of mast cells indicated by black arrows. c) DSS + BUD: No mast cells were observed. d) DSS + BUD-loaded Micelles: Absence of mast cells after treatment. e) DSS + Blank Micelles: Less mast cells appeared compared to diseased animals. f) Blank Micelles: No infiltrated mast cells. Magnification of images at 10X, scale bar = 200 µm (a-f), 20X, scale bar = 100 µm (a'-f').

6.2.5.2.1 Immunohistochemical analysis of iNOS and COX-2 expressions

Local expressions of proinflammatory enzymes COX-2 in inflammatory diseases like UC and iNOS which is accountable for the generation of NO at the site where disease confined have strong correlation with disease severity and progression.[46,47] COX-2 and iNOS estimation has been performed to the tissue sections of various *in-vivo* study groups by immunohistochemistry to evaluate the potential of BUD-loaded micelles in downregulation of these upregulated inflammatory enzymes (**Figure 6.22I&II**). Microscopic images of IHC observed and expression of COX-2 as well as iNOS has been estimated semi quantitatively. In healthy and blank group animals there was low expression of iNOS and COX-2 observed as evidenced by less appeared brown colored immune cells.

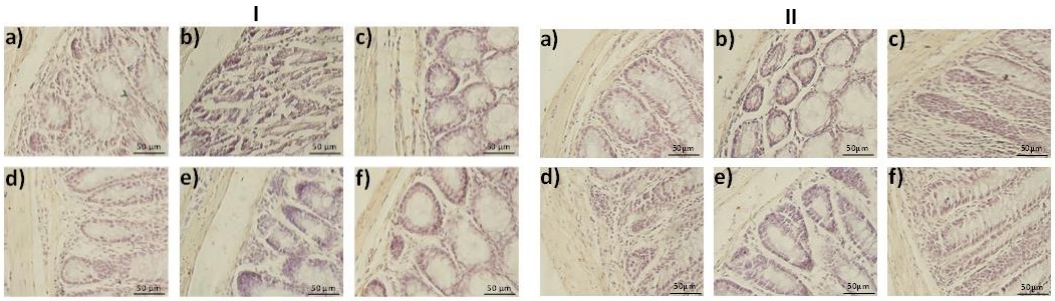

Figure 6.22 IHC stained colonic sections (I) COX-2 and (II) iNOS a) Healthy: Low expression of COX-2 and iNOS. b) DSS: Overexpressed COX-2 and iNOS level. c) DSS + BUD: Less expressed COX-2 and iNOS levels compared to diseased group. d) DSS + BUD-loaded Micelles: Significantly downregulated COX-2 and iNOS after treatment. e) DSS + Blank Micelles: Upregulated COX-2 and iNOS expressions. f) Blank Micelles: Observed COX-2 and iNOS expression comparable to normal. Magnification of images at 40X, scale bar = 50 µm (a-f).

After induction of disease marked upregulation of iNOS (***p ≤ 0.001) and COX-2 (***p ≤ 0.001) have been observed in contrast to healthy group. Administration of BUD (##p ≤ 0.01) and BUD-loaded micelles (###p ≤ 0.001) markedly decreased the level of overexpressed COX-2 and iNOS levels (**Figure 6.23**). BUD-loaded micelles have sufficient potential to attenuate the expression of inflammatory enzymes and hence provide the beneficial effects in UC.

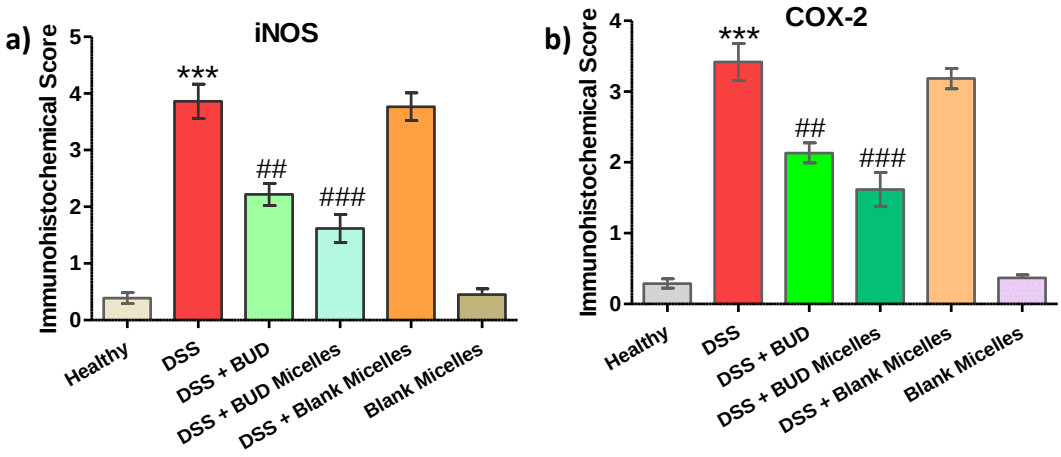

Figure 6.23 Semi-quantitative evaluation of (a) iNOS and (b) COX-2 expression. Group I – Healthy, Group II – DSS, Group III – DSS + BUD, Group IV – DSS + BUD-loaded Micelles, Group V – DSS + Blank Micelles. Group VI – Blank Micelles. Significant differences were indicated by ***p ≤ 0.001, as compared to control and #p ≤ 0.05, ##p ≤ 0.01 and ###p ≤0.001 as compared to DSS

group. The experiments were performed in triplicate (n = 3) and data are presented as mean ± standard deviation of three independent sets of observations.

6.2.5.3 *In-Vivo* Cytokines estimations

Various proinflammatory cytokines, tumor necrosis factor (TNF-α), interleukins (ILs)[38] etc. get overexpressed under the influence of activated mast cells and innate immune response at the site of inflammation.[39] These mediators play crucial role as pathogenic factor for UC and other related inflammatory ailments.[36,37] The unregulated inflammatory responses pathetically influence colon homeostasis that leads to the development and progression of colonic ailments.[40,41]

Nitrite production in colonic tissue reported to serve as a crucial biomarker responsible for the progression of inflammatory diseases and colitis.[42,43] In our study significant enhancement of tissue nitrite was observed in diseased group (***$p \leq 0.001$) in corelation to healthy group. Administration of BUD (#$p \leq 0.05$) and BUD-loaded micelle (##$p \leq 0.01$) markedly diminished the production of nitrite. Blank micelle administered in colitic animals also decreased nitrite but the level was insignificant. In healthy group and blank micelle administered group nitrite production was similar (**Figure 6.24a**). Observations of nitrite production is found similar to previous studies.[44,45]

Tissue myeloperoxidase (MPO) acts as an inflammatory biomarker which found over expressed in colitis.[46–48] Administration of DSS significantly enhances the level of MPO (***$p \leq 0.001$) in corelation to healthy group. Treatment with BUD (#$p \leq 0.05$) and BUD-loaded micelle (###$p \leq 0.001$) markedly decreased MPO and shows protective role of treatment in UC. Administration of blank micelles to the diseased animals has protective but insignificant in corelation to treatment groups. Tissue MPO expression in healthy and blank micelles group was similar and found to be very low (**Figure 6.24b**). In favour of MPO expression studies reported that it plays crucial role in regulation of inflammation in colitis and other related diseases.[49,50]

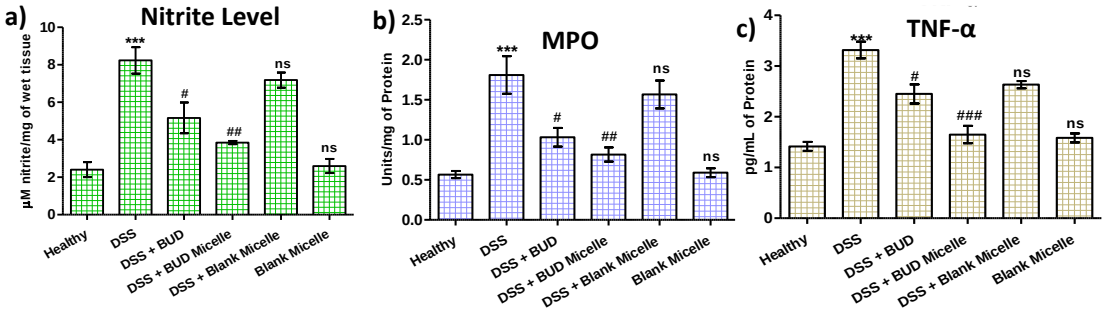

Figure 6.24 Assessment of inflammatory cytokines. a) Nitrite level, b) MPO in colonic tissues and c) TNF-α estimation in mice serum. Healthy group was compared with diseased and safety whereas diseased group compared with different treatment groups. (p ≤ 0.001, ###p ≤ 0.001, ##p ≤ 0.01, #p ≤ 0.05, ns = nonsignificant). (Data representation in average ± standard deviation).***

Induction of disease also evidenced with the overexpression of TNF-α (***p ≤ 0.001) in corelation to healthy group. Administration of BUD (#p ≤ 0.05) and (###p ≤ 0.001) markedly decreased the enhanced level of TNF-α. Administration of blank micelles to the diseased animals also decreased the level of TNF-α in comparison to other estimated cytokines but was not upto the mark with BUD/BUD-loaded micelles treatment. In healthy and blank micelles administered group TNF-α expression was found similar (**Figure 6.24c**). Observations of result shows that BUD-loaded micelles have potential to alleviate the overexpressed TNF-α and restrict the disease progression and inflammation.

6.3 Conclusion

In the present study caffeic acid and stearic acid conjugated amphiphile has been synthesized successfully. This amphiphile was self-assembled to form nanosized micelles that sufficiently encapsulated a hydrophobic drug budesonide. All the materials used in the micelle formation are USFDA approved and were safe for human use as they are GRAS classified. The prepared micelles have low CMC value that renders the micelles stable in suspending media. This micelle possesses all the favorable physicochemical properties in terms of morphology and hold the drug for longer duration in release media shows sustained behaviour. The *in-vivo* colitis study shows significant therapeutic efficacy of BUD-loaded micelle and its biocompatible

properties *in-vitro* as well as *in-vivo*. This study suggests that the formulated micelle significantly alleviate the inflammatory cytokines and enzymes and improve the inflammatory conditions in colitis.

6.4. Bibliography

(1) Shen, C.; Zhao, L.; Du, X.; Tian, J.; Yuan, Y.; Jia, M.; He, Y.; Zeng, R.; Qiao, R.; Li, C. Smart Responsive Quercetin-Conjugated Glycol Chitosan Prodrug Micelles for Treatment of Inflammatory Bowel Diseases. *Mol. Pharmaceutics* **2021**, *18* (3), 1419–1430. https://doi.org/10.1021/acs.molpharmaceut.0c01245.

(2) Fan, W.; Zhang, S.; Wu, Y.; Lu, T.; Liu, J.; Cao, X.; Liu, S.; Yan, L.; Shi, X.; Liu, G.; Huang, C.; Song, S. Genistein-Derived ROS-Responsive Nanoparticles Relieve Colitis by Regulating Mucosal Homeostasis. *ACS Appl. Mater. Interfaces* **2021**, *13* (34), 40249–40266. https://doi.org/10.1021/acsami.1c09215.

(3) Jayawardena, D.; Anbazhagan, A. N.; Guzman, G.; Dudeja, P. K.; Onyuksel, H. Vasoactive Intestinal Peptide Nanomedicine for the Management of Inflammatory Bowel Disease. *Mol. Pharmaceutics* **2017**, *14* (11), 3698–3708. https://doi.org/10.1021/acs.molpharmaceut.7b00452.

(4) Chen, Q.; Luo, R.; Han, X.; Zhang, J.; He, Y.; Qi, S.; Pu, X.; Nie, W.; Dong, L.; Xu, H.; Liu, F.; Lin, M.; Zhong, H.; Fu, C.; Gao, F. Entrapment of Macrophage-Target Nanoparticles by Yeast Microparticles for Rhein Delivery in Ulcerative Colitis Treatment. *Biomacromolecules* **2021**, *22* (6), 2754–2767. https://doi.org/10.1021/acs.biomac.1c00425.

(5) Chen, Q.; Gou, S.; Ma, P.; Song, H.; Zhou, X.; Huang, Y.; Kwon Han, M.; Wan, Y.; Kang, Y.; Xiao, B. Oral Administration of Colitis Tissue-Accumulating Porous Nanoparticles for Ulcerative Colitis Therapy. *International Journal of Pharmaceutics* **2019**, *557*, 135–144. https://doi.org/10.1016/j.ijpharm.2018.12.046.

(6) Citi, S. Intestinal Barriers Protect against Disease. *Science* **2018**, *359* (6380), 1097–1098. https://doi.org/10.1126/science.aat0835.

(7) Turner, J. R. Intestinal Mucosal Barrier Function in Health and Disease. *Nat Rev Immunol* **2009**, *9* (11), 799–809. https://doi.org/10.1038/nri2653.

(8) Halfvarson, J.; Brislawn, C. J.; Lamendella, R.; Vázquez-Baeza, Y.; Walters, W. A.; Bramer, L. M.; D'Amato, M.; Bonfiglio, F.; McDonald, D.; Gonzalez, A.; McClure, E. E.; Dunklebarger, M. F.; Knight, R.; Jansson, J. K. Dynamics of the Human Gut Microbiome in Inflammatory Bowel Disease. *Nat Microbiol* **2017**, *2* (5), 1–7. https://doi.org/10.1038/nmicrobiol.2017.4.

(9) Round, J. L.; Mazmanian, S. K. The Gut Microbiota Shapes Intestinal Immune Responses during Health and Disease. *Nat Rev Immunol* **2009**, *9* (5), 313–323. https://doi.org/10.1038/nri2515.

(10) Campbell, E. L.; Colgan, S. P. Control and Dysregulation of Redox Signalling in the Gastrointestinal Tract. *Nat Rev Gastroenterol Hepatol* **2019**, *16* (2), 106–120. https://doi.org/10.1038/s41575-018-0079-5.

(11) Ananthakrishnan, A. N.; Bernstein, C. N.; Iliopoulos, D.; Macpherson, A.; Neurath, M. F.; Ali, R. A. R.; Vavricka, S. R.; Fiocchi, C. Environmental Triggers in IBD: A Review of Progress and Evidence. *Nat Rev Gastroenterol Hepatol* **2018**, *15* (1), 39–49. https://doi.org/10.1038/nrgastro.2017.136.

(12) Thorsteinsdottir, S.; Gudjonsson, T.; Nielsen, O. H.; Vainer, B.; Seidelin, J. B. Pathogenesis and Biomarkers of Carcinogenesis in Ulcerative Colitis. *Nat Rev Gastroenterol Hepatol* **2011**, *8* (7), 395–404. https://doi.org/10.1038/nrgastro.2011.96.

(13) Mongia Raj, P.; Raj, R.; Kaul, A.; K. Mishra, A.; Ram, A. Biodistribution and Targeting Potential Assessment of Mucoadhesive Chitosan Nanoparticles Designed for Ulcerative Colitis via Scintigraphy. *RSC Advances* **2018**, *8* (37), 20809–20821. https://doi.org/10.1039/C8RA01898G.

(14) Wang, X.; Gu, H.; Zhang, H.; Xian, J.; Li, J.; Fu, C.; Zhang, C.; Zhang, J. Oral Core–Shell Nanoparticles Embedded in Hydrogel Microspheres for the Efficient Site-Specific Delivery of Magnolol and Enhanced Antiulcerative Colitis Therapy. *ACS Appl. Mater. Interfaces* **2021**, *13* (29), 33948–33961. https://doi.org/10.1021/acsami.1c09804.

(15) Cui, M.; Pang, G.; Zhang, T.; Sun, T.; Zhang, L.; Kang, R.; Xue, X.; Pan, H.; Yang, C.; Zhang, X.; Chang, J.; Liu, J.; Zhang, S.; Wang, H. Optotheranostic Nanosystem with Phone Visual Diagnosis and Optogenetic Microbial Therapy for Ulcerative Colitis At-Home Care. *ACS Nano* **2021**, *15* (4), 7040–7052. https://doi.org/10.1021/acsnano.1c00135.

(16) Lichtenstein, G. R. Budesonide Multi-Matrix for the Treatment of Patients with Ulcerative Colitis. *Dig Dis Sci* **2016**, *61* (2), 358–370. https://doi.org/10.1007/s10620-015-3897-0.

(17) Abdalla, M. I.; Herfarth, H. Budesonide for the Treatment of Ulcerative Colitis. *Expert Opinion on Pharmacotherapy* **2016**, *17* (11), 1549–1559. https://doi.org/10.1080/14656566.2016.1183648.

(18) Silverman, J.; Otley, A. Budesonide in the Treatment of Inflammatory Bowel Disease. *Expert Review of Clinical Immunology* **2011**, *7* (4), 419–428. https://doi.org/10.1586/eci.11.34.

(19) Patra, J. K.; Das, G.; Fraceto, L. F.; Campos, E. V. R.; Rodriguez-Torres, M. del P.; Acosta-Torres, L. S.; Diaz-Torres, L. A.; Grillo, R.; Swamy, M. K.; Sharma, S.; Habtemariam, S.; Shin, H.-S. Nano Based Drug Delivery Systems: Recent Developments and Future Prospects. *Journal of Nanobiotechnology* **2018**, *16* (1), 71. https://doi.org/10.1186/s12951-018-0392-8.

(20) Lombardo, D.; Kiselev, M. A.; Caccamo, M. T. Smart Nanoparticles for Drug Delivery Application: Development of Versatile Nanocarrier Platforms in Biotechnology and Nanomedicine. *Journal of Nanomaterials* **2019**, *2019*, e3702518. https://doi.org/10.1155/2019/3702518.

(21) Fan, Z.; Li, J.; Liu, J.; Jiao, H.; Liu, B. Anti-Inflammation and Joint Lubrication Dual Effects of a Novel Hyaluronic Acid/Curcumin Nanomicelle Improve the Efficacy of Rheumatoid Arthritis Therapy. *ACS Appl. Mater. Interfaces* **2018**, *10* (28), 23595–23604. https://doi.org/10.1021/acsami.8b06236.

(22) Kharat, M.; McClements, D. J. Recent Advances in Colloidal Delivery Systems for Nutraceuticals: A Case Study – Delivery by Design of Curcumin. *Journal of Colloid and Interface Science* **2019**, *557*, 506–518. https://doi.org/10.1016/j.jcis.2019.09.045.

(23) Ibaraki, H.; Hatakeyama, N.; Arima, N.; Takeda, A.; Seta, Y.; Kanazawa, T. Systemic Delivery of SiRNA to the Colon Using Peptide Modified PEG-PCL Polymer Micelles for the Treatment of Ulcerative Colitis. *European Journal of Pharmaceutics and Biopharmaceutics* **2022**, *170*, 170–178. https://doi.org/10.1016/j.ejpb.2021.12.009.

(24) Shi, H.; Zhao, X.; Gao, J.; Liu, Z.; Liu, Z.; Wang, K.; Jiang, J. Acid-Resistant ROS-Responsive Hyperbranched Polythioether Micelles for Ulcerative Colitis Therapy.

Chinese Chemical Letters **2020**, *31* (12), 3102–3106. https://doi.org/10.1016/j.cclet.2020.03.039.

(25) Thotakura, N.; Dadarwal, M.; Kumar, P.; Sharma, G.; Guru, S. K.; Bhushan, S.; Raza, K.; Katare, O. P. Chitosan-Stearic Acid Based Polymeric Micelles for the Effective Delivery of Tamoxifen: Cytotoxic and Pharmacokinetic Evaluation. *AAPS Pharm SciTech* **2017**, *18* (3), 759–768. https://doi.org/10.1208/s12249-016-0563-6.

(26) Negahban, Z.; Shojaosadati, S. A.; Hamedi, S. A Novel Self-Assembled Micelles Based on Stearic Acid Modified Schizophyllan for Efficient Delivery of Paclitaxel. *Colloids and Surfaces B: Biointerfaces* **2021**, *199*, 111524. https://doi.org/10.1016/j.colsurfb.2020.111524.

(27) Zhang, Z.; Wu, X.; Cao, S.; Wang, L.; Wang, D.; Yang, H.; Feng, Y.; Wang, S.; Li, L. Caffeic Acid Ameliorates Colitis in Association with Increased Akkermansia Population in the Gut Microbiota of Mice. *Oncotarget* **2016**, *7* (22), 31790–31799. https://doi.org/10.18632/oncotarget.9306.

(28) Wan, F.; Zhong, R.; Wang, M.; Zhou, Y.; Chen, Y.; Yi, B.; Hou, F.; Liu, L.; Zhao, Y.; Chen, L.; Zhang, H. Caffeic Acid Supplement Alleviates Colonic Inflammation and Oxidative Stress Potentially Through Improved Gut Microbiota Community in Mice. *Frontiers in Microbiology* **2021**, *12*.

(29) Zielińska, D.; Zieliński, H.; Laparra-Llopis, J. M.; Szawara-Nowak, D.; Honke, J.; Giménez-Bastida, J. A. Caffeic Acid Modulates Processes Associated with Intestinal Inflammation. *Nutrients* **2021**, *13* (2), 554. https://doi.org/10.3390/nu13020554.

(30) Guo, T.; Lin, Q.; Li, X.; Nie, Y.; Wang, L.; Shi, L.; Xu, W.; Hu, T.; Guo, T.; Luo, F. Octacosanol Attenuates Inflammation in Both RAW264.7 Macrophages and a Mouse Model of Colitis. *J. Agric. Food Chem.* **2017**, *65* (18), 3647–3658. https://doi.org/10.1021/acs.jafc.6b05465.

(31) Abdelmegid, A. M.; Abdo, F. K.; Ahmed, F. E.; Kattaia, A. A. A. Therapeutic Effect of Gold Nanoparticles on DSS-Induced Ulcerative Colitis in Mice with Reference to Interleukin-17 Expression. *Sci Rep* **2019**, *9* (1), 10176. https://doi.org/10.1038/s41598-019-46671-1.

(32) Mishra, R. K.; Ahmad, A.; Kumar, A.; Vyawahare, A.; Raza, S. S.; Khan, R. Lipid-Based Nanocarrier-Mediated Targeted Delivery of Celecoxib Attenuate Severity of Ulcerative Colitis. *Materials Science and Engineering: C* **2020**, *116*, 111103. https://doi.org/10.1016/j.msec.2020.111103.

(33) Balaha, M.; Kandeel, S.; Elwan, W. Garlic Oil Inhibits Dextran Sodium Sulfate-Induced Ulcerative Colitis in Rats. *Life Sciences* **2016**, *146*, 40–51. https://doi.org/10.1016/j.lfs.2016.01.012.

(34) Croix, J. A.; Carbonero, F.; Nava, G. M.; Russell, M.; Greenberg, E.; Gaskins, H. R. On the Relationship between Sialomucin and Sulfomucin Expression and Hydrogenotrophic Microbes in the Human Colonic Mucosa. *PLOS ONE* **2011**, *6* (9), e24447. https://doi.org/10.1371/journal.pone.0024447.

(35) Deplancke, B.; Gaskins, H. R. Microbial Modulation of Innate Defense: Goblet Cells and the Intestinal Mucus Layer. *The American Journal of Clinical Nutrition* **2001**, *73* (6), 1131S-1141S. https://doi.org/10.1093/ajcn/73.6.1131S.

(36) Branco, A. C. C. C.; Yoshikawa, F. S. Y.; Pietrobon, A. J.; Sato, M. N. Role of Histamine in Modulating the Immune Response and Inflammation. *Mediators of Inflammation* **2018**, *2018*, e9524075. https://doi.org/10.1155/2018/9524075.

(37) Luchini, A. C.; Costa de Oliveira, D. M.; Pellizzon, C. H.; Di Stasi, L. C.; Gomes, J. C. Relationship between Mast Cells and the Colitis with Relapse Induced by Trinitrobenzesulphonic Acid in Wistar Rats. *Mediators of Inflammation* **2009**, *2009*, e432493. https://doi.org/10.1155/2009/432493.

(38) Zhang, Y.; Wang, O.; Ma, N.; Yi, J.; Mi, H.; Cai, S. The Preventive Effect and Underlying Mechanism of Rhus Chinensis Mill. Fruits on Dextran Sulphate Sodium-Induced Ulcerative Colitis in Mice. *Food Funct.* **2021**, *12* (20), 9965–9978. https://doi.org/10.1039/D1FO01558C.

(39) Medicherla, K.; Sahu, B. D.; Kuncha, M.; Kumar, J. M.; Sudhakar, G.; Sistla, R. Oral Administration of Geraniol Ameliorates Acute Experimental Murine Colitis by Inhibiting Pro-Inflammatory Cytokines and NF-KB Signaling. *Food Funct.* **2015**, *6* (9), 2984–2995. https://doi.org/10.1039/C5FO00405E.

(40) Kaur, H.; Ali, S. A. Probiotics and Gut Microbiota: Mechanistic Insights into Gut Immune Homeostasis through TLR Pathway Regulation. *Food Funct.* **2022**. https://doi.org/10.1039/D2FO00911K.

(41) Ramadan, Q.; Gijs, M. A. M. In Vitro Micro-Physiological Models for Translational Immunology. *Lab Chip* **2015**, *15* (3), 614–636. https://doi.org/10.1039/C4LC01271B.

(42) Gawrońska, B.; Matowicka-Karna, J.; Kralisz, M.; Kemona, H. Markers of Inflammation and Influence of Nitric Oxide on Platelet Activation in the Course of Ulcerative Colitis. *Oncotarget* **2017**, *8* (40), 68108–68114. https://doi.org/10.18632/oncotarget.19202.

(43) Nagata, J.; Yokodera, H.; Maeda, G. In Vitro and in Vivo Studies on Anti-Inflammatory Effects of Traditional Okinawan Vegetable Methanol Extracts. *ACS Omega* **2019**, *4* (13), 15660–15664. https://doi.org/10.1021/acsomega.9b02178.

(44) Soufli, I.; Toumi, R.; Rafa, H.; Touil-Boukoffa, C. Overview of Cytokines and Nitric Oxide Involvement in Immuno-Pathogenesis of Inflammatory Bowel Diseases. *World J Gastrointest Pharmacol Ther* **2016**, *7* (3), 353–360. https://doi.org/10.4292/wjgpt.v7.i3.353.

(45) Avdagić, N.; Zaćiragić, A.; Babić, N.; Hukić, M.; Šeremet, M.; Lepara, O.; Nakaš-Ićindić, E. Nitric Oxide as a Potential Biomarker in Inflammatory Bowel Disease. *Bosn J Basic Med Sci* **2013**, *13* (1), 5–9.

(46) Chami, B.; Martin, N. J. J.; Dennis, J. M.; Witting, P. K. Myeloperoxidase in the Inflamed Colon: A Novel Target for Treating Inflammatory Bowel Disease. *Archives of Biochemistry and Biophysics* **2018**, *645*, 61–71. https://doi.org/10.1016/j.abb.2018.03.012.

(47) Garrity-Park, M.; Loftus, E. V., Jr; Sandborn, W. J.; Smyrk, T. C. Myeloperoxidase Immunohistochemistry as a Measure of Disease Activity in Ulcerative Colitis: Association with Ulcerative Colitis-Colorectal Cancer, Tumor Necrosis Factor Polymorphism and RUNX3 Methylation. *Inflammatory Bowel Diseases* **2012**, *18* (2), 275–283. https://doi.org/10.1002/ibd.21681.

(48) Bastaki, S. M. A.; Al Ahmed, M. M.; Al Zaabi, A.; Amir, N.; Adeghate, E. Effect of Turmeric on Colon Histology, Body Weight, Ulcer, IL-23, MPO and Glutathione in

Acetic-Acid-Induced Inflammatory Bowel Disease in Rats. *BMC Complementary and Alternative Medicine* **2016**, *16* (1), 72. https://doi.org/10.1186/s12906-016-1057-5.

(49) Hansberry, D. R.; Shah, K.; Agarwal, P.; Agarwal, N. Fecal Myeloperoxidase as a Biomarker for Inflammatory Bowel Disease. *Cureus* **2017**, *9* (1). https://doi.org/10.7759/cureus.1004.

(50) Iwao, Y.; Tomiguchi, I.; Domura, A.; Mantaira, Y.; Minami, A.; Suzuki, T.; Ikawa, T.; Kimura, S.; Itai, S. Inflamed Site-Specific Drug Delivery System Based on the Interaction of Human Serum Albumin Nanoparticles with Myeloperoxidase in a Murine Model of Experimental Colitis. *European Journal of Pharmaceutics and Biopharmaceutics* **2018**, *125*, 141–147. https://doi.org/10.1016/j.ejpb.2018.01.016.

Chapter 7

Summary & conclusion

7.1 Summary and conclusion

The development, physicochemical characterization, and pharmacological effectiveness of certain nanoformulations for drug delivery application in animal model of acute experimental colitis induced by dextran sodium sulphate are the main foci of this thesis. The attributes of nanoformulations, such as particle size (hydrodynamic diameter), shape, surface morphological characteristics, drug encapsulation efficacy, drug loading capacity of nanoformulations etc. were estimated. Following the physicochemical characterizations, these nanoformulations' *in-vitro* cytocompatibility was determined, and then their pharmacological activity in animal model of UC was evaluated.

Chapter 1 of thesis deals with introduction and overview of the literature on the use of nanoparticles to deliver pharmaceutical active ingredients for the treatment of inflammatory diseases such ulcerative colitis. It provides a background story of this inflammatory condition, outlines the basic pathophysiology involved, and discusses about various therapeutic modalities and therapeutic regimen application tactics for ulcerative colitis management. The use of medications in ulcerative colitis has some drawbacks, some of which have been briefly addressed. Various strategies for using different nanomaterials-based drug delivery systems to lessen the severity of ulcerative colitis have also been discussed.

In ***chapter 2*** of the thesis, various materials, methods, tools, and procedures used for conducting experiments are detailed in depth. This chapter discusses a variety of techniques from various sources that were used for formulation, physicochemical characterization, and biological evaluation of developed nanoformulations for their cytocompatibility and pharmacological activity *in-vitro* and *in-vivo*.

Chapter 3 of thesis describes formulation, characterization and anti-colitic activity of celecoxib loaded Eudragit S 100 coated nanostructured lipid carrier against animal model of colitis. Ulcerative colitis is a chronic mucosal inflammatory condition that adversely affects colon and rectum. Celecoxib is a selective inhibitor of

inducible cyclooxygenase-2 (COX-2) and is prescribed for the management of pain and other inflammatory disorders. The physicochemical properties of celecoxib limit its clinical potency. For the purpose of encapsulating celecoxib, we developed nanostructured lipid carriers (NLCs) utilising substances that are generally recognised as safe and US-FDA approved. Additionally, TEM, SEM, and AFM were used to confirm the formulation's size, shape, and morphology. The blank NLCs were cytocompatible against hTERT BJ cell shows safe biological properties of employed materials. As evidenced by the disease activity index, colon length, faecal occult blood test, and histological analysis, celecoxib-loaded NLC therapy reduced the severity of colitis. Treatment with celecoxib-loaded NLCs also restored sulfomucin in the colon while reducing goblets cell disintegration. Colonic inflammation was significantly lessened by celecoxib-nanoformulation, as shown by a decline in the immunohistochemistry expression of COX-2 and iNOS. The results of the study indicate that celecoxib administration tailored to the colon using lipids may be used to treat colitis.

In ***Chapter 4***, study on a colitis model induced by DSS, the formulation, characterizations, and therapeutic effectiveness of a cortisone-loaded nanostructured lipid carrier based on stearoyl ascorbic acid were examined. This study was entirely different from previous chapter in terms of materials and also therapeutic approach. As part of our study in this chapter, we used different materials from previously described to develop nanocarrier. According to reports, ascorbic acid has a considerable antioxidant activity, and the present formulation benefits from the same quality. It is a good material for the lipid-based nanoformulation when combined with stearic acid. Oxidative stress has a direct relationship to colitis and inflammation, both of which have a local corrosive effect at the illness site via different mechanisms. Together with the anti-inflammatory effects of the medication cortisone that is encapsulated, this formulation has good effects on oxidative stress defence. Treatment with CRT-loaded NLCs normalises physically observed measures like disease activity index, weight variation, and so forth. In terms of the colon's histoarchitecture, recovered goblet cells, mucin secretions, inhibition of pro-

inflammatory cytokines, etc., this NLCs was able to greatly lessen the severity of colitis. When CRT loaded NLC was used as a treatment, the overexpression of inflammatory enzymes including COX-2 and iNOS was successfully suppressed. The study's findings showed that this CRT loaded NLC effectively manages the disease severity induced by DSS.

Study in ***Chapter 5*** deals with the DSS-induced colitis model and the therapeutic effectiveness of previously synthesized Copperoxide nanoparticles. Colon inflammation, or UC, can progress to colon and rectum ulcers and colon cancer if it is not treated and allowed to become chronic. Current treatments for UC have significant drawbacks, including quick clearance, considerable first-pass metabolism, poor drug absorption, extremely low solubility, and limited bioavailability. Due to these limitations, managing UC necessitates a logical strategy that targets the drug delivery at the site of action in order to get beyond the therapeutic limitations. Metallic nanoparticles are effective in treating colitis, but their applications are restricted because of harmful side effects on the body. We have employed cellulose-grafted copper oxide nanoparticles (C-$Cu^{I/II}O$ NPs) which are biocompatible to cure UC. The length of the colon and other measured physical parameters show that the metal NPs improved the colitic state. Analysis of the histology showed that the DSS-induced colitis-damaged colon architecture had recovered. Treatment with C-$Cu^{I/II}O$ NPs lessens goblet cell breakdown and sulfomucin retention. Following treatment with C-$Cu^{I/II}O$ NPs, it was evidenced that levels of inflammatory indicators such as MPO, nitrite, and TNF- α were significantly decreased. Intestinal inflammation caused by colitis may be successfully treated intrarectally using cellulose-based C-$Cu^{I/II}O$ NPs, according to the study's findings.

Chapter 6 comprises of the development and evaluation of caffeic acid-based nanomicelle, as well as their therapeutic effectiveness against a model of colitis induced by DSS. In this study, a formulation that targets inflammation and has antioxidant properties due to caffeic acid has been produced and developed. This nanomicelle was formulated using the solvent evaporation process. Pyrene assay was initially used to characterise it for its critical micelle concentration. Accordingly,

physical and chemical analyses have been carried out using a variety of techniques, including DLS, SEM, TEM, and AFM. According to DLS measurements, the micelle had an average hydrodynamic diameter of 152 nm and estimated encapsulation efficacy was 87% for budesonide drug. Treatment with BUD-loaded micelles normalises physically observed parameters like disease activity index, weight variation whereas cytocompatibility study established the safety of formulation components. Through the restoration of goblet cells, the release of mucins, the inhibition of pro-inflammatory cytokines, and other factors, this micelle was able to greatly alleviate the severity of colitis. The overexpression of inflammatory enzymes like COX-2 and iNOS was successfully reduced by budesonide-loaded micelle therapy. The study's findings indicated that this BUD-loaded micelle manages the illness severity of DSS induced colitis.

Appendix

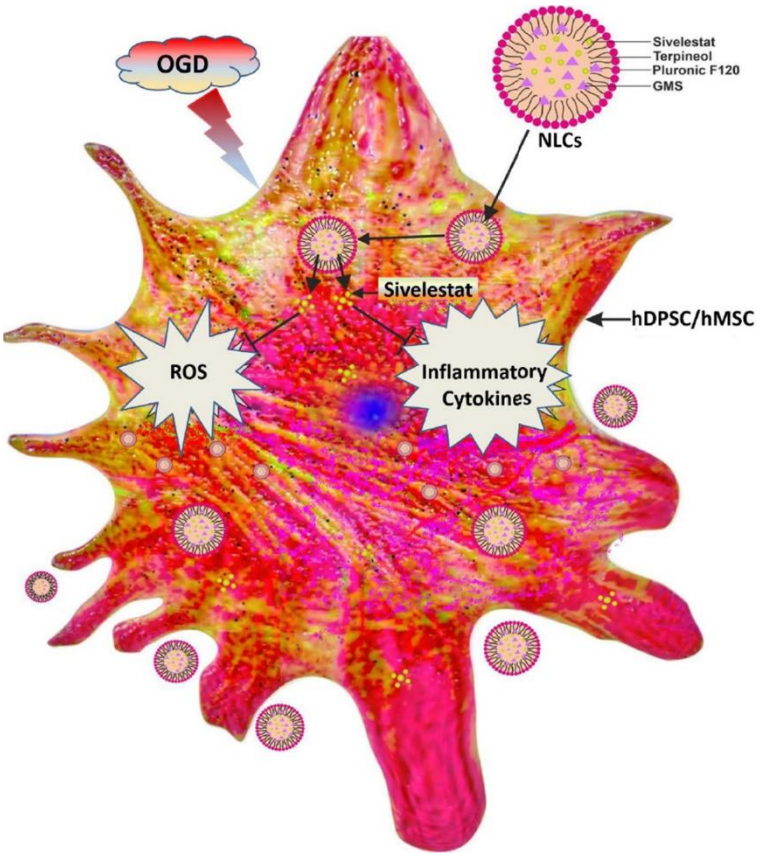
OGD
Sivelestat
Terpineol
Pluronic F120
GMS
NLCs
Sivelestat
hDPSC/hMSC
ROS
Inflammatory
Cytokines

Materials Science & Engineering C 120 (2021) 111700

Contents lists available at ScienceDirect

Materials Science & Engineering C

journal homepage: www.elsevier.com/locate/msec

Sivelestat-loaded nanostructured lipid carriers modulate oxidative and inflammatory stress in human dental pulp and mesenchymal stem cells subjected to oxygen-glucose deprivation

Ravi Prakash [a,1], Rakesh Kumar Mishra [b,1], Anas Ahmad [b], Mohsin Ali Khan [c], Rehan Khan [b,*,2], Syed Shadab Raza [a,d,**,2]

[a] Laboratory for Stem Cell & Restorative Neurology, Department of Biotechnology, Era's Lucknow Medical College and Hospital, Sarfarazganj, Lucknow 226003, Uttar Pradesh, India
[b] Department of Nano-Therapeutics, Institute of Nano Science and Technology, Habitat Centre, Phase 10, Sector 64, Mohali, Punjab 160062, India
[c] Era University, Lucknow 226003, Uttar Pradesh, India
[d] Department of Stem Cell Biology and Regenerative Medicine, Era University, Sarfarazganj, Lucknow 226003, Uttar Pradesh, India

ARTICLE INFO

Keywords:
Mesenchymal stem cells
Dental pulp stem cells
Oxygen-glucose deprivation
Sivelestat
Nanostructured lipid carriers
Oxidative and inflammatory stress

ABSTRACT

Stroke remains the leading cause of morbidity and mortality. Stem cell-based therapy offers promising hope for survivors and their families. Despite the clinical translation of stem cell-based therapies in stroke patients for almost two decades, results of these randomized controlled trials are not very optimistic. In these lines, an amalgamation of nanocarriers based drug delivery with stem cells holds great promise in enhancing stroke recovery. In the present study, we treated oxygen-glucose deprivation (OGD) exposed dental pulp stem cells (DPSCs) and mesenchymal stem cells (MSCs) with sivelestat-loaded nanostructured lipid carriers (NLCs). Various physicochemical limitations associated with sivelestat drug applications and its recent inefficacy in the clinical trials necessitates the development of novel delivery approaches for sivelestat. Therefore, to improve its efficacy on the survival of DPSCs and MSCs cell types under OGD insult, the current NLCs were formulated and characterized. Resulting NLCs exhibited a hydrodynamic diameter of 160–180 nm by DLS technique and possessed good PDI values of 0.2–0.3. Their shape, size and surface morphology were corroborated with microscopic techniques like TEM, SEM, and AFM. FTIR and UV–Vis techniques confirmed nanocarrier's loading capacity, encapsulation efficiency of sivelestat, and drug release profile. Oxidative stress in DPSCs and MSCs was assessed by DHE and DCFDA staining, and cell viability was assessed by Trypan blue exclusion test and MTT assay. Results indicated that sivelestat-loaded NLCs protected the loss of cell membrane integrity and restored cell morphology. Furthermore, NLCs successfully defended human DPSCs and MSCs against OGD-induced oxidative and inflammatory stress. In conclusion, modulation of oxidative and inflammatory stress by treatment with sivelestat-loaded NLCs in DPSCs and MSCs provides a novel strategy to rescue stem cells during ischemic stroke.

1. Introduction

Stroke is one of the significant causes of death and adult patient disability globally [1]. Survivors of stroke stay at the risk of recurrence, which often becomes more severe and disabling than the index event itself [2]. Out of the two categories of stroke, viz. ischemic and hemorrhagic, 90% of the cases are comprised of ischemic stroke and thus its acute management becomes of dire significance [3]. Despite of the approval and availability of recombinant tissue plasminogen activator (rtPA), and a speedy increment in the quantity of recanalization therapeutic approaches for ischemic stroke, their effects on decreasing stroke related chronic disablements stay restricted [4,5]. One of the

* Corresponding author.
** Correspondence to: S. S. Raza, Laboratory for Stem Cell & Restorative Neurology, Department of Biotechnology, Era's Lucknow Medical College Hospital, Sarfarazganj, Lucknow 226003, Uttar Pradesh, India.
E-mail addresses: rehankhan@inst.ac.in (R. Khan), drshadab@erauniversity.in (S.S. Raza).
[1] RP and RKM contributed equally and shares equal first-authorship.
[2] RK and SSR shares equal correspondence.

https://doi.org/10.1016/j.msec.2020.111700
Received 22 July 2020; Received in revised form 21 October 2020; Accepted 2 November 2020
Available online 6 November 2020

List of Publications

Research Articles

1. **Mishra RK**, Selim A, Gowri V, Ahmad A, Nadeem A, Siddiqui N, Raza SS, Jayamurugan G, Khan R. Thiol-Functionalized Cellulose-Grafted Copper Oxide Nanoparticles for the Therapy of Experimental Colitis in Swiss Albino Mice. ACS Biomaterials Science & Engineering. 2022 Apr 22.

2. Prakash R, **Mishra RK**, Ahmad A, Khan MA, Khan R, Raza SS. Sivelestat-loaded nanostructured lipid carriers modulate oxidative and inflammatory stress in human dental pulp and mesenchymal stem cells subjected to oxygen-glucose deprivation. Materials Science and Engineering: C. 2021 Jan 1; 120:111700.

3. **Mishra RK**, Ahmad A, Kumar A, Vyawahare A, Raza SS, Khan R. Lipid-based nanocarrier-mediated targeted delivery of celecoxib attenuate severity of ulcerative colitis. Materials Science and Engineering: C. 2020 Nov 1; 116:111103.

4. **Mishra RK**, Kumar A, Ali Aneesh, Kanika, Raza SS, Khan R. Cortisone loaded stearoyl ascorbic acid based nanostructured lipid carrier alleviate inflammatory changes in DSS induced colitis. **(Manuscript under revision)**

5. **Mishra RK,** Kumar A, Vyawahare A, Kanika, Sakla R, Nadeem A, Siddiqui N, Ahmad A, Raza SS, Khan R. Caffeic Acid Conjugated Budesonide Loaded Nanomicelle Attenuates Inflammation in Experimental Colitis. **(Manuscript under revision)**

6. Khan MM, Khanam N, Uddin M, **Mishra RK**, Khan R. Nanotized kinetin enhances essential oil yield and active constituents of mint via improvement in physiological attributes. Chemosphere. 2022 Feb 1; 288:132447.

7. Dar AH, Gowri V, **Mishra RK**, Khan R, Jayamurugan G. Nanotechnology-Assisted, Single-Chromophore-Based White-Light-Emitting Organic Materials with Bioimaging Properties. Langmuir. 2021 Dec 29.

8. Ahmad A, Ansari MM, **Mishra RK**, Kumar A, Vyawahare A, Verma RK, Raza SS, Khan R. Enteric-coated gelatin nanoparticles mediated oral delivery of 5-aminosalicylic acid alleviates severity of DSS-induced ulcerative colitis. Materials Science and Engineering: C. 2021 Feb 1; 119:111582.

9. Ahmad A, Ansari MM, Kumar A, Vyawahare A, **Mishra RK**, Jayamurugan G, Raza SS, Khan R. Comparative acute intravenous toxicity study of triple polymer-layered magnetic nanoparticles with bare magnetic nanoparticles in Swiss albino mice. Nanotoxicology. 2020 Nov 25;14(10):1362-80.

10. Ansari MM, Ahmad A, **Mishra RK**, Raza SS, Khan R. Zinc gluconate-loaded chitosan nanoparticles reduce severity of collagen-induced arthritis in Wistar rats. ACS Biomaterials Science & Engineering. 2019 May 27;5(7):3380-97.

11. Sinha P, Srivastava N, Rai VK, **Mishra RK**, Ajaya kumar PV, Yadav NP. A novel approach for dermal controlled release of salicylic acid for improved anti-inflammatory action: Combination of hydrophilic-lipophilic balance and response surface methodology. Journal of Drug Delivery Science and Technology. 2019 Aug 1; 52:870-84.

12. Ahmad A, Fauzia E, Kumar M, **Mishra RK**, Kumar A, Khan MA, Raza SS, Khan R. Gelatin-coated polycaprolactone nanoparticle-mediated naringenin delivery rescue human mesenchymal stem cells from oxygen glucose deprivation-induced inflammatory stress. ACS Biomaterials Science & Engineering. 2018 Dec 7;5(2):683-95.

Review Articles

1. **Mishra RK**, Ahmad A, Vyawahare A, Alam P, Khan TH, Khan R. Biological effects of formation of protein corona onto nanoparticles. International Journal of Biological Macromolecules. 2021 Apr 1; 175:1-8.

2. **Mishra RK**, Ahmad A, Vyawahare A, Kumar A, Khan R. Understanding the monoclonal antibody involvement in targeting the activation of tumor suppressor genes. Current Topics in Medicinal Chemistry. 2020 Aug 1;20(20):1810-23.

3. Ahmad A, **Mishra RK**, Vyawahare A, Kumar A, Rehman MU, Qamar W, Khan AQ, Khan R. Thymoquinone (2-Isopropyl-5-methyl-1, 4-benzoquinone) as a chemopreventive/anticancer agent: Chemistry and biological effects. Saudi Pharmaceutical Journal. 2019 Dec 1;27(8):1113-26.

4. Ahmad A, Khan F, **Mishra RK**, Khan R. Precision cancer nanotherapy: evolving role of multifunctional nanoparticles for cancer active targeting. Journal of medicinal chemistry. 2019 Jul 24;62(23):10475-96.

Book Chapters

1. Ahmad A, Imran M, Kumar A, **Mishra RK**, Vyawahare A, Khan AQ, Raza SS, Khan R. Black seeds of Nigella sativa: A remedy for advanced cancer therapeutics with special reference to nanotechnology. In Black Seeds (Nigella Sativa) 2022 Jan 1 (pp. 253-294). Elsevier.

2. Ali A, Yangchan J, Ahmad A, Kumar A, **Mishra RK**, Vyawahare A, Akhter R, Ashraf GM, Shakil S, Khan R. A Mechanistic Perspective on Chemopreventive and Therapeutic Potential of Phytochemicals in Honey. In Therapeutic Applications of Honey and its Phytochemicals 2020 (pp. 113-140). Springer, Singapore.

3. Rehman MU, Ahmad SB, Shah A, Kashani B, Ahmad A, **Mishra RK**, Khan R, Rashid SM, Ali R, Rasool S. An overview of the pharmacological properties and potential applications of lavender and cumin. The Glob. Floric. Ind. Shifting Dir. New Trends, Futur. Prospect. 2020 Nov 17;83.